GENETIC DETERMINANTS OF KEY ANTIRETROVIRAL PHARMACOKINETICS

Thesis submitted in accordance with requirements of the University of Liverpool for the degree of Doctor of Philosophy

by Marco Siccardi

June 2011

This thesis is the results of my own work. The material contained within the thesis has not been presented, either wholly or in part, for any other degree or qualification.

Marco Siccardi

This research was carried out in the

Liverpool HIV Pharmacology Group

Department of Molecular and Clinical Pharmacology

University of Liverpool, UK

TABLE OF CONTENTS

ACKNOWLEDGEMENTS

The studies presented in this thesis were carried out in the Department of Molecular and Clinical Pharmacology, University of Liverpool and Clinica Universitaria di Malattie Infettive, Università di Torino. Financial support was provided by Università di Torino for which I am grateful.

Completing a PhD is truly an odyssey and I would not have been able to complete this voyage without the aid and support of numerous people over the past three years. Foremost I would like to thank my supervisor Dr. Andrew Owen who has been a great scientific guide and his sound advice was essential throughout my studies. Our meetings have always been enriched by refreshing insight, critical questions and Bill Hick's razor-sharp humour that was crucial for my survival. Prof. David Back has been a great scientific mentor. His infinite knowledge on antiretroviral therapy was a central stimulus for developing new ideas and planning future studies. Prof Giovanni Di Perri and Prof. Stefano Bonora represented a rare example of dedication and passion for the clinical pharmacology of antiretrovirals. I would like also to thank Prof. Saye Khoo for clinical advice and suggestions. The development of bio-analytical methods would not be possible without the inspiring supervision of Dr. Antonio D'Avolio. My thanks go to Dr. Alessandro Schipani for the countless conversations on popPK and his help in Chapter 2. Dr. Sonia Rodríguez-Novoa had an essential role in Chapter 2 sharing her data. Thanks to everyone else in the Clinica Universitaria di Malattie Infettive and Liverpool HIV Pharmacology Group. In particular to Lorena, Marco, Mauro, Daniel, Andrea, Letizia, Marianna, Ilaria, Cristina, Mossy, Paul, Jay, Jae, Neill, Darren S, Deirdre, Phil, Ruben, Wai San, Laura's, Justin, Corinne, JT, Alieu, Sara and Beth who share with me part of their scientific life and drink coffee with me.

The crew of international friends that surrounded me during my time in Liverpool was a huge source of fun. Pipppe, Jonas, Kay, Chiara, Natalia, Alejandro, Ellie, Claudio M, Chao, Paul, Raluca, Claudio T, Mario, Marco, Meg, Angela, Michele, Kenneth, Virginie, Adolfo, Israel, Renee, Jonathan, Maria are just a few of the great persons I've had the luck to meet here.

A heartfelt thanks goes out to my Valentina who is my joy and an endless source of love and laughs. Lastly I would like to thank my parents, grandma and sister for all your love, support and encouragement even if a good portion of it was communicated through video-telephone.

ABBREVIATIONS

3TC	Lamivudine
μg	Microgram(s)
μl	Microliter(s)
μM	Micromolar
Ω	Ohms
ABC	ATP-binding cassette transporter
ACE	Angiotensin-converting enzyme
ADME	Absorption, distribution, metabolism, elimination
AIDS	Acquired Immunodefiency syndrme
APV	Amprenavir
ARV	Antiretroviral
ATV	Atazanavir
AUC	Area Under the Curve
AZT	Zidovudine
bid	Twice daily
BBB	Blood–brain barrier
BMI	Body mass index
CAR	Cellular Accumulation Ratio
CAR	Costitutuve Androstane Receptor
°C	Degree Celsius
C_{avg}	Average concentrations
CCR5	Chemokine (C-C motif) receptor 5
CXCR4	Chemokine (C-X-C motif) receptor 4
CD4	Cluster of differentiation 4
cDNA	Complementary DNA
CI	Confidence Intervals
Ci	Curie(s)
CL	Clearence
Cl_{int}	Intrinsic clearance

C_{max}	Maximum concentrations
CNS	Central nervous system
CSF	High cerebrospinal fluid
C_{trough}	Trough concentrations
CYP	Cytochrome P450
d4T	Stavudine
ddH_20	Double deionised water
ddI	Didanosine
DEPC	Diethylpyrocarbonate
dNTP	Deoxy nucleoside triphosphate
DNA	Deoxyribonucleic acid
DRV	Darunavir
E3S	Estrone-3-sulfate
EFV	Efavirenz
ESI	Electro spray Ionization
ETV	Etravirine
FDA	Food and drug administration
F	Bioavailability
fl	Femtoliter(s)
FTC	Emtricitabine
f_u	Free fraction
g	Gram(s)
gp41	Glycoprotein 41
gp120	Glycoprotein 120
gp160	Glycoprotein 160
GST	Glutathione–S-transferase
GWAS	Genome wide association studies
h	Hour(s)
HAART	Highly active antiretroviral therapy
HEPES	4-(2-hydroxyethyl)-1-piperazineethanesulfonic acid
HIV	Human Immunodeficiency Virus
HLM	Human Liver Microsome

HNF4α	Hepatocyte nuclear factor 4α
HPLC	High Performance Liquid Chromatography
HuPO	Human acidic ribosomal protein
IC	Intracellular
$IC_{50/95}$	Concentration required to produce 50/95% inhibition
IDV	Indinavir
Ind_{max}	Maximum induction
IQ	Inhibitory Quotient
IQR	Inter quartile range
I.S	Internal standard
ISEFi	Intersystem extrapolation factor
IVIVE	In vitro in vivo extrapolation
logP	Partition coefficient
Ka	Absorption rate constant
kD	KiloDalton
kg	Kilograms
K_i	Inhibitory constant
K_{inact}	Maximal inactivation rate constant
K_m	Michaelis constant
kV	KiloVolts
L	Liter(s)
Log_{10}	Logarithm to the base 10
LC-MS	Liquid Chromatography-Single Quadrupole
LC-MS/MS	Liquid Chromatography-Triple Quadrupole
LLQ	Lower Limit of Quantification
LOD	Lower Limit of Detection
LPV	Lopinavir
LTR	Long terminal repeats
LXR	Liver X receptor
LW	Liver Weight
m/z	Mass to charge ratio
M	Molar

MEC	Minimum effective concentrations
MCV	Mean Cellular Volume
mg	Milligram(s)
ml	Milliliter(s)
min	Minute(s)
mM	Millimolar
MPPGL	Microsomal protein per gram of liver
mRNA	Messenger RNA
MVC	Maraviroc
NFV	Nelfinavir
ng	Nanogram(s)
nm	Nanometer(s)
nM	Nanomolar
NNRTI	Non Nucleoside Reverse Transcriptase Inhibitors
NR	Nuclear receptor
NRTI	Nucleoside Reverse Transcriptase Inhibitors
NS	Not statistically significant.
NVP	Nevirapine
OBT	Optimised background therapy
OCT	Organic Cation Transporter
OF	Objective function
qid	Once daily
PAMPA	Parallel artificial membrane permeability assay
PBMC	peripheral blood mononuclear cell
PBPK	physiologically based pharmacokinetic
PCR	Polymerase chain reaction
PD	Pharmacodynamic
PDA	Photodiode Array Detector
PG	Pharmacogenetics
pH	$-\log_{10}$ hydrogen ion concentration
PI	Protease Inhibitor
pl	Picoliter(s)

PK	Pharmacokinetic
pmol	Picomole
popPK	Population pharmacokinetics
PPAR	peroxisome proliferator-activated receptors
PXR	Pregnane X receptor
QC	Quality control
QX	Quinoxaline
r^2	Correlation coefficient
RAL	Raltegravir
RNA	Ribonucleic acid
RSD	Relative standard deviation
RT	Reverse Transcriptase
RTV	Ritonavir
RXR	Retinoic acid receptor
s	Second(s)
SD	Standard Daviation
SE	Standard error
SI	Syncytia-forming
SLCO	Solute carrier organic anion transporter
SNP	Single nucleotide polymorphism
SPE	Solid phase extraction
SQV	Saquinavir
STD	Standard
SULT	Sulfotransferase
$t_{1/2}$	Half-life
TDF	Tenofovir
TFA	Trifluoroacetic acid
TDM	Therapeutic drug monitoring
TPV	Tipranavir
UGT	UDP-glucuronosyltransferase
UV	Ultraviolet
Vd	Volume of distribution

V_{max}	Maximum Velocity
vs	Versus

KEY POLYMORPHISMS discussed in the thesis

Gene	Traditional nomenclature	rs number
CYP3A4	*CYP3A4**1B	rs2740574
PXR	44477T>C	rs1523130
	63396C>T	rs2472677
	69789A>G	rs763645
CYP2B6	516G>T	(rs3745274
SLCO1B1	521T>C	rs4149056

PUBLICATIONS

Simiele M, D'Avolio A, Baietto L, **Siccardi M**, Sciandra M, Agati S, Cusato J, Bonora S, Di Perri G. Evaluation of the mean corpuscular volume of peripheral blood mononuclear cells of HIV patients by a coulter counter to determine intracellular drug concentrations. Antimicrob Agents Chemother 2011 Jun;55(6):2976-8.

D'Avolio A, Simiele M, **Siccardi M**, Baietto L, Sciandra M, Oddone V, Stefani FR, Agati S, Cusato J, Bonora S, Di Perri G. A HPLC-MS method for the simultaneous quantification of fourteen antiretroviral agents in peripheral blood mononuclear cell of HIV infected patients optimized using medium corpuscular volume evaluation. J Pharm Biomed Anal 2011 Mar 25;54(4):779-88.

Siccardi M, D'Avolio A, Nozza S, Simiele M, Baietto L, Stefani FR, Moss D, Kwan WS, Castagna A, Lazzarin A, Calcagno A, Bonora S, Back D, Di Perri G, Owen A. Maraviroc is a substrate for OATP1B1 in vitro and maraviroc plasma concentrations are influenced by SLCO1B1 521 T>C polymorphism. Pharmacogenet Genomics 2010 Dec;20(12):759-65.

Schipani A, **Siccardi M**, D'Avolio A, Baietto L, Simiele M, Bonora S, Rodriguez Novoa S, Cuenca L, Soriano V, Chierakul N, Saguenwong N, Chuchuttaworn C, Hoskins JM, Dvorak AM, McLeod HL, Davies G, Khoo S, Back DJ, Di Perri G, Owen A. Population pharmacokinetic modeling of the association between 63396C->T pregnane X receptor polymorphism and unboosted atazanavir clearance. Antimicrobial agents and chemotherapy 2010 Dec;54(12):5242-50.

D'Avolio A, Simiele M, Baietto L, **Siccardi M**, Sciandra M, Patanella S, Bonora S, Di Perri G. A validated high-performance liquid chromatography-ultraviolet method

for quantification of the CCR5 inhibitor maraviroc in plasma of HIV-infected patients. Therapeutic drug monitoring 2010 Feb;32(1):86-92.

D'Avolio A, Baietto L, **Siccardi M**, Sciandra M, Simiele M, Oddone V, Bonora S, Di Perri G. An HPLC-PDA method for the simultaneous quantification of the HIV integrase inhibitor raltegravir, the new nonnucleoside reverse transcriptase inhibitor etravirine, and 11 other antiretroviral agents in the plasma of HIV-infected patients. Therapeutic drug monitoring 2008 Dec;30(6):662-9.

Siccardi M, D'Avolio A, Baietto L, Gibbons S, Sciandra M, Colucci D, Bonora S, Khoo S, Back DJ, Di Perri G, Owen A. Association of a single-nucleotide polymorphism in the pregnane X receptor (PXR 63396C-->T) with reduced concentrations of unboosted atazanavir. Clin Infect Dis 2008 Nov 1;47(9):1222-5.

COMMUNICATIONS

Siccardi M, Almond LM, A. Schipani A, Owen A, Back DJ. In vitro-in vivo extrapolation of CYP2B6 genotype-based efavirenz dose reduction. 12th International Workshop on Clinical Pharmacology of HIV Therapy 13 – 15 April 2011, Miami, FL, USA.

Siccardi M, D'Avolio A, Baietto L, Simiele M, Bonora S, Back S, Di Perri G, and Owen A. Intracellular Pharmacokinetics of ATV/RTV Is Influenced by Solute Carrier Organic Anion Transporter 3A1 Expression. 18th Conference on Retroviruses and Opportunistic Infections (CROI), 27-3 Mar 2011, Boston, MA, USA

Siccardi M, D'Avolio A, Baietto L, Simiele M, Bonora S, Back S., Di Perri G, Owen A. SLCO3A1 expression is a major determinant of atazanavir PBMC penetration in

HIV infected patients. 10th International Congress on Drug Therapy in HIV Infection. Glasgow, UK. 7-11 November 2010. (Oral presentation)

Siccardi M, D'Avolio A, Simiele M., Sciandra M., Baietto L Stefani F.R., Agati S., Cusato J., Calcagno A., Owen A., Bonora S., Di Perri G. Intracellular Pharmacokinetics of Boosted and Unboosted Atazanavir in HIV Infected Patients 11th International Workshop on Clinical Pharmacology of HIV Therapy. 6-9 April 2010 Sorrento, Italy. (Oral presentation)

Simiele M, D'Avolio A, **Siccardi M**, Baietto L, Stefani FR, Agati S, Cusato J, Sciandra M, Bonora S, Di Perri G. Are intracellular drug concentrations underestimated? The role of mean corpuscolar volume (MCV) for a correct determination. 11th International Workshop on Clinical Pharmacology of HIV Therapy. 7-9 April 2010, Sorrento, Italy.

Schipani A, **Siccardi M**, Boffito M, D'Avolio A, Bonora S, Davies G, Khoo S, Back D, Di Perri G, and Owen A. A Population Pharmacokinetic Model Illustrates an Association Between a Pregnane-X-Receptor (PXR) Polymorphism and Boosted Atazanavir Clearance. 17th Conference on Retroviruses and Opportunistic Infections (CROI), 16-19 Feb 2010, San Francisco, CA, USA.

Siccardi M, Moss D, Kwan W.S, D'Avolio A, Bonora S, Khoo S, Back D, Di Perri G, and Owen A. Solute Carrier Organic Anion Transporter 1B1 (SLCO1B1) Mediates Transport of Maraviroc Using a X. leavis Model. 17th Conference on Retroviruses and Opportunistic Infections (CROI), 16-19 Feb 2010, San Francisco, CA, USA

Siccardi M, Bonora S, Nozza S, Castagna A, D'Avolio A, Michelazzo M, Chiesa M, Calcagno A, Lazzarin A, Di Perri G. Pharmacokinetics and pharmacogenetics of

maraviroc in the clinical setting. ICAR (Italian Conference on AIDS and Retroviruses), 24-26 May 2009, Milan, Italy. (Oral presentation)

Siccardi M, D'Avolio A, Bonora S, Baietto L, Gatti D, Calcagno A, Ghisetti V, Lanzafame M, Penco G, Back D, Owen A, Di Perri G. Combined effect of SLCO1B1 521T>C, PXR 63396C>T, and ABCB1 3435C>T on the achievement of therapeutic concentrations of unboosted Atazanavir. 10th International Workshop on Clinical Pharmacology of HIV Therapy, 15-17 April 2009, Amsterdam, The Netherlands. (Oral presentation)

Siccardi M, D'Avolio A, Nozza S, Bonora S, Castagna A, Baietto L, Stefani F.R, Moss D, Calcagno A, Sciandra M, Lazzarin L, Back D, Owen A, Di Perri G. Is Maraviroc a substrate for SLCO1B1? 10th International Workshop on Clinical Pharmacology of HIV Therapy, 15-17 Apr 2009, Amsterdam, The Netherlands.

Siccardi M, D'Avolio A, Baietto L, Calcagno A, Gibbons S, Sciandra M, Bonora S, Khoo S, Back D, Di Perri G, Owen A. Plasma concentration of boosted and unboosted Atazanavir are predicted by 63396C>T SNP in the PXR gene. 9th International Congress on Drug Therapy in HIV Infection, 09-13 Nov 2008 Glasgow, UK

ABSTRACT

Antiretroviral pharmacokinetics is one of the most important predictors of therapy efficacy and correlations between virological suppression and plasma concentrations have been described for all antiretroviral classes. Plasma concentrations are the result of absorption, distribution, metabolism and elimination (ADME) processes which are mediated by numerous proteins in different tissues. Single nucleotide polymorphisms (SNPs) in genes encoding for individual proteins may be an important determinants drug exposure. The aim of this thesis was to characterise the role of some key SNPs determining antiretroviral plasma concentrations in order to improve the current understanding of dose-dependent efficacy and toxicity.

A number of different strategies to investigate the role of genetic variability in antiretroviral exposure were developed in this thesis. The polymorphism 63396 C>T in the *PXR* gene, a nuclear factor regulating the expression of CYPs and transporter in hepatocytes, was proven to influence unboosted atazanavir clearance using a pharmacogenetic based population pharmacokinetic model and patients with 63396TT genotype had a increment in ATV clearance of 17% (Chapter 2). In Chapter 3, the predictors of intracellular pharmacokinetic of unboosted and boosted atazanavir were investigated and expression of *SLCO3A1,* an uptake transporter expressed on PBMC was correlated with cellular accumulation of boosted and unboosted atazanavir (rho=0.706, p=0.010; rho = 0.830, p = 0.005, respectively). An *in vitro in vivo* extrapolation model for efavirenz was developed in Chapter 4 and the effect of CYP2B6 516 G>T on standard regimens or dose reduction was quantified. Efavirenz pharmacokinetics was predicted with good accuracy compared to available data; simulated Ctrough was 2119 ng/ml vs 1764 ng/ml, simulated Cmax was 3725 ng/ml vs 4063 ng/ml. The effect of 516G>T on simulated EFV clearance (GT = -24% and TT = -58%) was comparable to previously published population pharmacokinetic data (GT =-36%, TT =-66%). Maraviroc, a CCR5 inhibitor was identified as a substrate for SLCO1B1 with a K_m of 33.85 μM and V_{max} of 187.9 fmol/oocyte/min and the inhibitory potential of concomitant protease inhibitors on this transporter was investigated using *Xenopus laevis* oocytes heterologous protein expression system (Chapter 5). Moreover the SNP *SLCO1B1* 521 T>C was correlated with maraviroc C_{trough} in a cohort of HIV infected patients; MVC C_{trough} in SLCO1B1 521 heterozygote patients (TC) (n=8) was higher than in wild type homozygotes (TT) (n=22), 103 ng/ml (69 - 124) vs 46 ng/ml (28 - 66), p=0.003 (Chapter 6).

The convergence of different factors under study permitted partial definition of the complex interplay in which drug-drug interactions and physical characteristics interact with genetic variability to define the pharmacokinetic phenotype. These findings will help identify patients with a higher risk of achieving sub-therapeutic or

potentially toxic plasma concentrations and will serve as a knowledge-base from which to grow and validate strategies for optimisation of therapy.

CHAPTER 1
General Introduction

1.1. HIV Replication Cycle

HIV is a Retrovirus, an RNA virus that uses the transcription of its RNA into linear double-stranded DNA with subsequent integration into the host genome (Gelmann et al. 1983). HIV is able to infect new cells interacting with a CD4 receptor and one of two co-receptors on the surface of a CD4+ cell. CD4 is a receptor present on 60% of T-lymphocytes, T-cell precursor, monocytes, macrophages, eosinophils, dendritic cells and microglial cells of the central nervous system (Fauci and Lane 2006).

The HIV replication cycle can be divided into several stages. The attachment/uncoating process is firstly mediated by the interaction between the viral glycoprotein gp120 and the CD4 host receptor (Lundin et al. 1987). This interaction causes a conformational change in the gp120 that favours the binding to the coreceptor CCR5 and/or CXCR4, followed by a conformational change in the gp41 (Gallo et al. 2001). Subsequently the host and viral membrane fuse and the capsid is uncoated followed by release of its contents into the host cell. Reverse transcriptase mediates the reverse transcription of the viral RNA genome into proviral HIV DNA (Chandra et al. 1986). The process of reverse transcription begins in the cytoplasm as DNA synthesis is initiated from the transfer RNA primer bound to the viral genomic RNA just downstream of the 5' LTR. When the minus strand of DNA is completed the RNA is degraded by the viral ribonuclease H (Starnes and Cheng 1989). Unlike most retroviruses, which integrate into the host cellular DNA as the nuclear membrane is disrupted during cell division, HIV-1 can be imported into the nucleus and integrate into non dividing cells (Lewis et al. 1992). Integrase catalyses two separate chemical reactions: an initial 3′ processing of the nascent cDNA ends, which

is followed in the cell nucleus by their covalent attachment to the 5′ phosphates of a double-stranded staggered cut in chromosomal DNA. Integration does not appear to be site-directed. However, virus may preferentially integrate into or near two repeated DNA elements, L1 and Alu, that move throughout the genome as retrotransposons (Stevens and Griffith 1994).

Once integrated, the provirus is not transcribed and remains integrated in the host genome until cellular transcription factors, such NF-kB, start the transcription (Pazin et al. 1996). Proviral DNA is quiescient in CD4 T-cells and monocytes, macrophages and microgial cells which represent an important cellular reservoirs of HIV (Zhu et al. 2002). A cellular stimulus can cause the transcription of the host cell DNA and the HIV DNA. Transciption is mediated by host RNA polymerase using endogenous dNTPs and viral mRNA undergoes a splicing process that generates smaller mRNAs (Feinberg et al. 1986; Lightfoote et al. 1986). The viral mRNA is translated using host amino acids and ribosomes into viral polyproteins. Viral polyproteins are then cleaved by the HIV-protease: large gp160 precursor molecules are cleaved by the HIV-1 protease into gp120 and gp41 and the Gag and Pol proteins are also derived from a large 160 kD precursor molecule (Oroszlan et al. 1984). The formation of new viral particles is a stepwise process: two viral RNA strands associate with replication enzymes and core proteins and forms the virus capsid. This immature particle migrates towards the cell surface. During the budding process, the viral lipid membranes incorporate various host cell proteins that can include phospholipids and cholesterol (Katsumoto et al. 1990).

1.2. Natural History of HIV Infection

HIV infection can be divided into three phases: primary infection (acute infection), clinical latency phase and immunodeficiency syndrome, as shown in Figure 1.1.

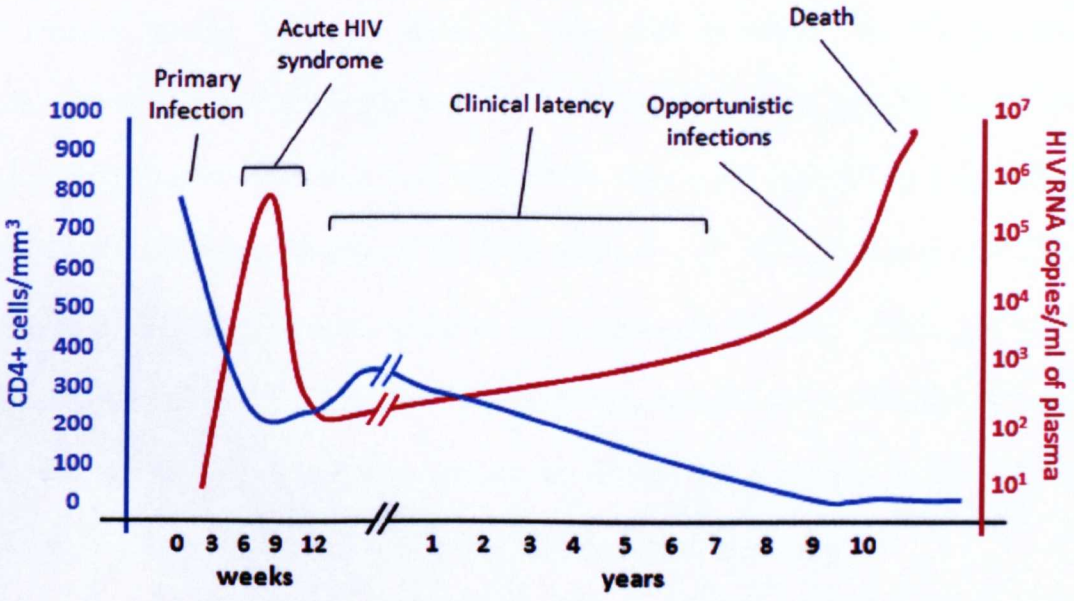

Figure 1.1. Variation of CD4 count and HIV RNA copies in plasma during the infection phases. Red line represent HIV vial load and blue line represent the CD4 count.

Primary acute infection is characterised by a transient symptomatic illness associated with an intense viral replication and high number of HIV RNA copies (Cooper et al. 1985; Daar et al. 1991). The HIV-specific immune response can reduce the plasma viremia and initially limit the evolution of the disease (Phillips 1996). However, the viremia at this stage is strongly correlated with the progression of the infection in the later stages of the infection (Ruffault et al. 1995)

During the clinical latency phase low HIV RNA copies can be found in plasma or in peripheral blood lymphocytes and, initially, the number of CD4+ cells stays constant or is only slightly decreased (Moss et al. 1988). Although the viremia is reduced during clinical latency, the virus is still detectable (Michael et al. 1992). After the initial peak of virus, the virus reaches a "set point", which predicts the time of onset of clinical disease. With set point less than 1000 copies/ml, the symptomatic syndrome usually has a latency period of more than 10 years. Most patients with more than 100,000 copies/ml, lose their CD4+ cells more rapidly and progress to AIDS before 10 years (Mellors et al. 1996; Mellors et al. 1997; Vlahov et al. 1998). Though no clinical signs and symptoms are apparent, the immune system, primarily through depletion of CD4 lymphocytes, deteriorates (Kaslow et al. 1987). Emergence of HIV infection from clinical latency is marked by a decline in the CD4+ lymphocyte count and an increase in viremia (Nicholson et al. 1989).

The last stage of the disease is characterised by immunodefiency syndrome and is marked by the appearance of one or more of the typical opportunistic infections (Mildvan et al. 1982). The progression to clinical AIDS is also marked by the appearance of syncytia-forming (SI) variants of HIV in approximately 50% of HIV-infected patients (Tersmette et al. 1988; Tersmette et al. 1989). These SI viral variants have greater CD4+ cell tropism and are temporally associated with a more rapid CD4+ cell decline (Schuitemaker et al. 1992). The development of signs and symptoms of AIDS typically occurs when the total CD4+ cell count falls below 200 cells/μl (Masur et al. 1989; Hanson et al. 1993).

1.3. Antiretroviral therapy

Worldwide, the total number of people accessing antiretroviral therapy at the end of 2009 was estimated to be more than 6 million (UNAIDS/WHO 2010). In low-and middle-income countries approximately 5 million patients were receiving antiretroviral therapy, more than 1.2 million more people than at the end of 2008. This represents a 30% increase in 1 year and a 10-fold increase in 5 years. The number of people receiving antiretroviral therapy in high-income countries is estimated to be at least 700,000, with approximately 385,000 patients in Europe and 300,000 patients in North America (UNAIDS/WHO 2010).

Highly Active Antiretroviral Therapy (HAART) is based on the co-administration of drugs from two or three different classes, aiming to inhibit multiple viral targets, maximising the inhibition of viral replication and reducing the risk of developing drug resistance. To date 6 classes of antiretrovirals are available: nucleoside/nucleotide reverse transcriptase inhibitors (NRTIs), non nucleotide reverse transcriptase inhibitors (NNRTI), protease inhibitors (PIs), fusion inhibitors, CCR5 antagonists and integrase inhibitors. Although the introduction of HAART has led to an intense decline in mortality and morbidity, therapeutic failure occurs in an estimated 8% of treatment naïve and 33% of experienced patients (Palella et al. 2006). Therapeutic failure is due to several factors such as a high rate of viral replication (with more than 10^9 virions produced daily) and the high error rate of the reverse transcriptase resulting in a high mutation rate. Host factors such as pharmacological variability and immunological characteristics are also important.

1.3.1. Nucleoside/Nucleotide Reverse Transcriptase Inhibitors (NRTIs)

There is structural diversity in the eight NRTIs that have been approved by regulatory agencies for HIV treatment. The viral reverse transriptase (RT) is a crucial enzyme in the viral life cycle and it has been one of the most active targets for drug discovery. The first antiretrovirals were inhibitors of this enzyme. RT catalyses the incorporation of endogenous deoxynucleotide triphosphates (dNTPs) into the forming DNA strand and the NRTIs act as competitive inhibitors. Once incorporated, NRTIs serve as chain-terminators of viral RT.

NRTIS can undergo hepatic metabolism; for example, zidovudine (AZT) is metabolised by UGT2B7 (Belanger et al. 2009). This class of antiretrovirals requires phosphorylation to 5'-triphosphates in order to become active, and this process occurs within the host cell and involves host kinases (Bazzoli et al. 2010). Activation of NRTIs is first dependent on cellular entry by passive diffusion or carrier-mediated transport. NRTIs have low membrane permeability and are hydrophilic molecules. Therefore, transporters such as the members of the equilibrative and concentrative families of nucleoside transporters play an important role in the cellular diffusion of NRTIs (Cass et al. 1999). NRTIs predominantly undergo renal excretion unchanged but some NRTIs are subject to catabolism, mainly depurination and depyrimidation (e.g zidovudine, didanosine, abacavir and stavudine). Mitochondrial toxicity is thought to underlie many NRTI-related adverse effects. In particular, the development of lipoatrophy and fat wasting or myopathy and cardiomyopathy (Cote et al. 2002).

1.3.2. Non Nucleoside Reverse Transcriptase Inhibitors (NNRTIs)

NNRTIs are noncompetitive inhibitors of RT with respect to primer-template and nucleoside triphosphate binding. These drugs bind directly to heterodimeric HIV-1 RT and appear to inhibit viral RNA- and DNA-dependent polymerase activities by disrupting the catalytic site of the enzyme. The NNRTIs are a class of potent antiretrovirals. One member of this class, efavirenz (EFV), is recommended as the first-line antiretroviral for naïve patients according to treatment guidelines (DHHS 2010). To date, four NNRTIs are currently approved for treatment of HIV infection. EFV and nevirapine (NVP) are predominantly used in treatment-naïve patients, while etravirine (ETV) is indicated for treatment-experienced patients. Due to its less favourable pill burden, dosing frequency, and adverse event profile, delavirdine is rarely used (DHHS 2010).

NNRTIs are generally characterised by favourable pharmacokinetics and rare major side effects but have a low genetic barrier to resistance. Most common toxicities for EFV are central nervous system side effects that can occur in the first weeks of treatment and in some cases cause treatment discontinuation (Fumaz et al. 2005). Treatment with NVP is associated with mild or moderate rash and in 1% of cases severe toxicity such as Stevens-Johnson syndrome, toxic epidermal necrolysis and hypersensitivity (Kontorinis and Dieterich 2003; Rivero et al. 2007). Moreover, symptomatic events involving the liver occur in around 5% of patients (Stern et al. 2003).

1.3.3. Protease Inhibitors (PIs)

HIV-1 protease inhibitors have had a major role in the chronic management of HIV disease, providing a very effective pharmacological tool that began a new era of therapy. PIs are typically characterised by use with dual NRTIs in regimens that were and are described as HAART. The PIs target the HIV protease enzyme, which mediates the cleavage of HIV precursor polyproteins into functional viral proteins, binding tightly to a peptide moiety in the catalytic pocket.

To date, nine PIs are available on the market (Table 1.1). Each PI has specific characteristics in terms of their side effects, potency and resistance profile. Therefore, patients can be treated with different PIs based on their infection status. PIs have unfavourable pharmacokinetics, with a very short half-life and extremely low plasma concentrations during the dose interval. This results from the activity of cytochrome P450 (CYP) isoform 3A4 (CYP3A4), the main enzyme responsible for their oxidation. Therefore, most PIs (with the exception of nelfinavir, fosamprenavir and atazanavir) have to be administered with an inhibitor of their metabolism and the only "booster" currently available is ritonavir (RTV). RTV was originally developed as an antiretroviral but was subsequently selected for its intense inhibitory effect on CYP3A4 (Eagling et al. 1997; Koudriakova et al. 1998). However, new boosters, such as cobicistat, that lack anti-HIV activity are currently under development (Mathias et al. 2010).

Table 1.1. Approved protease inhibitors

Active molecule	Drug Name	Year of market approval
Saquinavir	Invirase Fortovase	1995 1997
Ritonavir	Norvir	1996
Indinavir	Crixivan	1996
Nelfinavir	Viracept	1997
Amprenavir	Agenerase	1999
Lopinavir/Ritonavir	Kaletra	2000
Atazanavir	Reyataz	2003
FosAmprenavir	Lexiva	2003
Tipranavir	Aptivus	2005
Darunavir	Prezista	2006

1.3.4. CCR5 Inhibitors

HIV enters new cells by interacting with the CD4 receptor and a chemokine receptor such as CCR5 or CXCR4. CCR5 is the main co-receptor by which HIV infects cells. Maraviroc (MVC) effectively inhibits the interaction between HIV and CCR5, blocking HIV entry into the host cells. It is the only licensed CCR5-antagonist and standard dosing is 300 mg bid but its metabolic profile justifies dose adjustments when co-administered with other drugs. Specifically, with inhibitors of CYP3A4, such as RTV where the dose of MVC should be reduced to 150 mg bid (Abel et al. 2008; Abel et al. 2008). If co-administered with ETV, an inducer of CYP3A4, the dose of MVC should be increased to 600mg bid (Abel et al. 2008; Abel et al. 2008).

In several clinical studies MVC at standard doses was generally well tolerated over a year of treatment and the tolerability profile of MVC was broadly similar to that of placebo (Gulick et al. 2008; Pfizer Inc 2010). Upper respiratory tract infections, cough, pyrexia, rash and dizziness were the most common (>8% incidence) treatment-emergent adverse events (Gulick et al. 2008; Pfizer Inc 2010).

1.3.5. Integrase Inhibitors

Integrase inhibitors target the viral integrase enzyme, responsible for the integration of the viral DNA (generated by reverse transcription of the RNA genome) into the host cell genome. To date, raltegravir (RAL) is the only integrase inhibitor available and other integrase inhibitors, such as elvitegravir, will be licensed in the coming years (Prada and Markowitz 2010).

RAL is commonly administered 400 mg bid but has been proven to effectively inhibit viral replication even at lower doses in Phase I and II studies (Markowitz et al. 2006). Doses ranging from 10 to 1600 mg have been demonstrated to be safe and well tolerated (Iwamoto et al. 2008). In treatment-naive patients, pharmacokinetic parameters increased up to 400 mg with no further increase for the 600mg dose (Markowitz et al. 2006). Consequently, 400 mg twice daily was selected as the licensed dose (DHHS 2010). RAL is metabolised mainly in hepatic tissue by UDP-glucuronosyltransferase 1A1 (UGT1A1) to the RAL glucuronide (Kassahun et al. 2007). RAL was generally well tolerated in Phase II/III clinical trials (Markowitz et al. 2006). In the combined BENCHMRK studies, serious drug related adverse events occurred in 2.5% of patients treated with RAL. Moderate to severe adverse events

occurring in >2% of RAL-treated patients included diarrhea (4.3%), injection-site reactions probably attributable to concomitant use of enfuvirtide (2.8%), headache (2.6%) and nausea (2.4%) (Steigbigel et al. 2008).

1.4. Pharmacokinetics of antiretrovirals

1.4.1. Main pharmacokinetic variables

Pharmacokinetics is the study of what the body does to administered foreign compounds. One of the main biological matrixes analysed in pharmacokinetic studies is plasma, because it is easily obtainable and represents a marker for global exposure to a drug. This is the case for antiretrovirals despite most antiretrovirals acting inside cells. The exposure to drugs is commonly measured through three different variables. C_{max} is the maximum concentration achieved during the dose interval, C_{trough} is the concentration reached just before the next dose and Area Under the Curve (AUC), is the area under the plot of plasma concentration of drug against time after drug administration.

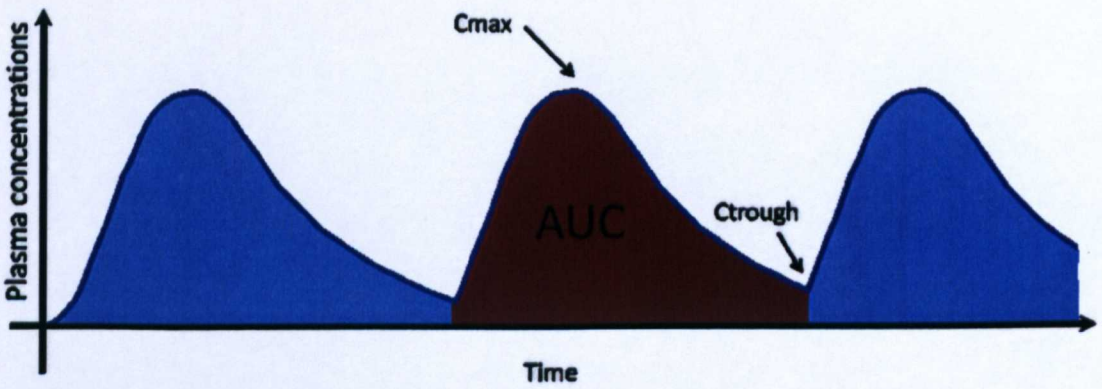

Figure 1.2. Example of pharmacokinetic profile: C_{max}, C_{trough} and AUC are indicated.

C_{avg} is another measure of exposure and represents the average concentrations during the dose interval and is normally calculated from the area under the plasma concentration-time curve during a dosing interval divided by time (AUC/T). Moreover C_{all}, the geometric mean of all sparse plasma concentrations, regardless of time of collection is another marker of exposure. However this does not represent a precise measurement, since it does not take into account the effect of time on concentrations, and therefore the use of other pharmacokinetic variables is preferable.

1.4.2. Pharmacokinetic/Pharmacodynamic (PK/PD) relationship

Heterogeneity in the response to antiretroviral agents has been attributed to multiple factors, such as adherence to therapy, characteristics of the virus, immunological status, and pharmacokinetic exposure to antiretrovirals. All of these factors which are characterised by a large inter-patient variability. A PK/PD relationship is evident for viral suppression and has been demonstrated for a broad number of antiretrovirals. However, plasma exposure does not always explain the variability observed in side effects.

Antiretroviral plasma exposure has been investigated in many clinical trials and its influence on viral suppression is widely recognised (DHHS 2010). For drugs with a low genetic barrier, for which a single mutation can cause high level resistance (e.g. NNRTIs), PK has a direct correlation with efficacy. However, for PIs resistance involves several mutations having a cumulative effect and PK cannot be considered as an independent predictor of efficacy. In this case PK needs to be interpreted in the context of viral resistance data and drug concentrations can be used to calculate the

inhibitory quotient (IQ). IQ validation for newer drugs such as RAL and MVC has not been finalised and therefore utility of its clinical application is not yet clear (la Porte 2008).

To represent resistance, viral phenotypic and genotypic data can be used to calculate the IQ. Genotypic inhibitory quotient (gIQ) is the ratio of C_{trough} to the number of mutations conferring resistance, derived from a genotypic resistance test. When phenotypic resistance data are used C_{trough} is related to the 50% *in-vitro* inhibitory concentration (IC_{50}), giving the phenotypic inhibitory quotient (PIQ). IQ cut-off values have been successfully identified for fosAPV, 300 ng/ml/mutation for gIQ and 1 PIQ (Pellegrin et al. 2007); ATV, 100ng/ml/mutation for gIQ (Pellegrin et al. 2006); DRV, 600ng/ml/mutation (Gonzalez de Requena et al. 2011); LPV, 90 ng/ml/mutation (Hoefnagel et al. 2006). An example of the probability of virological failure based on gIQ cut-off for DRV/r is represented in Figure 1.3.

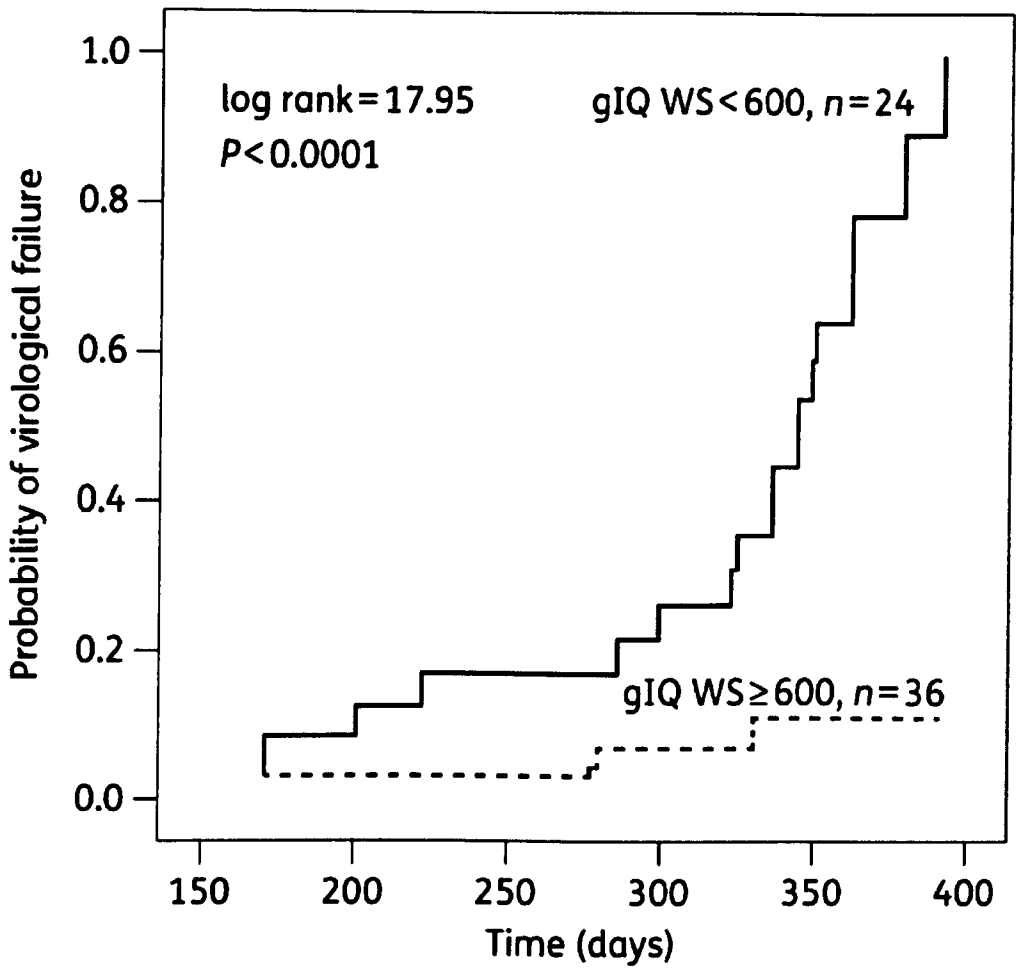

Figure 1.3. Kaplan–Meier curve for the time of maintenance of virological response over 48 weeks. The probability represents the proportion of patients treated with DRV/r who presented virological failure according to qIQ in respect of the 600 ng/ml/mutation cut-off (Gonzalez de Requena et al. 2011).

Variability in IQ can be influenced by the set of mutations considered in the analysis and complete standardisation of this PK/PD measure is therefore essential prior to widely accepted clinical application (la Porte 2008; Gonzalez de Requena et al. 2011).

1.4.3. Pharmacokinetic/Pharmacodynamic (PK/PD) relationship

1.4.3.1. Efavirenz

EFV PK/PD has been investigated in numerous clinical studies of efficacy or side effects. There is not a perfect homogeneity in the available literature but some interesting trends have been described. In 2001, Marzolini *et al* described an association between EFV plasma exposure, probability of virological suppression and side effects in 130 patients (Marzolini et al. 2001). Unfortunately, this study had some limitations. Firstly the majority of patients had tolerated EFV for at least twelve weeks, underestimating the development of side effects in the first three to four weeks of treatment. Also, some patients were concomitantly treated with boosted protease inhibitors, although the description of treatment history was limited. Adherence was not assessed, concentrations were measured for a broad range of time after dose, viral load was measured with an older standard (viral load > 400 copies/ml) and the definition of side effect was not rigorous. Despite these limitations, a clear association between EFV plasma exposure and efficacy was observed. Patients with EFV concentrations from 8 to 20 hours below the cut-off of 1000 ng/ml had a much higher probability of therapeutic failure (50%) compared to patients with higher EFV concentrations (20-25%). Moreover, CNS toxicity was observed in 24% of patients with efavirenz concentrations > 4000 ng/ml and in only 9% with concentrations 1000 - 4000 ng/ml. Therefore, a range of mid-interval drug levels (1000 - 4000 ng/l) was proposed according to toxicity and efficacy in viral suppression (Marzolini et al. 2001).

Regarding efficacy, similar conclusions were made in other clinical studies on 235 patients (Csajka et al. 2003), on 68 patients (Stahle et al. 2004) and on 300 patients

(Leth et al. 2006). However, in a more recent study of 71 patients (3 of which had therapeutic failure) this was not replicated (Josephson et al. 2010). The small sample size of non-responders in this latter study is one of the main reasons for the inconsistency with respect to efficacy. For neuropsychiatric side effects a correlation with high plasma exposure was not confirmed in all studies and a clear description of the PK role in the definition of CNS side effects has not yet been finalised.

1.4.3.2. Maraviroc

MVC is a clear example of a drug for which a correlation between plasma exposure and suppression of viral replication has been demonstrated. MVC blocks the CCR5 receptor, which is used by HIV to enter CD4+ cells. Consequently, on a theoretical level higher concentrations of MVC will occupy a higher proportion of CCR5 receptors and thereby block the penetration of HIV into CD4+ cells with higher efficacy. This effect was clearly observed in the monotherapy investigation, where 44 patients received maraviroc under food restrictions at 25 mg once daily, 50, 100, or 300 mg twice daily, or placebo for 10 days in a randomized, double-blind, placebo-controlled, multicenter study (Rosario et al. 2006). The mean log10 viral load declines from baseline to day 11 for placebo, 25 mg once daily, 50 mg twice daily, 100 mg twice daily and 300 mg twice daily were 0.02 [range: -0.45 to 0.56], -0.43 [range: -1.08 to 0.02], -0.66 [range: -1.37 to 0.40], -1.42 [range: -1.84 to -1.04], and -1.60 [range: -2.42 to -0.78], respectively (Rosario et al. 2006). This dose dependent effect was subsequently confirmed to be correlated with plasma exposure and was demonstrated also for more commonly used combination therapies where MVC was co-administered with other antiretrovirals agents. Results of the MOTIVATE 1-2 study highlighted a good association of MVC C_{trough} and C_{avg} with

probability of virological failure (>50 copies/ml). As shown in Figure 1.4, higher MVC plasma exposure is correlated with lower probability of virological failure.

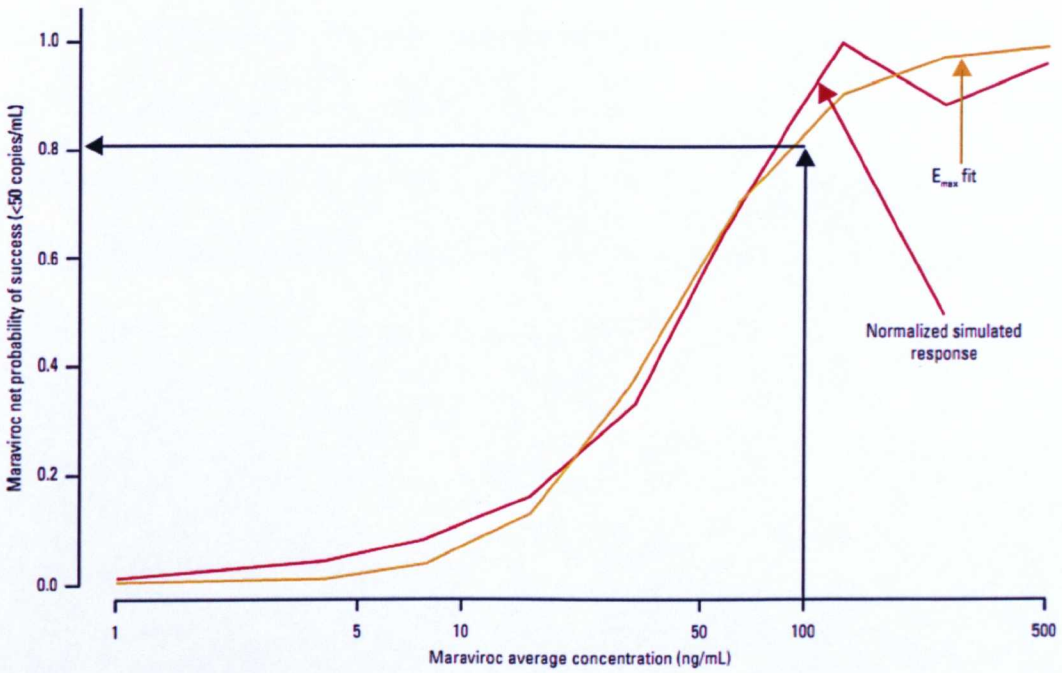

Figure 1.4. MVC net virological success rate versus Cavg. The probability represents the proportion of patients treated with MVC who with presented virological success (<50 copies/ml) and MVC plasma concentrations (McFadyen et al. 2007).

Two cut-off values have been proposed for MVC with C_{trough} above 50 ng/ml or C_{avg} above 100 ng/ml having a higher probability of viral suppression (McFadyen et al. 2007). This PK/PD analysis indicates that factors lowering plasma concentrations below the cut-off should be investigated in order to reduce the risk of therapeutic failure. MVC is therefore a good candidate for Therapeutic Drug Monitoring in patients at high risk of low plasma concentrations.

1.4.3.3. Raltegravir

RAL PK/PD is complicated. Several clinical studies initially showed an equal response even for a broad range of doses. RAL was initially tested in 35 HIV infected treatment naive patients receiving monotherapy at four dose levels (100, 200, 400, or 600 mg twice daily) with a matching placebo administered orally, without regard to food. As shown in Figure 1.5 the four groups had a comparable viral suppression resulting in an approximately 2.0 log10 reduction in plasma HIV-1 RNA levels after 10 days (Markowitz et al. 2006).

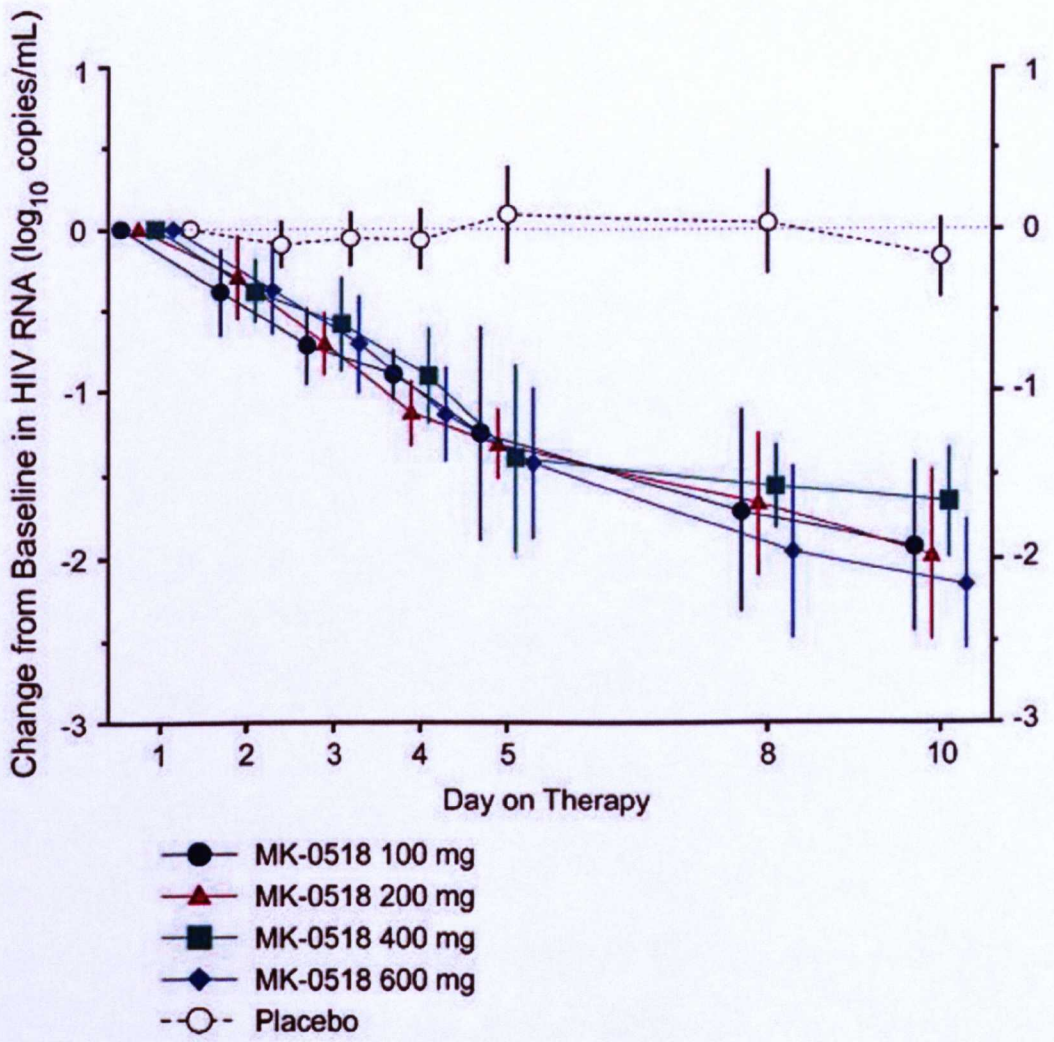

Figure 1.5. Change in log10 HIV RNA after 10 days therapy with RAL (with 95% CI). Error bars indicate 95% CIs. Data for a total of 7 patients (from 4 of the 5 treatment groups) were not available on day 5 (Markowitz et al. 2006).

Safety and efficacy of RAL have also been evaluated in combination therapy with TDF and 3TC in treatment naive and treatment-experienced HIV-1–infected patients (Grinsztejn et al. 2007; Markowitz et al. 2007). In both these studies the range of doses under investigation gave similar results and for naive-patients RAL achieved HIV-1 RNA levels below detection at a more rapid rate compared to EFV. As shown in Figure 1.6 achievement of virological suppression was comparable in the four dose groups and significantly faster compared to an EFV standard regimen.

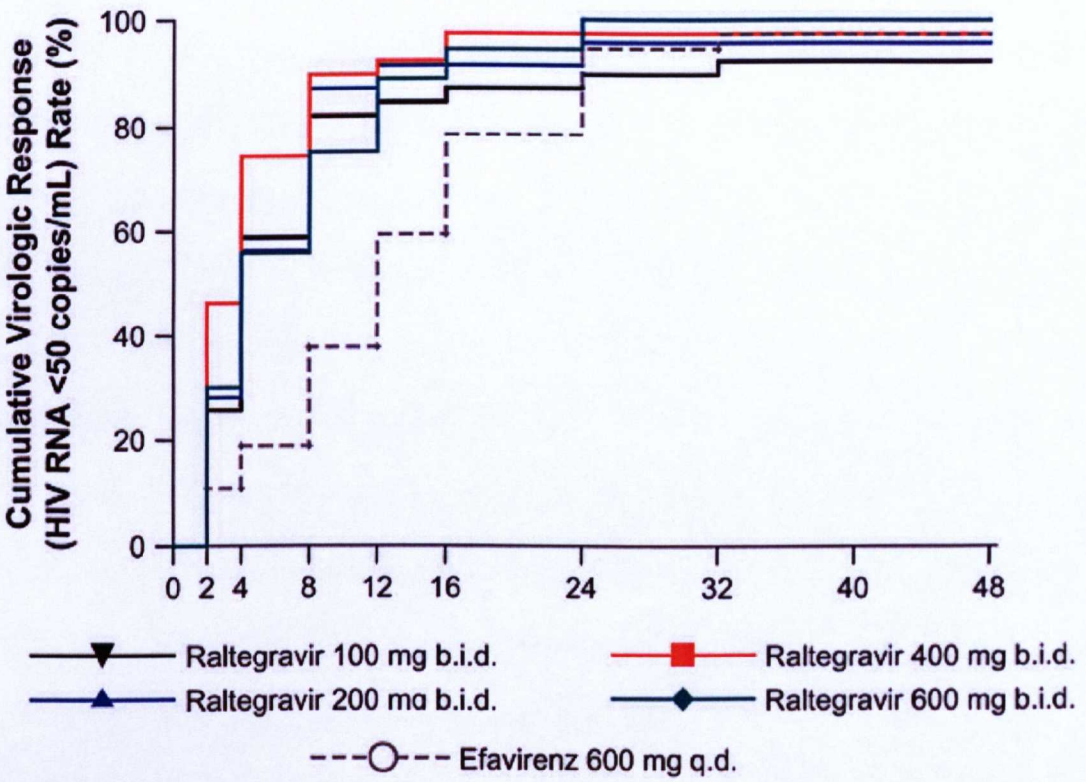

Figure 1.6. Efficacy outcomes through week 48; time to achieve an HIV-1 RNA level <50 copies/ml (Markowitz et al. 2007).

For treatment experienced patients, the relationship between C_{all} (the geometric mean of all sparse raltegravir plasma concentrations, regardless of time of collection) and suppression was less predictive of outcome than other covariates such as use of other active agents in optimised background therapy (OBT) and HIV RNA at baseline

(Wenning et al. 2008). Therefore, the relationship between RAL concentrations and outcome appears to fall near the end of the concentration–response curve for most patients. Consequently, the PK/PD relationship for RAL was temporarily thought to be less relevant than other factors. The clinical pharmacology of this drug was therefore focused on other issues such as drug-drug interactions and correct management of RAL administration in special populations.

Protocols for dose reduction and simplification of RAL have been developed that take into consideration its potency and its hypothetical clinical use as a first line treatment. A promising simplification strategy appears to involve a once daily regimen doubling the dose to 800mg + NRTIs (FTC and TDF, similarly to ATRIPLA). The results for the qid dosage study (QDMRK) showed high virological response rates and good immunologic effects for both bid and qid RAL in combination with TDF/FTC (Eron et al. 2011). However, for patients with baseline HIV-RNA above 100,000 copies/ml a higher failure rate was recorded [53 of 382 (13.9%) and 35 of 388 (9.0%) in the once-daily and twice-daily groups, respectively] (Eron et al. 2011). Moreover, nine patients from the once-daily vs two patients from the twice-daily groups, experienced virological failure with integrase (and FTC) - resistant virus. Interestingly, in the once daily arm higher C_{trough} and C_{all} were associated with a greater probability of treatment success and in the lowest C_{trough} quartile group the response rate was statistically lower compared to the other three quartiles [80% vs >90%] (Eron et al. 2011). RAL plasma exposure, which initially was thought to be unimportant was the main cause of failure in this simplification study, and a major obstacle for future development of a RAL qid.

1.5. Absorption, Distribution, Metabolism and Elimination (ADME)

Antiretroviral plasma concentrations (as for other drugs) are influenced by numerous absorption, distribution, metabolism and elimination processes which can take place in several tissues and are mediated by many proteins and therefore genes (summarised in Figure 1.7).

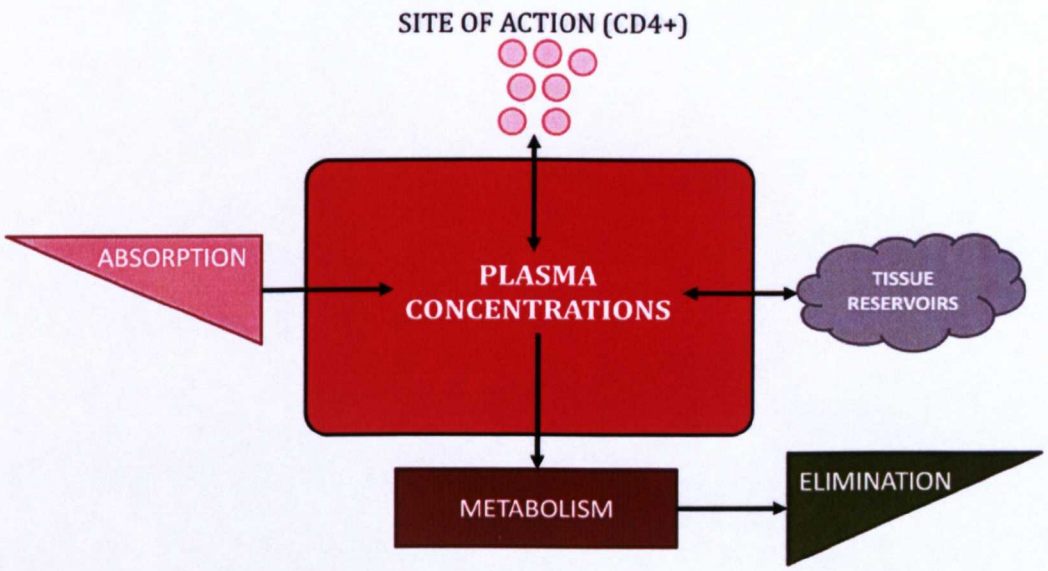

Figure 1.7. Schematic representation of ADME. 9

1.5.1. Genes regulating intestinal absorption

Most antiretrovirals are administered orally and therefore the first stage in absorption involves intestinal tissue. The small intestine represents the principal site of absorption for any ingested xenobiotic whether dietary, therapeutic or environmental and is a critical factor in the determination of overall bioavailability. Enterocytes constitute a selective barrier to drugs and the activity of this barrier is strictly regulated by specific membrane transport systems and metabolic enzymes. Several

lipophilic orally administered drugs undergo passive diffusion into enterocytes or are specifically transported into enterocytes by uptake transporters such as solute carrier organic anion (SLCO) isoforms (Kobayashi et al. 2003). Drugs can also be substrates for apical efflux transporters which can mediate their extrusion into the intestinal lumen (Evers et al. 1998; Walgren et al. 2000). ATP-binding cassette (ABC) transporters such as ABCB1, ABCC2 and ABCG2 are the main apical efflux transporters involved in the intestinal absorption. Moreover the apical efflux transporters can secrete other compounds that are already present in the blood stream. Other efflux transporters such as ABCC1 and ABCC3 can mediate the passage of substrates towards the blood (Lagas et al. 2009). As well as efflux pumps, the transcellular route of absorption exposes drugs to intracellular metabolic enzymes and in the intestinal tissue represents the first site for CYP mediated metabolism (Thelen and Dressman 2009).

1.5.2. Genes regulating hepatic metabolism

Antiretrovirals that escape intestine metabolism or efflux pass into the blood stream and on to the liver via the portal system. They can then be subject to further metabolism and biliary excretion, by a similar system of enzymes and transporters to that present in the intestine. Xenobiotics can diffuse across the basolateral membrane of hepatocytes by passive diffusion or by active transport, mainly mediated by SLCO1B1 and secondarily by SLCO1B3 and SLCO1A2 (Hartkoorn et al. 2010).

SLCO1B1 (also known as OATP2, OATP-C and LST-1) is encoded by the *SLCO1B1* gene and it is a key hepatic uptake transporter. SLCO1B1 is principally expressed on the sinusoidal membrane of hepatocytes but SLCO1B1 mRNA has also

been detected in other tissues, including small intestine (Glaeser et al. 2007). SLCO1B1 is a 691 amino acid protein and has a broad range of endogenous and exogenous substrates. Endogenous substrates include bile acids (cholate and taurocholate), conjugated steroids (estradiol-17b-glucuronide, estrone-3-sulfate and dehydroepiandrosterone-3-sulfate), eicosanoids (leukotrienes C4 and E4, prostaglandin E2 and thromboxane B2) and thyroid hormones (thyroxine and triiodothyronine) (Abe et al. 1999; Hsiang et al. 1999; Tamai et al. 2000). Numerous classes of drugs have also been identified as SLCO1B1 substrates, including HMG-CoA reductase inhibitors, statins, angiotensin-converting enzyme (ACE) inhibitors, and angiotensin II receptor antagonists (Katz et al. 2006; Pasanen et al. 2006; Kohlrausch et al. 2010) and PIs (Hartkoorn et al. 2010).

A large number of SNPs and other sequence variations have been described in the *SLCO1B1* gene, and their allele frequencies vary between different populations (Tirona et al. 2001; Pasanen et al. 2008). At least three SNPs in the *SLCO1B1* gene have been correlated with clinical outcome or alteration of pharmacokinetics, -11187G>A, 388A>G (rs2306283, Asn130Asp), and 521T>C (rs4149056, Val174Ala). Two functional SNPs, 521T > C and 388A > G have been reported in *SLCO1B1* and collectively define four haplotypes: *SLCO1B1*1A* (388A-521T, reference allele), **1B* (388G-521T), **5* (388A-521C) and **15* (388G-521C). In several *in vitro* studies the haplotypes **5* and **15* have been associated with a reduced activity using a wide range of substrates. Both haplotypes contain the 521C allele. Therefore this polymorphism appears to have a predominant effect and this has recently been demonstrated (Kameyama et al. 2005). The 521T>C polymorphism has previously been correlated with increased plasma concentrations of atrasentan,

fexofenadine, simvastatin acid, pitavastatin, atorvastatin, rosuvastatin, pravastatin and lopinavir (Niemi et al. 2004; Katz et al. 2006; Pasanen et al. 2007; Hartkoorn et al. 2010; Kohlrausch et al. 2010).

The hepatic tissue is the main site of Phase I and II metabolism of all antiretrovirals except NRTIs (which are phosphorylated). CYPs are highly expressed in hepatocytes and mediate the transformation of a broad range of substrates, both endogenous and exogenous. The nomenclature of this class of genes is based on a number indicating the gene family (>40% of amino-acid homology), a letter indicating the subfamily (55% of amino-acid homology) and a number for the gene (Nelson et al. 1996). The CYPs in families 1–3 are responsible for 70–80% of all phase I dependent metabolism of clinically used drugs (Bertz and Granneman 1997; Evans and Relling 1999). As shown in Figure 1.8 CYP3A4/5 is the most abundant isoform in the hepatic tissue and is responsible for the catabolism of a high number of therapeutic agents, including all PIs and MVC (Koudriakova et al. 1998; Hyland et al. 2004; Walker et al. 2005). NNRTIs are mainly metabolised by CYP2B6 but other isoforms such as 1A2, 2A6, 2D6 and 3A4 can account for up to 30% of their metabolism (Erickson et al. 1999; Faucette et al. 2007; di Iulio et al. 2009; Ogburn et al. 2010).

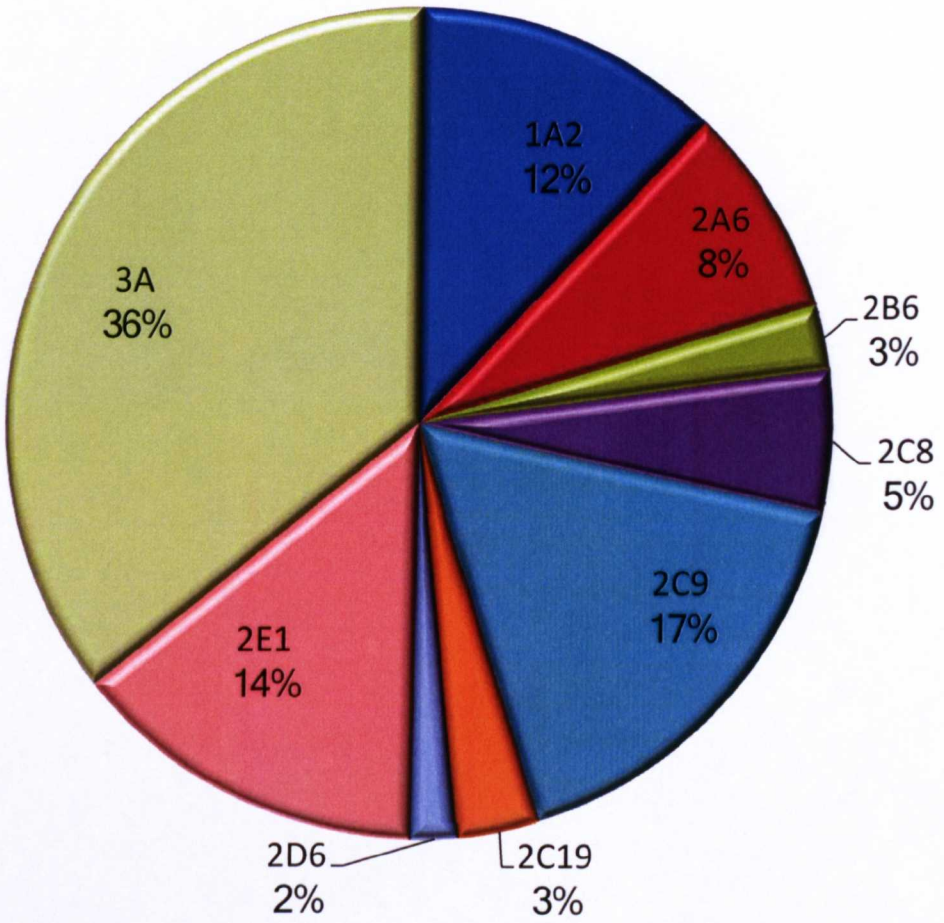

Figure 1.8. Relative amount of the hepatic human CYPs in liver (Rowland Yeo et al. 2003).

EFV metabolism is summarised in Figure 1.9, CYP2B6 is the main enzyme metabolising EFV into 8-hydroxy EFV, the most abundant metabolite with a minor contribution of CYP1A2 and CYP3A4/5 (Ward et al. 2003). The transformation to 7 hydroxy EFV is mainly mediated by CYP2A6 (Ogburn et al. 2010). Moreover, UDP-glucuronosyltransferase (UGT) 2B7 has recently been identified as the main enzyme involved in EFV N-glucuronidation (Belanger et al. 2009).

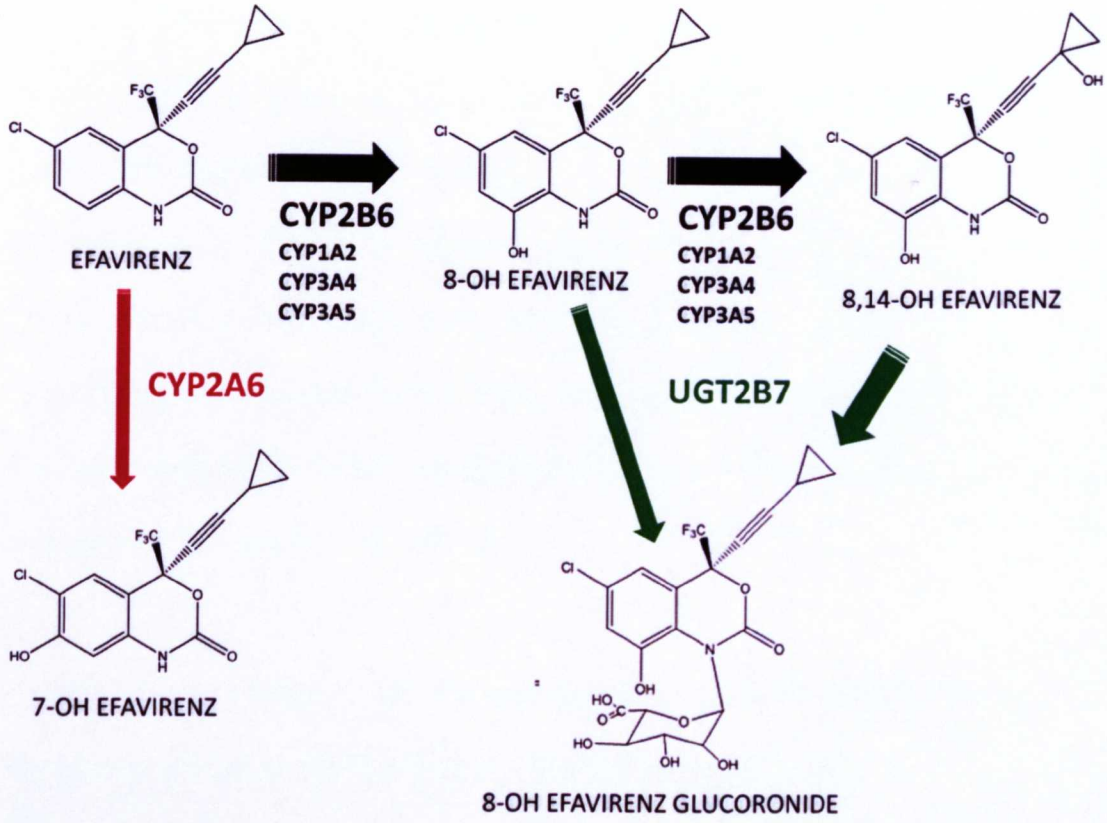

Figure 1.9. Schematic of EFV metabolism. Main metabolism pathway is represented by a black arrow and secondary pathway by red and green.

A number of studies have shown that the 516G>T (rs3745274) and 983 T>C (rs28399499) SNPs in the *CYP2B6* gene are associated with EFV plasma concentrations (Klein et al. 2005; Rotger et al. 2005; Saitoh et al. 2007; Mahungu et al. 2009). More recently studies have also demonstrated that in the presence of defective CYP2B6 metabolism, there is a significant association between EFV exposure and *CYP3A4*, *CYP2A6* and *UGT2B7* genetic variants (Arab-Alameddine et al. 2009; Kwara et al. 2009). These findings illustrate the simultaneous effects of major and minor metabolic pathways and their genetic variants on EFV pharmacokinetics.

Phase II metabolism represents an important step in the elimination of some antiretrovirals in hepatic tissue. RAL is mainly metabolised by UDP-glucuronosyltransferase (UGT) isoforms 1A1 and secondarily by 1A9 and 1A3 (Kassahun et al. 2007). As indicated above UGT2B7 mediates the secondary metabolism of EFV (Belanger et al. 2009). Metabolised or unaltered molecules are subsequently extruded into the bile ducts and secondarily into the intestine by active transport mediated by several transporters including members of the ABC family such as ABCB1, ABCC2 and ABCG2.

Another class of proteins which can play an active role in the ADME processes are the nuclear receptors (NRs). NRs are a broad set of transcription factors whose primary function is to recognise exogenous or endogenous toxic substances and to activate the detoxification pathways, increasing the expression of several proteins. In the liver and intestine the main regulators of the phase I and II metabolism and transporters are the constitutive androstane receptor (CAR; *NR1I3*) and the pregnane-X receptor (PXR; *NR1I2*). PXR and CAR expression is also regulated by other nuclear receptor such as PPAR, LXR and HNF4α (Iwazaki et al. 2008; Lim and Huang 2008). It is well established that PXR and CAR regulate metabolism and elimination of many xenobiotics and endogenous compounds by inducing CYPs, primarily CYP3A and CYP2B isoforms, respectively (Waxman 1999). They also regulate glutathione–S-transferases (GSTs), UDP-glucuronosyltransferases (UGTs) and sulfotransferase (SULTs) (Alnouti and Klaassen 2008; Knight et al. 2008; Mackenzie et al. 2010). PXR can also induce the expression of transporters such as ABCB1, ABCC1 and 2 and SLCOs (Geick et al. 2001; Hagenbuch et al. 2001; Synold et al. 2001; Kast et al. 2002).

PXR is encoded by the nuclear receptor subfamily 1, group I, member 2 (*NR1I2*) gene which is located at 3q12–q13.3 and consists of 9 exons. Exons 2–9 contain the coding region for a 434 amino acid protein (Zhang et al. 2001). PXR is resident in the cellular cytoplasm and upon binding to ligands, it translocates to the nucleus, heterodimerises with the 9-cis retinoic acid receptor (RXR) and binds as a complex to regulatory regions of target genes. Upon release of co-repressor proteins and the recruitment of co-activators, there is a transcription stimulation of several genes involved in the xenobiotic metabolism and elimination, such as ABCB1, CYPs and SLCOs as shown in Figure 1.10 (Woods et al. 2007).

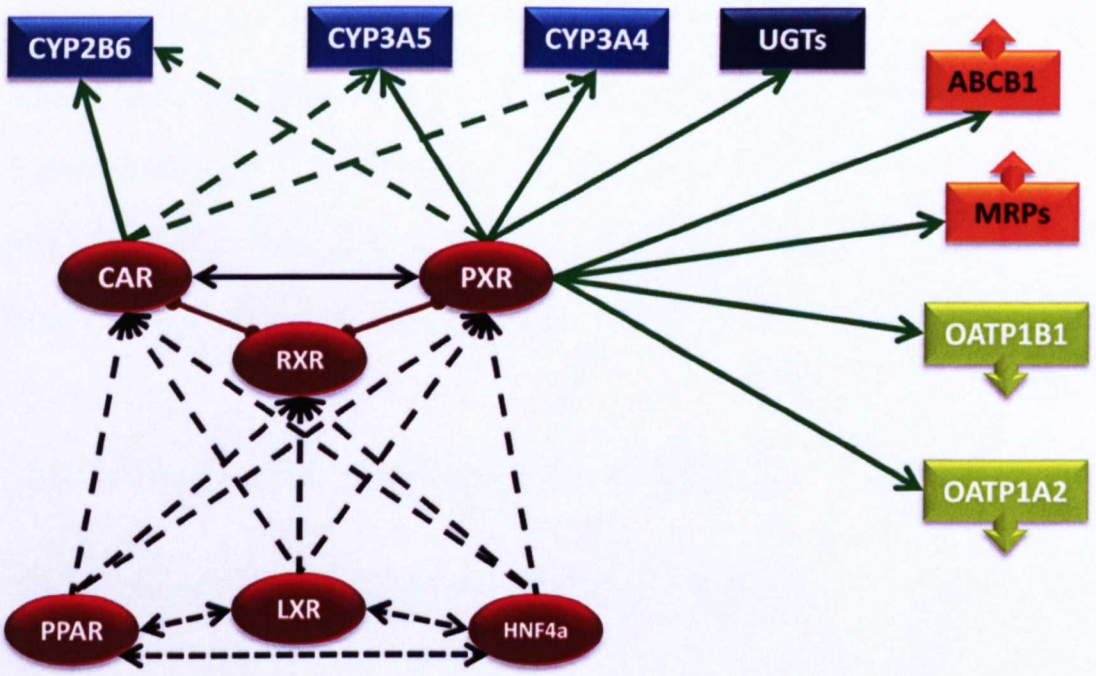

Figure 1.10. Regulatory networks controlled by PXR reveal induction or direct regulation of a number of phase I and II enzymes and transporters.

Several studies have scanned for polymorphisms in the regulatory and coding regions of *PXR*. Polymorphisms in the promoter, DNA binding domain, and ligand binding domain regions of the *PXR* gene have been reported to have significant functional

consequences (Hustert et al. 2001; Zhang et al. 2001; Woods et al. 2007; Lamba et al. 2008). The key activity of PXR in the regulation of metabolism and drug transport means that it is also involved in clinical drug–drug interactions (Amacher 2010). Most of the genes regulated by PXR have a broad range of substrates and their induction is potentially capable of affecting the metabolism and clearance of co-consumed drugs. Rifampicin is a potent PXR agonist and has been proven to be prone to drug–drug interactions with several classes of drugs including NNRTI, PIs and CCR5 inhibitors (Chen and Raymond 2006; Maartens et al. 2009).

Recently, three polymorphisms, 44477T>C (rs1523130), 63396C>T (rs2472677), 69789A>G (rs763645), were reported in the regulatory regions, which can alter the expression of PXR and the activity of CYP3A4 in primary hepatocytes and liver. The T allele for the 44477T>C SNP and the G allele for the 69789A>G were correlated with a lower *PXR* and *CYP3A4* expression whereas the T allele for 63396C>T was associated with higher expression of *PXR* (Lamba and Lamba et al. 2008).

1.5.3. Genes regulating transport into tissues

A key subsequent stage in ADME is the distribution of antiretrovirals into peripheral tissues and their site of action. Penetration of antiretrovirals into the central nervous system (CNS) which is a major site of HIV replication, is limited by the blood–brain barrier (BBB) (Varatharajan and Thomas 2009) and antiretrovirals have been classified into three major groups (low penetration, intermediate penetration, higher penetration) based on their high cerebrospinal fluid (CSF) penetrations, as shown in Table 1.2 (Letendre et al. 2008).

Table 1.2. Antiretrovirals penetration in to CSF (Letendre et al. 2008).

Drug Class	0: Low Penetration	0.5: Intermediate Penetration	1: Higher Penetration
Nucleoside/nucleotide reverse transcriptase inhibitors	ddC (zalcitabine; Hivid [discontinued]) ddI (didanosine; Videx) tenofovir (Viread)	d4T (stavudine; Zerit) 3TC (lamivudine; Epivir) emtricitabine (Emtriva)	AZT (zidovudine; Retrovir) abacavir (Ziagen)
Non-nucleoside reverse transcriptase inhibitors		efavirenz (Sustiva)	nevirapine (Viramune) delavirdine (Rescriptor)
Protease inhibitors	nelfinavir (Viracept) ritonavir (Norvir) saquinavir (Invirase, boosted or unboosted) tipranavir/ritonavir (Aptivus)	unboosted amprenavir (Agenerase [discontinued]) unboosted fosamprenavir (Lexiva) atazanavir (Reyataz, boosted or unboosted) unboosted indinavir (Crixivan)	amprenavir/ritonavir fosamprenavir/ritonavir indinavir/ritonavir lopinavir/ritonavir (Kaletra)
Entry inhibitors	enfuvirtide (T-20; Fuzeon)		

Several transporters are expressed on the BBB and a complex interplay between efflux and uptake transporters determine antiretroviral diffusion into CSF. ABC transporters are thought to be crucial in the protection of the brain: ABCB1, ABCC1, ABCC2, ABCC4 and ABCC5 cooperate to extrude substrates from the brain into the blood stream (Varatharajan and Thomas 2009).

Although plasma concentrations are used clinically as a marker of drug exposure, antiretrovirals act within HIV infected cells and therefore intracellular concentrations may be a better correlate of therapeutic efficacy. Consequently, the characterisation of transporters involved in the transport of antiretrovirals into peripheral blood mononuclear cells (PBMC) is an important field of research. To date, the factors that define antiretroviral passage into PBMC are not fully characterised (Bazzoli et al. 2010). Intracellular pharmacokinetics have been studied in more detail for PIs than other antiretrovirals and their penetration is influenced by the physiochemical characteristics, being higher for lipophilic compounds such as nelfinavir and saquinavir (Ford et al. 2004). Furthermore, antiretroviral penetration into PBMC can

be influenced by the interplay of several efflux and influx transporters. ABCB1, ABCC1 and ABCC2 are key efflux transporters expressed on PBMC and have a broad range of substrates ranging from anticancer drugs and immunosuppressive agents to antibiotics and antiretrovirals (Chan et al. 2004). To date, only one member (3A1) of the SLCO family has been identified on PBMC (Adachi et al. 2003).

Antiretrovirals might undergo intracellular metabolism in PBMC. CYP isoforms are expressed in PBMC, including CYP3A4 and 2B6 (Liptrott et al. 2008; Liptrott et al. 2009). The degree of metabolism in PBMC is not fully characterised but the intracellular pharmacokinetic variability observed between patients can be partially explained by the interplay of efflux/influx transporters and metabolic enzymes. Moreover, NRs can regulate metabolic enzymes and transporter expression in lymphocytes. Several studies indicate that expression of transporters, such as ABCC1, ABCC2, ABCB1 and CYPs are directly correlated with PXR expression suggesting an effect of PXR on the regulation of these proteins basal expression (Owen et al. 2004; Albermann et al. 2005). The interplay of transporters, CYPs and PXR expressed on PBMC is represented in Figure 1.11.

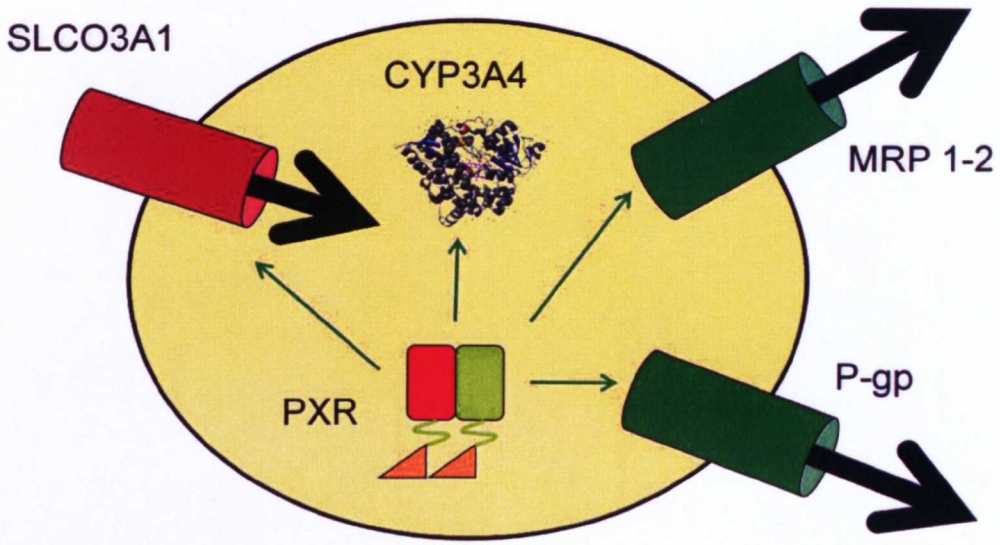

Figure 1.11. Schematic representation of uptake and efflux transporters that may influence intracellular concentrations of antiretroviral drugs in peripheral blood cells.

1.6. Strategies for the investigation of Pharmacokinetics/ Pharmacogenetics

Genetic polymorphisms in genes coding for proteins involved in ADME processes account for part of the inter-individual variability in antiretroviral pharmacokinetics. Although other factors might affect pharmacokinetics, including age, organ function, drug interactions, disease states, it is estimated that genetics can account for different proportions of inter-patient variability in drug disposition and efficacy (Kalow et al. 1999). An example of this is warfarin-based treatment, where CYP2C9 genetic factors can explain between 13% and 22.5% of the maintenance dose requirement (Caldwell et al. 2007; Sangviroon et al. 2010). For efavirenz, CYP2B6 516 G>T accounts for 45% of the total pharmacokinetic variability and other genetic factors

such as CYP2A6*9 and UGT2B7*1A might explain 10% of the remaining interpatient variability (Kwara et al. 2009). Polymorphisms do not usually independently influence pharmacokinetics because plasma concentrations usually result from several processes mediated by numerous proteins. Consequently, multiple polymorphisms in many human genes may affect pharmacokinetics and pharmacogenetic studies should take into account the interplay between genetics factors.

As summarised in Figure 1.12, two main strategies have been applied to identify the influence of genetic variants on pharmacokinetics. Candidate gene studies are based on *in-vitro* investigation of molecular mechanisms responsible for phenotypes and may be referred to as a "Bottom-Up" approach. Conversely, genome wide association studies (GWAS) involve hypothesis-free identification of specific genetic determinants of phenotypes and are based on a scan of genetic markers across the whole genome or exone. These may be defined as "Top-Down" approaches. Irrespective of the strategy used, all pharmacogenetic associations need to have biologically plausible mechanisms and need to be replicated in multiple cohorts.

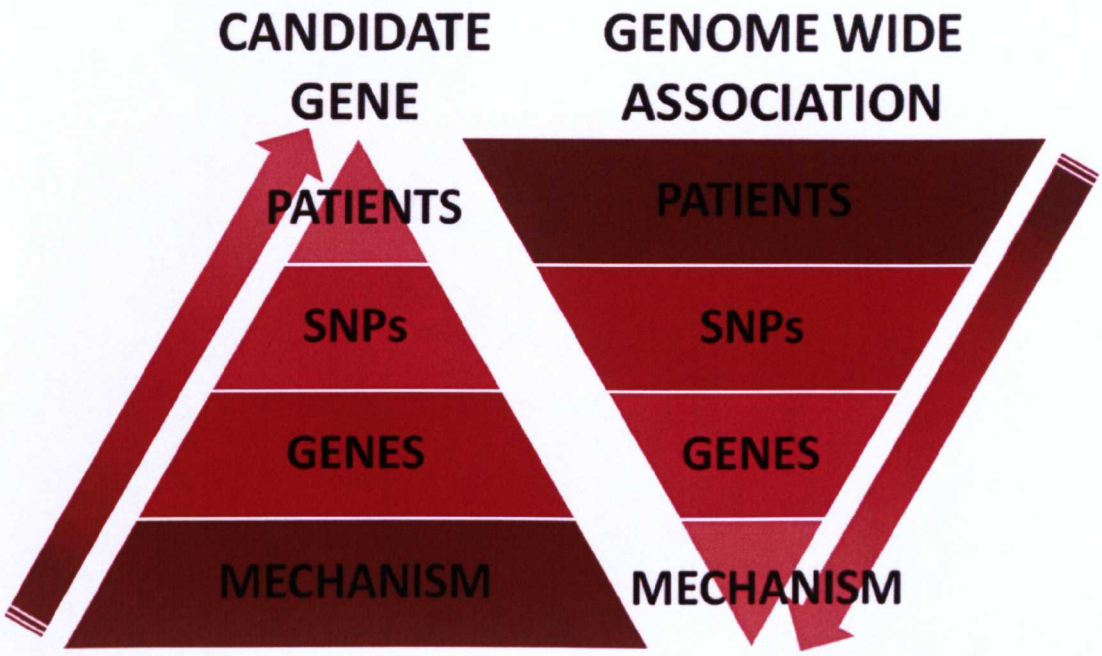

Figure 1.12. Schematic representation of gene candidate approach vs GWAS

1.6.1. Candidate Gene Studies

Candidate gene studies require a comprehensive knowledge of individual elements of ADME on a drug-specific basis which is then used to identify a hypothesis for the cause of variability. If biological mechanisms responsible for ADME are sufficiently clarified, genes coding for involved proteins can be scanned for genetic variants and pharmacogenetic associations can be elucidated in selected patient cohorts. Because a low number of SNPs are selected in candidate gene studies, the number of patients that need to be included in order to obtain sufficient statistical power is generally considered to be lower making these studies more feasible. These investigations are appealing because they are hypothesis-driven. However, our current lack of knowledge about the complex interplay of proteins (and therefore genes) defining the pharmacokinetics is a major limitation. Moreover, this approach is low throughput,

due to the need for development of new techniques which involve cloning and establishment of expression systems followed by functional characterisation.

1.6.2. Genome Wide Association Studies (GWAS)

GWAS is a hypothesis-free identification of genetic determinants of phenotypes. It involves a screen of genetic markers across the whole genome of subjects with defined phenotypes compared to controls. Novel sequencing technologies have allowed the analysis of millions of SNPs across the whole genome, capturing the influence of genetic variants even with unknown function. However, the mechanisms for associations discovered by this method still require confirmation in order to establish biological plausibility. Furthermore the genomic regions containing tagging SNPs should be re-sequenced to identify functional variants. Because GWAS is hypothesis-free and does not require any knowledge of the biological processes it offers new opportunities for breakthrough research. However some limitations can be highlighted. Firstly these studies require high throughput sequencing technologies which are costly and not uniformly available (although cost per SNP is lower than for candidate gene studies). Secondly, millions of SNPs may be typed and therefore to obtain sufficient statistical power very large case/control cohorts of patients need to be included in the studies. For some phenotypes, the number of patients required is prohibitive. This is particularly true for pharmacokinetic studies. Moreover SNPs that have a minor contribution in the definition of phenotypes or have low frequency might easily be classified as false negative. Pharmacokinetics results from a complex interplay of proteins and can therefore be influenced by several genetic factors. A large proportion of these have a minor effect but a synergistic interplay can be hypothesised. Consequently, the net effect of some SNPs may be underestimated in

GWAS studies. Moreover GWAS normally investigates a clearly defined phenotype (categorical) such as a particular toxicity or outcome while pharmacokinetic data is continuous leading to further statistical challenges that must be faced. Standardisation of procedures and correct storage of samples containing antiretrovirals to be quantified is another logistic issue that may jeopardise GWAS studies.

1.6.3. Pharmacogenetic-based population Pharmacokinetic models

For the analysis of pharmacokinetic determinants, a novel technique is represented by pharmacogenetics-based population pharmacokinetic modelling. Population pharmacokinetics (popPK) is a statistical evaluation of variability in drug exposure and quantitatively describes the processes of absorption, distribution, metabolism and elimination of a drug. It can either be prospectively planned as part of clinical trial development or it can be based on the mathematical modelling and statistical analysis of existing data, selected according to the objective of the study (Aarons et al. 2001). Many patient characteristics can potentially influence pharmacokinetics and these include demographical, pathophysiological, body weight, excretory and metabolic functions and concomitant therapies (among others). Pharmacogenetics-based popPK models include all these factors but also include genetic markers which can explain part of the variability within the population. Variability can be observed within subjects (intra-patient) or between subjects (inter-patients). Models of this nature can use sparse data and therefore samples derived from retrospective studies can be included in the analysis. Intense sampling, which may not always be optimal in the clinical setting, can therefore be avoided. Considering the clinical pharmacology of antiretrovirals, some recent examples of this application have been

published but strategies to incorporate large numbers of variants are still evolving (Lubomirov et al. 2010).

1.6.4. *In vitro in vivo* extrapolation

Another promising "Bottom-up" approach is represented by *in vitro in vivo* extrapolation (IVIVE) (Rostami-Hodjegan and Tucker 2007). This technique involves the use of physiologically based pharmacokinetic (PBPK) models to investigate pharmacokinetics in virtual populations. PBPK modelling uses anatomical, physiological, physical and chemical principles to describe complex ADME processes. PBPK relies on multi-compartment models where different tissues and organs represent compartments connected via blood flow. Interplay of differential equations simulating concentration of drugs in each compartment is used and parameters included in the equations represent blood flow, organ volume and diffusion into tissues. As shown in Figure 1.13, known variability in demographic and biological (genetic and environmental) factors can then be incorporated into PBPK models. Drug-specific physicochemical properties and *in vitro* data on absorption, metabolism and transport processes can also be used to simulate the potential impact of PK and optimise design of clinical studies.

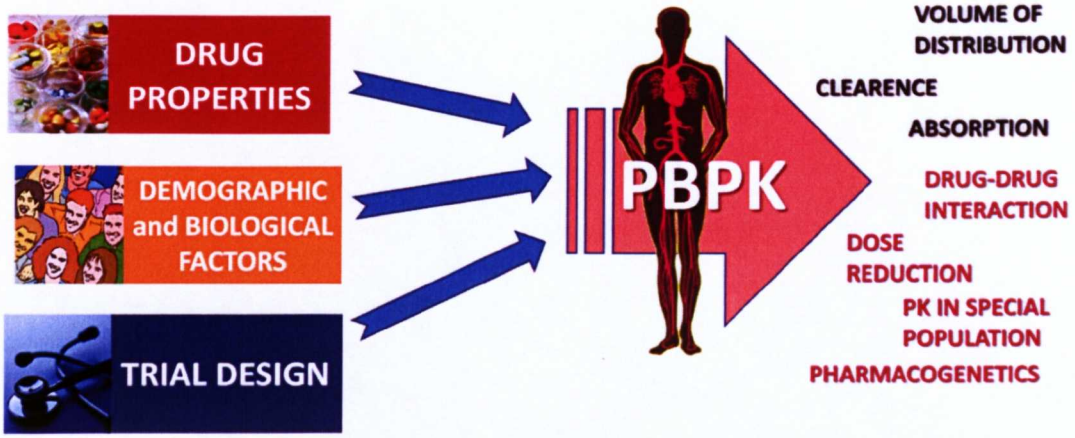

Figure 1.13. Representation of IVIVE and possible applications. Drug properties, demographic and trial design information are considered into physiologically based pharmacokinetic models.

A number of model systems can be employed to generate data to inform PBPK modelling. For example, absorption can be predicted using *in vitro* cell systems such as Caco-2 cells, or artificial monolayers such as PAMPA. Metabolism of drugs can be characterised *in vitro* using recombinant CYPs or human liver microsomes. The V_{max} (maximum metabolism rate achievable) and K_m (concentration at which 50% of V_{max} is reached) are essential *in vitro* variables that are normally investigated for IVIVE (Rostami-Hodjegan and Tucker 2007). Several other physiochemical properties of the drugs also need to be described such as the fraction unbound in plasma (a major determinant of clearance) and the logP (that influences diffusion into tissue and consequently the volume of distribution). One advantage of IVIVE is that *in vitro* information generated during drug discovery and pre-clinical evaluation can be used and early *in vivo* pharmacokinetic studies become less exploratory.

Various anatomical factors such as weight, height, body surface area, liver volume, cardiac output are correlated and based on known covariation of these factors, virtual

individuals can be simulated. Thus clinical trials can be simulated in groups of virtual individuals to understand inter-patient variability. IVIVE can estimate mean parameters and variability for clearance, volume of distribution and absorption. Possible applications of this method include simulation of drug-drug interactions, pharmacokinetics in special populations, dose reduction strategies and pharmacogenetic associations. Genetic factors with known effects on expression and activity of enzymes can be included in the simulations and their effect on ADME processes and therefore pharmacokinetic variability can be estimated.

1.7. Aim of the thesis

Response to treatment is generally characterised by a broad variability between patients. In most cases patients are treated with a fixed dose based on empirical guidelines and with no regards to potential differences in drug response. The correct management of disparities in efficacy and toxicity between patients poses an essential clinical challenge which can be overcome if the factors regulating inter-patient variability can be sufficiently elucidated. Efficacy of antiretroviral therapy can be affected by dose-dependent and dose independent processes. Dose dependent processes are normally defined as variation of the intensity of adverse drug reaction or efficacy which correlates with dosage and consequently with pharmacokinetic exposure. Conversely, dose independent processes do not correlate with the administered dosage and are commonly regulated by immunological or virological factors.

The overall aim of this thesis was the identification of genetic determinants of antiretroviral pharmacokinetics, in order to improve the current understanding of dose-dependent efficacy and toxicity. Antiretroviral exposure has been demonstrated to have a direct effect on efficacy and toxicity for drugs of different classes. Antiretroviral concentrations are the results of numerous absorption, distribution, metabolism and elimination (ADME) processes which are mediated by several proteins and take place in different tissues. Consequently, a complex interplay of metabolism enzymes and transporters determine the antiretroviral pharmacokinetic exposure and change in expression and/or activity of one of these proteins can have a direct effect on pharmacokinetics. Genes coding for proteins involved in ADME processes are polymorphic and a consistent proportion of polymorphisms have a direct or indirect influence on expression and activity affecting amino acid sequence in key regions of the proteins or altering regulation of expression. Therefore, a comprehensive knowledge of genetic factors will be essential for a correct management of drug-drug interactions, dose reduction, regimen simplification and future individualisation of antiretroviral therapy.

The selected antiretrovirals are some of the most commonly used agents and represent optimal candidates for pharmacogenetic studies. In Chapter 2 a population pharmacokinetic model was developed for unboosted ATV, and used to quantify the impact of *PXR* genetic variants on ATV clearance. ATV is one of the few protease inhibitors that can be administered without ritonavir and therefore can be used to investigate genetic determinants of CYP3A4 activity. Chapter 3 evaluated the intracellular pharmacokinetics of unboosted and boosted ATV, indentifying genes influencing cellular accumulation of ATV and RTV. EFV is used as a first line anti-

HIV agent and CYP2B6 polymorphisms have been confirmed to influence its pharmacokinetics. *CYP2B6* 516 G>T is one of the main genetic determinants of EFV pharmacokinetics and genotype based dose adjustments have been previously hypothesised. In Chapter 4 an IVIVE model was developed in order to simulate EFV pharmacokinetics at the standard regimen or with dose reductions. MVC is a novel antiretroviral that inhibits the interaction between HIV and CCR5. A relationship between MVC exposure and efficacy has been recently identified; consequently understanding factors which can alter MVC pharmacokinetics can have a crucial importance in future improvements of MVC-based therapy. Chapter 5 examines the substrate specificity of SLCO1B1 for MVC and the inhibitory effect of PIs on MVC uptake using a Xenopus *laevis* oocytes heterologus protein expression system. In Chapter 6 the effect of SLCO1B1 521 polymorphism on MVC pharmacokinetics has been investigated, taking into account the different dosage and concomitant antiretrovirals.

CHAPTER 2

The effect of PXR SNPs on plasma concentrations of unboosted atazanavir

2.1. Introduction

Atazanavir (ATV) is a protease inhibitor (PI) commonly administered once a day at a dose of 300 mg with 100 mg of ritonavir (RTV) to boost its plasma concentrations. However, ATV can be used without boosting at 400 mg once daily, recently validated by a simplification trial (Delfraissy et al. 2008). Therefore, although the 400 mg once a day dose is not yet licensed in Europe, this could be an attractive choice for patients with RTV intolerance. In a recent study approximately 20% of ATV recipients were reported to be administered off-label with an unboosted regimen (Quirino et al. 2008).

ATV plasma exposure has been shown to correlate with virological response, and a trough concentration (C_{trough}) value of 150 ng/mL proposed as a minimum effective concentration (MEC) (DHHS 2010). The pharmacokinetics (PK) of unboosted ATV could be more fragile compared to boosted dosing, leading to considerable inter-individual variability and potential suboptimal exposure in a significant proportion of subjects, considering that up to 50-60% of ATV 400 mg recipients showed C_{trough} below the MEC (Colombo et al. 2006).

Plasma concentrations of ATV are determined by several processes which are mediated by different transporters and metabolic enzymes. ATV metabolism is effected mainly by cytochrome P450 3A4 (CYP3A4) and the boosting activity of RTV affects CYP3A4, increasing ATV plasma concentrations if co-administered.

The only SNP that substantially influences CYP3A4 expression and activity is the *CYP3A4**1B (rs2740574), which has a low frequency in Caucasians (Lamba et al. 2002). P-glycoprotein, coded by the *ABCB1* gene, is involved in the disposition of several CYP3A4 substrates, including ATV, and influences intestinal absorption and excretion into the bile (Kim et al. 1998; Choo et al. 2000). The expression of *CYP3A4* is influenced by the pregnane-X receptor (PXR; *NR1I2*), an important regulator of genes involved in the metabolism and efflux of drugs. PXR has been shown to be activated by many PIs, and although PXR is classically considered to be a ligand-activated receptor that regulates gene expression in response to xenobiotics, it is important to recognise that expression of *PXR* is correlated with *CYP3A4* and *ABCB1* in liver and PBMC. Several studies have searched for polymorphisms in the coding and regulator region of *PXR*. Recently three SNPs (44477T>C, rs1523130; 63396C>T, rs2472677; 69789A>G , rs763645) have been identified in transcription factor binding sites of PXR regulatory regions and have been associated with an alteration of PXR expression and the activity of CYP3A4 (Lamba et al. 2008). The 63396TT genotype has been recently described as a predictor of suboptimal ATV C_{trough} and therefore the 63396C>T polymorphism was included in the current analysis (Siccardi et al. 2008).

Identification of factors influencing the variability in pharmacokinetics is important in the clinical management of HIV infection and may guide dosage optimization. The main purpose of this study was to identify covariates which affect the pharmacokinetic variability of unboosted ATV, in particular to evaluate the influence of the polymorphism *PXR* 63396C>T which is involved in the regulation of *PXR* expression and consequently CYP3A4 regulation (Lamba et al. 2008). A secondary

purpose was to assess the frequency of *PXR* 63396 T in several ethnic groups. However in order to develop the phenotype-genotype approach it was essential to have a robust chromatographic method for the quantification of atazanavir along with other antiretrovirals in plasma. Therefore the initial aspect of the study was to develop and subsequently validate novel analytical methodology following the FDA guidelines (Food and Drug Administration 2001).

2.2. Methods

2.2.1. Quantification of antiretrovirals in plasma

2.2.1.1. Chemicals

Compounds were kindly supplied by the following pharmaceutical companies: nevirapine (NVP) from Boehringer Ingelheim Pharmaceuticals, Inc. (Ridgefield, CT, USA); efavirenz (EFV) and atazanavir (ATV) from Bristol Myers Squibb Company (Princeton, NJ, USA); indinavir (IDV) and raltegravir (RAL) from Merck Sharp & Dohme Laboratories (West Point, PA, USA); amprenavir (APV) from GlaxoSmithKline (Brentford, UK); darunavir (DRV) and etravirine (ETV) from Tibotec (Mechelen, Belgium); saquinavir (SQV) from Roche (Mannheim, Germany); nelfinavir (NFV) and M-8 from Pfizer, Inc. (Groton, CT, USA) and lopinavir (LPV) and ritonavir (RTV) from Abbott Laboratories (Chicago, IL). Acetonitrile HPLC grade was purchased from J.T. Baker (Deventer, Holland). HPLC grade water was produced with a Milli-DI system coupled with a Synergy 185 system (Millipore, Milan, Italy). Quinoxaline (QX), ortho-phosphoric acid, potassium dihydrogen phosphate, formic acid and trifluoroacetic acid (TFA) were obtained from Sigma-Aldrich (Milan, Italy). Solid phase extraction (SPE) cartridges C-18 (100 mg, 40–63

mm particle size) were obtained from VWR (Milan, Italy). Blank plasma from healthy donors was kindly supplied by the Blood Bank of Maria Vittoria Hospital (Turin, Italy).

2.2.1.2. Stock solutions, Standards and Quality Controls

DRV, NVP, IDV, APV, SQV, M-8, NFV, ATV, QX and RGV stock solutions were made in a solution of methanol and HPLC grade water (90:10 vol/vol), and EFV, ETV, RTV, and LPV were made in a solution of methanol and HPLC grade water (95:5 vol/vol) to obtain a final concentration of 1 mg/mL; TPV stock solution was made with methanol to obtain a concentration of 10 mg/mL; all stock solutions were then refrigerated at 4°C until use, within 1 month. The Internal Standard (IS) working solution was prepared with QX (2 μg/mL) in methanol and HPLC grade water (50:50, v/v) and stored at 4 °C until use (maximum 1 month).

2.2.1.3. Chromatographic Conditions, Standard and QC concentrations.

The HPLC-PDA instrument used was a Waters 2695 HPLC system (Milan, Italy), including a degasser and an autosampler, coupled with a 2998 PDA detector. Empower 2 Pro software (version year 2005; Waters, Milan, Italy) was used for management of the HPLC-PDA system. Chromatographic separation was performed by a Luna 5μm C18 column (150 x 4.6 mm; Phenomenex, CA, USA), protected by a SecurityGuard with C18 (4.0 x 3.0 mm ID; Phenomenex, CA, USA) at 45°C using a Temperature Control Module II (Waters). The run was performed at 1 ml/min; the mobile phase was composed of solvent A (KH_2PO_4 50 mM with ortho-phosphoric acid, final pH = 3.23) and acetonitrile, and the gradient is reported Table 2.1. The run

was monitored in the range of 210–320 nm by the PDA detector. The wavelength for quantification, standards and QC concentrations are listed in

Table **2.2**. 500 µl of plasma was diluted with 500 µl of HPLC solvent A. 50 µl of IS working solution was added to each tube, and the samples were vortexed for 10 seconds. SPE C-18 cartridges were placed on a vacuum elution manifold WAT 200677 (Waters, Milan, Italy) and activated with 1 ml of methanol, followed by 1 ml of HPLC solvent A before loading of the samples. Loading was carried out under gravity. Then, the cartridges were washed with 500 µl of HPLC solvent A, followed by 250 µl of HPLC grade water, and then elution was carried out using 500 µl of methanol and acetonitrile solution (90:10, vol/vol). Eluted solutions were collected into glass tubes and treated by vortex vacuum evaporation to dryness at 60°C. Each extract was reconstituted with 150 µl of HPLC grade water and acetonitrile solution (60:40, vol/vol), and 30 µl was injected into the column.

Table 2.1. Chromatographic conditions (gradient). Mobile Phase A consisted of KH_2PO_4 50 mM with orthophosphoric acid, final pH = 3.23, and Mobile phase B consisted of HPLC grade acetonitrile

TIME (min.)	% Mobile Phase A	% Mobile Phase B
0.0	70	30
5.0	61	39
7.0	56	44
10.0	54	46
11.0	51	49
13.0	48	52
15.5	47	53
18.0	47	53
19.8	46	54
19.9	41	59
20.0	30	70
23.9	30	70

24.0	70	30
28.0	70	30

Table 2.2. PDA wavelengths used to quantify IS and each drug, nominal concentrations of STD 8, STD 1 (LOQ), QCs (QC High, QC Medium, and QC Low), and LOD.

		Concentrations (ng/mL)					
Drugs	Wavelengths (nm)	STD 8	STD 1/LOQ	QC High	QC Medium	QC Low	LOD
NVP	284	8000	62.5	6000	1500	150	15.6
IDV	261	8000	62.5	6000	1500	150	31.3
M8	253	4000	31.25	2000	500	50	15.6
RGV	304	3000	23.4	2000	500	50	11.7
SQV	240	7000	54.7	4000	1000	100	13.7
NFV	253	8000	62.5	4000	1000	100	15.6
APV	284	10000	78.1	8000	2000	200	19.5
DRV	284	10000	78.1	8000	2000	200	19.5
ATV	284	6000	46.8	4000	1000	100	11.7
RTV	240	2500	19.5	2000	500	50	9.8
EFV	294	8000	62.5	6000	1500	150	31.3
LPV	260	15000	117.1	10000	2500	250	58.6
ETV	304	3000	23.4	2000	500	50	11.7
TPV	260	45000	351.5	25000	6250	625	43.9
IS	260	—	—	—	—	—	—

2.2.1.4. Validation

Interference from endogenous compounds was investigated by analysis of six different blank solutions. Other possible concomitant drugs were also investigated, including amodiaquine, desacetyl amodiaquine, amoxicillin, caspofungin, ceftazidime, ciprofloxacin, clavulanic acid, ethambutol, furosemide, insulin, isoniazid, levofloxacin, nimesulide, omeprazole, pravastatin, and ribavirin.

Intra-day and inter-day accuracy and precision were determined by assaying 4 sets of QCs in each session. Accuracy was calculated as the percent deviation from the nominal concentration. Inter-day and intra-day precision were expressed as the standard deviation at each QC concentration. The calibration curve was obtained using 8 calibration points in duplicate. A quadratic through zero calibration curve was used. The limit of detection (LOD) was defined as the concentration that yields a signal-to-noise ratio of 3/1. Percent deviation from the nominal concentration (measure of accuracy) and relative standard deviation (measure of precision) of the concentration considered as the limit of quantification (LOQ) had to be < 20%, and it was considered the lowest calibration standard, as requested by FDA guidelines (Food and Drug Administration 2001). Average recovery of all analytes was determined by comparing the peak area of the drug extracted from the three QCs with those obtained by direct injection of the same amount of drug in the reconstitution solution. The stability of RAL, NNRTIs, and PIs at different conditions has been assessed in several studies (Marzolini et al. 2002; Crommentuyn et al. 2003; Turner et al. 2003; Crommentuyn et al. 2004; D'Avolio et al. 2007; Merschman et al. 2007; ter Heine et al. 2009; Ter Heine et al. 2009) and for this reason, assessment of stability before assay for these drugs was not performed, but it was evaluated for post extraction conditions. Stability of drugs and IS in plasma extracts at room temperature (20–25°C, the autosampler rack temperature) was evaluated; processed QCs, at 3 different concentrations, were analyzed immediately after preparation and after being left for 24 hours at room temperature.

2.2.2. Patients

The population pharmacokinetic (PK) model was developed in collaboration with Dr. Alessandro Schipani using data from adult HIV-positive patients receiving a regimen containing ATV 400 mg once daily, and no known concomitant interacting medication (except for tenofovir, TDF), from three independent cohorts. Cohort A included 11 patients with 5 to 6 plasma concentrations in the dosing interval and 64 patients with at least 2 random plasma concentrations from the Department of Infectious Diseases at the University of Turin (Turin, Italy). Cohort B included 42 patients with a single plasma concentration data point from the Department of Infectious Diseases, Hospital Carlos III (Madrid, Spain). Cohort C comprised 65 patients with plasma samples collected at random time points from the Liverpool Therapeutic Drug Monitoring Registry (Liverpool, UK). All blood sampling was performed after written informed consent had been obtained in accordance with local ethics committee indications. All samples were obtained under steady-state conditions. The following covariates were available: age, gender, body weight, time post-dose, concomitant ARVs and other medications.

2.2.3. Frequency analysis

The frequency of the *PXR* 63396 T variant allele has been investigated in 563 unrelated healthy individuals among 8 ethnic groups. 87 Ghanaians, 47 Kenyans, 78 Peruvians, 87 Saudis, 45 Sudanese were all assessed at a USA study centre (UNC Institute for Pharmacogenomics and Individualized Therapy, University of North

Carolina, Chapel Hill, NC, USA), 82 Italians were recruited and assessed at the Italy study centre (Department of Infectious Diseases at the University of Turin, Turin, Italy). 53 Spanish patients were recruited and assessed at the Spain study centre (Department of Infectious Diseases, Hospital Carlos III, Madrid, Spain) and 84 Thai subjects were recruited and assessed at the Thai study centres (Siriraj Hospital, Bank Thailand and Bamrasnaradura Infectious Diseases Institute, Nonthaburi, Thailand).

2.2.4. Genotyping analysis

DNA was extracted from whole blood (100µl) using GenElute Blood Genomic DNA kit (Sigma-Aldrich, Poole, UK), according to the manufacturer's instructions. Genotyping was conducted by real time PCR based allelic discrimination. PCR reaction volume was 25 µl; 12.5 µl Taq Man MasterMix (Applied Biosystem, UK), 1.25 µl of primers and probes (*PXR* 63396 C>T, rs2472677, Applied Biosystem code = C__26079845_10). The Taq DNA Polymerase was activated at 95°C for 10 min and subsequently 50 cycles with a denaturation phase of 15 sec at 95°C and annealing/extension phase of 1 min at 60°C.

2.2.5. Population pharmacokinetic analysis

The PK model was developed using NONMEM® (ICON, version VI 2.0) installed under nmqual (Metrum institute). Data processing and graphical analyses were done using Microsoft® Office Excel 2007 for Windows (Microsoft Corporation, Redmond. WA, USA).

The model building strategy was as follows: One- and two- compartment models with first- or zero-order absorption without and with lag-time were fitted to the data using the First Order Conditional method of estimation. Proportional, additional and combined proportional and additional error models were evaluated to describe residual variability. In the model, residual variability was best described by a purely proportional structure. Inter-individual random effects were described by an exponential model, but supported only for apparent clearance (CL/F):

$$CL/F_i = \theta_1 * \exp(\eta_i)$$

where CL/F*i* is the atazanavir CL/F of the *i*th individual; θ_1 is the population parameter estimate; and η_i is the inter-individual variability with a mean of zero and variance ω^2. The minimal objective function value (OFV; equal to -2 log likelihood) was used as a goodness-of-fit diagnostic with a decrease of 3.84 points corresponding to a statistically significant difference between models (P=0.05, χ^2 distribution, one degree of freedom). Residual plots were also examined. Once the appropriate structural model was established, the following covariates were explored: body weight, age, gender, PXR 63396 genotype. Tenofovir use (300 mg once daily) was also included in the covariate analysis because an unexpected interaction has been reported (VIREAD®, Gilead Sciences Inc., Foster City, CA, USA). Graphical methods were used to explore the relationship of covariates versus individual predicted pharmacokinetics parameters. Each covariate was introduced separately into the model and only retained if inclusion in the model produced a statistically significant decrease in OFV of 3.84 ($P \leq 0.05$) and was biologically plausible. A backwards elimination step was then carried out once all relevant covariates were

incorporated and covariates retained if their removal from the model produced a significant increase in OFV (**>6.63 points; P≤0.01, χ^2 distribution, one degree of freedom).**

Dichotomous (gender and co-medications) and continuous (body weight and age) variables, here defined as X, were introduced into the model using the following parameterizations, respectively:

(1) TVCL $=\theta_0 * (1+\theta_1 * X)$

(2) TVCL $= \theta_0 + \theta_1 *$ (X-Median value)

where TVCL is the typical value of ATV CL/F of the population; in the equation 1 θ_0 is the value of CL/F for the individuals X=0; and θ_1 is the relative difference in CL/F for the individuals X=1. In the equation 2, for example θ_0 is typical CL/F at the median body weight and θ_1 is the change in CL/F per kg.

Genotype information was coded as an index variable, which is shown below for CL/F:

TVCL $=\theta_0+\theta_1 * X_1+ \theta_2 * X_2$

where θ_0 is the typical value of CL/F for individuals with homozigosity for the C allele [C/C], θ_1 is the relative difference in CL/F for patients with CT when X_1=1, and θ_2 is the relative difference in CL/F for patients with TT when X_2=1.

To assess the stability and performance of the model a visual predictive check was carried out, 1000 datasets were simulated using the parameter estimates defined by the final model with the SIMULATION SUBPROBLEMS option of NONMEM®. Datasets were simulated for unboosted ATV 400 mg once daily. From the simulated data, 95% prediction intervals (P2.5-P97.5) were constructed and observed data from the original dataset were superimposed. 95% of data points within the prediction interval was indicative of an adequate model.

In addition, in order to confirm the stability and robustness of the model, a bootstrap re-sampling was used. Bootstrapping was performed with the software package Perl-speaks-NONMEM 5.1. The median values and 95% confidence intervals for the parameter estimates were obtained from 200 bootstrap replicates of the original data set and compared with the original population parameters.

2.3. Results

2.3.1. Validation of HPLC-PDA method for quantification of antiretrovirals in plasma

The retention time of each analyte was: NVP 3.9 ± 0.1 min, IDV 5.7 ± 0.1 min, M8 7.2 ± 0.1 min, RAL 8.5 ± 0.1 min, SQV 9.7 ± 0.1 min, NFV 10.5 ± 0.1 min, IS 11.1 ± 0.1 min, APV 11.6 ± 0.1 min, DRV 11.6 ± 0.1 min, ATV 16.2 ± 0.1 min, RTV 18.6 ± 0.1 min, EFV 19.3 ± 0.1 min, LPV 19.8 ± 0.1 min, ETV 21.5 ± 0.1 min, TPV 24.0 ± 0.1 min. It has to be noticed that APV and DRV co-eluted at the same

retention time due to their very similar physio-chemical properties, therefore two separate lots of STD and QCs were made, one containing DRV and the other APV. Chromatograms representing a STD1 and STD8 are shown in Figure 2.1 and Figure 2.2.

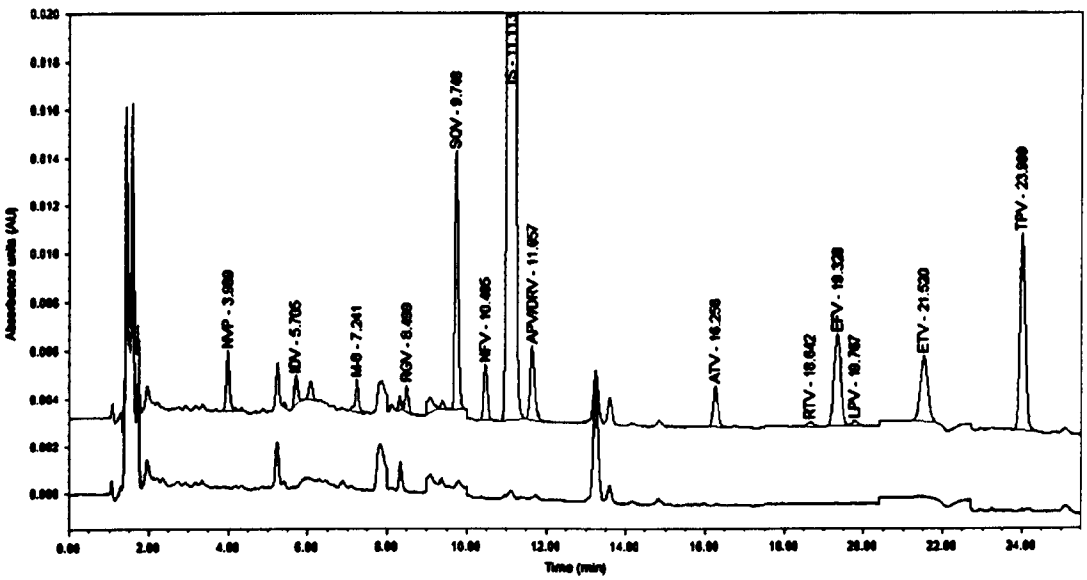

Figure 2.1 Overlapped chromatograms of STD 1 and drug-free plasma. Y axis is absorbance and X axis is time. STD1 chromatogram is the above line and drug-free plasma is represented by the line below.

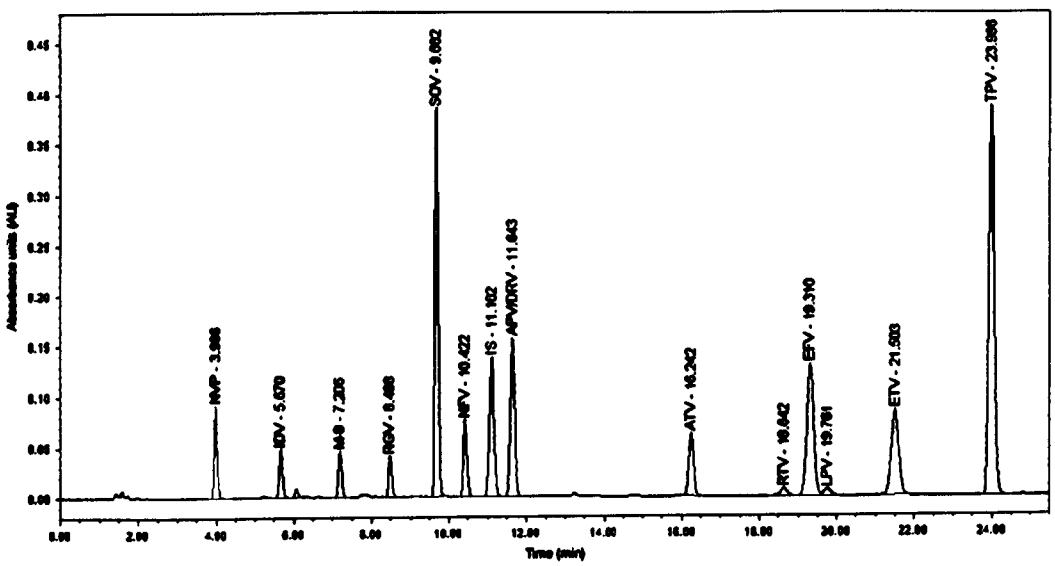

Figure 2.2. Chromatogram of STD 8. Y axis is absorbance and X axis is time.

The assay did not show any relevant interference with antiretrovirals or other concomitant drugs administered to the patients at therapeutic doses, excluding the above-mentioned overlap between DRV and APV.

The mean regression coefficient of determination (r^2) of all calibration curves was higher than 0.998. A linear through zero regression was chosen due to an excellent linear response for all the drugs up to STD 8. Results of the validation of the methods are listed in Table 2.3. All observed data (intraday and interday precision as percent relative standard deviation, RSD%) were below 15.0%, in line with FDA guidelines (Food and Drug Administration 2001).

Table 2.3. Accuracy (%) and Intraday and Interday Precision (RSD%) for all drugs

	QC High			QC Medium			QC Low		
		Precision (RSD%)			Precision (RSD%)			Precision (RSD%)	
Drugs	Acc %	Intraday	Interday	Acc %	Intraday	Interday	Acc %	Intraday	Interday
NVP	2.85	3.76	5.52	4.44	5.15	6.23	11.59	7.17	8.82
IDV	1.61	5.04	8.35	8.65	3.60	3.39	8.25	3.03	8.94
M-8	1.17	2.79	9.50	2.27	1.36	4.83	9.73	6.45	8.79
RGV	2.13	5.57	6.98	2.58	2.56	3.54	3.50	4.00	8.43
SQV	2.64	3.25	5.64	1.05	5.27	5.98	8.79	4.64	8.44
NFV	3.79	4.48	5.55	4.30	3.44	4.88	8.30	3.24	14.54
APV*	0.17	2.16	4.38	9.88	3.67	8.16	2.36	6.05	7.51
DRV†	0.88	2.34	4.55	8.83	3.62	8.46	3.24	5.15	7.86
ATV	0.02	4.83	6.81	3.87	3.48	4.61	13.73	3.37	6.63
RTV	6.87	2.39	2.87	1.73	2.36	6.07	7.74	3.45	3.53
EFV	3.92	2.96	4.13	0.16	2.81	3.53	2.61	1.47	4.61
LPV	6.51	2.28	3.77	0.96	6.33	13.52	8.42	2.80	5.19
ETV	5.53	4.00	5.35	7.59	1.82	3.05	9.16	3.87	7.26
TPV	4.59	1.65	3.30	13.45	3.61	5.81	14.56	3.58	8.11

Multiple aliquots (n=6) at each of the three QC concentrations were assayed. Mean recovery of all drugs ranged from 75% to 83%. The mean IS recovery was 89% (mean CV 2.9%). The stability study of drugs and IS in plasma extracts, kept for 24

hours in the autosampler rack at room temperature, showed a variation of less than 7% for IS and all drugs at each concentration.

2.3.2. Genotyping analysis

The fluorogenic probe complementary to the T allele had a FAM dye and the fluorogenic probe complementary to the C allele had a VIC dye. A shown in Figure 2.3, patients with TT genotype resulted in amplification of just the FAM-probe (open circle), patients who were heterozygous had amplification of both probes (open triangle) and patients with CC genotype resulted in amplification of just the VIC-probe.

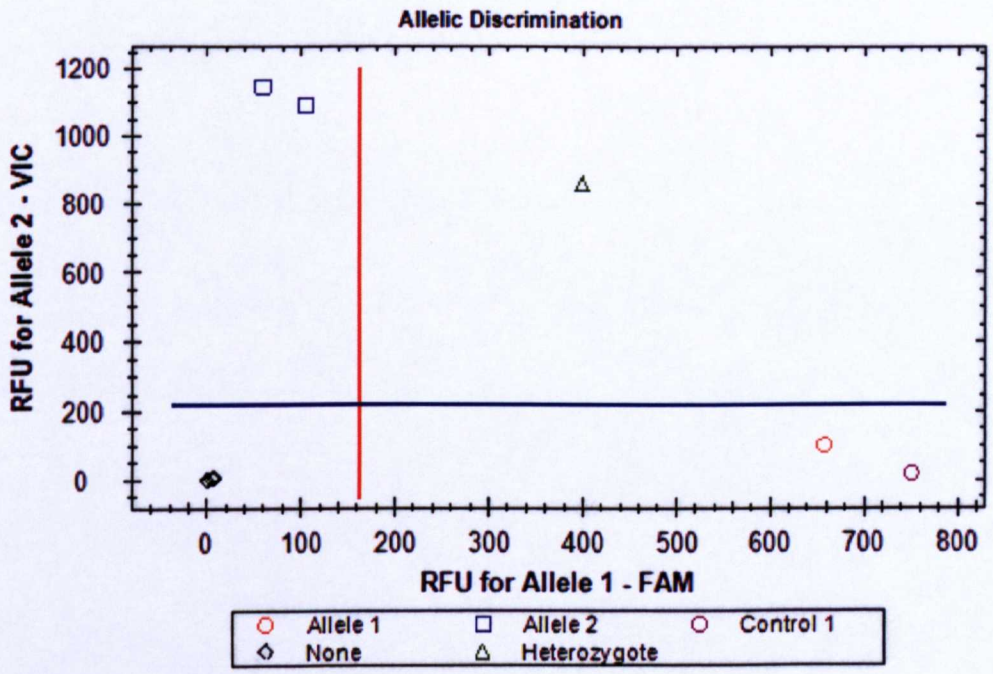

Figure 2.3. Representative allelic discrimination plot for *PXR* 63396C>T. Open square represents the CC genotype, the open triangle heterozygosity and the open circle TT genotype. The orange line is the threshold for FAM-probe amplification and the blue line for the amplification of VIC-probe.

2.3.3. Population PK analysis

A total of 182 HIV infected individuals receiving once-daily unboosted-ATV at 400 mg, were included in the population analysis. 11 of the patients had full concentration-time profiles of 5-6 samples at steady state obtained between 0 and 24 hours after dosing, the remaining patients had blood samples drawn at random points (sparse data set) at least 1 month after initiation of the atazanavir regimen. For this group of patients, timing of sampling relative to dose intake and dosing with food was obtained from patient self-reporting. A total of 323 plasma samples were available, 64 from the rich data set and 259 from the sparse data set. The demographic characteristics of these patients and their concomitant medications are shown in Table 2.4.

Table 2.4. Summary of patient demographics and baseline clinical characteristics.

Parameter		**Median (range)**
Study participants n [M/F]	182 [116/66]	
Age (years)		44 (19-74)
Weight (kg)		76 (46-115)
TDF 300 mg *qd (%)*	103 (57)	
n: number of patients; M: male; F: female; TDF: tenofovir; *qd*: once daily.		

The base model was adequately described by a 1-compartment model with first-order absorption. In the model, residual variability was best described by a proportional structure; the inclusion of an additive component did not improve the model. Inter-

individual random effects were described by an exponential model, but supported only for apparent clearance (CL/F):

$$CL/Fi = q1 * \exp(\eta i)$$

where CL/Fi is the atazanavir CL/F of the individual; q1 is the population parameter estimate; and ηi is the inter-individual variability with a mean of zero and variance ω2. The introduction of a lag time significantly improved the fit (ΔOF=16.8). Parameter estimates for the base model are summarized in Table 2.5. A stepwise backward elimination approach was applied to the intermediate model to identify the following as covariates ($P<0.001$): body weight, age, gender and co-medications for CL/F. Continuous and dichotomous variables, here defined as X (body weight, age, gender and co-medications) in the following equation were applied for the demographic model as shown below:

$$TVCL = q0 * (1+q1*X)$$

where TVCL is the typical value of ATV CL/F of the population; q0 is the value of CL/F for the individuals X=0; and q1 is the relative difference in CL/F for the individuals X=1. None of the demographic covariates and co-medication (TDF) showed a significant decrease in objective function, and therefore were not retained in the final model.

Table 2.5. Atazanavir parameter estimates and standard errors obtained from the final population pharmacokinetic model.

	Basic Model		Final Model	
Parameter	**Estimate**	**RSE (%)**	**Estimate**	**RSE (%)**
CL/F (L/h)	18.4	12.4	19.7	6.1
V/F (L)	122	17.13	136	16.5
k_a (h^{-1})	2.27	37.05	2.3	3.9
Lag-time (h)	1.3	0.12	1.3	0.005
IIV CL/F (%)	25.3	39.28	21.5	26.1
Residual error				
Proportional (%)	36.5	11.04	38.5	8.6
Factor associated with Het on ATV CL/F[a]	-	-	-0.2	63
Factor associated with Mut on ATV CL/F[a]	-	-	3.4	4.7
F diurnal			1.34	10

RSE (%): relative standard error; CL/F: apparent oral clearance; V/F: apparent volume of distribution; k_a: absorption rate constant; IIV: interindividual variability; Het: heterozygous alleles; Mut: homozygous mutate alleles; RSE defined as: ($SE_{estimate}$/estimate)*100; [a] Het and Mut as a covariate not included in the basic model.

2.3.4. Pharmacogenetics

The impact on CL/F for each variant genotype of *PXR* was tested using several equations which are shown in Table 2.6.

Table 2.6. Models explored to determine the influence of covariates on atazanavir pharmacokinetic parameters following genotype-variant analysis.

Covariate	Model	θ_0	θ_1	θ_2	ΔOFV	*p* value
Influence of sex on CL/F	$CL = \theta_0 * (1+\theta_2 \cdot SEX)$	18.5	0.996		0.007	NS
Influence of weight on CL/F	$CL = \theta_0 + \theta_2 * (WT-76)$	11.2	-0.022		-2.6	NS
Influence of age on CL/F	$CL = \theta_0 + \theta_2 * (AGE-44)$	14.5	-0.424		0.446	NS
Influence of TDF on CL/F	$CL = \theta_0 * (1+\theta_2 \cdot TDF)$	18.5	0.029		0.228	NS
Genotype-variant analysis	**Model**	θ_0	θ_1	θ_2	ΔOFV	*p* value
Rich equation Influence of *Het* and *Mut* on CL/F	$CL = \theta_0 + \theta_1 \cdot Het + \theta_2 \cdot Mut$	17.6	-0.20	3.04	10.50	< 0.01
Reduced equation1 Influence of Het on CL/F	$CL = \theta_0 + \theta_1 \cdot (Het+Mut)$	18.5	1.21	-	-37	NS
Reduced equation2 Influence of *Mut* on CL/F	$CL = \theta_0 + \theta_2 \cdot Mut$	17.5	-	3.18	10.42	< 0.01
Linear equation n= 0, 1, 2	$CL = \theta_0 + \theta_1 \cdot n$	18.5	-0.46		0.13	NS
Power equation n= 0, 1, 2	$CL = \theta_0 + \theta_1^{\,n}$	18.0	0.71		-29	NS
Square root equation n= 0, 1, 2	$CL = \theta_0 + \theta_1 \cdot \sqrt{n}$	19.0	-0.015		-29	NS

CL/F: apparent oral clearance; θ_0: typical value of the parameter; $\theta_{1\text{-}2}$: estimate of the factor associated with the covariate; ΔOFV: change in objective function value; TDF: tenofovir; WT: weight; Het: heterozygous alleles; Mut: homozygous mutate alleles; NS: not statistically significant.

Genotype information was coded as an index variable, which is shown below for CL/F:

TVCL =q0+q1*X1+ q2*X2

where q0 is the typical value of CL/F for individuals carrying wild-type alleles (CC), q1 is the relative difference in CL/F for patients carrying heterozygous alleles (CT) when X1=1, and q2 is the relative difference in CL/F for patients carrying homozygous variant type alleles (TT) when X2=1. A rich model which assigned a

separate fixed effect for wild-type, heterozygote and homozygote variant carriers, showed the best fit of the data (ΔOFV=10.5). A reduced model, grouping wild-type and heterozygote carriers also showed an improvement of fit (ΔOFV=10.4), similar to the rich model. A second reduced model, grouping T allele carriers, showed no significant model improvement (ΔOFV=-37). Simplified models were also tried to estimate CL/F as a function of the number of *PXR* polymorphisms, assigned a value of 0 for wild-type, 1 for heterozygotes and 2 for homozygotes. With this method, linear, power and square root models were tested. None of these models showed a significant improvement of the objective function, and therefore this method was not used for the design of the final model.

The rich model showed the best fit, with general decreases in standard errors (SEs) for all the parameters. Therefore, it was chosen as the final model, which estimated an average CL/F of 19.7 liters/h in individuals carrying two C alleles. In heterozygotes the CL/F decreased by 0.18 liters/h, and in individuals with a T/T genotype, the model showed an increase in CL/F of 3.4 liters/h. Based on these values the half life of ATV was calculated using the following formula:

The half life was therefore equal to 4.59 hours for the whole population, 5.35 hours for patients with 63396CC, 5.41 hours for patients with 63396CT and 4.48 for patients with 63396TT. As shown in Table 2.5, the introduction of PXR 63396 genotype in the final model reduced the CL/F interindividual variability from 25.3 to 21.5 and consequently PXR 63396 TT accounts for 3.8% of the total interindividual variability.

In order to evaluate the possible impact of diurnal variation in combination with *PXR* genotype, a relative bioavailability value, $F_{diurnal}$, was introduced. The results showed that administration of ATV in the evening increased the bioavailability by 34% over that with morning dosing. A summary of the final population estimates is presented in Table 2.6. The diagnostic plots for the final model showed that predicted and observed data were in agreement (Figure 2.4). The individual weighted residuals did not reflect any particular systematic trends.

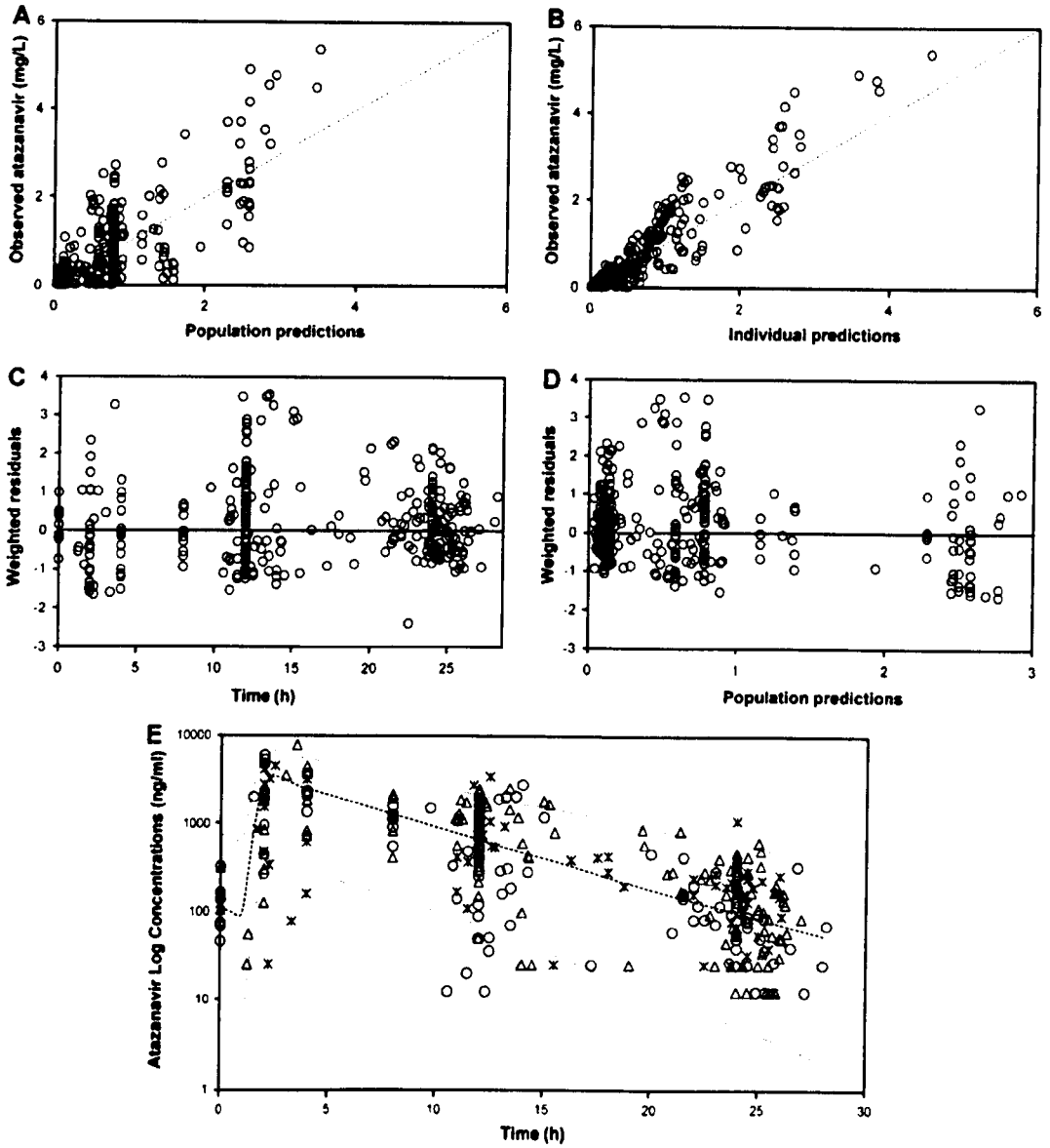

Figure 2.4. (A and B) Goodness-of-fit plots for the final pharmacokinetic model illustrating population predictions of atazanavir versus observed concentrations (A) and individual predictions of atazanavir versus observed concentrations (B); the broken line describes the line of unity. (C) Weighted residuals versus time postdose. (D) Population predictions of atazanavir versus weighted residuals; the thin black line is at ordinate value zero. (E) Ninety-five percent prediction intervals (P2.5 to P97.5) determined from simulated data of unboosted atazanavir administered at 400 mg once daily. Atazanavir plasma concentrations (n = 323) in 182 patients are superimposed, asterisks represent concentrations in individuals carrying wild-type alleles (41 patients), open circles represent concentrations in individuals carrying heterozygous alleles (85 patients), and open triangles represent concentrations in individuals carrying homozygous mutant alleles (56 patients).

A 95% prediction interval was generated from 1,000 simulations for unboosted ATV 400 mg once daily, with the covariate values of those individuals used in the building process, as shown in Figure 2.4E. Observed data from patients used in the model-building process were superimposed onto the prediction interval. Of 323 plasma concentrations, 4.3% were above P97.5 and 4.6% were below P2.5, which suggests that overall the final model performed adequately. In the final model, the TT genotype increased the CL/F by 3.04 liters/h (17.2%). Heterozygosity did not significantly affect the CL/F (–0.9%), suggesting that homozygosity for the T allele is required to influence the disposition of ATV, as shown in Figure 2.5.

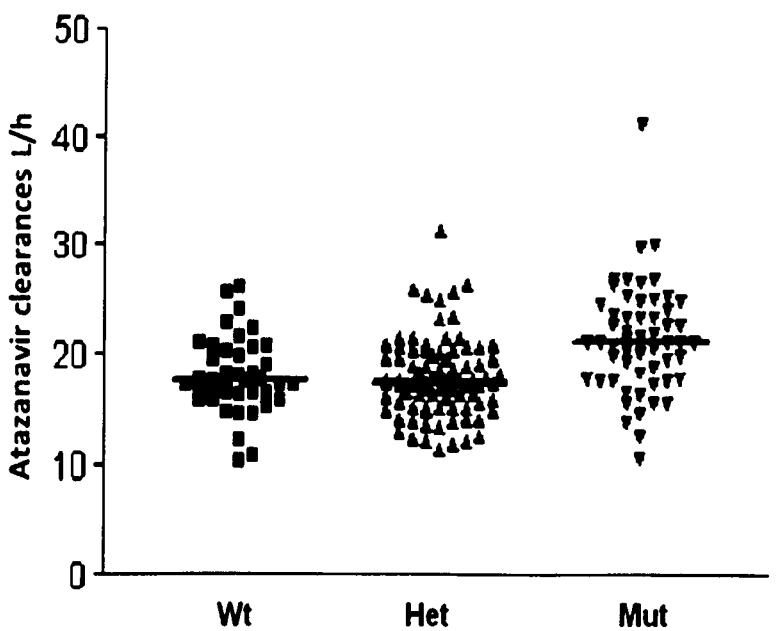

Figure 2.5. Atazanavir individual clearance values associated with the *PXR* 63396C>T genotype. Wt, wild-type C/C alleles; Het, heterozygous C/T alleles; Mut, homozygous T mutant alleles. Median values are shown by thick horizontal lines.

To investigate the effect of the combination of genetic and diurnal variation in a population, simulated concentration-time courses of a single dose of unboosted ATV at steady state were performed as shown in Figure 2.6. The simulations were carried

out firstly with a population of individuals homozygous for the common allele (63396CC) and secondly with a population of individuals homozygous for the variant allele *PXR* 63396TT, stratifying each group into individuals who took the drug in the morning and individuals who took the drug in the evening. For the morning simulations, the proportion of individuals with C_{trough} below the suggested MEC (150ng/ml) was 62% *PXR* 63396CC versus 80% *PXR* 63396TT. For the evening simulations, the proportions were 49% *PXR* 63396CC versus 70% *PXR* 63396TT.

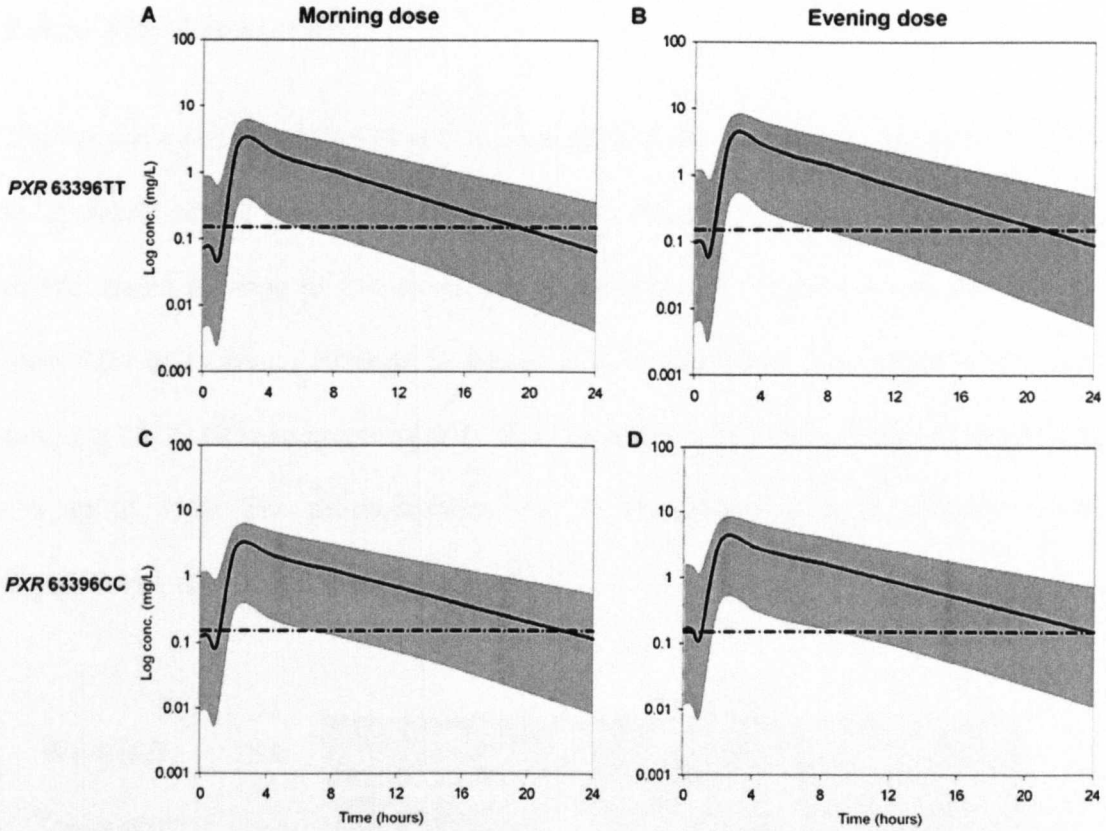

Figure 2.6. Steady-state 95% prediction intervals (P2.5 to P97.5) determined from simulated data of unboosted ATV stratified for *PXR* 63396C>T genotype and for evening versus morning dosing. The mean population prediction (continuous thick line) and the 95% prediction interval (gray area) are represented for each category. The broken horizontal line is at an ordinate value of 0.150 mg/liter (proposed MEC). (A) Steady-state ATV concentrations predicted for patients with *PXR* 63396TT with morning dose (median time to below MEC = 19.32 hours). (B) Steady-state ATV concentrations predicted for patients with PXR 63396TT receiving an evening dose (median time to below MEC = 21 hours). (C) Steady-state ATV concentrations predicted for patients with PXR 63396CC with morning dose (median time to below MEC = 22.15 hours). (D) Steady-state ATV concentrations predicted for patients with *PXR* 63396CC with evening dose (median time to below MEC = 24.08 hours).

2.3.5. Allele frequency

The frequency of the *PXR* 63396 T mutant allele has been investigated in a total of 8 independent ethnic groups, as summarized in Figure 2.7. The T allele has been demonstrated to have highly frequency in several different ethnic groups, ranging from 0.25 in Peruvian subjects to 0.6 in Italian, Saudi and Thai subjects. Patients carrying the T allele in homozygosity were therefore a high proportion, ranging from 4% up to 41%. The polymorphism was in Hardy-Weinberg equilibrium in all populations other than Sudanese ($p = 0.02$).

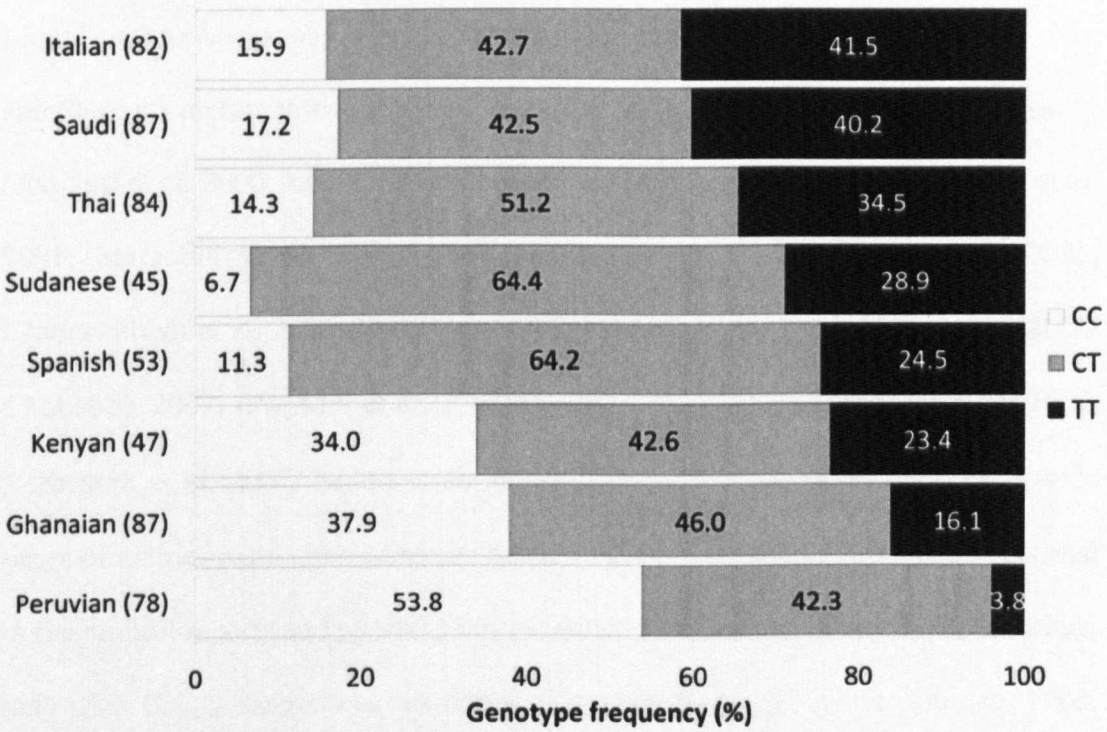

Figure 2.7. Genotype frequencies of *PXR* 63396C>T in eight ethnic groups. Vertical bars represent genotype frequencies of the different populations arranged from those with the highest frequency to those with the lowest frequency of the T allele. Percent frequencies of genotypes are shown in white for CC, gray for CT, and black for TT. The number of patients included for each population is given in parentheses next to the ethnicity.

2.4. Discussion

Unboosted ATV is characterised by low pill burden, favourable lipid profile and pharmacokinetics which allows once-daily dosing and can represent a valuable antiretroviral dosing strategy in patients unable to tolerate RTV.

In this chapter a novel analytical method for quantification of 13 antiretroviral agents in the plasma of HIV-infected patients was developed using SPE with a PDA/UV detector. Other UV-based, Liquid Chromatography-Single Quadrupole (LC-MS), and Liquid Chromatography-Triple Quadrupole (LC-MS/MS) methods for the simultaneous measurement of antiretrovirals in plasma have been reported previously (Aymard et al. 2000; Marzolini et al. 2000; Sarasa-Nacenta et al. 2001; Simon et al. 2001; Marzolini et al. 2002; Crommentuyn et al. 2003; Turner et al. 2003; Crommentuyn et al. 2004; Dailly et al. 2004; Pelerin et al. 2005; Notari et al. 2006; Choi et al. 2007; D'Avolio et al. 2007; Goldwirt et al. 2007; Takahashi et al. 2007; Verbesselt et al. 2007; Notari et al. 2009). The calibration curves included a wide range of antiretroviral concentrations based on the lowest and highest values reported in the clinical reports and plasma pharmacokinetic studies, except for TPV, for which only the C_{trough} range was explored (Kappelhoff et al. 2004; Tibotec 2006; MacArthur and Novak 2008; Hughes et al. 2009). Reliability, costs, difficulty of performance, and reproducibility are issues with regard to measurement of drug plasma concentrations. The method described which relies on SPE coupled with a PDA/UV detector, is simple, reliable, sensitive, and not expensive in consumables and instrumentation when compared with other methods developed for LC-MS or LC-MS/MS (Aymard et al. 2000; Marzolini et al. 2000; Sarasa-Nacenta et al. 2001;

Simon et al. 2001; Marzolini et al. 2002; Crommentuyn et al. 2003; Turner et al. 2003; Crommentuyn et al. 2004; Dailly et al. 2004; Pelerin et al. 2005; Notari et al. 2006; Choi et al. 2007; D'Avolio et al. 2007; Goldwirt et al. 2007; Takahashi et al. 2007; Verbesselt et al. 2007; Fayet et al. 2009). Reliability has been demonstrated for all concentrations tested. Moreover the use of QX as IS, an inexpensive and easy to purchase compound, improved reliability (compared to no IS) and reproducibility of the assays. The absence of interfering peaks, excluding the overlapping of DRV and APV, allowed accurate measurement of drug plasma concentrations. The APV/DRV co-elution is a negligible issue because co-administration of APV and DRV is not a current therapeutic option. Multiple channel acquisition in the range of 210–320 nm with a PDA detector allowed assessment of peak purity, ensuring the absence of interference. The choice of a specific wavelength for each drug was based on the need for adequate sensitivity and high specificity. An example is LPV, for which quantification at 260 nm was chosen to ensure the absence of interference, despite a reduction in sensitivity (Figure 2.1).

This method found application in the clinical study where a population pharmacokinetic model was developed for the evaluation of the *PXR* polymorphism on unboosted ATV plasma pharmacokinetics. Of the covariates evaluated, only the *PXR* 63396C>T was significantly correlated with ATV plasma levels, increasing the CL/F of ATV by 17.3%.

ATV pharmacokinetics was best described by a one-compartment model with first-order absorption, similar to previous studies of ritonavir-boosted ATV (Colombo et al. 2006). Although the great majority of pharmacokinetic samples were collected at

certain discrete and previously defined times (sparse data), CL/F, V/F, and in particular Ka, could be estimated with acceptable standard errors (SEs). Literature values of Ka are variable, from 0.405 to 3.4 h^{-1}, with relatively high SEs, which highlights the difficulty in evaluating the absorption phase of ATV (Colombo et al. 2006; Solas et al. 2008; Dickinson et al. 2009). Variability in Ka may be due to several factors including drug-drug interactions, lack of regard to food recommendations, other genetic variants and suboptimal adherence to treatment. In boosted treatment, ritonavir is an inhibitor of ABCB1 and CYP3A4, which are expressed both in the hepatic and intestinal tissue. Consequently RTV potentially inhibits metabolism and absorption and influences Ka. The Ka was estimated at 2.25 h^{-1}, which is in the range of the previous analysis, but with relatively low SE (0.0862 h^{-1}) as compared to studies with ritonavir -boosted ATV (Colombo et al. 2006; Solas et al. 2008; Dickinson et al. 2009). Therefore despite a limited number of samples collected in the absorption phase (3 or 4 hours after dose intake), the estimation of Ka was less variable, which might be explained by the absence of ritonavir. The lag time was 1.30 h, which was slightly higher compared to previous population pharmacokinetic models for boosted ATV (from 0.86 to 0.96 h), suggesting an effect of RTV on ATV absorption. As mentioned previously, ATV absorption can be affected by many factors, and accurate estimation of Ka and lag time can be particularly difficult with a low number of samples.

Increased bioavailability of ATV was observed for the evening dose and similar diurnal variation of plasma concentrations has previously been reported for other PIs. (Justesen 2008). Possible mechanisms include variation in physiological processes such as gastric emptying time, gastric and urinary pH, blood flow to liver and

intestine which can affect absorption and metabolism (Lemmer 2005). The pharmacokinetic parameter results in this study showed an increased CL/F compared to data obtained with boosted ATV presented in previous studies, which can be explained by considering the absence of RTV. However, the median (range) individual estimate of half-life was 4.6 h and consistent with previous reports (Colombo et al. 2006). Among the different demographic covariates tested, there was no apparent affect of age, gender and body weight on ATV PK parameters, thus confirming other data (Colombo et al. 2006; Solas et al. 2008; Dickinson et al. 2009). Here the presence of TDF did not increase the ATV clearance, which was unexpected since TDF has been shown to affect unboosted ATV concentrations (Agarwala et al. 2005). However previous population PK studies did not show any significant effect on boosted ATV concentrations (Colombo et al. 2006; Dickinson et al. 2009).

C_{trough} can be considered a predictive parameter of virologic efficacy and or toxicity for many antiretroviral drugs, and a C_{trough} value of 150 ng/mL has been proposed the MEC (DHHS 2010). However, as ATV is administered once daily and most of the patients take ATV in the evening, plasma C_{trough} is not always readily obtained consequently ATV therapeutic drug monitoring can be difficult to interpret.

The data show an association between *PXR* 63396C>T and unboosted ATV clearance which explains a proportion of the pharmacokinetic variability. The association is likely to be mediated through an effect on hepatic *PXR* expression and therefore expression of its target genes (e.g. *CYP3A4*, *ABCB1*, *ABBCs* and *SLCOs*), which are known to be involved in ATV clearance. Several transporters, such as

ABCB1, ABCCs, SLCOs mediate the passage of ATV through biological membranes and consequently have an effect on intestinal absorption, intestinal uptake and efflux into the bile. CYP3A4 is highly expressed in the hepatic and intestinal tissues and represents an important determinant of ATV metabolic rate. Several polymorphisms in these genes influence their expression or activity, potentially determining an alteration of the absorption and/or elimination of ATV. Consequently the prediction of ATV pharmacokinetics might be improved by including other genetic variables into population pharmacokinetics models.

A potential utility of pharmacogenetic testing is in optimizing dose and/or choice of regimen in different ethnicities or subpopulations. Therefore, we also investigated the frequency of the PXR 63396T allele across different ethnic groups and observed considerable differences in the frequency. Of note, the frequency of the T allele was lower in Ghanaian subjects than in Sudanese subjects. The genotype frequency was in Hardy–Weinberg equilibriumin for all the groups included in the analysis except the Sudanese subjects. This could be caused by a high degree of ethnic diversity among the people living in Sudan (Babiker et al. 2011). Also of interest was that the T allele was more frequent in Spanish individuals than in native Peruvians, and this large difference in frequency may have implications for dosing of CYP3A4 substrates in Latin America, a possibility which warrants further investigation. Conversely, no marked differences in allele frequency were observed between Thai and Caucasian individuals, and this polymorphism therefore does not explain why lower-dose-boosted ATV (200/100 mg once daily) gives pharmacokinetic parameters in Thai patients similar to those reported for the standard dose (300/100 mg OD) in Caucasians (Chetchotisakd and Anunnatsiri 2008; Avihingsanon et al. 2009).

Nonetheless the investigation of 63396 C>T effect on ATV pharmacokinetics in various ethnicities is needed before hypothesising any genotype-based dose adjustment or prospective and interventional clinical trials.

In this chapter a robust statistical method (nonlinear mixed-effects) was used to provide a better understanding of sparse datasets. In total 182 patients from three cohorts were analysed, and a correlation between ATV plasma concentrations and *PXR* 63396C>T was identified. In conclusion, the pharmacokinetic parameters of unboosted ATV in HIV patients were adequately described by the population model, which might be used to improve therapeutic drug monitoring interpretation. C_{trough} can be extrapolated from the value obtained after the absorption phase using the calculated half-life considering the patient genotype.

CHAPTER 3

SLCO3A1 expression is a determinant of atazanavir PBMC penetration in HIV infected patients treated with boosted and unboosted atazanavir

3.1 Introduction

Although plasma concentrations are used clinically as a marker of drug exposure, PIs act within HIV infected cells and therefore intracellular concentrations may be a better correlate of therapeutic efficacy. To date the factors that define PI penetration into peripheral blood mononuclear cells (PBMC) are not fully characterised (Bazzoli et al. 2010). Intracellular concentrations are influenced by the physiochemical characteristics of PIs being higher for lipophilic compounds such as nelfinavir and saquinavir (Ford et al. 2004). Furthermore, PIs are substrates for several efflux and influx transporters which may influence intracellular pharmacokinetics (Choo et al. 2000; Janneh et al. 2010). Inter-individual variability between patients is high for antiretrovirals and can be influenced by several factors such as genetic variants, induction/inhibition of transporter expression by nuclear factors and competitive interaction with other substrates.

P-glycoprotein (*ABCB1*), ATP-binding cassette, sub-family C member 1 (*ABCC1*) and 2 (*ABCC2*) are key efflux transporters expressed on PBMC. These transporters have a broad range of substrates ranging through anticancer drugs, immunosuppressive agents, antibiotics and antiretrovirals (Chan et al. 2004). Influx transporters of the solute carrier organic anion transporter (SLCO) family are also emerging as important determinants of antiretroviral pharmacokinetics (Hartkoorn et al. 2010). The only member of this family to be expressed on PBMCs is SLCO3A1 (Janneh et al. 2008).

The expression of many genes involved in xenobiotic disposition is regulated by the pregnane-X receptor (PXR, *NR1I2*). PXR has been shown to be activated by PIs (Svard et al. 2008). and influences expression of *CYP3A4* (Moore and Kliewer 2000), *ABCB1* (Geick et al. 2001) and *SLCO1B1* (Jigorel et al. 2006) in intestinal and hepatic cells. Moreover a correlation between *PXR* with *ABCB1*, *ABCC1* and *ABCC2* expression has been described in PBMC (Albermann et al. 2005).

Several reports have hypothesised a contribution of efflux/influx transporters to intracellular accumulation of PIs but there are only a limited number of reports investigating this effect *in vivo* (Bazzoli et al. 2010). The main aim of this study will be to evaluate gene expression of transporters and *PXR* in relation to the cellular accumulation of boosted and unboosted ATV. In order to achieve this a suitable method for the quantification of antiretrovirals in PBMC was developed and validated.

3.2 Methods

3.2.1 Quantification of ATV in plasma

Measurements were conducted in samples collected 20-26 hr post dose. ATV plasma concentrations were quantified using a validated HPLC-PDA method (described in chapter 2) which has been externally validated by successful participation in an international interlaboratory QC program (KKGT, the Hague, the Netherlands).

3.2.2 Quantification of ATV in PBMC

3.2.2.1 Chemicals

Compounds and chemicals were purchased as indicated in Chapter 2. Solid phase extraction (SPE) cartridges C-18 (100 mg, 40–63 mm particle size) were obtained from VWR (Milan, Italy). Blank plasma from healthy donors was kindly supplied by the Blood Bank of Maria Vittoria Hospital (Turin, Italy).

3.2.2.2 Stock solutions

Darunavir (DRV), nevirapine (NVP), iIndinavir (IDV), amprenavir (APV), saquinavir (SQV), M-8, nelfinavir (NFV), atazanavir (ATV), quinoxaline (QX) and raltegravir (RAL) stock solutions were made in a solution of methanol and HPLC grade water (90:10 vol/vol), and efavirenz (EFV), etravirine (ETV), ritonavir (RTV), and lopinavir (LPV) were made in a solution of methanol and HPLC grade water (95:5 vol/vol) to obtain a final concentration of 1 mg/mL; TPV stock solution was made with methanol to obtain a concentration of 10 mg/mL; all stock solutions were then refrigerated at 4°C until use, within 1 month. The Internal Standards (IS) working solution was prepared with QX (2 μg/mL) in methanol and HPLC grade water (50:50, v/v) and stored at 4 °C until use (maximum 1 month).

3.2.2.3 Chromatographic Conditions, Standard and QC concentrations.

The HPLC-MS instrument used was a Waters system (Milan, Italy), with binary pump model 1525, AF degasser, 717-plus autosampler, and Micromass ZQ mass detector. LC-MS Empower Pro software (version year 2002, Waters, Milan, Italy)

was used. The chromatographic separation was performed at 35°C using a column oven, on Atlantis T3 C-18 3μ column (150 x 2.1 mm I.D.; Waters, Milan, Italy), protected by a C18 Security Guard (4.0 x 3.0mm I.D.) pre-column (Phenomenex; CA, USA). The chromatographic run was performed with a gradient (Table 3.1), and the mobile phase was composed of HPLC grade water + 0.05% formic acid, for mobile phase A, and HPLC grade acetonitrile + 0.05% formic acid, for mobile phase B.

Table 3.1. Chromatographic conditions (gradient): Mobile phase: solvent A (HPLC grade water + 0.05% formic acid); mobile phase B: solvent B (HPLC grade acetonitrile + 0.05% formic acid). The flow was 0.3 ml/min.

TIME (min.)	% Mobile phase A	% Mobile phase B
0.0	59	41
0.1	58	42
2.0	45	55
4.0	40	60
9.0	30	70
9.5	25	75
9.6	5	95
14.0	5	95
14.1	95	5
15.0	95	5
15.1	70	30
25.0	60	40

Detector settings were: ESI, positive polarity ionization (except for EFV which was detected by negative polarity ionization, in the same run simultaneously using instantaneous switching); capillary voltage, 3.5 kV; source temperature 110°C; desolvation temperature 350°C; nitrogen desolvation flow 400 l/hr; nitrogen cone flow 40 l/hr. Ions detected, cone voltages, standard and QCs concentrations are listed in Table 3.2.

Table 3.2 Detected mass (Dalton), cone voltage used (Volts) and retention time (RT, in minutes) used to quantify Internal Standard and each drug, and relative concentrations from STD8 to STD1 (LOQ), QCs (QC high, QC medium and QC low) and LOD.

Drugs	TPV	IS	ETV	LPV	EFV*	RTV	ATV	DRV	APV	SQV	RGV	NFV	M-8	NVP	IDV
RT (minutes)	16.2	8.6	15.2	14.0	13.9	13.5	10.3	10.2	10.2	8.3	8.2	8.1	5.4	3.5	3.3
Mass (dalton)	603.10	313.30	434.90	629.20	313.85	580.20	705.22	548.10	506.10	671.25	445.00	568.18	584.15	267.15	614.2
Cone Voltage	28	50	60	25	30	25	33	19	18	37	30	32	35	30	42
STD 8 (ng/ml)	320	-	32	32	32	32	32	32	32	32	32	32	32	32	32
STD 7 (ng/ml)	160	-	16	16	16	16	16	16	16	16	16	16	16	16	16
STD 6 (ng/ml)	80	-	8	8	8	8	8	8	8	8	8	8	8	8	8
STD 5 (ng/ml)	40	-	4	4	4	4	4	4	4	4	4	4	4	4	4
STD 4 (ng/ml)	20	-	2	2	2	2	2	2	2	2	2	2	2	2	2
STD 3 (ng/ml)	5	-	0.5	0.5	0.5	0.5	0.5	0.5	0.5	0.5	0.5	0.5	0.5	0.5	0.5
STD 2 (ng/ml)	2.5	-	0.25	0.25	0.25	0.25	0.25	0.25	0.25	0.25	0.25	0.25	0.25	0.25	0.25
LOQ / STD 1 (ng/ml)	1.250	-	0.125	0.125	0.125	0.125	0.125	0.125	0.125	0.125	0.125	0.125	0.125	0.125	0.125
QC High	150	-	15	15	15	15	15	15	15	15	15	15	15	15	15
QC Medium	50	-	5	5	5	5	5	5	5	5	5	5	5	5	5
QC Low	10	-	1	1	1	1	1	1	1	1	1	1	1	1	1
LOD	0.15	-	0.06	0.06	0.06	0.06	0.06	0.06	0.06	0.06	0.06	0.06	0.06	0.06	0.06

3.2.2.4 Standards, Quality Controls and Sample Preparation

PBMC were isolated from 12 to 14 ml of blood using lymphoprep density gradient centrifugation (700 *g*, 25 min, 4°C with a Jouan Centrifuge, Model BR4i, Saint-Herblain, France). PBMC were then fast washed twice in 40 ml cold-ice phosphate-buffered saline and centrifuged (750 *g*, 6 min, 4°C). Cell number and mean cellular volume (MCV) were determined by a Bekman Coulter Z2 (Instrumentation Laboratory, Milan, Italy) and managed by Z2 AccuComp Software (Version 3.01, Instrumentation Laboratory, Milan, Italy). The resulting pellet of washed PBMC was dissolved with 1 ml extraction solution (methanol:water, 70:30 vol/vol), switched in two cryovials (500 µl each) and then stored at –80°C until analyses, and for no longer than three months. The time taken to process PBMC from phlebotomy to methanol extraction solution was less than 1 h, ensuring that sampling conditions were ice cold to prevent drug loss. Blank PBMC isolated from the blood of healthy donors, were stored in aliquots of around $5x10^6$ cells. The stored aliquots of STDs, QCs and patient samples PBMC were defrosted with HIV inactivation thermal treatment (58 °C for 35min). Fifty µl of IS working solution were added to each tube and the samples were vortexed for 10 s. STDs, QCs and patient tube samples were sonicated in an ice–water bath three time (cycle 0.75; amplitude 80%), to fully lyse the PBMCs, using a sonicator UP-50 H (Dr Hielscher GmbH, Teltow, Germany). After centrifugation (7000×g, 10min at 4°C), the supernatants were collected into glass tubes, and the remaining pellets were washed by vortexing for 10 s with 200 µl of acetonitrile:methanol solution (50:50, v/v). This was followed by centrifuging (7000 × g, 10 min at 4°C) and each supernatant was collected in the indicated glass tubes to be treated by vortex–vacuum evaporation to dryness at 60 °C. Each extract was reconstituted with 60 µl of HPLC-grade water and acetonitrile solution (60:40,

v/v) and 20 µl were injected into the column. For validation purposes, all samples were extracted and analyzed in duplicate. All procedure steps were carried out at room temperature, excluding that of sonication.

3.2.2.5 Validation

Interferences from endogenous compounds was investigated by analysis of six different blank PBMC. Other possible concomitant drugs were also investigated, including amodiaquine, desacetyl amodiaquine, amoxicillin, caspofungin, ceftazidime, ciprofloxacin, clavulanic acid, ethambutol, furosemide, insulin, isoniazid, levofloxacin, nimesulide, omeprazole, pravastatin, and ribavirin. Intra-day and inter-day accuracy and precision were determined by assaying 4 set of QCs in each session. Accuracy was calculated as the percent deviation from the nominal concentration. Inter-day and intra-day precision were expressed as the standard deviation at each QC concentration. The calibration curve was obtained using 8 calibration points in duplicate. A quadratic through zero calibration curve was used. The limit of detection (LOD) was defined as the concentration that yields a signal-to-noise ratio of 3:1. Percent deviation from the nominal concentration (measure of accuracy) and relative standard deviation (measure of precision) of the concentration considered as the limit of quantification (LOQ) had to be < 20%, and it was considered the lowest calibration standard, as indicated by FDA guidelines (Food and Drug Administration 2001; DHHS 2010).

Average recovery of all analytes was determined by comparing the peak area of the drug extracted from the three QCs with those obtained by direct injection of the same amount of drug in the reconstitution solution. The matrix effect was investigated

using six different blank PBMCs comparing peak areas obtained from standard solutions of water and acetonitrile (60:40, vol/vol), containing all analytes at three different concentrations, and peak areas obtained from blanks post extraction solution with the same amount of analytes (Taylor 2005). The possible matrix effect was calculated, as the deviation %, comparing the peak area obtained from the PBMC extract with the peak area obtained from the standard solution. The stability of RAL, NNRTIs, and PIs at different conditions has been assessed and assayed in several studies (Marzolini et al. 2002; Crommentuyn et al. 2003; Turner et al. 2003; Crommentuyn et al. 2004; D'Avolio et al. 2007; Merschman et al. 2007; ter Heine et al. 2009; Ter Heine et al. 2009) and for this reason, assessment of stability before assay for these drugs was not performed, but it was evaluated for post extraction conditions. Stability of drugs and IS in PBMC extracts at room temperature (20–25°C, the autosampler rack temperature) was evaluated; processed QCs, at 3 different concentrations, were analyzed immediately after preparation and after being left for 24 hours at room temperature.

3.2.3 RNA isolation and Retrotranscription

RNA was isolated from PBMC using TRIzol (Gibco BRL, Life Technologies, UK). Quality and concentration were measured spectrophotometrically, and isolated RNA was stored at −80°C until retrotranscription for no longer than 6 months. From each sample, 1 μg of RNA was used to generate complementary DNA using the MultiScribe™ Reverse Transcriptase according to the manufacturer's protocol (Applied Applied Biosystems, Foster City, CA, USA).

3.2.4 Quantification of gene expression

ABCB1, ABCC1, ABCC2, SLCO3A1 and *PXR* expression were normalised to the human acidic ribosomal protein (HuPO) which has been previously validated as the most suitable housekeeping gene for PBMC (Dheda et al. 2004). Gene expression was evaluated by relative quantification and PCR amplification was carried out in a 20-μL reaction volume containing template cDNA equivalent to 10 ng of RNA, TaqMan® Gene Expression Master Mix and primer and probes from TaqMan® Gene Expression Assays (Hs01067802_m1 for *ABCB1*, Hs00166123_m1 for *ABCC2*, Hs00243666_m1 for *PXR*, Hs00203184_m1 for *SLCO3A1*, Hs00219905_m1 for *ABCC1*; Applied Applied Biosystems, Foster City, CA, USA) following manufacturer's specification. Specifically the ingredients of a 20 μL reaction were: 2 μL of 10X TaqMan RT Buffer, 4.4 μL 25mM Magnesium Chloride, 4 μL of deoxyNTPs Mixture, 1 μL Random Hexamers, 0.4 μL RNase Inhibitor and 0.5 μL of MultiScribe Reverse Transcriptase (50 U/μL); the Reverse Transcriptase was activated at 95°C for 10 min and subsequently 50 cycles with a denaturation phase of 15 sec at 95°C and annealing/extension phase of 1 min at 60°C.

3.2.5 Patients

Inclusion criteria were: receiving unboosted ATV (400 mg once a day) or boosted ATV (300mg with 100mg of RTV), older than 18 years, not receiving drugs known to alter plasma concentration of ATV, such as proton pump inhibitors or non-nucleoside reverse transcriptase inhibitors, adherence >95% assessed by analyses of clinical and pharmacy records. Patients were recruited in Torino, Italy and sampling was done after obtaining written informed consent according to local Ethics

Committee indications. All samples were obtained under steady-state conditions. The following covariates were available: age, gender, body weight, ethnicity, other coinfections, time post-dose, time of sample, concomitant ARVs and other medications.

3.2.6 Statistical analysis

Results for categorical data are expressed as median with interquartile range (IQR). All data were assessed for normality using a Shapiro-Wilk test and categorical data were compared using a Mann Whitney statistical test. To investigate continuous data, a Pearson or Spearman correlation was used. Bonferroni correction was applied for multiple comparisons.

3.3 Results

3.3.1 Validation of HPLC-MS method for quantification of antiretrovirals in PBMCs

Analyte retention times were: IDV 3.3 ± 0.1 min NVP 3.5 ± 0.1 min, M-8 5.4 ± 0.1 min, NFV 8.1 ± 0.1 min, RGV 8.2 ± 0.1 min, SQV 8.3 ± 0.1 min, APV 10.2 ± 0.1 min, DRV 10.2 ± 0.1 min, ATV 10.3 ± 0.1 min, RTV 13.5 ± 0.1 min, EFV 13.9 ± 0.1 min, LPV 14.0 ± 0.1 min, ETV 15.2 ± 0.1 min, IS 8.6 ± 0.1 min, TPV 16.2 ± 0.1 min. APV and DRV eluted at the same retention time, due to their similar chemical structure and physiochemical properties, but this co-elution did not affect the quantification of the two drugs. Representative chromatograms of a blank PBMCs extracted and STD1 are shown in Figure 3.1.

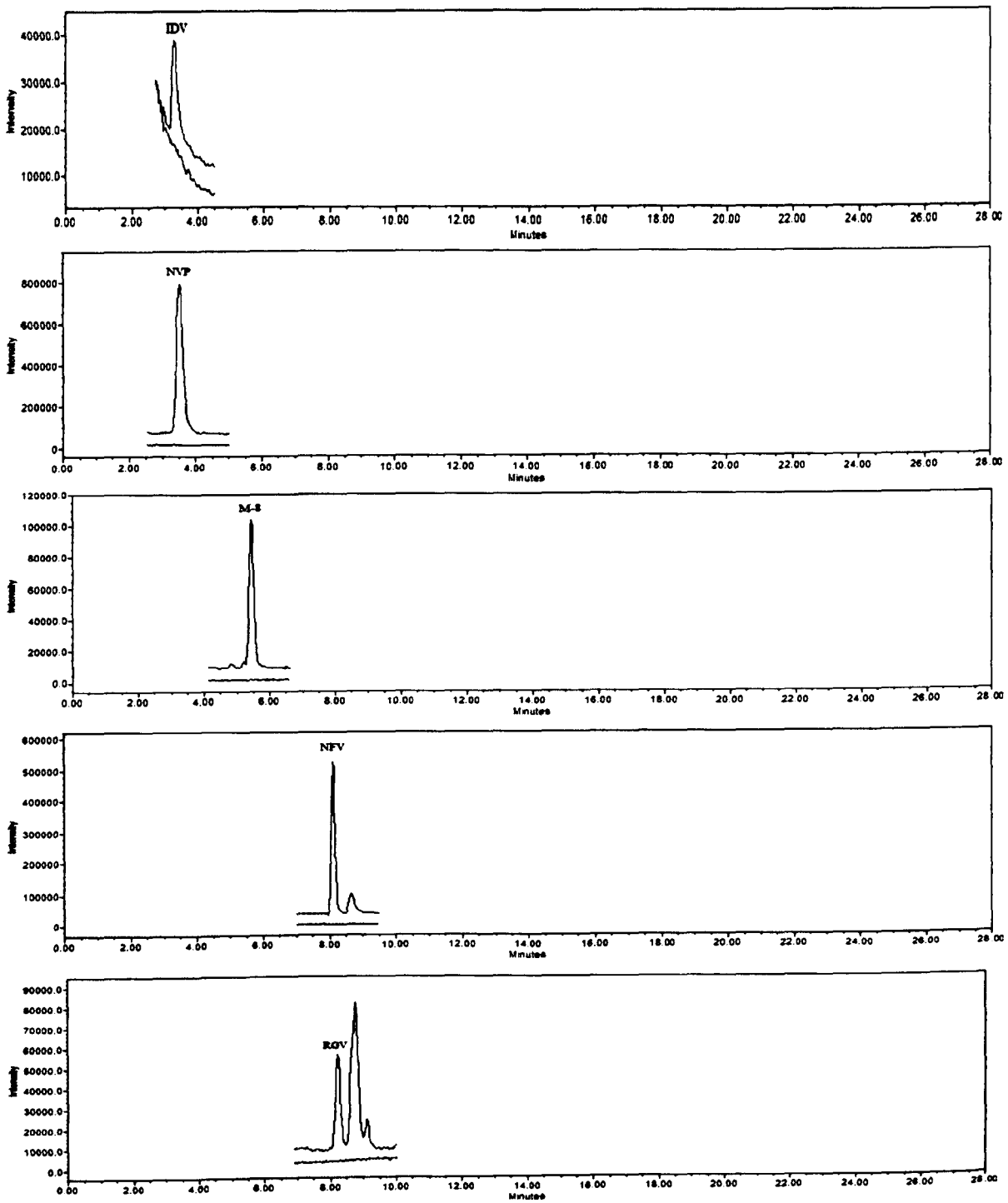
IDV
NVP
M-8
NFV
RGV
Intensity
Minutes

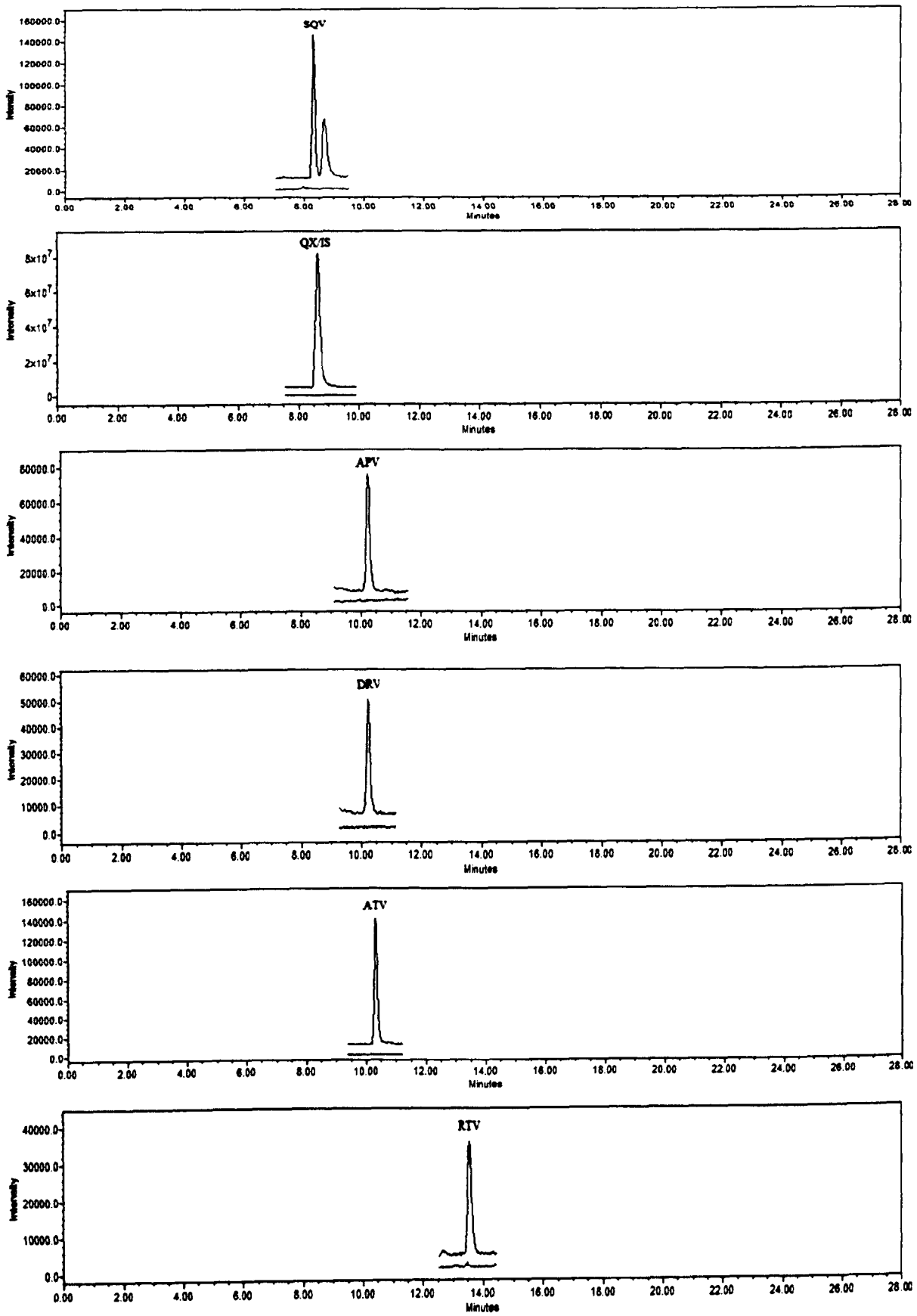
SQV
QX/IS
APV
DRV
ATV
RTV
Intensity
Minutes

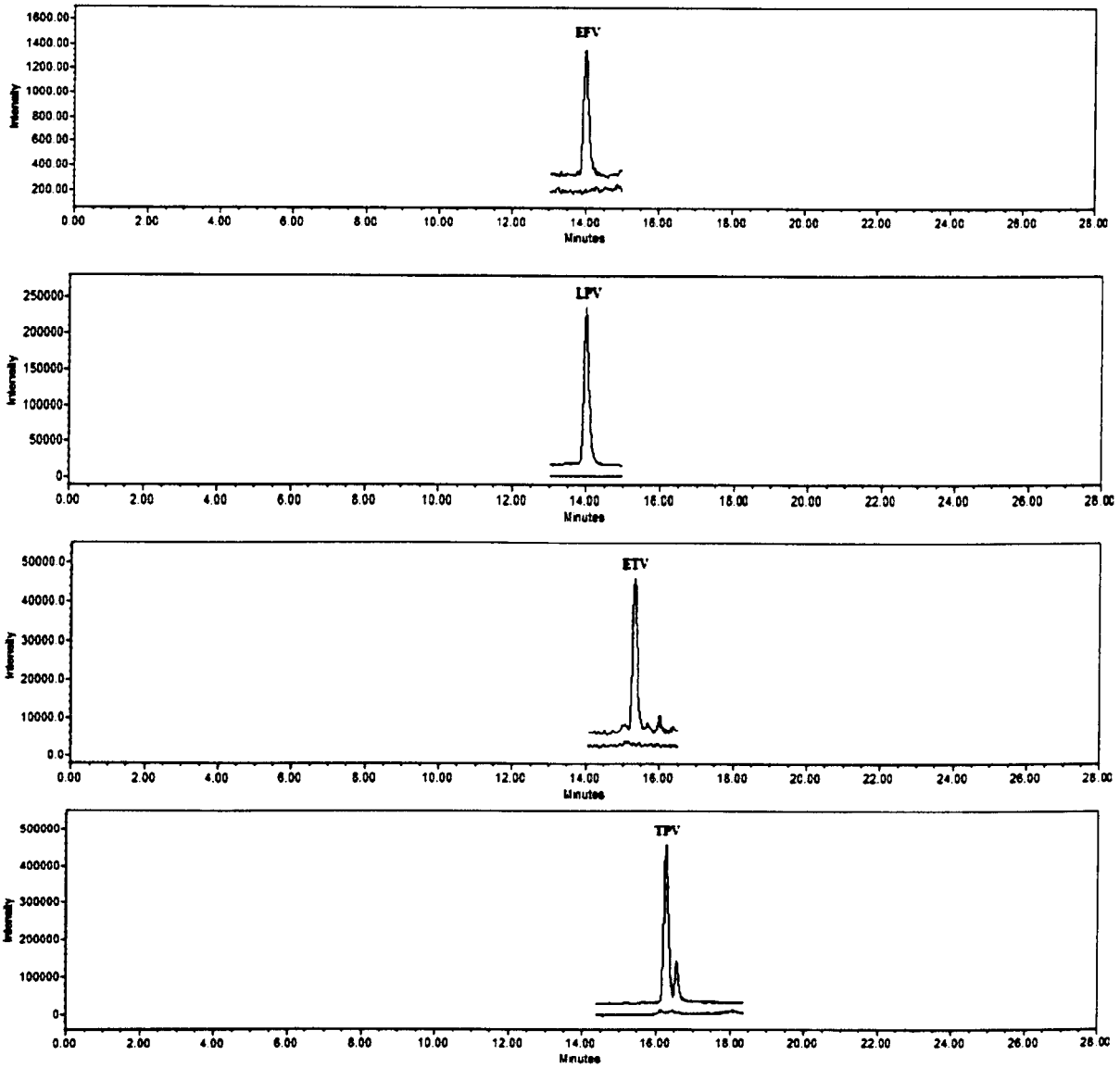

Figure 3.1. Overlapping of SDT1 and blank PBMCs extracted ions detection.

The assays did not show any relevant interference with antiretrovirals or other concomitant drugs administered to the patients at therapeutic doses. Mean regression coefficient (r^2) of all calibration curves was higher than 0.998. A $1/X$ weighted quadratic regression was chosen due to its r^2 higher than other equations. The results of the validation of the methods are listed in

Table 3.3 for all analytes. All observed data (Intraday and Interday precision [RSD%]) were below 15.0 %, according to FDA guidelines. Results of the validation of the method is listed in

Table 3.3.

Table 3.3. Accuracy (%), Intraday and Interday Precision (RSD%) for all drugs (n=6).

	QC High			QC Medium			QC Low		
		Precision (RSD%)			Precision (RSD%)			Precision (RSD%)	
Drugs	Acc %	Intraday	Interday	Acc %	Intraday	Interday	Acc %	Intraday	Interday
IDV	4.80	5.29	9.14	8.94	9.19	9.48	-2.76	9.70	14.89
NVP	-3.44	6.25	10.30	9.70	6.36	10.80	5.81	7.79	13.96
M-8	2.67	4.55	7.82	9.54	6.66	7.94	5.79	7.48	11.48
NFV	1.73	6.29	7.24	6.29	8.22	10.35	9.43	12.92	11.21
SQV	7.41	4.39	8.50	8.39	11.97	10.91	5.55	7.57	8.81
RGV	8.19	2.60	7.27	8.35	3.42	5.92	-0.87	14.02	14.46
APV	3.08	5.22	6.37	4.42	5.74	10.59	-2.22	9.52	13.48
DRV	-2.18	6.04	11.71	-1.33	5.04	10.97	-1.64	11.14	14.70
ATV	3.88	3.41	6.42	1.57	5.40	8.85	-3.44	9.69	13.76
RTV	2.49	4.43	4.84	3.68	6.04	6.89	-7.85	11.63	10.56
LPV	-3.41	4.00	10.11	1.70	8.77	10.36	7.42	10.75	10.21
EFV	0.17	7.13	10.25	0.93	7.72	9.69	-6.24	8.65	12.22
ETV	0.26	3.84	3.99	3.74	7.12	10.01	-1.13	9.82	13.13
TPV	3.04	3.88	9.41	8.38	11.09	11.80	8.38	11.09	11.80

Mean recovery of all drugs ranged from 76% to 98% (mean CV 6.7%). Mean IS recovery was 92% (mean CV 4.3%). For matrix effect, the deviation % of the peak area at the three concentrations for all analytes was comparable, ranging from – 17.0% to + 8.8% (mean -3.1%), showing the absence of a "matrix effect". The lowest

percentage (-17%) was related to IDV, which has the shortest retention time and could be potentially affected by poor column retained analytes. The stability study of drugs and IS in PBMC extracts, kept for 24 hours in the autosampler rack at room temperature, showed a variation of less than 7% for IS and all drugs at each concentration.

3.3.2 Evaluation of mean cellular volume of PBMC of HIV positive patients

Included were patients from the current study (n=30) and an additional cohort of 56 patients. MCV (±CV%) from 86 patients (200 samples) was 282.5 fl (232.5–341.2) as summarised in Figure 3.2.

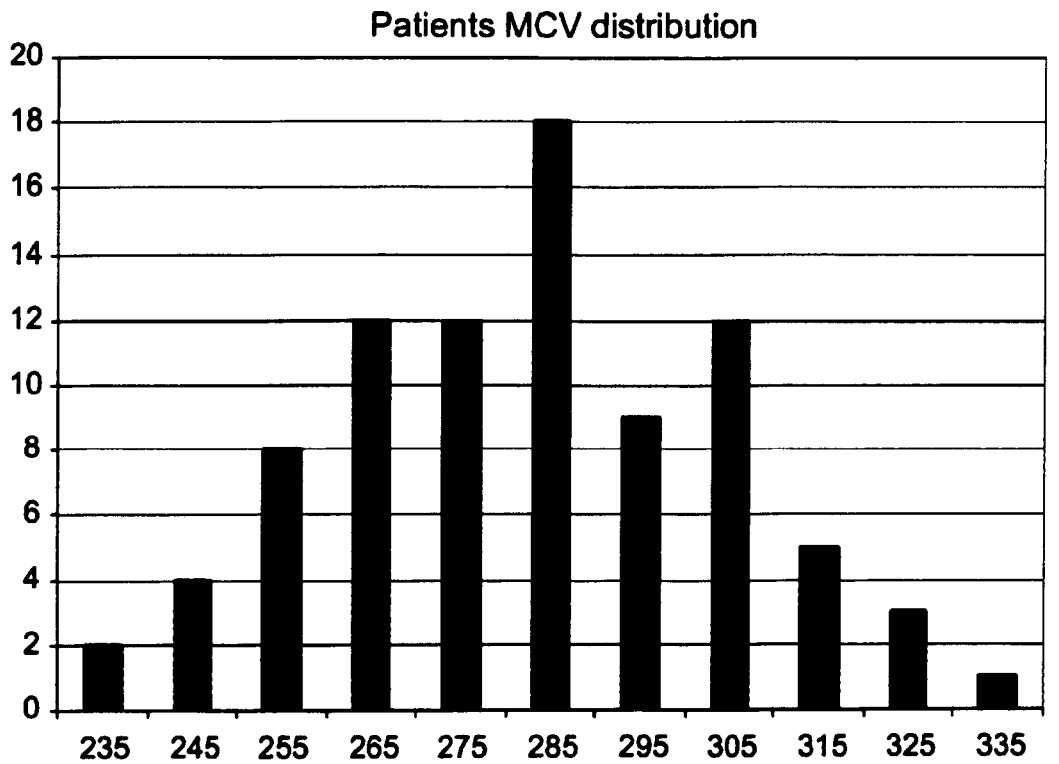

Figure 3.2. Distribution of patient MCV. 86 samples were clustered in 11 classes according to MCV value and their frequencies plotted.

3.3.3 Gene expression analysis

A standard curve was constructed using reference cDNA (Clontech Laboratories Inc., Mountain View, CA, USA) and values were within a linear range for all genes ($r^2 > 0.991$) as shown in Figure 3.3 for *ABCB1*.

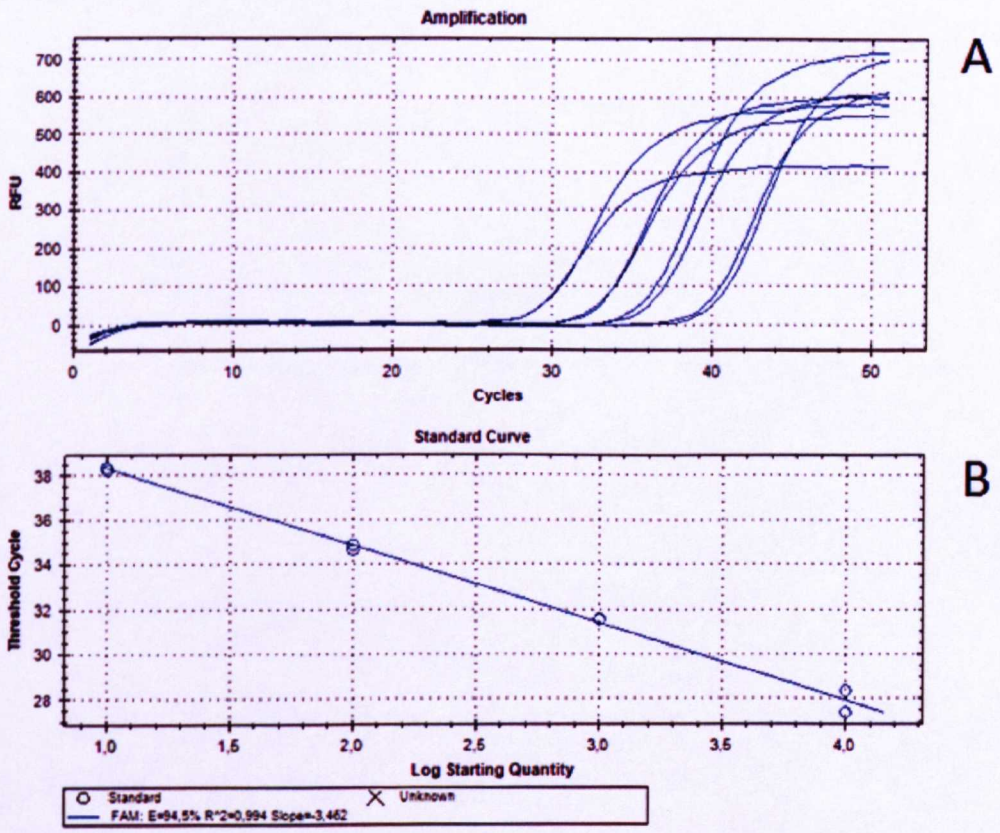

Figure 3.3. Representative amplification of *ABCB1* at different concentrations of reference cDNA (1µg to 1 ng). A) amplification curves of four serial dilutions of

reference cDNA; Y axis represents fluorescence and X axis number of cycles and B) linearity of amplifications; Y axis threshold cycle and X concentration of cDNA.

Amplification of all genes had minor variability, as shown in Figure 3.4 and all patients had a threshold cycle inferior to 36 cycles.

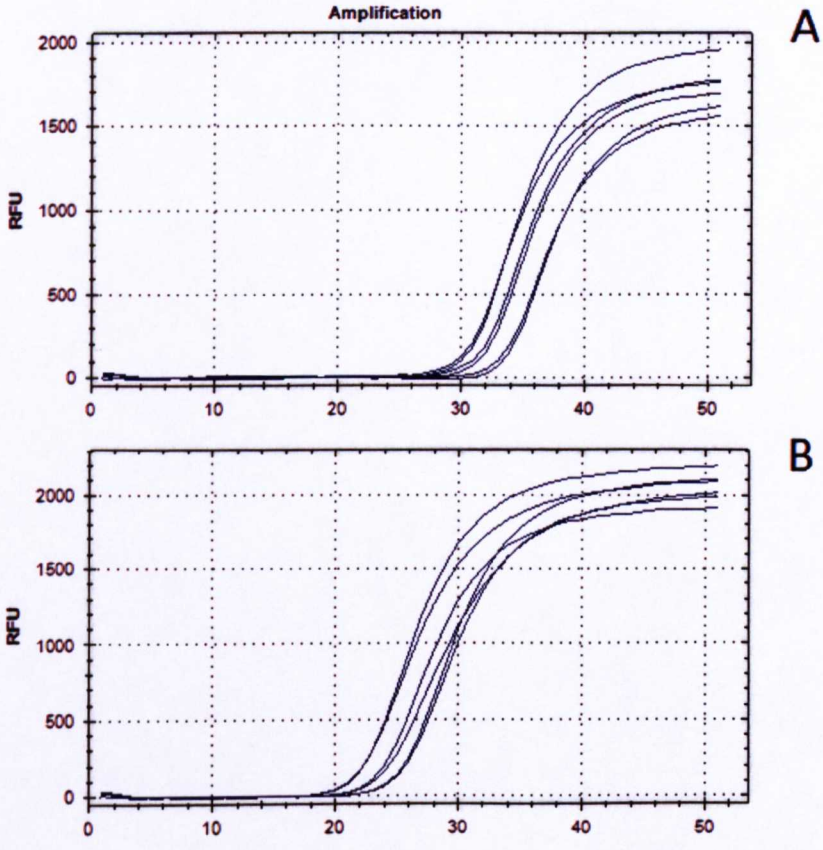

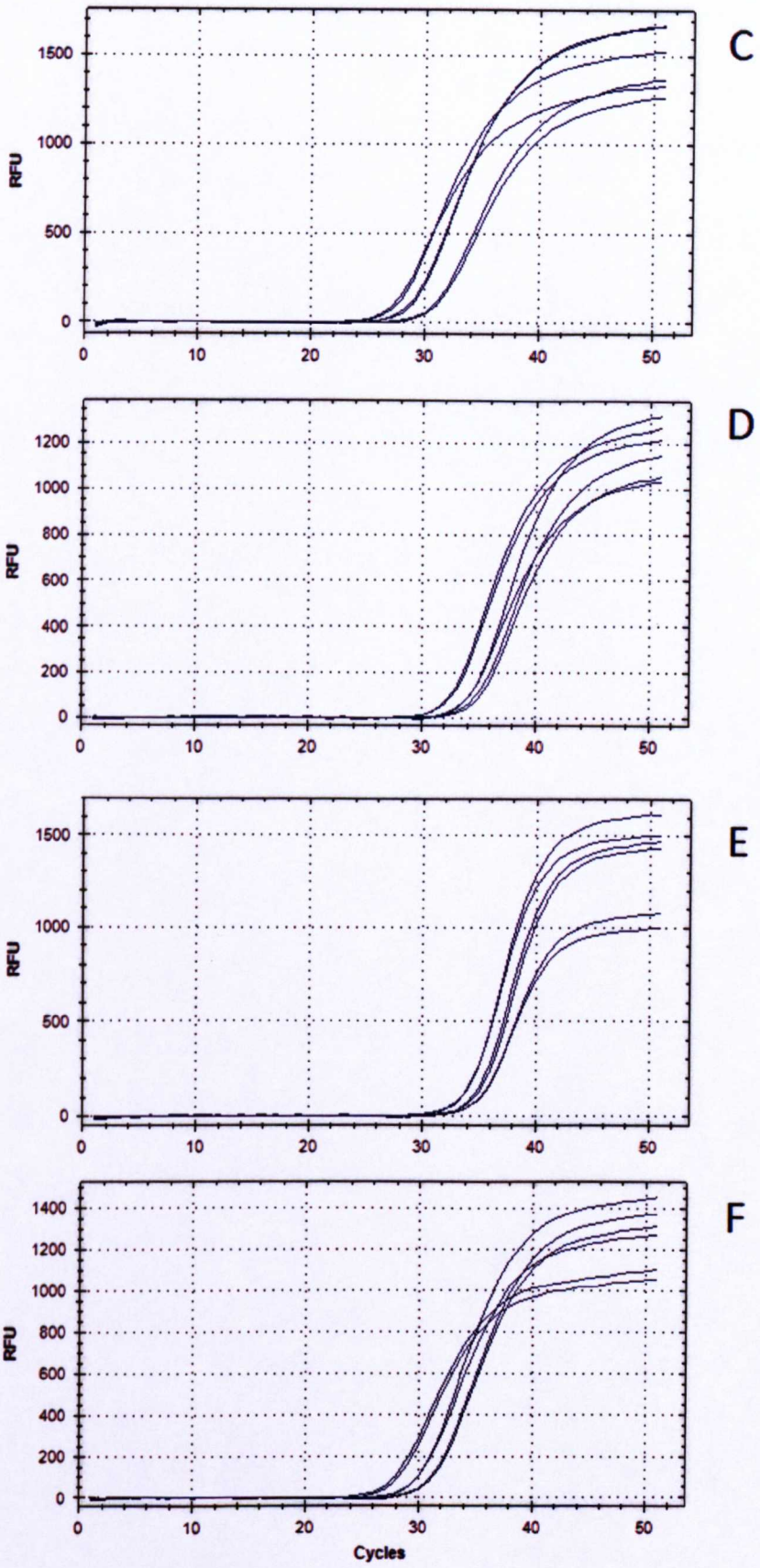
C
RFU
1500
1000
500
0
0
10
20
30
40
50
D
RFU
1200
1000
800
600
400
200
0
0
10
20
30
40
50
E
RFU
1500
1000
500
0
0
10
20
30
40
50
F
RFU
1400
1200
1000
800
600
400
200
0
0
10
20
30
40
50
Cycles

Figure 3.4. Representative amplification of genes in three patients A) *ABCB1*, B) *HuPO*, C) *SLCO3A1*, D) *ABCC2*, E) *PXR*, F) *ABCC1*. Y axis represents fluorescence and X axis number of cycles.

3.3.4 Clinical study

30 Caucasian patients met the inclusion criteria and were included in the study. 17 patients were treated with unboosted ATV and 13 patients with boosted ATV. Median age was 46 years (IQR, 35 - 55), median BMI was 23.1 kg/m2 (IQR, 20.9 – 29.5). 25 (83%) patients were male.

For patients treated with unboosted ATV, median plasma concentrations were 134 ng/ml (IQR, 99 - 171) and intracellular concentrations were 322 ng/ml (IQR, 165 - 448), as shown in Figure 3.5.

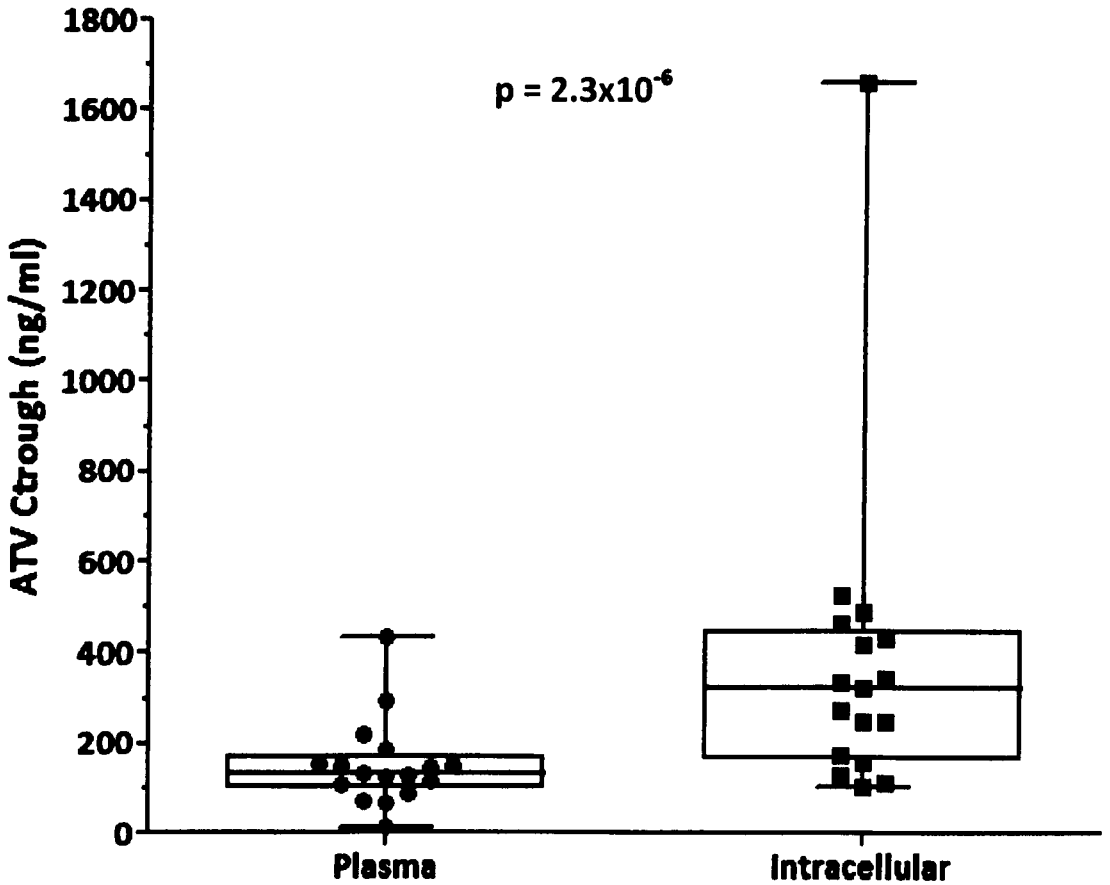

Figure 3.5. ATV plasma and intracellular C_{trough} in 17 patients on unboosted ATV. Median values (horizontal line), IQR (bars), patient values (black dots for plasma values and squares for intracellular values), highest and lowest value (whiskers) are given.

Median cellular accumulation ratio (CAR) was 1.92 (IQR, 1.39 – 4.71), as shown in Figure 3.6, suggesting that ATV accumulates inside PBMC.

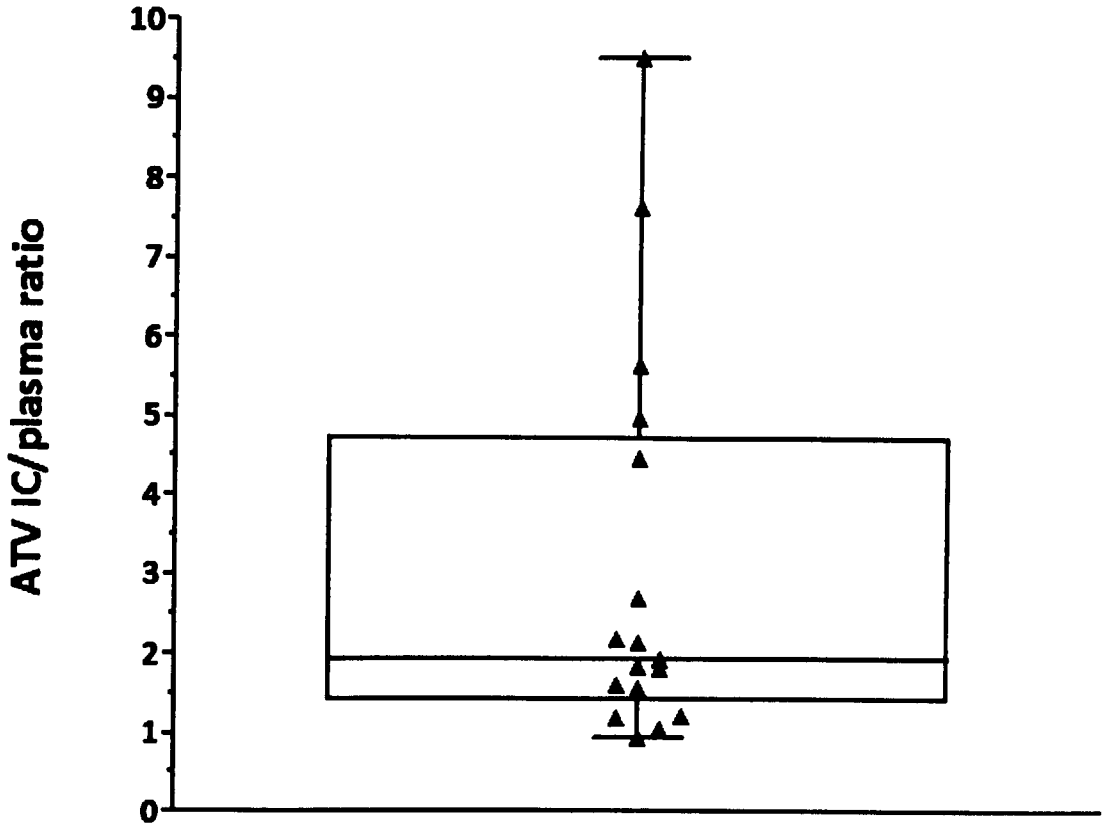

Figure 3.6 ATV CAR in 17 patients on unboosted ATV. Median values (horizontal line), IQR (bars), patient values (black square), highest and lowest value (whiskers) are given.

No association between demographic or physical characteristics such as age, weight, height, BMI and plasma, and intracellular ATV C_{trough}, and accumulation ratio were observed. Plasma ATV C_{trough} were not correlated with weight (rho= 0.24 p=0.35), height (rho= 0.20 p=0.44), age (rho = 0.39 p=0.12), BMI (rho = 0.23 p=0.38). Similarly, intracellular ATV C_{trough} were not correlated with weight (rho = -0.09, p=0.73), height (rho = -0.84, p = 0.75), age (rho = 0.22, p = 0.39), BMI (rho = -0.11, p=0.67). CAR were not correlated with weight (rho= 0.34, p=0.18), height (rho= 0.02, p = 0.93), age (rho = -0.13, p = 0.63), BMI (rho = -0.42, p = 0.09). Intracellular concentrations were not correlated with plasma concentrations, as shown in Figure 3.7 (rho = -0.36, p = 0.155).

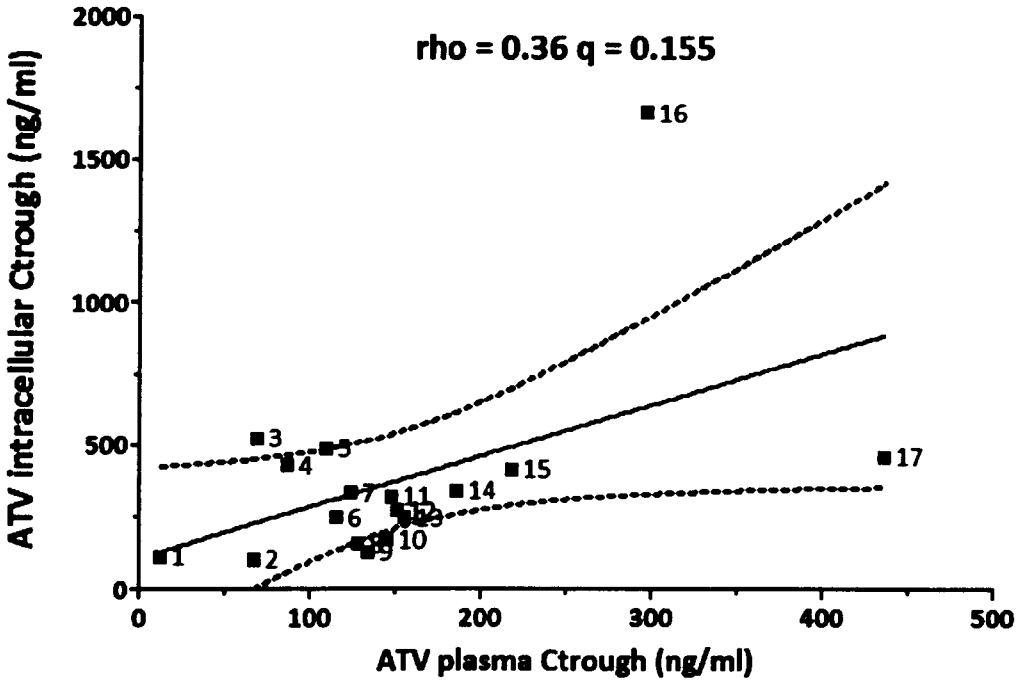

Figure 3.7. Scatter plot representing the correlation between ATV plasma and intracellular C_{trough} in 17 patients on unboosted ATV. Patient values (black dots), linear regression (filled line) and 95% CI (dotted line) are given.

For patients treated with boosted ATV, median plasma concentrations were 543 ng/ml (IQR, 430 - 724), intracellular concentrations were 1461 ng/ml (IQR, 872 - 2344) as shown in Figure 3.8. Median CAR was 2.45 (IQR, 1.91 – 5.88), as shown in Figure 3.9.

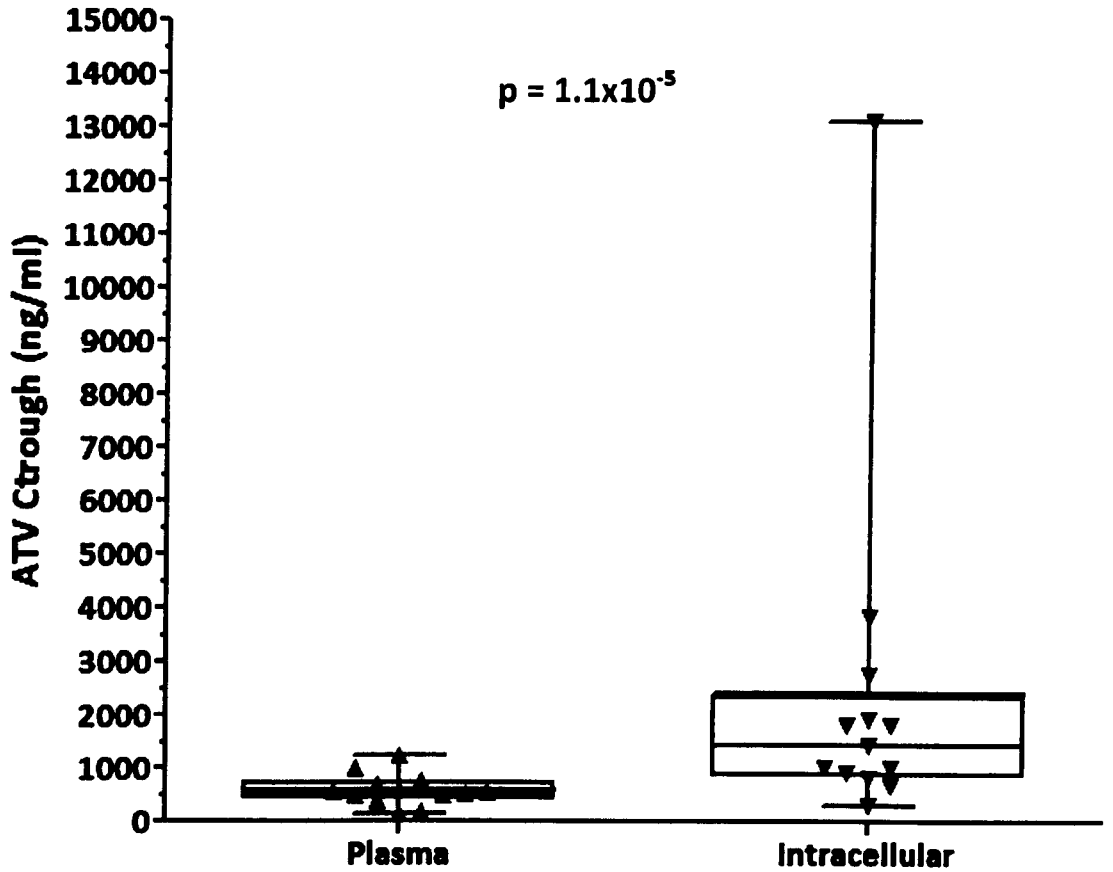

Figure 3.8. ATV plasma and intracellular C_{trough} in 13 patients on boosted ATV. Median values (horizontal line), IQR (bars), patient values (black dots for plasma values and square for intracellular values), highest and lowest value (whiskers) are given.

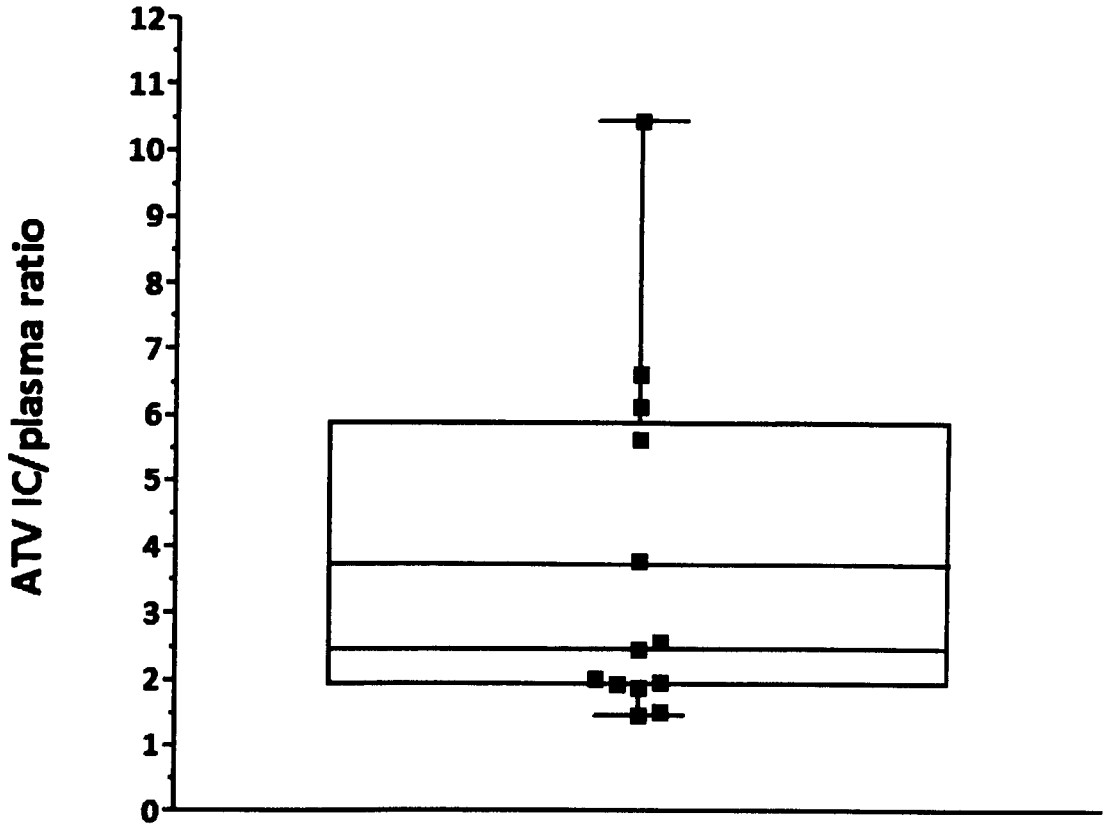

Figure 3.9. ATV CAR in 13 patients on boosted ATV. Median values (horizontal line), IQR (bars), patient values (black square), highest and lowest value (whiskers) are given.

No association between demographic or physical characteristics such as age, weight, height, BMI and plasma and intracellular ATV C_{trough} and CAR were observed. In more detail, plasma ATV C_{trough} were not correlated with weight (rho = 0.29 p = 0.32), height (rho = 0.28 p = 0.36), age (rho = 0.51 p = 0.08) or BMI (rho = 0.26 p = 0.39).

Similarly, intracellular ATV C_{trough} were not correlated with weight (rho = 0.15, p = 0.63), height (rho = 0.01, p = 0.99), age (rho = 0.18, p = 0.56 or, BMI (rho = 0.12, p = 0.69).

CAR was not correlated with weight (rho= -0.27, p=0.38), height (rho= -0.12, p=0.68), age (rho= -0.31, p=0.30) or BMI (rho= -0.36, p=0.23). For patients treated with boosted ATV, ATV intracellular concentrations were correlated with ATV plasma concentrations (rho=0.687 p=0.003, as shown in Figure 3.10), and intracellular RTV (rho=0.819, p=0.003) concentrations.

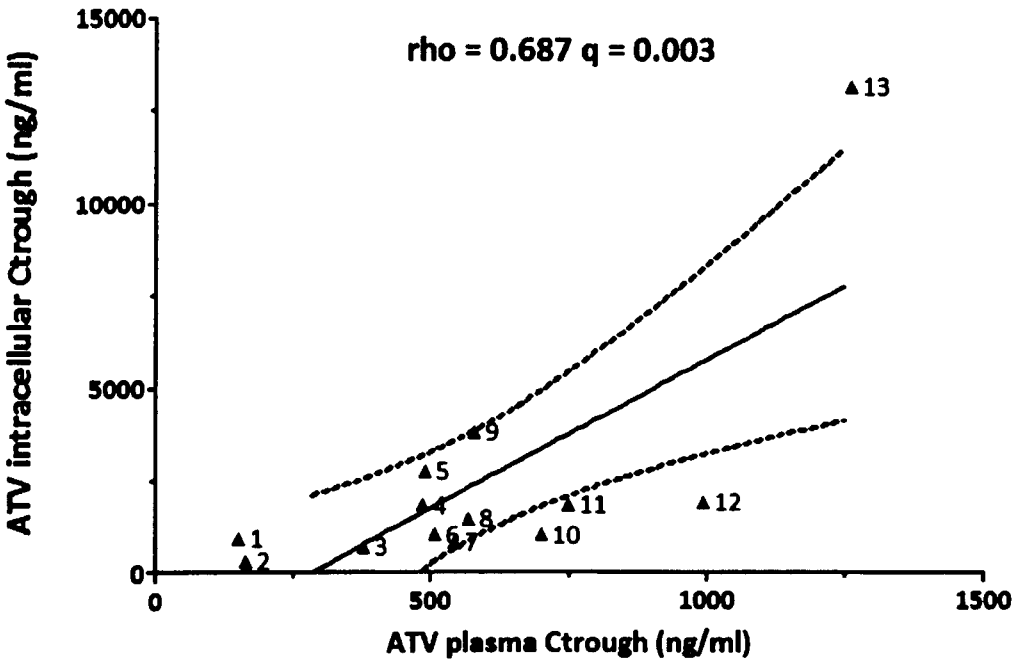

Figure 3.10. Scatter plot representing the correlation between ATV plasma and intracellular C_{trough} in 13 HIV patients on boosted ATV. Patient values (black dots), linear regression (filled line) and 95% CI (dotted line) are given.

ABCB1, *ABCC1* and *SLCO3A1* expression was detectable in all samples; *PXR* expression was detectable in 26 out 30 samples and *ABCC2* in 28 out 30 samples. *PXR* expression was correlated with *ABCB1* (rho = 0.467, p = 0.046), ABCC1 (rho = 0.797, p = 6.95E-07), *ABCC2* (rho = 0.856, p = 8.52E-09), *SLCO3A1* (rho = 0.830, p = 7.14E-08), as summarised in Table 3.4. Expression of transporters and *PXR* did not

differ between the two treatment groups (*ABCB1* p = 0.785, *ABCC1* p = 0.156, *ABCC2* = 0.156, *PXR* p = 0.111 and *SLCO3A1* p = 0.111).

Table 3.4 Correlations between gene expression. Bonferroni correction was applied for multiple comparisons. *p<0.05, **p<0.01

		SLCO3A1	ABCC2	ABCC1	ABCB1
PXR	rho	0.830 **	0.856 **	0.797 **	0.467 *
	p value	7.14E-09	8.52E-10	6.95E-08	4.65E-03
	corrected p value	7.14E-08	8.52E-09	6.95E-07	4.65E-02
ABCB1	rho	0.602 **	0.530 **	0.560 **	
	p value	2.15E-04	1.29E-03	6.46E-04	
	corrected p value	2.15E-03	1.29E-02	6.46E-03	
ABCC1	rho	0.939 **	0.819 **		
	p value	9.09E-15	1.55E-08		
	corrected p value	9.09E-14	1.55E-07		
ABCC2	rho	0.825 **			
	p value	1.06E-08			
	corrected p value	1.06E-07			

For patients treated with unboosted ATV, two genes were significantly correlated with cellular accumulation ratio. *PXR* (rho = 0.736. p = 0.005) and *SLCO3A1* (rho = 0.706. p = 0.010), as shown in Figure 3.11 and Figure 3.12, respectively. For patients on boosted ATV, two genes were significantly correlated with cellular accumulation ratio, *ABCC1* (rho = 0.830. p = 0.005) and *SLCO3A1* (rho = 0.846. p = 0.001), as shown in Figure 3.13 and Figure 3.14, respectively.

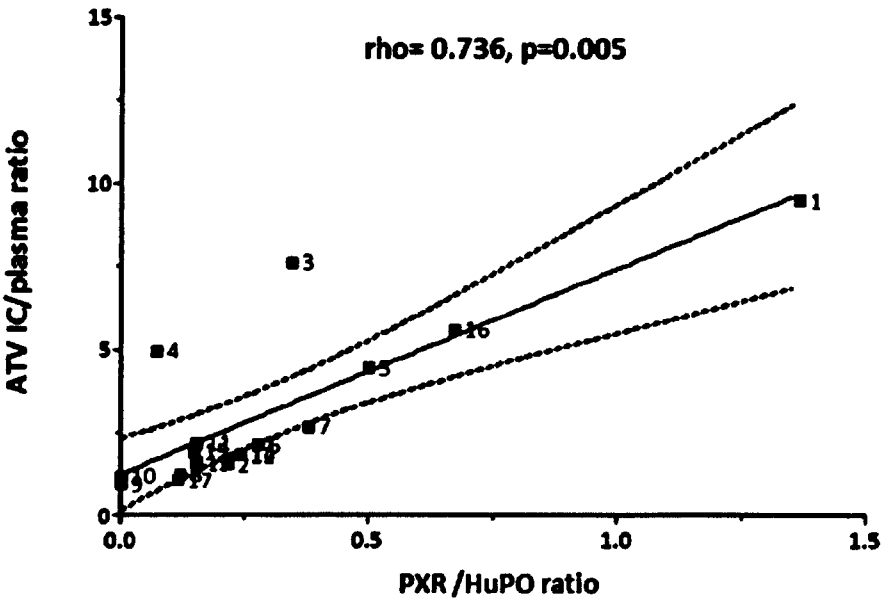

Figure 3.11 Scatter plot representing the correlation between ATV CAR and *PXR* expression in 17 HIV patients on unboosted ATV. Patient values (black dots), linear regression (filled line) and 95% CI (dotted line) are given.

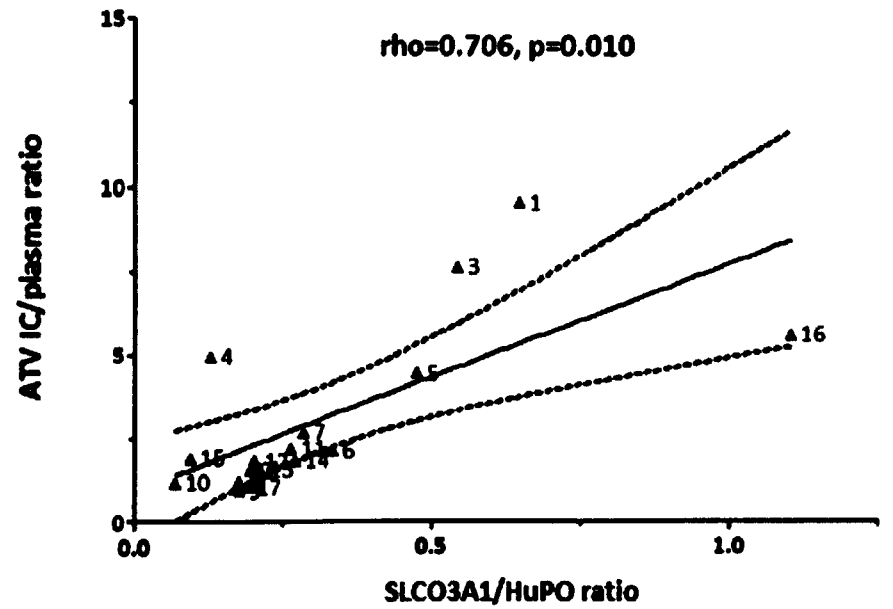

Figure 3.12. Scatter plot representing the correlation between ATV CAR and *SLCO3A1* expression in 17 HIV patients on unboosted ATV. Patient values (black dots), linear regression (filled line) and 95% CI (dotted line) are given.

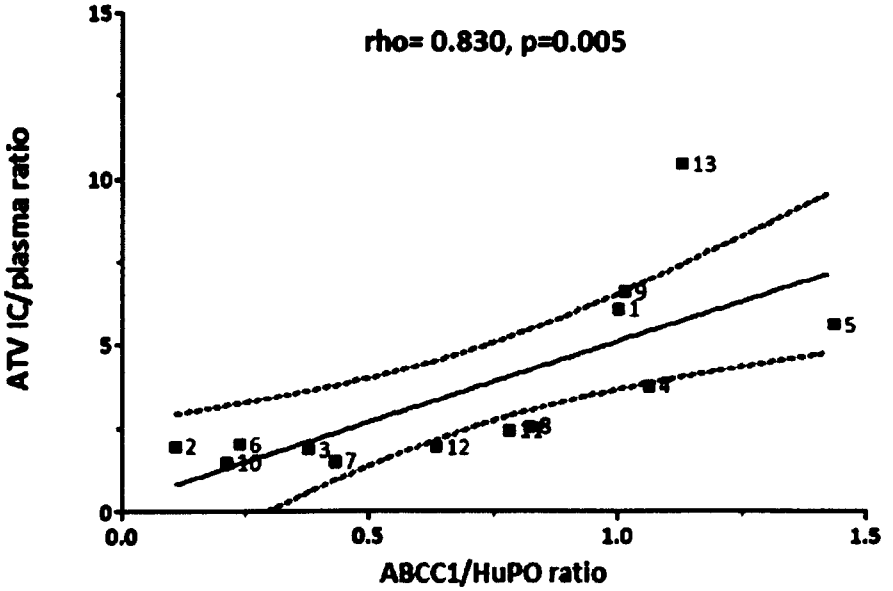

Figure 3.13. Scatter plot representing the correlation between ATV CAR and *ABCC1* expression in 13 HIV patients on boosted ATV. Patient values (black dots), linear regression (filled line) and 95% CI (dotted line) are given.

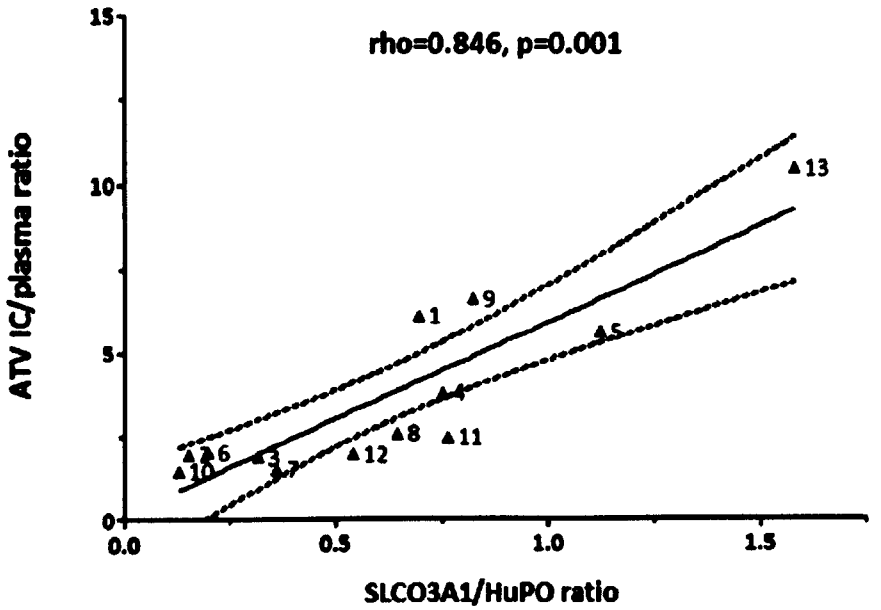

Figure 3.14. Scatter plot representing the correlation between ATV CAR and *SLCO3A1* expression in 13 HIV patients on boosted ATV. Patient values (black dots), linear regression (filled line) and 95% CI (dotted line) are given.

3.4 Discussion

Most antiretrovirals (with the exception of entry inhibitors) inhibit viral replication inside cells and as such intracellular pharmacokinetics is likely to be a key determinant of therapeutic efficacy. Intracellular pharmacokinetics are likely to impact on the efficacy and toxicity of antiretroviral treatments and are potentially influenced by several factors such as binding to plasma proteins, intracellular-free fraction, influx and efflux transporters and intracellular drug metabolism.

To date, intracellular drug levels have not been fully investigated *in vivo*, due to methodological difficulties and the relatively large volumes of blood required. However, standardized methods have to be applied, and there is no reference technique for measuring intracellular drug concentrations.

A novel HPLC-MS method has been developed and validated in this chapter. To increase the recovery and sensitivity of extraction, two additional steps were added to the extraction procedure: namely, PBMC sonication and a 100% organic extraction treatment. In fact, the storage at −80 °C in water:methanol (30:70) lead to a first PBMC lyses and the sonication step allowed to fully lyse PBMC membranes. The remaining pellets from sonication and centrifugation were washed by vortexing for 10 s with 200 µl of acetonitrile:methanol organic solution (50:50). This step was required in order to avoid loss of lipophilic drugs such as LPV, ETV and TPV. The extraction steps were therefore optimized to reach a low limit of quantification for all the drugs, below the clinically relevant range of concentrations encountered in patient PBMC contained in 12–14 ml blood (Hennessy et al. 2003; Breilh et al. 2004;

Crommentuyn et al. 2004; Ford et al. 2004; Ford et al. 2004; Hennessy et al. 2004; Colombo et al. 2005; Colombo et al. 2006; Djabarouti et al. 2006; Ford et al. 2006; Elens et al. 2009; ter Heine et al. 2009; Ter Heine et al. 2009; Ter Heine et al. 2009).

The extraction procedure and the HPLC–MS method here described allow accurate and reproducible simultaneous quantification of fourteen antiretroviral agents in PBMC by a single assay. A low blood volume, good extraction efficiency and a low limit of quantification make this a suitable method for use in clinical trials and for the study of intracellular concentrations of RAL, PIs and NNRTIs, including ETV. Moreover the observed mean MCV from 86 patients (200 samples) was 282.5 fl (SD = 22.4, min 232.5–max 341.2, CV% = 7.9) as summarized in Figure 3.2. The mean MCV value was around 30% lower than the 400 fl (Gao et al. 1993), used in most methodological and clinical publications (Hennessy et al. 2003; Breilh et al. 2004; Crommentuyn et al. 2004; Ford et al. 2004; Ford et al. 2004; Hennessy et al. 2004; Colombo et al. 2005; Colombo et al. 2006; Djabarouti et al. 2006; Ford et al. 2006; Elens et al. 2009; ter Heine et al. 2009; Ter Heine et al. 2009; Ter Heine et al. 2009). Use of the latter as a presumptive standard value could significantly bias the method of quantification, and consequently previous reports could have potentially underestimated intracellular drug exposure. The PBMC volume varies according to the state of the cells (quiescent or stimulated) or the nature of the cells (cell volume of human lymphoblast: around 2.1 pl) (Bazzoli et al. 2010). This suggests that the calculation of individual MCV gives a more accurate and reliable tool to quantify intracellular antiretroviral drugs concentrations.

In the current study we investigated intracellular concentrations of ATV in a cohort of 30 patients, treated with boosted or unboosted regimens. An accumulation of ATV in PBMC was observed in all patients, indicating a role for influx transporters in this phenomenon, with a median cellular accumulation ratio of 1.92 (IQR, 1.39 – 4.71) for patients treated with unboosted ATV and 2.45 (IQR, 1.91 – 5.88), for patients on boosted ATV.

SLCO3A1 expression was correlated with ATV accumulation in both cohorts, rho=0.706, p=0.010 for patients on unboosted ATV and rho = 0.830. p = 0.005 for patients on boosted ATV. Although there is no direct evidence that PIs are SLCO3A1 substrates we have shown that they are substrates for at least 3 other members of this family, SLCO1B1, SLCO1B3 and SLCO1A2 (Hartkoorn et al. 2010). Furthermore, previous studies have indicated a role for SLCO transporters in lymphocytes (Janneh et al. 2008; Janneh et al. 2009).

Intracellular concentrations of ATV did correlate with plasma concentrations in patients on boosted ATV but not for patients treated with unboosted ATV, indicating that RTV may influence cell specific mechanisms regulating penetration of ATV to its target cells. Another factor that can potentially influence intracellular concentrations of PIs is the activity of *PXR*, which regulates the expression of several transporter/enzymes involved in drug disposition. PXR is expressed in several tissues such as liver, intestine, lung, and PBMC where it plays an important role in xenobiotic sensing and acts as a master regulator of detoxifying phase I and II enzymes. The correlation between *PXR* and *SLCO3A1* reported here suggests that *PXR* may also regulate transcription of this transporter. Our data confirm the role of

PXR in regulation of the *ABCB1*, *ABCC1* and *ABCC2* transcription in PBMC (Albermann et al. 2005).

SLCO3A1 could represent a novel pharmacological target in the treatment of HIV infection. Induction of its expression could enhance the influx of ATV and potentially other PIs, causing higher intracellular concentrations, and consequently favour the inhibition of viral replication. The expression of *SLCO3A1* on PBMC could be screened prior to antiretroviral selection in order to identify patients with a better chance to have higher PBMC accumulation of ATV and other PIs.

However the correlation between ATV intracellular pharmacokinetics and SLCO3A1 mRNA expression does not constitute definitive evidence for the role of SLCO3A1 in ATV PBMC accumulation. Further data on protein expression and SLCO3A1 activity are needed in order to fully elucidate SLCO3A1 relevance. Inclusion of more patients could increase the statistical power of the study and clarify the importance of proteins involved in the regulation of PI intracellular pharmacokinetics.

Identification of SNPs with an impact on *SLCO3A1* expression and activity could be the basis for future pharmacogenetic studies. rs1517618 C/G, which causes a Asp/Glu transition, rs72655652 A/C, coding for a Arg/Ser transition, and rs3924426 recently investigated in a whole genome association study and correlated with a QT prolongation during iloperidone treatment of schizophrenia (Volpi et al. 2009) are good potential candidates to affect *SLCO3A1* activity and could influence the definition of intracellular pharmacokinetics.

Potential drug-drug interactions could be mediated by *SLCO3A1* and requires further investigation. Recently SLCOs have emerged as key determinants of drug-drug interactions for numerous drugs; primarily inhibition of drug hepatic uptake by *SLCO1B1* can lead to increased plasma concentrations (Niemi et al. 2001; Kajosaari et al. 2005; Kajosaari et al. 2006; Kalliokoski et al. 2008). A similar mechanism could also potentially influence the SLCO3A1 uptake activity in PBMC, giving a lower intracellular accumulation in patients treated with SLCO3A1 inhibitors and consequently affecting ATV antiretroviral activity.

To summarise, these data suggest that the SLCO3A1 uptake transporter is a determinant of intracellular ATV concentrations and potentially mediates the uptake of ATV into PBMC. Further studies to investigate the role of *SLCO3A1* genetic variants on plasma and intracellular protease inhibitors pharmacokinetics are now warranted.

CHAPTER 4

In vitro-in vivo extrapolation of CYP2B6 genotype-based efavirenz dose reduction

4.1. Introduction

The pharmacokinetics of efavirenz (EFV) is characterized by marked inter-patient variability (Csajka et al. 2003). CYP2B6 is the main enzyme responsible for EFV metabolism and *CYP2B6* polymorphisms can markedly affect EFV exposure, with 516G>T considered to be the main genetic variant accounting for as much as 45% of the observed variability in efavirenz concentrations (Arab-Alameddine et al. 2009; Kwara et al. 2009). EFV is commonly administered at 600 mg once daily and the current strategy to administer an equal dose of EFV to all patients without regard to heterogeneity in biological and genetic factors may explain part of the variability observed in treatment efficacy or toxicity.

Several dose reduction or individualization strategies have been hypothesised (Gatanaga et al. 2007; van Luin et al. 2009; Cabrera Figueroa et al. 2010; Fayet Mello et al. 2011). Indeed a good proportion of patients might be over dosed, reaching plasma exposure above the concentrations needed for inhibition of viral replication. Moreover neuropsychiatric side effects have been correlated with higher plasma concentrations in several studies (Marzolini et al. 2000; Nunez et al. 2001; Gallego et al. 2004; Haas et al. 2004; Gutierrez et al. 2005) but to date these findings have not been replicated in all cohorts (Stahle et al. 2004; Josephson et al. 2010). Dose reduction strategies might be applied for patients achieving high concentrations due to genetic or biological factors or who have already reached viral suppression and therefore require a lower maintenance dose. Dose reduction can include lowering of dosage, e.g. from 600 mg to 400 mg or 200mg, or administration on a non-daily

basis, which has been applied on selected populations with good clinical results. In the FOTO study, HIV+ patients characterised by durable viral suppression on daily HAART changed their usual treatment schedule (600 mg of EFV once daily) to 5 consecutive days on treatment (typically Monday through Friday) followed by 2 days off treatment (Five-On, Two-Off, or FOTO treatment schedule). At 48 weeks, although plasma exposure was below the suggested minimum effective concentration (1000 ng/ml), suppression of viral load was maintained in all subjects (Marzolini et al. 2001; Csajka et al. 2003). These findings suggest that plasma exposure needed for viral suppression, in patients which who have reached an undetectable viral load, might be reduced compared to patients with higher viral load (Cohen et al. 2007).

Another example of successful dose individualization/reduction is represented by a study conducted by Gatanaga et al. where patients with a genetic profile linked to extremely high plasma concentrations (*CYP2B6**6/*6 or *6/*26) and C_{avg} > 6000 ng/ml were switched to a lower dosage of EFV, either 400 mg or 200 mg in order to achieve C_{avg} in the suggested range of concentrations. Plasma EFV concentrations decreased proportionally in most patients although same patients had a higher decrease compared to the dose ratio. At 400 mg EFV concentrations were in the therapeutic range (1000-4000 ng/ml) for all the patients with *6/*6 and *6/*26 and a significant portion of patients had an improvement of the CNS side effects (Gatanaga et al. 2007).

The *in vitro in vivo* extrapolation (IVIVE) is a "Bottom-Up" approach to model the pharmacokinetics of drugs using *in vitro* data such as the physiochemical

characteristics of a drug, intrinsic clearance in human liver hepatocytes and transporter affinity. This technique uses physiologically based pharmacokinetic (PBPK) models in order to simulate the pharmacokinetics of drugs. PBPK models are based on multi-compartmental equations that mimic the absorption, distribution, metabolism and elimination processes in the human body. Absorption can be symbolised by kinetic parameters of absorption in different loci. Organs represent compartments in communication through blood or lymph flow which can be simulated in silico. Metabolism can be represented by intrinsic clearance in the liver or other organs, and might be equal to the sum of clearance for each CYP or UGT isoform. Moreover the role of transporters regulating the passage of substrates into tissues can be included into PBPK, describing a complex interplay which thereby defines plasma pharmacokinetics.

The Simcyp Simulator is a platform for IVIVE and can simulate oral absorption, tissue distribution, metabolism and excretion of drugs in virtual populations. Inter-patient variability in demographic and biological (genetic and environmental) factors is incorporated in the PBPK models with drug-specific physicochemical properties. Covariation between demographic and physiological parameters is the basis for the definition of virtual individuals and consequently the pharmacokinetics of drugs can be described not only by mean values but an estimation of inter-patient variability can be given. Variation of the above mentioned covariates is possible in different ethnic groups or special populations which can all be included in the simulations. Moreover several dosing strategies, including different administration routes such as oral, intravenous and dermal can be simulated by the program.

The aim of this chapter was to develop an IVIVE model for EFV pharmacokinetics. The effect of *CYP2B6* genotype on EFV plasma exposure will be evaluated on traditional dosage and dose reduction strategies.

4.2. Methods

Efavirenz pharmacokinetics were simulated using a generic PBPK model implemented in the Simcyp™ ADME simulator (version 10.11, Simcyp™ Ltd., UK). *In vitro* data describing the physiochemical properties (Figure 4.1), absorption and metabolism of EFV and the effect of CYP2B6 516 genotype on CYP2B6 protein expression in liver tissue were obtained from published literature and are summarized in Table 4.1 and Table 4.2.

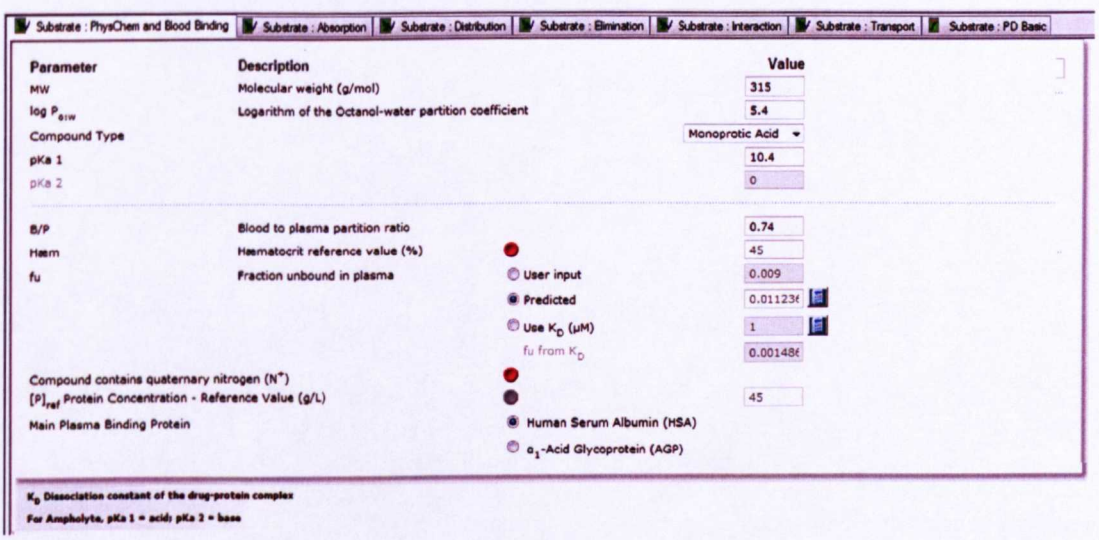

Figure 4.1. SIMCYP physiochemical characteristic menu.

Table 4.1 EFV physiochemical and metabolic characteristic

Input paramenter	Value	Reference
Molecular weight	315.7	(Bristol-Myers Squibb 2009)
logP	5.4	(Rowe et al. 1999)
Free fraction in plasma (f_u)	1%	Simulated by Simcyp
Caco-2 permeability	8.92 (10^{-6} cm/s)	(Takano et al. 2006)
Vd in rat	5.5 L/kg	(Balani et al. 1999)
EFV metabolism to 8-OH		
rCYP2B6 Cl_{int}	0.55 μL/min/pmol	(Ward et al. 2003)
rCYP1A2 Cl_{int}	0.07 μL/min/pmol	(Ward et al. 2003)
rCYP2A6 Cl_{int}	0.08 μL/min/pmol	(Ward et al. 2003)
rCYP3A4 Cl_{int}	0.007 μL/min/pmol	(Ward et al. 2003)
rCYP3A5 Cl_{int}	0.03 μL/min/pmol	(Ward et al. 2003)
EFV metabolism to 7-OH		
rCYP2A6	0.05 μL/min/pmol	(Ogburn et al. 2010)
EFV metabolism to glucuronide		
rUGT2B7	0.05 μL/min/pmol	(Belanger et al. 2009)
CYP induction		
CYP2B6 Ind_{max}	6	(Faucette et al. 2007)
CYP3A4 Ind_{max}	1.5	(Mouly et al. 2002)

Note: Vd, Volume of distribution; Cl_{int} intrinsic clearance; Ind_{max}, Maximum induction

Absorption was investigated *in vitro* using a Caco-2 monolayer and the apparent permeability value obtain was 8.92 (10^{-6} cm/s) (Takano et al. 2006). Volume of distribution was scaled from rat to man by means of allometric scaling using the equation suggested by Caldwell et al ($\log Vd_h = 0.83 \cdot \log Vd_r - 0.18$ (L kg−1) (Caldwell et al. 2004).

The intrinsic metabolic clearance (CL_{int}) was described by:

$$hCL_{int} = \sum_i \frac{rCL_{int\,i}}{fu_{mic_i}} x\ ISEF_i\ x\ CYPabundance_i\ x\ MPPGL\ x\ LW$$

Where i indicates the isoform of CYP involved in metabolism, rCl_{int} is the intrinsic clearance for recombinant CYP, f_{umic} is the fraction of unbound drug in the *in vitro* system used to quantify rCl_{int}, ISEFi is a scaling factor that compensates for any differences in enzyme activity between different recombinant and hepatic systems. Indeed, ISEF is a dimensionless number used as a direct scaler to convert data obtained with a rCYP system to an 'Human Liver Microsomes (HLM) environment'. ISEF values for the different *in vitro* system have been thoroughly determined and reference values are available in the software (Proctor et al. 2004). CYP abundance is the concentration of CYP isoform per mg of liver protein, MPPGL is the amount of protein per gram of liver and LW is liver weight. The software provides information on occurring variability in MPPGL and LW.

rClint values for CYP isoforms and UGT2B7 were obtained from available *in vitro* data on EFV metabolism (Ward et al. 2003; Belanger et al. 2009; Ogburn et al. 2010). Three different metabolic pathways have been included: hydroxylation to 7-hydroxy EFV mediated by CYP2A6, hydroxylation to 8-hydroxy EFV mediated by CYP2B6, CYP2A6, CYP1A2, CYP3A4 and CYP3A5, glucuronidation mediated by UGT2B7. A screenshot of the SIMCYP metabolism menu is represented in Figure 4.2.

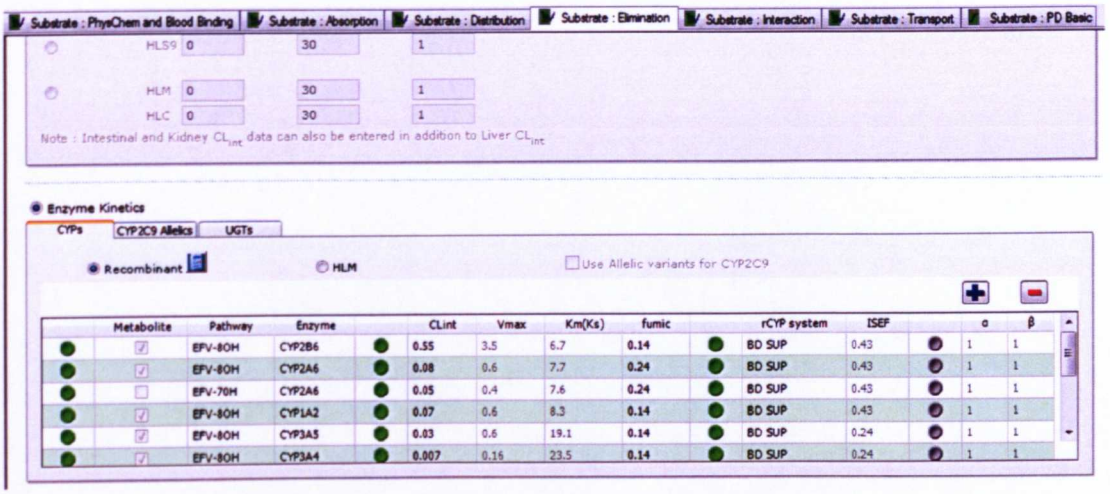

Figure 4.2. SIMCYP metabolism menu. Cl_{int} for the different CYP isoforms. rCYP used is BD SUP for all isoforms with an ISEF value of 0.43 and 0.24

The effect of the *CYP2B6* 516 G>T polymorphism on protein abundance was defined by Lang et al. and summarised in Table 4.2 (Lang et al. 2001).

Table 4.2. Influence of CYP2B6 516G>T genotypes on CYP2B6 expression in hepatocytes.

Genotype	CYP2B6 expression
516GG	24 pmol/mg-of protein
516GT	17 pmol/mg of protein
516TT	8 pmol/mg of protein

These data were used to simulate EFV (600mg once daily) pharmacokinetics in a virtual population of 100 patients using Simcyp Population-based Simulator. Simulated pharmacokinetic parameters, such as C_{trough}, C_{max}, AUC, and the impact of 516G>T genotype were compared with observed values available in the literature (Nyakutira et al. 2008). Moreover simulated pharmacokinetics of EFV were

compared with data from the Therapeutic Drug Monitoring (TDM) registry of the "Department of Infectious Diseases, University of Turin, Amedeo di Savoia Hospital, Turin, Italy" containing data from 532 plasma from 367 patients receiving standard dosage of EFV. These samples were collected from January 2003 to August 2010. Patients were receiving stable highly active antiretroviral therapy containing EFV were older than 18 years old and not receiving potentially interfering drugs.

Two dosing strategies were then simulated in 100 virtual patients for each genotype. Firstly, dose reduction to 400mg once daily and secondly a regimen where subjects received 600 mg once daily for 5 days followed by 2 days without EFV therapy (5 days on and 2 days off; FOTO study).

4.3. Results

Simulated pharmacokinetic variables at steady state (mean ± SD), C_{trough} (2119 ± 2192 ng/ml), C_{max} (3725 ± 2398 ng/ml), AUC (71865 ± 56689 ng/mL.h) were in agreement with previously published pharmacokinetic data (mean ± SD) C_{trough} (1764 ± 1008 ng/ml), C_{max} (4063 ± 1165 ng/ml), AUC (57960 ± 22995 ng/mL.h) (Vrouenraets et al. 2007). As shown in Figure 4.3, the majority of measurements from the TDM registry were included between the 5^{th} and 95^{th} percentile of the simulation with, 55 out of 532 (10.3%) measurement outside the calculated range.

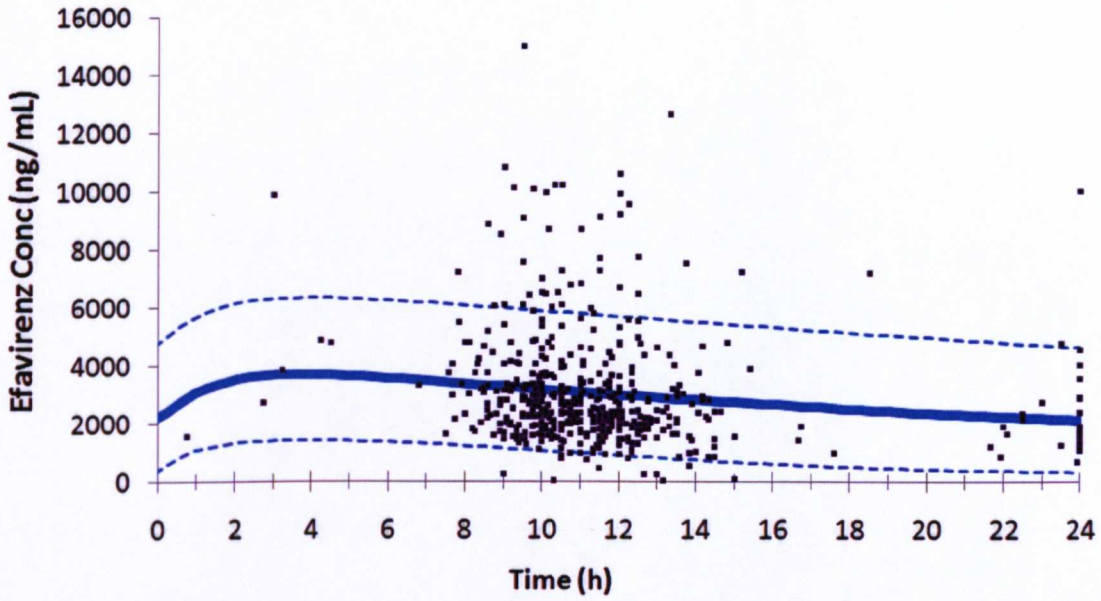

Figure 4.3. Simulated efavirenz concentration-time profile at steady state in the cohort receiving 600 mg once daily. The full line represents the mean and dotted lines represent the 5th and the 95th percentiles. Black squares represent individual values from the TDM registry.

The prediction of oral clearance, volume of distribution and other PK variables are summarised in Table 4.3.

Table 4.3. Comparison between simulated and reference PK value.

	Simulation	Real value	Diff%	Reference
C_{trough} (ng/ml)	2119	1764	+20%	(Vrouenraets et al. 2007)
C_{max} (ng/ml)	3725	4063	-9%	(Vrouenraets et al. 2007)
AUC (ng/mL.h)	71865	57960	+23%	(Vrouenraets et al. 2007)
Clearence (L/h)	12.9	11.3	+ 14%	(Arab-Alameddine et al. 2009)
Vd (L/kg)	2.7	4.2	- 43%	(Arab-Alameddine et al. 2009)

The effect of 516G>T on simulated EFV clearance (GT = -24% and TT = -58%) was comparable to previously published population pharmacokinetic data (GT =-36%, TT =-66%) (Nyakutira et al. 2008; Cabrera et al. 2009). Simulated EFV PK profiles of 100 patients with different genotypes are represented in Figure 4.4. The mean C_{trough} was 1781 ± 1580 ng/ml for GG virtual patients, 2949 ± 2572 ng/ml for GT virtual patients and 4910 ± 3353 ng/ml for TT virtual patients.

Considering a dose reduction to 400 mg once daily, the mean C_{trough} was 1185 ± 1012 ng/ml for GG virtual patients, 1964 ± 2102 ng/ml for GT virtual patients and 3278 ± 2235 ng/ml for TT virtual patients Figure 4.5.

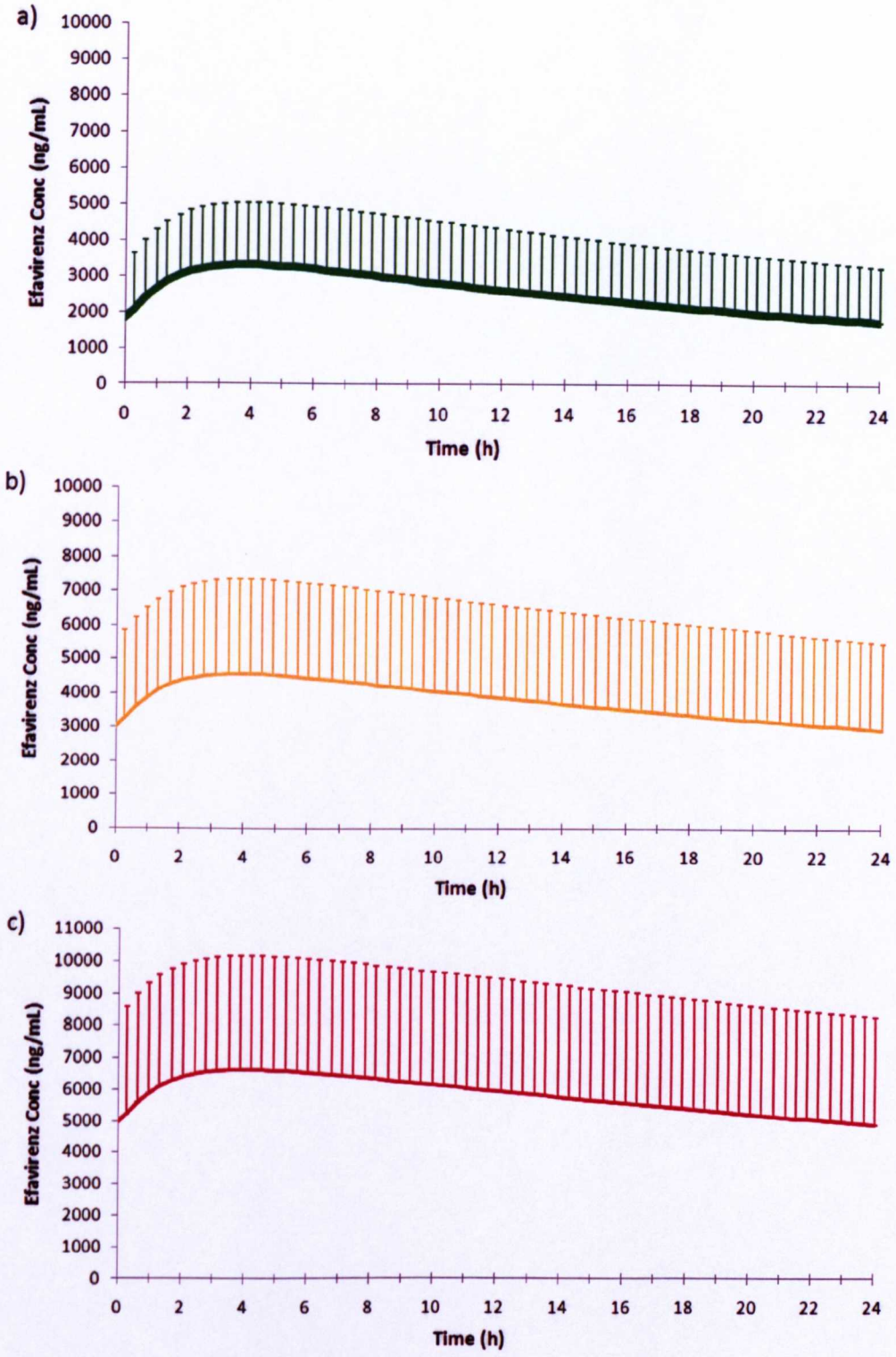

Figure 4.4. Simulated efavirenz concentration-time profiles at steady state following administration of 600 mg once daily in the three genetic groups. a, 516 GG, green; b, 516GT yellow; c,516 TT, red. The full lines represent the mean and bars represent SD.

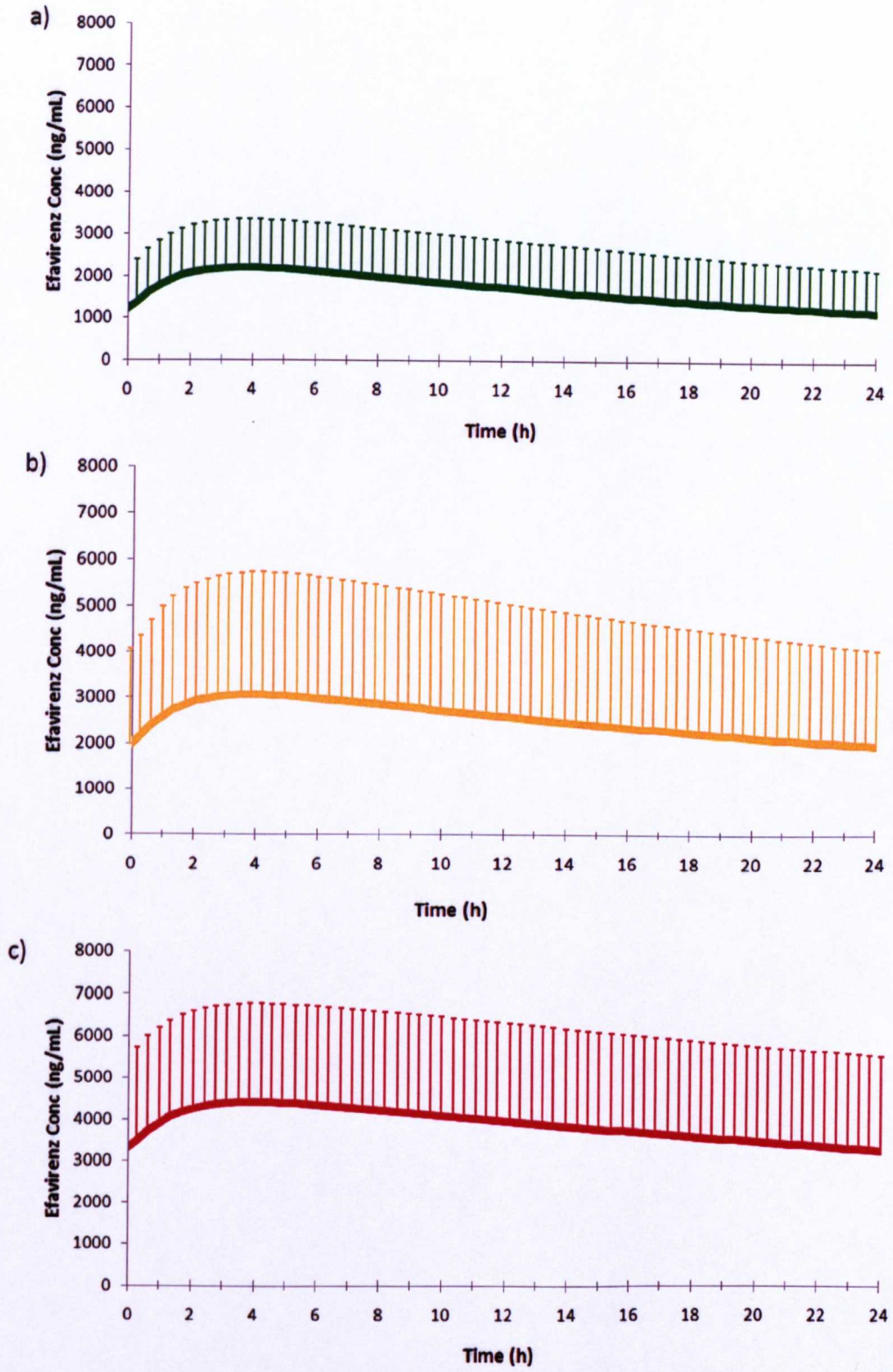

Figure 4.5. Simulated efavirenz concentration-time profiles at steady state following administration of 400 mg once daily in the three genetic groups. a, 516 GG, green; b, 516GT yellow; c,516 TT, red. The full lines represents the mean and bars represent SD.

Simulation of FOTO-like administration resulted in a mean C_{trough} value at the end of two days without EFV administration of 489 ng/ml ± 691 for GG virtual patients, 1091 ng/ml ± 1431 for GT virtual patients and 2191 ng/ml ± 2134 for TT virtual patients, as represented in Figure 4.6. This is comparable to what has been recently described in the FOTO study, ie 7 patients with unknown CYP2B6 genotype had EFV PK available and median (range) concentrations were 595 ng/ml (<10-747) (Cohen et al. 2007).

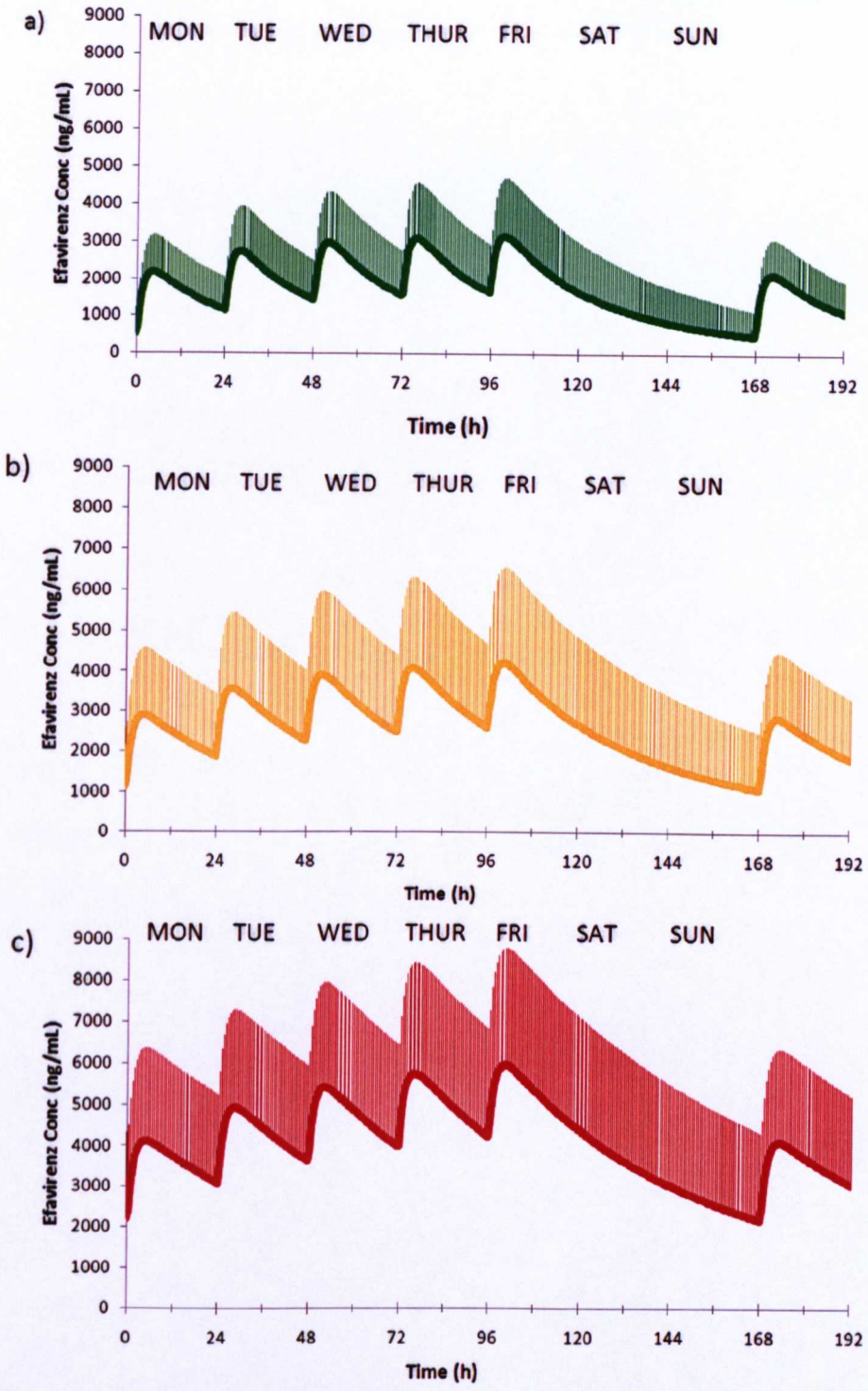

Figure 4.6. Simulated efavirenz concentration-time profiles in patients receiving 600 mg once daily for 5 days followed by 2 days without EFV therapy (5 days on and 2 days off; FOTO study) in the three genetic groups. a, 516 GG, green; b, 516GT yellow; c,516 TT, red. The full lines represent the mean and bars represent SD

4.4. Discussion

The developed IVIVE model predicted the *in vivo* pharmacokinetics of EFV in individuals with different *CYP2B6* genotypes. The main PK variables for different dosing strategies have been simulated and the effect of *CYP2B6* 516 G>T on EFV clearance has been characterised. The identification of genetic and demographic factors influencing EFV clearance has clinical relevance considering how EFV concentrations are important in relation to viral suppression and side effects. IVIVE gives novel approach to clarify factors important in the pharmacokinetics of a drug. However to use this "Bottom-up" modelling ADME key data need to be available. Fortunately this is the case of EFV, for which absorption and metabolism has been investigated *in vitro* and the main enzymes responsible for EFV clearance have been identified (Ward et al. 2003; Takano et al. 2006; Ogburn et al. 2010).

EFV is metabolised by several CYPs in the liver and intestine, CYP2B6, 1A2, 2A6 and 3A4. Previous publications have investigated EFV metabolism *in vitro* and CYP2B6 has been identified as the main isoform mediating EFV hydroxylation to the most abundant metabolite, 8 hydroxy EFV (Ward et al. 2003), and CYP2A6 for EFV hydroxylation to 7 hydroxy EFV (Ogburn et al. 2010). Successively a third metabolic pathway has been identify and UGT2B7 is responsible for direct glucuronidation of EFV (Belanger et al. 2009). The knowledge of the enzymes involved in EFV metabolism was essential to develop the IVIVE model although the description of enzyme induction by EFV was another important factor for the simulations. EFV strongly influences the expression of CYPs through the nuclear

receptor CAR, inducing CYP2B6 activity up to 6 fold and CY3A4 up to 1.5 fold (Faucette et al. 2007). Complete description of the genetic influence on enzyme expression and activity was available for CYP2B6 516 G>T only (Lang et al. 2001). EFV absorption was based on *in vitro* data from Caco-2 monolayers which is a cell system to investigate the intestinal passage of xenobiotics and gives a good estimation of EFV bioavailability (Takano et al. 2006). Volume of distribution was evaluated using data from an animal model, using the equation develop by Caldwell et al (Caldwell et al. 2004), which gives a good quantification of Vd compared to the reference value, as shown in Table 4.3.

An over-prediction of inter-patient variability was detected and simulated PK variables had a CV% of around 100% compared to real variables ranging between 40-60%. Reference values were measured in a controlled setting during clinical studies in a small cohort therefore variability might be underestimated. The main PK variables were predicted with good accuracy (<2 fold difference, Table 4.3). As shown in Figure 4.3, around 10% of real measurements from the Therapeutic Drug Monitoring registry were not included between the 5^{th} and 95^{th} percentile of the simulation. It is important to note that the simulation was of a generic Caucasian cohort (with a low frequency of 516T), and the ethnicity of a substantial proportion of patients included in the TDM cohort was unknown. African-Americans are characterised by a higher frequency of the T variant allele for CYP2B6 516G>T and therefore higher plasma concentrations. The presence of an unknown number of African-Americans in the TDM cohort could be the reason why there are values well above the simulated range of concentrations.

The simulated effect of CYP2B6 516 G>T on EFV clearance was similar to the reference values (Nyakutira et al. 2008; Cabrera et al. 2009). Recently two investigations of the influence of CYP2B6 genetic variability on EFV have been published. In a population pharmacokinetic study in Zimbabwean patients, the effect of 516 GT was to decrease EFV clearance by 22% and 57% for 516 TT (Nyakutira et al. 2008). In a more recent study on a Caucasian cohort the effect of 516G>T on EFV clearance was greater with the 516GT genotype causing a decrease of 50% in the EFV clearance while the 516 TT genotype was correlated with a decrement of 75% (Cabrera et al. 2009). The effect on EFV clearance simulated by IVIVE (GT = -24% and TT = -58%) was comparable to the above mentioned studies and reflected what has been observed in the clinical setting. The good concordance between the IVIVE data and the *in vivo* pharmacokinetics of 600 mg of EFV was essential to proceed with further simulations of dose reductions. The measurement of PK variables of EFV is not easily achievable, and a complete description of EFV PK in the clinical setting is challenging. Actual C_{trough} values are rarely measured due to administration of EFV at night and the consequent difficulty in the collection of C_{24} samples. Notwithstanding the lack of data for EFV C_{trough} all the main PK variables had minor differences compared to reference values, as shown in Table 4.3.

Dose reduction strategies, such as 400mg once daily and 600 mg once daily for 5 days followed by 2 days without EFV therapy (5 days on and 2 days off; FOTO study) were successfully simulated considering the three different genetic groups and plasma exposure was predicted at steady state. The only possible direct comparison with reference values was for the FOTO study, for which some PK data are available. Seven patients with unknown CYP2B6 genotype had EFV PK available

and median (range) concentrations were 595 ng/ml (<10-747), similar findings in the current simulation, ie C_{trough} value at the end of two days without EFV administration of 489 ng/ml ± 691 for GG virtual patients, 1091 ng/ml ± 1431 for GT virtual patients and 2191 ng/ml ± 2134 for TT virtual patients (Cohen et al. 2007).

Since EFV is metabolised by other CYPs isoforms, the inclusion of other genetic variants and a more detailed description of metabolism and induction of enzyme expression could improve the accuracy of clearance simulation. CYP2A6 and 3A4 are of secondary importance in the metabolism of EFV, but an effect of their genetic variants on EFV clearance has already been shown, consequently the inclusion of these genetic variants might improve reliability of EFV IVIVE simulation (Arab-Alameddine et al. 2009). Moreover the role of transporters in the regulation of EFV absorption, diffusion and elimination has not been fully investigated. To date EFV has not been identified as a substrate of any major transporters, but clarification of the role of transporters in the disposition of EFV might help to explain part of the variability observed in EFV pharmacokinetics. EFV is a strong inducer of *ABCB1* and other transporters, so the future investigation of EFV effects on transporter expression and activity will additionally improve the understanding of EFV pharmacokinetics and interaction with other drugs (Weiss et al. 2009). EFV pharmacokinetics are known to correlate with efficacy and toxicity. Inclusion of pharmacodynamic/pharmacokinetic data in the IVIVE models provides the opportunity to elucidate the consequences of EFV dose reduction on efficacy or side effects.

This simulation approach can be used to investigate clinically relevant 'what-if' questions, such as whether genotype-based dose reduction strategies are feasible to

manage inter individual differences in exposure. Patients who have already achieved suppression of viral replication or who have a favourable genetic profile might be overdosed on a standard EFV dosage and dose reduction strategies could be implemented to optimize EFV exposure. Moreover EFV can interact with several other drugs and alteration of exposure of EFV or the interacting drug might affect clinical efficacy of therapies. IVIVE models can represent a useful tool for simulation of these clinical scenarios and help optimization of antiretroviral therapy. This information can now be used to design prospective clinical studies and to develop PK/PD models in order to predict the effect of dose reductions on outcome.

CHAPTER 5

Substrate specificity of SLCO1B1 for maraviroc and in-vitro evaluation of drug-drug interaction between maraviroc and protease inhibitors

5.1 Introduction

Similarly to several other antiretrovirals, maraviroc (MVC) is metabolised by CYP3A4 (Hyland et al. 2008). Consequently the inhibitory effect of protease inhibitors (PIs) on CYP3A4 alters MVC pharmacokinetics (Abel et al. 2008). PIs and MVC are concomitantly administered in a substantial proportion of patients and this interaction therefore impacts on the antiretroviral therapy. SQV/r, LPV/r, ATV, ATV/r and RTV caused an increase in MVC C_{max} and AUC in the range of two-to threefold and three-to five fold, respectively (Abel et al. 2008). SQV/r had a greater effect on MVC exposure (four and eightfold increase in C_{max} and AUC, respectively) than other PIs. Consequently the dose of MVC is reduced to 150 mg bid if co-administered with a boosted PI (except TPV/r).

This increase in MVC exposure reflects the fact that HIV PIs are both substrates and inhibitors of CYP3A and thus compete for the same metabolic enzyme at both hepatic and intestinal sites. HIV PIs exhibit potent competitive inhibition although the inhibitory effect can persist after discontinuation and protease inhibitor concentrations are below detectable levels (Washington et al. 2003). This demonstrates a mechanism based inhibition in which decreased enzyme activity persists after the inhibitor has been cleared from the body (Kanamitsu et al. 2000). RTV is the most potent inhibitor with a Ki of 0.17 μM compared to 0.65 μM for SQV, 2.3 μM for ATV and 1 μM for LPV (Ernest et al. 2005; Hyland et al. 2008). The ratio between maximal inactivation rate constant (K_{inact}) and Ki is a measure of inhibition efficiency and RTV results in the most efficient inhibition with a K_{inact}/Ki

of 2353 min^{-1} x nM compared to 400 min^{-1} x nM for SQV, 110 min^{-1} x nM for LPV and 26 min^{-1} x nM for ATV (Ernest et al. 2005; Hyland et al. 2008).

Other mechanisms may also contribute to the increase in MVC pharmacokinetics enhancement when co-administered with PIs. MVC has been shown to be an ABCB1 substrate (Walker et al. 2005) and all PIs are known inhibitors of this transporter with a ranking order of inhibition of RTV > LPV > SQV > AMP > ATV (Storch et al. 2007). ABCB1 is localised to the apical membrane of many epithelial and endothelial cells and participates in absorption and excretion through its influence on the efflux from intestinal and hepatic cells.

Moreover, influx transporters of the SLCO family are also emerging as important determinants of pharmacokinetics for antiretrovirals and other classes of drugs. The SLCO1B1 transporter is located on the basolateral membrane of hepatocytes and mediates hepatic uptake of a number of drugs (Kalliokoski and Niemi 2009). The 521T>C SNP (rs4149056) has previously been correlated with increased plasma concentrations of pravastatin and lopinavir (Niemi et al. 2004; Hartkoorn et al. 2010). Consequently, SLCO1B1 might be relevant in the definition of pharmacokinetics and drug-drug interactions for MVC as has been recently shown for other drugs such as repaglinide and statins (Kalliokoski et al. 2008; Amundsen et al. 2010).

Therefore, the main aim of this chapter was to investigate the substrate specificity of MVC for SLCO1B1 and the inhibitory effect of PIs on MVC uptake using the *Xenopus laevis* oocytes heterologus protein expression system.

5.2 Methods

5.2.1 Materials

T3 mMessage mMachine Transcription kits were purchased from Ambion Ltd. (Huntingdon, UK). Ultima Gold scintillation fluid was purchased from Perkin Elmer (Boston, USA). Cyclosporin A, formic acid, NaCl, HEPES, $CaCNO_3 \cdot 6H_2O$, $CaCl_2 \cdot 6H_2O$ and KCl were purchased from Sigma-Aldrich Company Ltd (Poole, UK). $MgSO_4 \cdot 7H_2O$ was purchased from VWR (Lutterworth, UK). Restriction enzymes were purchased from New England Biolabs (Hitchen, UK). Adult female X. *laevis* frogs were purchased from Xenopus Express (Lyon, France). [^{3}H] Estrone-3-Sulfate (E3S, specific activity, 50Ci/mmol) was purchased from American Radiolabeled Company Inc. (St. Louis, MO, USA), pBluescriptIIII-KSM was a kind gift from WJ Joiner (Yale University, CT, USA). Maraviroc was kindly supplied by Pfizer Inc (Groton, CT, USA). Acetonitrile HPLC grade was purchased from J.T. Baker (Deventer, Holland). The water was further purified to 18.2 MΩ with a Purelab Classic UVF (Elga LabWater, High Wycombe, UK). Cyclosporin A and formic acid were obtained from Sigma-Aldrich (UK).

5.2.2 Oocyte expression strategy

Ovary lobes were extracted from adult female X. *laevis* frogs. Experiments with *SLCO1B1*-KSM injected oocytes with respective water injected controls were conducted using oocytes extracted by collagenease treatment and oocytes were incubated for 3 days post injection. The overall strategy is illustrated in Figure 5.1.

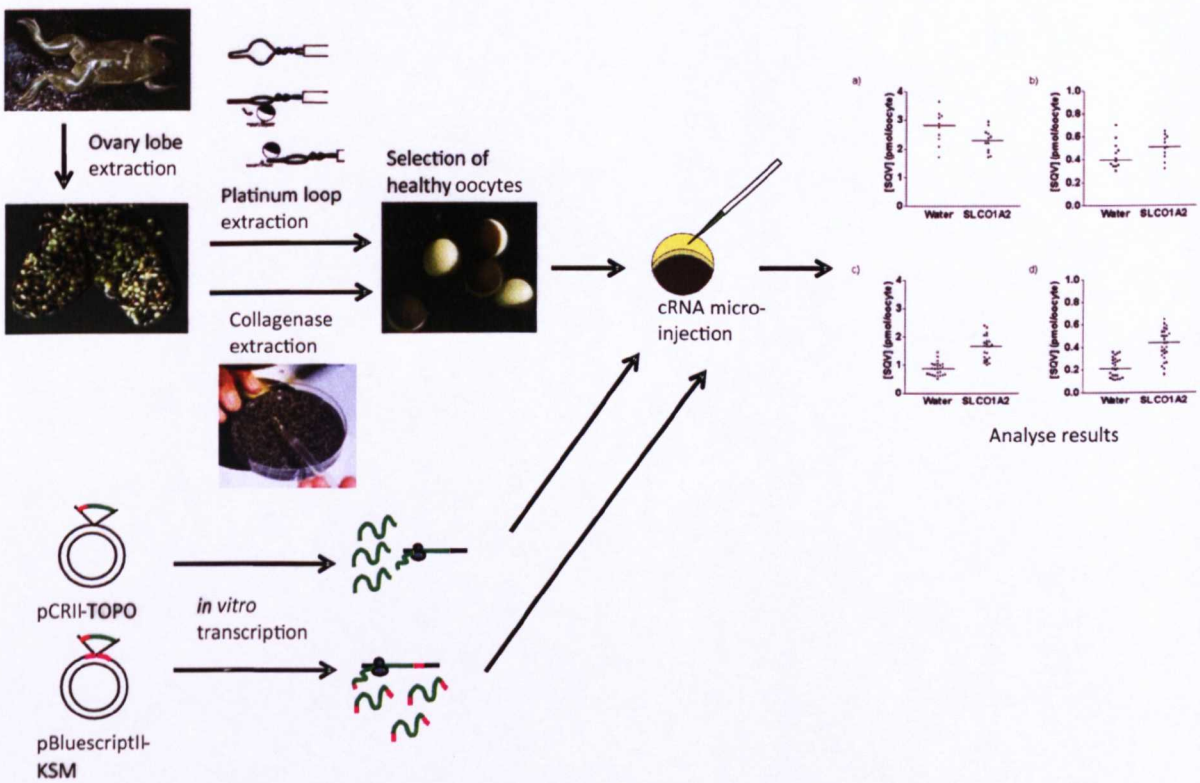

Figure 5.1. The experimental strategy for expression of SLCOs in X. *laevis* oocytes.

5.2.3 Site-directed mutagenesis

To generate *SLCO1B1* containing the 521T>C polymorphism a two-step site directed mutagenesis was performed using SLCO1B1-KSM previously generated as a template (Hartkoorn et al. 2010). QuickChange II Site-Directed Mutagenesis Kit

(Stratagene, LaJolla, CA, USA) was used to introduce the polymorphism following the manufacturer indication. Primers used for mutagenesis were as follows: 5'CTG GGT CAT ACA TGT GGA TAT ATG CGT TCA TGG GTA ATA TGC 3' (forward) and 5'GCA TAT TAC CCA TGA ACG CAT ATA TCC ACA TGT ATG ACC CAG 3' (reverse). The procedure utilizes a supercoiled double-stranded DNA (dsDNA) vector with an insert of interest and two synthetic oligonucleotide primers, containing the desired mutation. The primers, each complementary to opposite strands of the vector, are extended during temperature cycling by PfuUltra HF DNA polymerase. The reaction volume was 50 µl; 5 µl of 10× reaction buffer, 1 µl (50 ng) of dsDNA template, 1 µl (125 ng) of oligonucleotide primer #1 and 1 µl (125 ng) of oligonucleotide primer #2, 1 µl of dNTP mix, 1 µl of PfuUltra HF DNA polymerase (2.5 U/µl), ddH2O to a final volume of 50 µl. Cycling PCR parameters were: first segment, one cycle 95°C for 30 seconds; second segment, 20 cycles, 95°C for 30 seconds, 55°C for 1 minute and 68°C for 1 minute/kb of plasmid length. Extension of the oligonucleotide primers generates a mutated plasmid containing staggered nicks. Following temperature cycling, the product is treated with Dpn I (1 µl, 10U/µl), an endonuclease specific for methylated and hemimethylated DNA. DpnI digests the parental DNA template and selects for mutation-containing synthesized DNA.

5.2.4 In vitro transcription

The T3 mMessage mMachine *in vitro* transcription kit was used to generate *SLCO1B1* with 5' and 3' flanking UTR cRNA from pBluescriptII-KSM. The pBluescriptII-KSM-*SLCO1B1* plasmid was linearised with SacI (1× final concentration of NEBuffer 1, 1× BSA, 1µg DNA, 37°C, 10mins) and purified using the GenElute PCR Clean-Up kit. The linearised DNA was concentrated by LiCl

DNA precipitation, 8M LiCl was added to the DNA (final concentration LiCl 800mM, 30mins), precipitated with isopropanol (equal volume, centrifuge 13, 000 × g, 4°C, 15mins) and washed with absolute ethanol (1ml, centrifuge 13,000 × g, 4°C, 15mins). The DNA pellet was solubilised in nuclease free water to a concentration of 1μg/μl. 10X Reaction Buffer (10μl, 1× final concentration, room temperature), 2× NTP/CAP (2μl, 1× final concentration), template DNA (1μg), RNA Polymerase Enzyme Mix (1μl) and nuclease-free water (up to 20μl) was assembled at room temperature and incubated (37°C, 2 hours). The DNase treatment was performed following the incubation (1μl TURBO DNase, 37°C, 15mins). The cRNA was purified by LiCl precipitation. The reaction mix was incubated with nuclease-free water (30μl) and LiCl precipitation solution (30μl, -20°C, 30mins). The mixture was centrifuged (13000 × g, 4°C, 15mins) to pellet the cRNA. The supernatant was removed and the pellet was washed with ethanol (70%, 1ml) and again centrifuged (13000 × g, 4°C, 15mins). The ethanol was removed and the pellet was resuspended in nuclease-free water, quantified with spectrophotometry, diluted to 1μg/μl and stored in aliquots (5μl, -80°C).

5.2.5 X. laevis maintenance

Adult female X. *laevis* frogs were kept in fresh water and cleaned once a week. Frogs were handled with a net and fed dried pellets twice a week. Frogs were sacrificed by an anaesthetic solution (MS222, 8g/l, 45mins).

5.2.6 X. laevis oocyte isolation by collagenase treatment

Oocytes were isolated by dissection of the abdomen of the frog and excising ovary lobes with forceps into Barth's solution without calcium (NaCl 88mM, KCl 1mM, HEPES 15mM, pH 7.6) containing collagenase (1mg/ml, shaking, 2h). The oocytes were washed twice with Barth's solution without calcium, followed by a wash with Barth's solution containing calcium (NaCl 88mM, KCl 1mM, HEPES 15mM, $CaCNO_3 \cdot 6H_2O$ 0.3mM, $CaCl_2 \cdot 6H_2O$ 41μM, $MgSO_4 \cdot 7H_2O$, 0.82mM, pH 7.6). The cells were incubated (18°C 1h) and healthy stage V-VI oocytes (Dumont 1972; Rasar and Hammes 2006) were selected and maintained in Barth's solution with calcium supplemented with 10 μg/ml penicillin and streptomycin (18°C, overnight).

5.2.7 X. laevis micro-injection

Needles were made from thin wall glass capillaries (1mm diameter, 102mm length) using the PUL-1 machine (World Precision Instruments, UK). One needle was loaded onto the micro-manipulator and trimmed using forceps. cRNA (1μg/μl, 7.5μl, TOPO origin) or DEPC treated water (7.5μl) was loaded into the needle by the vacuum pump DA7C (Charles Austen Pumps, UK) and held in the needle using the picopump PV830 (World Precision Instruments, UK) supplied with compressed air. The drop size of the sample was calibrated to one third the size of an oocyte (~50nl). Fifty oocytes were injected per condition and uptake was performed 3 days following injection.

5.2.8 Uptake experiments in X. laevis oocytes

SLCO1B1 with X. *laevis* β-globin UTR flanking region cRNA (50nl, 1μg/μl) or DEPC treated water was injected into oocytes. Uptake was performed in a 24 well plate (5 oocytes per condition, room temperature, 1 well in a 24 well plate, shaking at 150rpm). MVC or [^{3}H] E3S (1μM, 0.33μCi/ml) were diluted in Hanks balanced salt solution. After incubation, oocytes were transferred into cell strainers and washed with ice cold Hanks balanced salt solution (3 wells in a 6 well plate) and individual oocytes were transferred into scintillation vials or eppendorfs. For the quantification of [^{3}H] E3S, after incubation, oocytes were lysed with 10% SDS and scintillation fluid was added. Radioactivity was then counted by liquid scintillation spectroscopy. (Packard 1900CA Tri-Carb Liquid Scintillation Analyser). MVC was quantified using an LC-MS/MS method. Firstly, the transport rate of [^{3}H] E3S and MVC was evaluated as the ratio of uptake obtained in *SLCO1B1*-cRNA-injected oocytes and water-injected oocytes and saturation of MVC uptake was investigated at 5 μM up to 120min. Subsequently, to estimate kinetic parameters for the uptake of MVC, SLCO1B1-mediated transport rate was obtained by subtracting the transport rate of water-injected oocytes from that of *SLCO1B1*-cRNA-injected oocytes at increasing concentrations (2, 5, 10, 15, 25, 50, 100μM). The transport rate of MVC was plotted against the initial concentrations, and a Michaelis–Menten equation was fitted to the data to estimate kinetic parameters, such as V_{max} and K_m, using GraphPad Prism version 5.00 for Windows (GraphPad Software, San Diego California USA, www.graphpad.com). The Cl_{int} was then obtained from V_{max}/K_m .

To further confirm the uptake of MVC by SLCO1B1, the effect of cyclosporin A, a known inhibitor of SLCO1B1, was evaluated. The transport rate of MVC was investigated at 5 and 25 μM in the presence of 30 μM of cyclosporin A (Kitamura et

al. 2007). The effect of the 521T>C polymorphism was also investigated *in vitro* by injecting X. laevis oocytes with SLCO1B1-KSM 521C mRNA and then evaluated the uptake of MVC at 5 and 25 μM.

For interaction between MVC and PIs, drugs were diluted in Hanks balanced salt solution. For experiments in which the effect of inhibitors was investigated, cells were pre-incubated for 5 min with 0.5 ml of the standard buffer containing the inhibitor at desired concentration. Subsequently, 0.5 ml of double-concentrated substrate solution was added to initiate the actual incubation. After 30 minutes of incubation, oocytes were transferred into cell strainers and washed with ice cold Hanks balanced salt solution (3 wells in a 6 well plate) and individual oocytes were transferred into eppendorfs. Firstly, the inhibition of MVC transport rate by PIs was evaluated as uptake obtained in SLCO1B1-cRNA-injected oocytes in the presence of 50μM of DRV, SQV, LPV, ATV and 30 μM of cyclosporin A. To determine the concentration required to inhibit MVC uptake activity by 50% (IC_{50}), experiments were performed at 0.1, 0.3, 1, 3.3, 10, 33 and 100 μM of each inhibitor. The transport rate of MVC was plotted against the inhibitor concentration, and a log(inhibitor) vs. response curves curve was fitted to the data using GraphPad Prism version 5.00 for Windows.

5.2.9 LC-MS/MS method for quantification of MVC in X. laevis oocytes

5.2.9.1 Chemicals

MVC was kindly supplied by Pfizer Inc (Groton, CT, USA). Acetonitrile HPLC grade was purchased from J.T. Baker (Deventer, Holland). HPLC grade water was produced with Milli-DI system coupled with a Synergy 185 system by Millipore (UK), formic acid was obtained from Sigma-Aldrich (UK).

5.2.9.2 Stock solutions, Standards and Quality Controls

MVC stock solution was made in methanol and HPLC grade water (90:10 v/v) to obtain a final concentration of 1 mg/ml and was refrigerated at 4°C until use, within 1 month. Blank solution was prepared for each experiment, solubilising 20 oocytes in 3 ml of Acetonitrile. The highest calibration standard (STD 8) and three quality controls (QCs) were made by spiking the stock solution in 150 ul of blank solution; the others STDs were prepared by serial dilution from STD 9 (20000 fmol/oocyte) to STD 1 (78 fmol/oocyte) with blank solution, to obtain 9 different spiked concentrations plus a blank sample (STD 0). QC concentrations were 13650 fmol/oocyte, 1950 fmol/oocyte and 390 fmol/oocyte for QC-High, QC-Medium and QC-Low, respectively.

5.2.9.3 Chromatographic Conditions

The LC-MS/MS system used to assay MVC consisted of a pump and autosampler model Surveyor, and LCQ DecaXP ion trap detector (Thermo, UK). Chromatographic separation was performed at 37°C using a column oven, on a Fortis C-18 3μ column (50 mm × 2.1 mm I.D., Fortis Technologies, UK), protected by a Column Saver with pre-column (Thermo, UK). The chromatographic run was

performed at 0.4 mL/min with a gradient (Table 5.1), and the mobile phase was composed of Buffer A (HPLC grade water 95% - Acetonitrile 5% + 0.05% formic acid) and Buffer B (HPLC grade water 20% - Acetonitrile 80% + 0.05% formic acid).

Table 5.1. Chromatographic conditions (gradient): Mobile phase A (HPLC grade water 95% - Acetonitrile 5% + 0.05% formic acid) and Mobile phase B (HPLC grade water 20% - Acetonitrile 80% + 0.05% formic acid).

TIME (min.)	% Mobile phase A	% Mobile phase B	Flow (ml/min)
0.0	95	5	0.4
0.5	95	5	0.4
1.0	0	100	0.4
3.0	0	100	0.4
3.1	95	5	0.4
6.5	95	5	0.4

5.2.9.4 Ion trap conditions

Detector settings were ElectroSpray Ionization and positive polarity ionization. Spray voltage 5kV; capillary voltage 6V; capillary temperature 360 °C; stealth gas flow rate 65 l/h; nitrogen cone flow 100 l/h. MVC main parent ion was isolated at 514 (m/z) with collision energy 40V and the main daughter ion was detected at 389 (m/z).

5.2.9.5 Standards, Quality Controls and Sample Preparation

150µl of acetonitrile was added to a single oocyte, in a glass tube. After solubilising the oocyte and vortexing for 10 seconds, the mixture was centrifuged at 6,000 rpm

for 10 min at 4°C. 100µl of supernatant was transferred into a vial, 100µl of distilled water was then added and the vial was vortexed for 10 seconds. 10µl was injected into the column. All procedure steps were carried out at room temperature. This was repeated for all standard, quality controls and samples.

5.2.9.6 Validation

Interference from endogenous compounds was investigated by analysis of six different blank solutions. Intra-day and inter-day accuracy and precision were determined by assaying 4 sets of QCs in each experiment. Accuracy was calculated as the percent deviation from the nominal concentration. Inter-day and intra-day precision were expressed as the standard deviation at each QC concentration. The calibration curve was obtained using 9 calibration points in duplicate, ranging from 20000 fmol/oocyte to 78 fmol/oocyte, and considering MVC peak area. A quadratic through zero calibration curve was used. The limit of detection (LOD) in plasma was defined as the concentration that yielded a signal-to-noise ratio of 3/1. Percent deviation from the nominal concentration (measure of accuracy) and relative standard deviation (measure of precision) of the concentration considered as the limit of quantification (LOQ) was < 20%. This was used as the lowest calibration standard, as requested by FDA guidelines (Food and Drug Administration 2001). MVC pre-assay stability was not evaluated, relying on the manufacturer's data and on a previous publication (Fayet et al. 2009). Therefore, stability studies were performed only in post-extraction conditions. Processed QCs were analysed immediately after extraction and after being incubated for 24 h at room temperature by comparing peaks areas.

5.3 Results

5.3.1 Validation of LC-MS for MVC quantification in oocytes

Maraviroc retention time was 4.5 ± 0.1 minutes. Representative chromatograms of a blank and STD1 are shown in Figure 5.2. A 1/X weighted quadratic regression was chosen and mean regression coefficient (r^2) of all calibration curves was at least 0.991. Lowest limit of quantification (LOQ) and detection (LOD) were 78 fmol/oocyte.

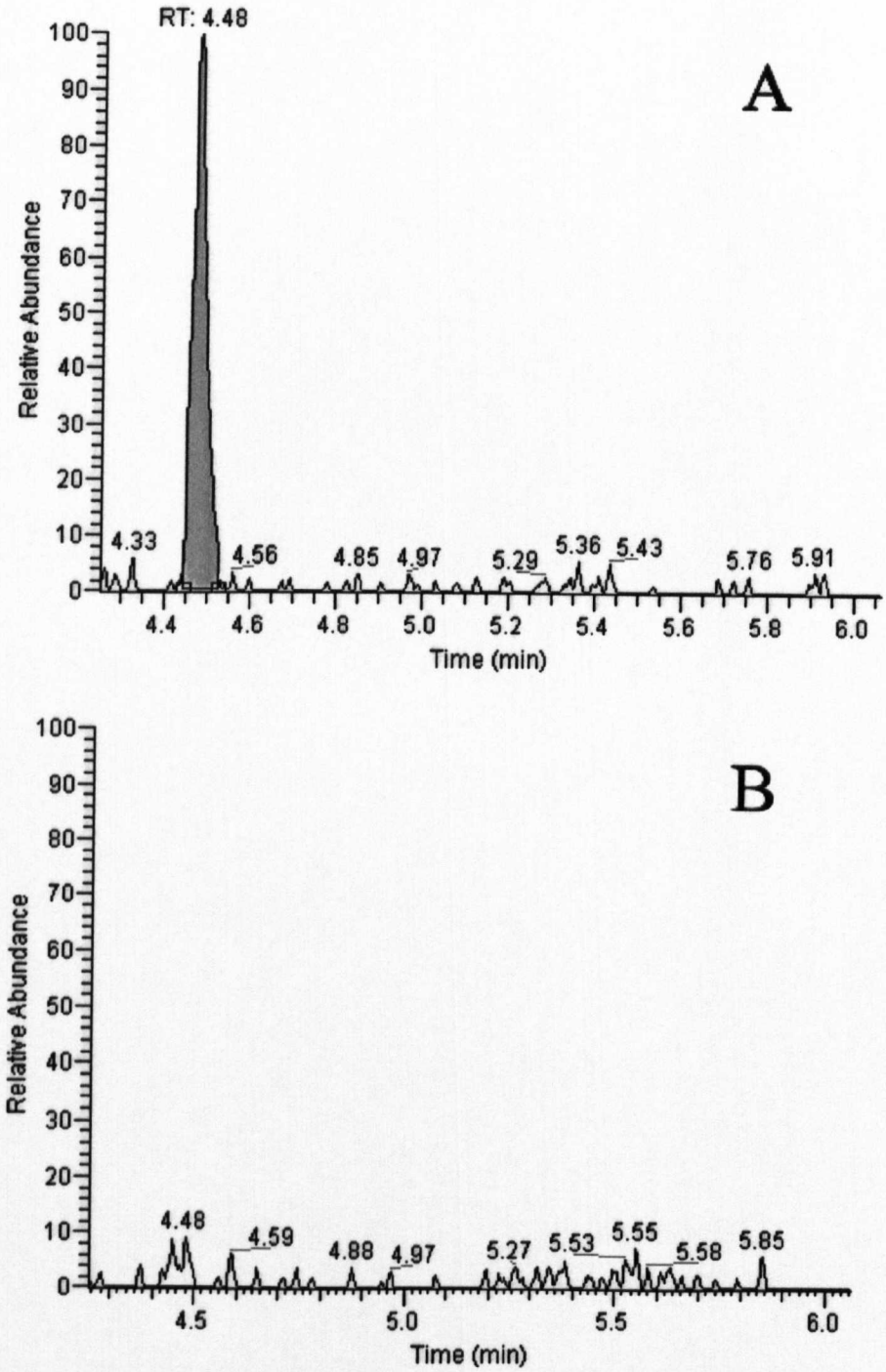

Figure 5.2. Chromatograms of Standard 1 (A) and a blank sample (B).

Results of the validation are listed in Table 5.2. All observed data (intra-day and inter-day precision [R.S.D.%]) were below 15.0%, in accordance with FDA guidelines (Food and Drug Administration 2001). Multiple aliquots (n=8) of each of the three MVC QCs were assayed and mean recovery ranged from 90% to 105%

(mean = 93%). The stability study of MVC in extracts, showed a coefficient of variation below 8%, therefore the samples were considered stable throughout the analysis.

Table 5.2. Validation results: accuracy (%), intra-day and inter-day precision

High Quality Control			Medium Quality Control			Low Quality Control		
Accuracy (%)	Precision (RSD%)		Accuracy (%)	Precision (RSD%)		Accuracy (%)	Precision (RSD%)	
	Interday	Intraday		Interday	Intraday		Interday	Intraday
8.05	9.03	8.47	4.32	9.81	10.57	-3.72	8.00	5.28

5.3.2 Substrate specificity of SLCO1B1 for MVC

E3S was used as a positive control and had significantly increased accumulation in oocytes injected with *SLCO1B1*-KSM (3945 ± 980 fmol/oocyte) compared to water controls (95 ± 42 fmol/oocyte; n=4; $p < 0.05$, 41.4-fold; Figure 5.3).

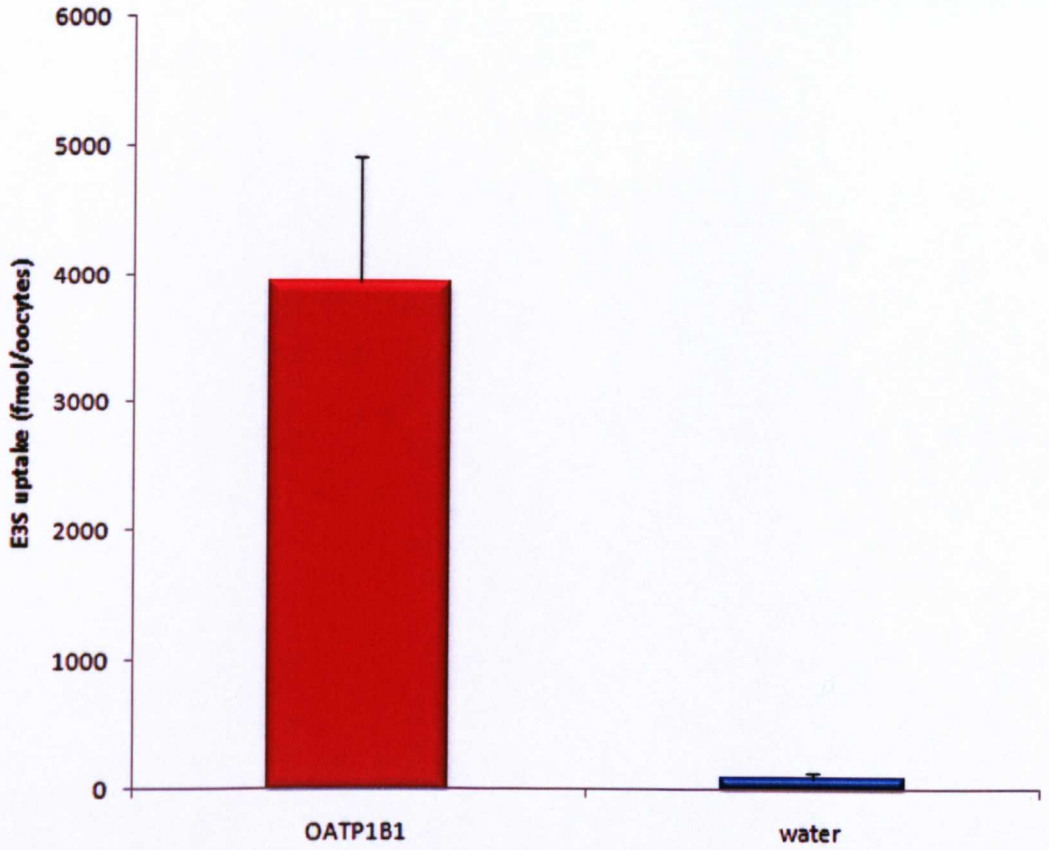

Figure 5.3. Water injected and *SLCO1B1*-KSM injected X. *laevis* oocytes uptake of E3S (n=4)

The uptake of MVC at 5μM increased up to 60 min in oocytes injected with *SLCO1B1*-KSM and then slowed between 60 and 120 min while the uptake in water injected oocytes was exponential as summarized in Table 5.3 and Figure 5.4. 60 min was identified as the timepoint at which the best ratio between *SLCO1B1*-KSM cRNA and water injected oocytes was reached (9.1) and it was therefore selected as the timepoint for subsequent experiments.

Table 5.3. The uptake of MVC at 5μM up to 120min obtained in water and *SLCO1B1*-KSM injected oocytes. (n = 3; mean ± SD)

Time (min)	Water (fmol/oocytes)	*SLCO1B1*-KSM (fmol/oocytes)	ratio
30	76.7 ± 9	482 ± 148	6.2
60	224 ± 193	2045 ± 537	9.1
90	598 ± 147	2851 ± 722	4.7
120	1321 ± 161	3860 ± 831	2.9

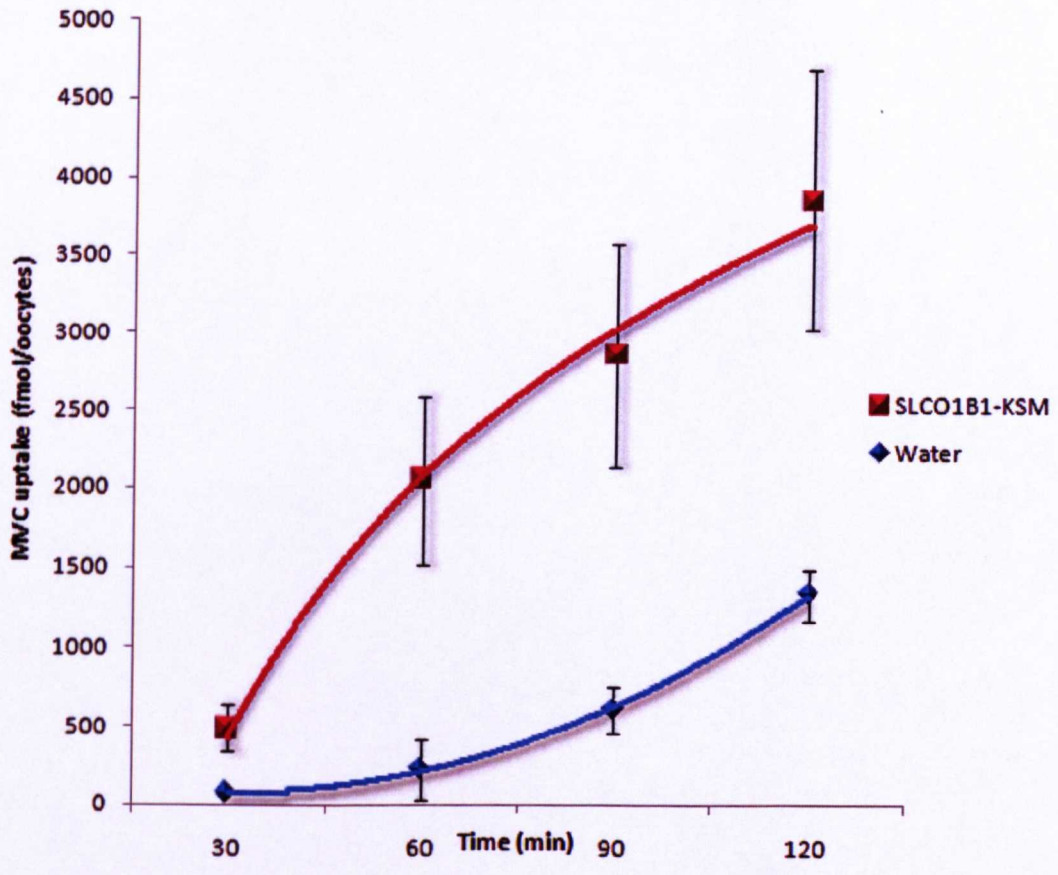

Figure 5.4. Water injected and *SLCO1B1*-KSM injected X. *laevis* oocytes uptake of MVC (n=3, mean ± SD)

MVC uptake rate showed concentration dependency with increasing concentrations, reaching saturation at 100μM as summarized in Table 5.4 and Figure 5.5. The K_m

was 33.85 μM and V_{max} was 187.9 fmol/oocyte/min. Cl_{int} (V_{max}/K_m) was equal to 5.5 nl/min/oocytes.

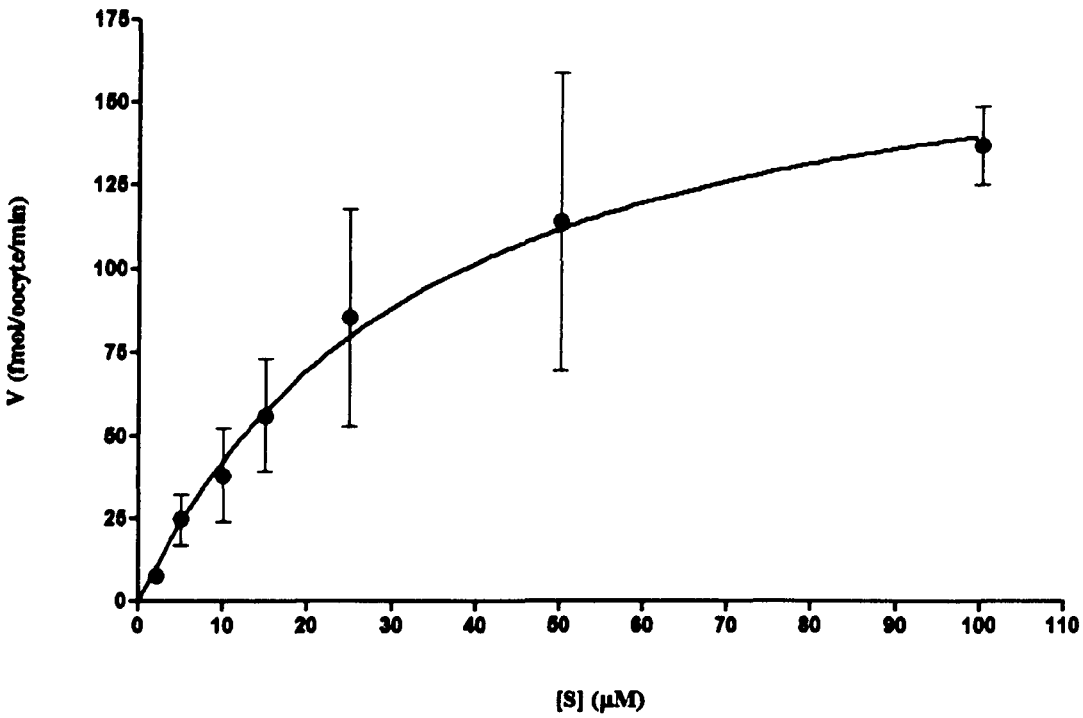

Figure 5.5. Concentration dependency of the uptake of MVC measured in a concentration range of 2–100 μM. (n = 4; mean ± SD)

Table 5.4. The uptake of MVC obtained by subtracting the transport rate of water-injected oocytes from that of *SLCO1B1*-KSM injected oocytes at increasing concentrations (2-100μMn = 4; mean ± SD).

Concentration (μM)	Velocity (fmol/oocyte/min)
2	8.1 ± 1.4
5	24.8 ± 7.6
10	38.25 ± 14.2
15	56.2 ± 16.9
25	85.4± 32.3
50	114.2± 44.5
100	137.5± 11.7

The uptake of MVC was significantly reduced ($p = 0.01$) by 75 ± 7.7 % at 5 μM and 73 ± 13 % at 25 μM by 30 μM cylosporin A (Figure 5.6). Oocytes injected with *SLCO1B1*-KSM 521C mRNA exhibited a lower MVC uptake compared to the oocytes injected with SLCO1B1-KSM 521T. MVC transport rate was 69 ± 7 % lower at 5 μM and 74 ± 8 % lower at 25 μM ($p = 0.01$) with the variant allele (Figure 5.6).

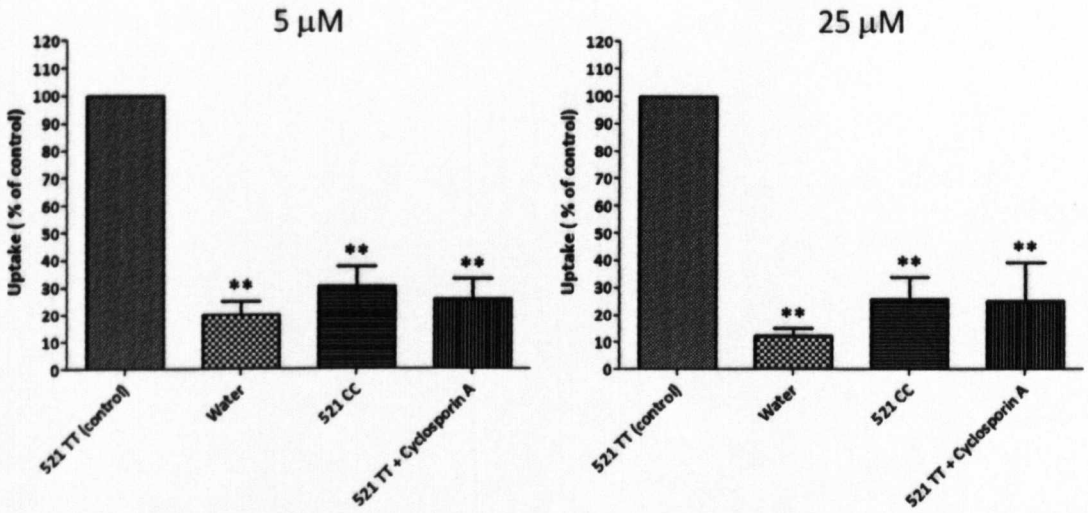

Figure 5.6. Effect of the 521C variant and cyclosporin A on MVC transport at two different concentrations of MVC (5 and 25 μM). The data are shown as the percentages of control value and expressed as mean ± SD (n=3). **p=0.01 significant difference by Dunnett's test.

5.3.3 Inhibition of MVC uptake by protease inhibitors

Uptake of MVC at 10μM in oocytes expressing SLCO1B1 was effectively inhibited by cyclosporin A and all PIs at high concentration (50 μM). As summarised in Figure 47, the uptake (% of control) with inhibitors was as follows: 23.% ± 4.2 for 50μM ATV, 36.01% ± 12.65 for 50μM DRV, 42.7% ± 21.9 for 50μM LPV, 30.5% ± 11.3 for 50μM RTV, 38% ± 4, 50μM SQV, 13.2% ± 3.5 for 30μM cyclosporin A; uptake ratio in water injected oocyte was 9% ± 3,8.

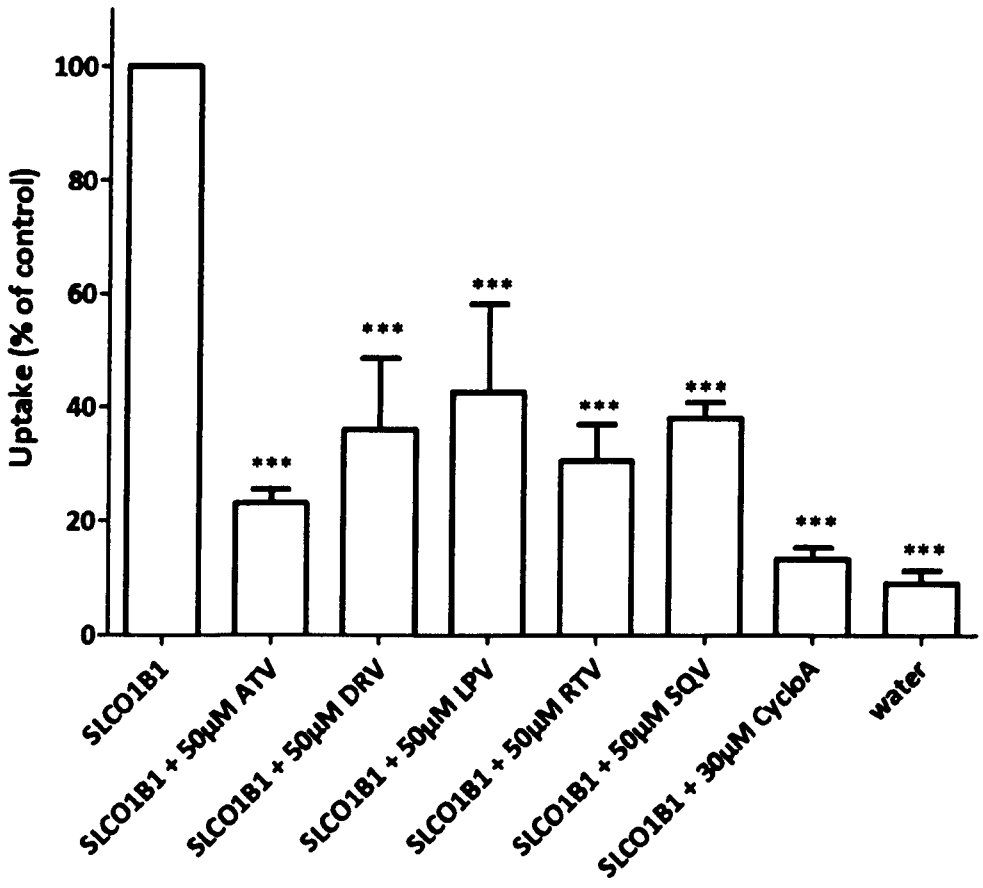

Figure 5.7 Effect of PIs and cyclosporin A on MVC uptake at 10µM. The data are shown as the percentage of control value and expressed as mean ± SD (n= 3). ***P=0.001.

The effect on 5µM MVC uptake at of increasing concentrations of inhibitors was tested in three independent experiments with three oocytes for each condition (0.1, 0.3, 1, 3.3, 10, 33 and 100 µM of inhibitor). Maximum inhibitory effects (% of control) reached at 100 µM for the inhibitors were 8.7% for ATV, 6.6 % of DRV, 5 % for LPV, 18.7% for RTV, 24.7% for SQV and 3.3% for cyclosporin A. A log(inhibitor) vs. response curves curve was fitted to the data in order to identify the IC_{50}, representing the concentration at which 50% of the maximum inhibitory effect is reached. Mean IC_{50} (µM; 95% CI) values were 1.8 (0.9 to 3.4) for ATV, 0.4 (0.3 to

0.6) for DRV, 1.0 (0.6 to 1.7) for LPV, 0.3 (0.2 to 0.4) for RTV, 0.6 (0.2 to 2.0) for SQV and 0.25 (0.1 to 0.5) for cyclosporin A.

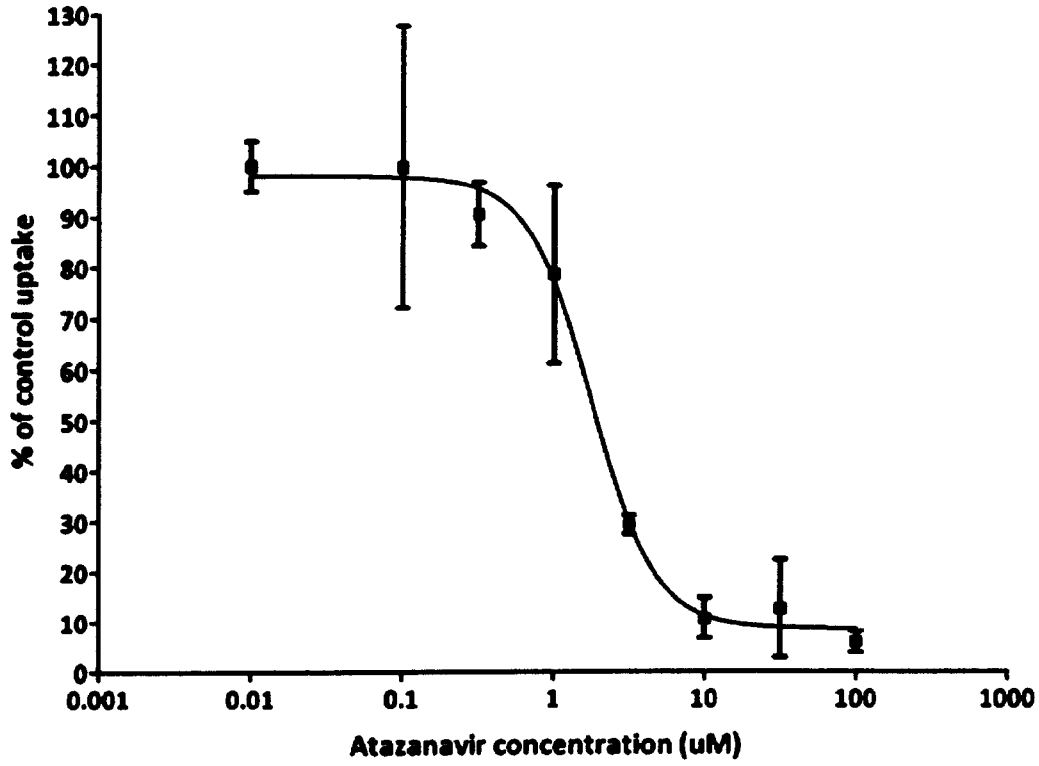

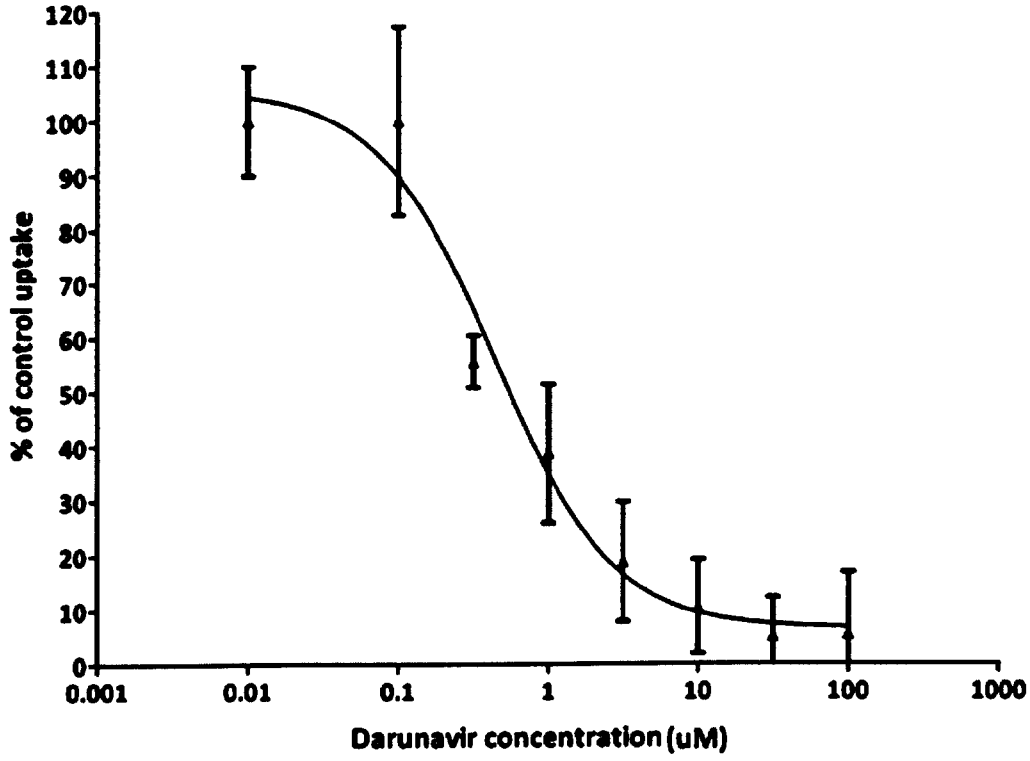
% of control uptake
120
110
100
90
80
70
60
50
40
30
20
10
0
0.001
0.01
0.1
1
10
100
1000
Darunavir concentration (uM)

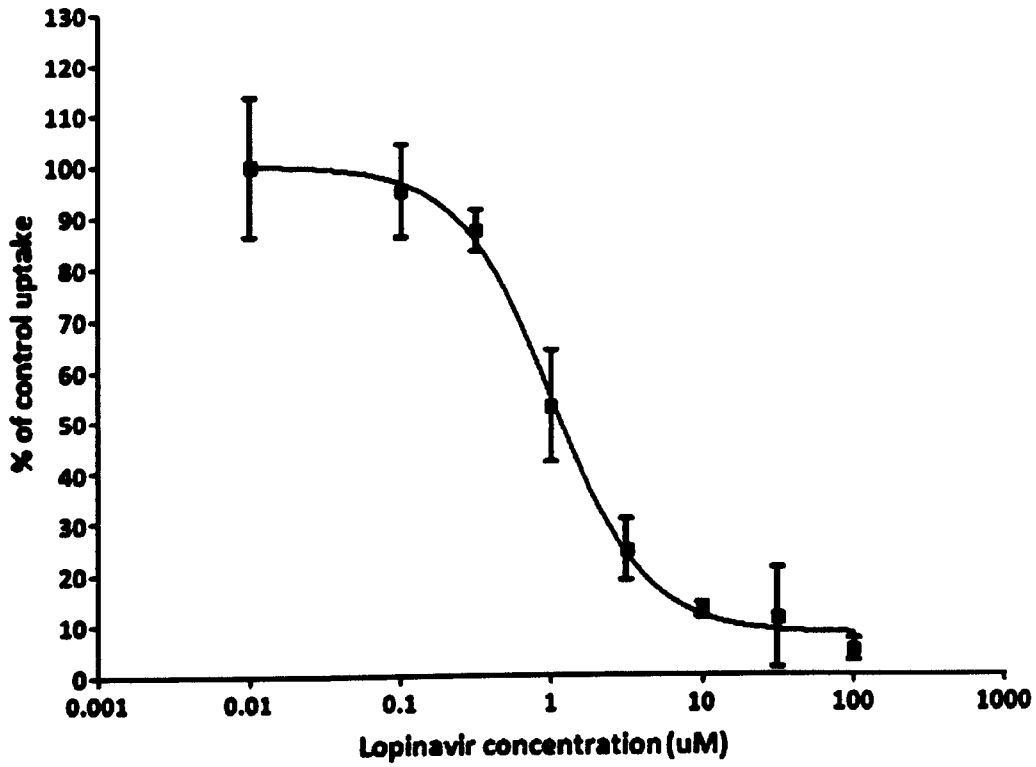
% of control uptake
130
120
110
100
90
80
70
60
50
40
30
20
10
0
0.001
0.01
0.1
1
10
100
1000
Lopinavir concentration (uM)

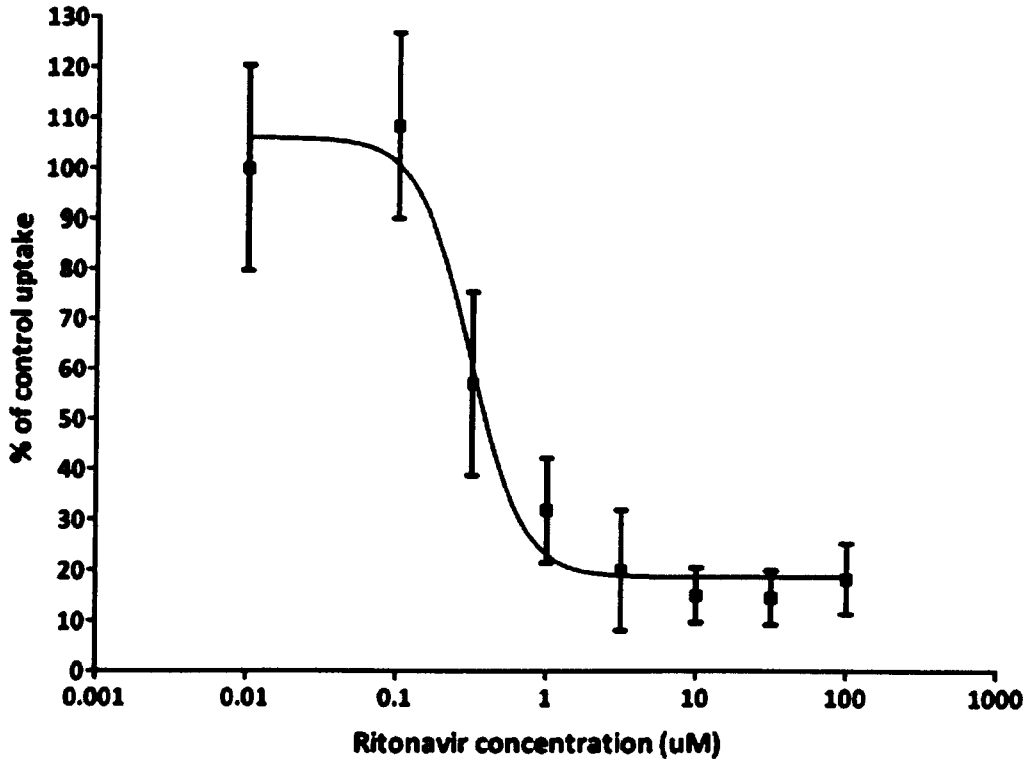
% of control uptake
130
120
110
100
90
80
70
60
50
40
30
20
10
0
0.001
0.01
0.1
1
10
100
1000
Ritonavir concentration (uM)

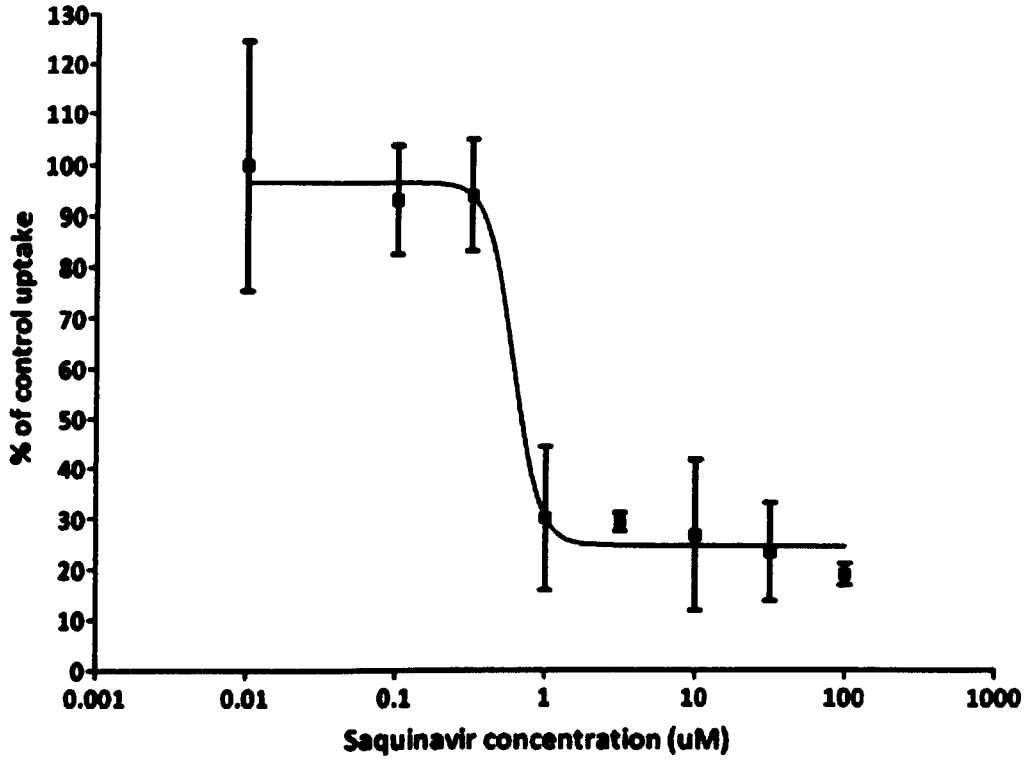
% of control uptake
130
120
110
100
90
80
70
60
50
40
30
20
10
0
0.001
0.01
0.1
1
10
100
1000
Saquinavir concentration (uM)

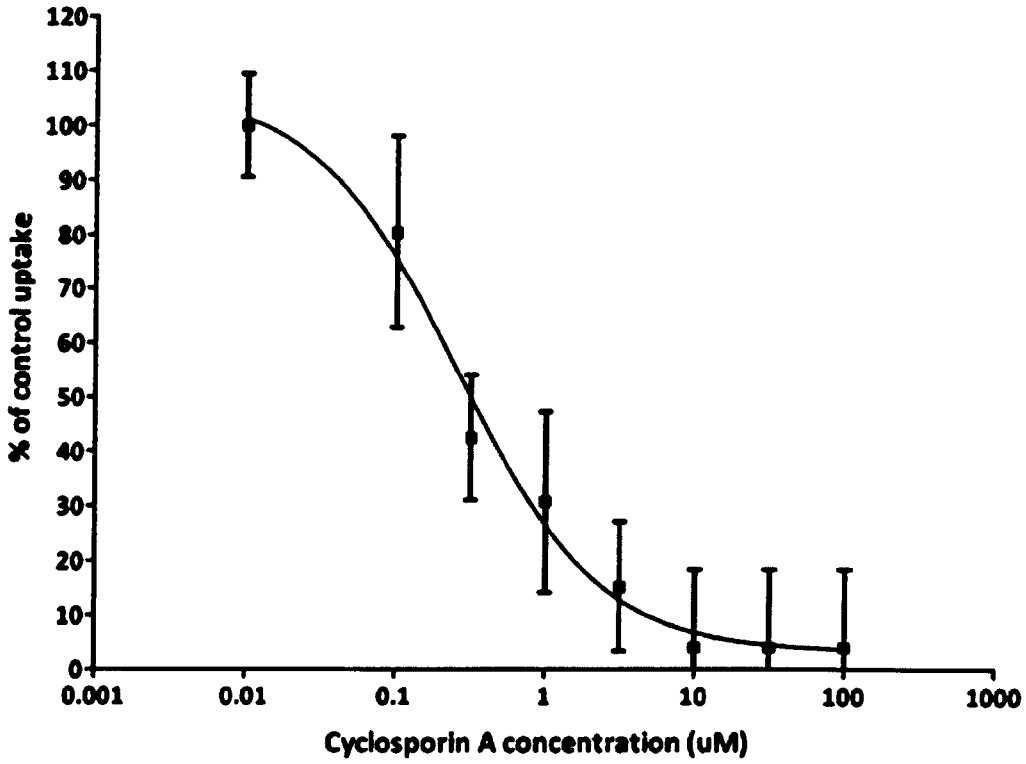

Figure 5.8. Concentration-dependent inhibition of MVC uptake in SLCO1B1-expressing oocytes. Accumulation of 5 μM MVC was measured in the presence of different concentrations of PIs and cycloA. Uptake was obtained by subtracting accumulation in water injected oocytes from uptake in SLCO1B1-expressing oocytes. Triangles represent the mean (± SD) of triplicate measurements. Lines represent the best fit to the data according to the log(inhibitor) vs. response curves curve.

5.4 Discussion

Several *in-vitro* systems have been developed in order to characterise the metabolism and transport affinity for substrates, therefore representing a useful tool to identify key proteins involved in the ADME process. Cell lines and primary cells are the most common cell population used in this sort of investigation. Primary hepatocytes, Chinese hamster ovary cells and *Xenopus laevis* oocytes are commonly used to investigate uptake transporters such as OCTs and SLCOs.

Xenopus laevis oocytes were successfully used to express heterologus transporters and to study the role of SLCOs for uptake of several antiretrovirals and other class of drugs and LPV, SQV, DRV (Hartkoorn et al. 2010), statins (Fujino et al. 2005), imatinib (Hu et al. 2008) were identified as substrates of SLCO1B1. The pharmacokinetics of many substrates can be influenced by 521 C>T polymorphism (Zair et al. 2008) and consequently *X. laevis* expression system could be used to predict pharmacogenetic associations. Recently several *in-vitro in-vivo* extrapolation (IVIVE) algorithms that include SLCO1B1 as a hepatic uptake transporter have been developed giving the opportunity to simulate the impact of SLCO1B1 genetic variants on substrate pharmacokinetics (Jamei et al. 2009).

Moreover this *in-vitro* system was use to investigate potential interactions mediated by uptake transporters between RAL and TDF (Moss et al. 2011), gemfibrozil and pravastatin (Shitara et al. 2004), theophylline with erythromycin (Kobayashi et al.

2005), rifamycin SV and rifampicin (Vavricka et al. 2002) and methotrexate and nonsteroidal anti-inflammatory drugs (Uwai et al. 2000).

Substrate specificity of MVC for SLCO1B1 was determined using the X. *laevis* expression system. This kind of assay is low-throughput and labour intensive and complicated by variations in quality of oocytes, causing large variations in oocyte uptake. Nonetheless the heterologus expression system using *X. laevis* oocytes represents a flexible *in-vitro* technique that can be used to successfully identify substrates of various uptake and efflux transporters. Statistically significant differences between *SLCO1B1*-KSM and water injected oocytes uptake could be described and MVC was confirmed as a good substrate for this transporter. *SLCO1B1*-KSM injected oocytes accumulate MVC when compared to their respective water injected controls (2045 ± 537 fmol/oocytes vs 224 ± 193 fmol/oocytes, ratio 9.1, p= 0.005, after 60 min, 5μM). Uptake of MVC by SLCO1B1 was confirmed using a specific inhibitor of this transporter, cyclosporin A with a significant decrease in the MVC uptake rate at 5 μM and 25 μM. The concentration-dependent uptake of MVC in oocytes overexpressing SLCO1B1 demonstrate that MVC is a substrate of the uptake transporter, with K_m equal to 33.85 μM, V_{max} equal to 187.9 fmol/oocyte/min and a Cl_{int} (V max/Km) equal to 5.5 nl/min/oocytes.

Similar results were obtained in other *in-vitro* studies of SLCO1B1 substrates, such as olmesartan with a K_m of 42.5 μM (Nakagomi-Hagihara et al. 2006), pravastatin with a Km of 57.47 μM, pivatastatin with a Km of 6.70 μM and fluvastatin with a K_m of 31.1 μM (Deng et al. 2008). The range of MVC plasma concentrations (10-

300 ng/ml) is much lower than the K_m value (33.85 μM) of maraviroc uptake, suggesting that SLCO1B1 may play an important role in vivo.

Moreover, in this chapter *Xenopus laevis* oocytes heterologus protein expression system was used to screen PIs for potential interaction with MVC mediated by SLCO1B1, and a range of PIs was tested in order to quantify the IC_{50}, measure of the inhibitory concentration at which 50% of the maximum inhibition can be achieved.

All tested drugs resulted in a intense inhibition of MVC uptake by SLCO1B1 at high concentrations, decreasing the uptake of MVC by 77% for ATV, 64% for DRV, 57 LPV, 69% for RTV, 62% for SQV, and 87% for cyclosporine A. This first set of data suggest that the effect of PIs on SLCO1B1 activity is comparable to cyclosporin A, a well known inhibitor of SLCO1B1 which cause interactions with several drugs, such as statins (Shitara et al. 2003), repaglinide (Kajosaari et al. 2005), methotrexate (Fox et al. 2003) and bosentan (Binet et al. 2000).

MVC uptake was further investigated using a broad range of inhibitor concentrations (0.1 to 100 μM) and all PIs proved to have an IC_{50} below 2μM; mean IC50 (μM; 95% CI) were 1.79 (0.94 to 3.38) for ATV, 0.44 (0.29 to 0.64) for DRV, 1.0 (0.6 to 1.7) for LPV, 0.3 (0.23 to 0.39) for RTV, 0.6 (0.17 to 2.1) for SQV and 0.25 (0.13 to 0.47) for cyclosporin A. The minor difference between IC_{50} for a known inhibitor of SLCO1B1 such as cyclosporin A and the tested PIs suggests a similar potency for PIs, consequently the clinical relevance of this inhibitory effect can be hypothesised. Cyclosporin A is able to cause an increment of 2-20 times in the plasma exposure of

statins, which are well characterised substrates of SLCO1B1 and the enhancement of statin pharmacokinetics is characterised by a marked increase in the peak plasma concentration and AUC, without a significant effect on terminal half-life (Muck et al. 1999; Hedman et al. 2004).

The overall effect of PIs on MVC and other SLCO1B1 substrates pharmacokinetics may also be influenced by inhibition of several other proteins such as efflux transporters and metabolism enzymes, since PIs are known inhibitors of ABCB1 and CYPs. This complex interplay of inhibition determines increased absorption, altered passage into tissues, decreased metabolism and elimination. Therefore investigation of the overall effect of PIs on MVC and other SLCO1B1 substrates pharmacokinetics should take into account several transporters and enzymes. Moreover the use of other cell lines or primary cells to investigate the substrate specificity of MVC and the inhibitory effect of PIs on SLCO1B1, could improve our understanding of SLCO1B1 relevance in the determination of antiretroviral pharmacokinetics and drug-drug interactions.

Genetic polymorphisms in the SLCO1B1 gene reduce the expression or functionality of SLCO1B1, therefore patients carrying genetic profile which can cause a decrement in the SLCO1B1 activity might have a more intense drug-drug interaction or a broader range of variability. Moreover, a large portion of HIV positive patients are receiving an increasing number of drugs for the treatment of concomitant pathologies. Consequently patients treated with SLCO1B1 substrates should be monitored for multiple drug-interactions caused by two or more inhibitors of

SLCO1B1 which may determine a synergistic effect on the liver uptake of SLCO1B1 substrates and their pharmacokinetics.

CHAPTER 6

SLCO1B1 521 T>C effect on maraviroc pharmacokinetics in the clinical setting

6.1 Introduction

The traditional targets of most HAART regimes are the viral reverse-transcriptase and viral protease however the appearance of mutations in these proteins conferring resistance can limit therapeutic use. Therefore, new antiretrovirals that target other steps in the viral life cycle have been crucial for effective treatment of multidrug-resistant viral strains. HIV enters new cells by interacting with the CD4 receptor and a chemokine receptor such as CCR5 or CXCR4. CCR5 is one co-receptor involved in the activation of leucocytes and is the main co-receptor by which HIV infects cells. Maraviroc (MVC) effectively inhibits the interaction between HIV and CCR5, blocking HIV entry into the host cells and is the first licensed CCR5-antagonist, representing a useful clinical tool in the treatment of treatment-experienced patients.

MVC standard dosing is 300 mg bid but dose adjustments are recommended when co-administering with inhibitors and inducers of its metabolism (Abel et al. 2008; Abel et al. 2008). MVC is a CYP3A4 substrate and is transported by P-glycoprotein. Ritonavir (RTV), which is commonly administered as a booster for protease inhibitors, is a strong inhibitor of CYP3A4 and ABCB1, and can consequently cause an increase in MVC plasma concentrations. Therefore the dose of MVC is reduced to 150 mg bid if co-administered with a boosted protease inhibitor, except tipranavir (TPV) (Abel et al. 2008). Etravirine (ETV) and efavirenz (EFV) are known inducers of CYP3A4 and cause a decrease in the MVC plasma concentrations, and the MVC dose has to be increased to 600 mg (Abel et al. 2008). When patients are not receiving these drugs 300mg bid is adequate to achieve sufficient plasma exposure of

MVC. Moreover CYP4A4 activity is characterized by a marked inter-individual variability. However this variability cannot be explained by currently described SNPs, such as *CYP3A4**1B (rs2740574), which has been controversially associated with altered CYP3A4 expression (Ingelman-Sundberg et al. 2007).

P-gp, coded by the *ABCB1* gene, is involved in the disposition of several CYP3A4 substrates, including MVC (Walker et al. 2005), and influences intestinal absorption and excretion into the bile (Kim et al. 1998; Choo et al. 2000). One of the most extensively studied SNPs in *ABCB1* is the synonymous transition 3435C>T (rs1045642), which has been correlated with the alteration of plasma concentrations of several drugs (Owen 2006).

As demonstrated in Chapter 5, MVC is a substrate of the influx transporter SLCO1B1 which is emerging as an important determinant of the pharmacokinetics of antiretrovirals and other classes of drugs. The 521T>C SNP (rs4149056) has previously been correlated with increased plasma concentrations of several substrates such as pravastatin and lopinavir (Niemi et al. 2004; Hartkoorn et al. 2010). The C variant allele causes a Val-174 → Ala substitution in the transmembrane-spanning domain, altering cell surface expression (Tirona et al. 2001).

Other proteins which can play an active role in the ADME process are the nuclear receptors (NRs). One of the main regulators of Phase I and II metabolism and transporters is the pregnane – X – receptor (PXR; *NR1I2*). PXR has been shown to

be activated by many PIs (Svard et al. 2008) and to regulate the expression of *CYP3A4* (Moore and Kliewer 2000), *ABCB1* (Geick et al. 2001) and *SLCO1B1* (Jigorel et al. 2006). Three polymorphisms have been associated with expression of PXR and the activity of *CYP3A4* (Lamba et al. 2008). Furthermore homozygosity of 63396C>T has been recently identified as a predictor of sub-optimal ATV C_{trough} and in Chapter 2 has been proven to influence ATV clearance (Siccardi et al. 2008).

The aim of this chapter was to evaluate the effect of i) concomitant antiretrovirals and ii) SNPs (*CYP3A4**1B, *ABCB1* 3435C>T, *SLCO1B1* 521T>C and *PXR* 63396C>T) on MVC plasma C_{trough} exposure in patients treated with several antiretroviral regimens. Initially, bio-analytical methodology for the quantification of MVC in human plasma was developed and validated.

6.2 Methods

6.2.1 HPLC-UV method for the quantification of MVC in human plasma

6.2.1.1 Chemicals

Quinoxaline (QX), orto-phosphoric acid, potassium dihydrogen phosphate, formic acid and trifluoroacetic acid (TFA) were obtained from Sigma-Aldrich (Milan, Italy). Blank plasma from healthy donors was kindly supplied by the Blood Bank of Maria Vittoria Hospital (Turin, Italy).

6.2.1.2 Stock solutions, Standards and Quality Controls

MVC and QX stock solutions were made in a solution of methanol and HPLC grade water (90:10 vol/vol). The Internal Standards (IS) working solution was prepared with QX (2 μg/mL) in methanol and HPLC grade water (50:50, v/v) and stored at 4°C until use (maximum 1 month).

6.2.1.3 Chromatographic Conditions

The HPLC system used to assay MVC consisted of two pumps model 515, an 717 autosampler, and 2487 UV detector (Waters, Milan, Italy). The detector was operated at a wavelength of 193 nm and, after a switch and autozero of the wawelength at 9.2 minutes of run, at a wavelength of 352 nm. A Pump Control Module (PCM) interface and Empower 2 Pro software (version year 2005, Waters; Milan, Italy) were used for management of the HPLC system. Chromatographic separation was performed by a Luna 5μ C18 column (150x4.6 mm I.D, Phenomenex, CA, USA), protected by a C18 Security Guard (4.0x3.0 mm I.D, Phenomenex, CA, USA), at 44°C using a column thermostat TS130 (Phenomenex, CA, USA). The run was performed at 1 ml/min, the mobile phase was composed of Solvent A (KH_2PO_4 50 mM with ortho-phosphoric acid, final pH = 3.23) and Solvent B (acetonitrile), as Table 6.1. The calibration curve was obtained using standards ranging from 19.5 to 2500 ng/mL. QC concentrations were 2000, 500, and 50 ng/ml.

Table 6.1. Chromatographic conditions (gradient): Mobile phase: Solvent A (KH_2PO_4 50 mM with ortho-phosphoric acid, final pH = 3.23) and Solvent B (acetonitrile).

TIME (min.)	% Solvent A	% Solvent B	Flow (ml/min)
0.00	74	26	1
3.00	71	29	1
5.00	70	30	1
5.45	65	35	1
5.50	30	70	1
10.00	30	70	1
10.10	74	26	1
15.00	74	26	1

6.2.1.4 Standards, Quality Controls and Sample Preparation

1400 µl of protein precipitation solution (acetonitrile + TFA 0.1%) and 50 µl of IS working solution were added to 600 µl aliquots of plasma samples, in a PTFE microfuge tube. After vortexing for 30 seconds, the mixture was centrifuged at 12,000 rpm for 10 min at 4°C. All the supernatant was transferred into glass tubes, and evaporated to dryness using a vortex-vacuum (60°C). Each extract was reconstituted with 60 µl of mobile phase solution (50 mM KH2PO4 pH 3,2 and acetonitrile; 70:30, v/v) and 30 µl were injected into the column.

6.2.1.5 Validation

Interference from endogenous compounds was investigated by analysis of six different blank solution. Other possible concomitant drugs were also investigated, including amodiaquine, desacetyl amodiaquine, amoxicillin, caspofungin,

ceftazidime, ciprofloxacin, clavulanic acid, ethambutol, furosemide, insulin, isoniazid, levofloxacin, nimesulide, omeprazole, pravastatin, and ribavirin.

Intra-day and inter-day accuracy and precision were determined by assaying 4 sets of QCs in each session. Accuracy was calculated as the percent deviation from the nominal concentration. Inter-day and intra-day precision were expressed as the standard deviation at each QC concentration. The calibration curve was obtained using 8 calibration points in duplicate. A quadratic through zero calibration curve was used. The limit of detection (LOD) was defined as the concentration that yields a signal-to-noise ratio of 3/1. Percent deviation from the nominal concentration (measure of accuracy) and relative standard deviation (measure of precision) of the concentration considered as the limit of quantification (LOQ) had to be < 20%, and it was considered the lowest calibration standard, as requested by FDA guidelines.

Average recovery of all analytes was determined by comparing the peak area of the drug extracted from the three QCs with those obtained by direct injection of the same amount of drug in the reconstitution solution.

6.2.2 Clinical study

Patients were recruited in the Department of Infectious Diseases, University of Torino, Amedeo di Savoia Hospital, Torino, Italy and Clinic of Infectious Diseases, San Raffaele Scientific Institute, Milano, Italy. Inclusion criteria were as follows: older than 18 years old, not receiving interfering drugs, in good general medical

condition and having a good adherence record as assessed by analyses of clinical and pharmacy records. Sampling was performed after written informed consent was obtained in accordance with local ethics committee indications. 42 patients receiving MVC as part of their therapy were included in the study. 3 patients were treated with MVC 300 mg bid + NVP (200 mg bid) and 1 + TPV/r (500 mg + 200 mg of RTV bid), 7 patients received MVC 150 mg bid + DRV/r (600 mg + 100 mg of RTV bid), and 29 patients received 600 mg bid + ETV (200 mg bid) and one patient received 600 mg bid + 600 mg od EFV. MVC C_{trough} was measured in samples collected 10-14 hr post dose.

DNA was extracted from whole blood (100µl) using GenElute Blood Genomic DNA kit (Sigma-Aldrich, Poole, UK), according to the manufacturer's instructions. Genotyping was conducted by real time PCR based allelic discrimination. PCR reaction volume was 25 µl; 12.5 µl Taq Man MasterMix (Applied Biosystem, UK), 1.25 µl of primers and probes (SLCO1B1 521 T>C, rs4149056, Applied Biosystem code = C__30633906_10; ABCB1 3435 C>T, rs1045642, Applied Biosystem code = C___7586657_20; PXR 63396 C>T, rs2472677, Applied Biosystem code = C__26079845_10), 1 µl of DNA and ddH2O to a final volume of 25 µl. PCR parameters were: first segment, one cycle 95°C for 10 minutes; second segment, 50 cycles, 95°C for 30 seconds, 60°C for 1 minute. The fluorescence plate reading was set to excite FAM and VIC dyes at 488 nm and quantify fluorescence at 518 nm for FAM and 552 for VIC. Fluorescence, proportional to amplification, was measured using Opticon 2 and Chromo4 real-time detector (Biorad, Hemel Hempstead, UK). The genotypes were determined from fluorescence intensity at the endpoint. All genotyping experiments were performed in duplicate and included positive controls

for each possible genotype. A genotype was only assigned when both duplicates were in agreement.

Data were processed in Microsoft Excel 2007 and statistical analyses were performed using SPSS 14 or R. Results for categorical data are expressed as median with IQR. All data were assessed for normality using a Shapiro-Wilk test and categorical data were compared using a Mann Whitney or Kruskal-Wallis statistical test. All variants were tested for Hardy-Weinburg equilibrium by $\chi 2$ test of observed and predicted genotype frequencies. To investigate continuous data, a Spearman Rank correlation was utilised. Univariate and stepwise logistic regression analyses were conducted to identify factors associated with MVC C_{trough}.

6.3 Results

6.3.1 Validation of the HPLC-UV for MVC quantification in plasma

IS and MVC retention times were 11.1 ± 0.25 minutes and 7.2 ± 0.25 minutes, respectively. Representative chromatograms of STD1 and STD8 are shown in Figure 6.1 and Figure 6.2.

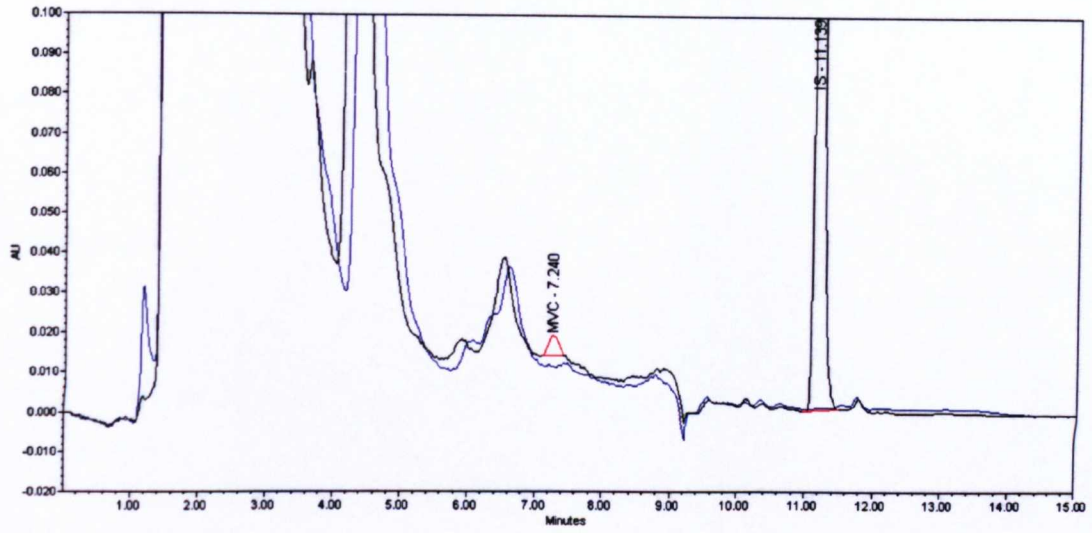

Figure 6.1. Chromatogram representing retention time for MVC and IS from extracted plasma samples at STD1 (overlapped with blank plasma extract).

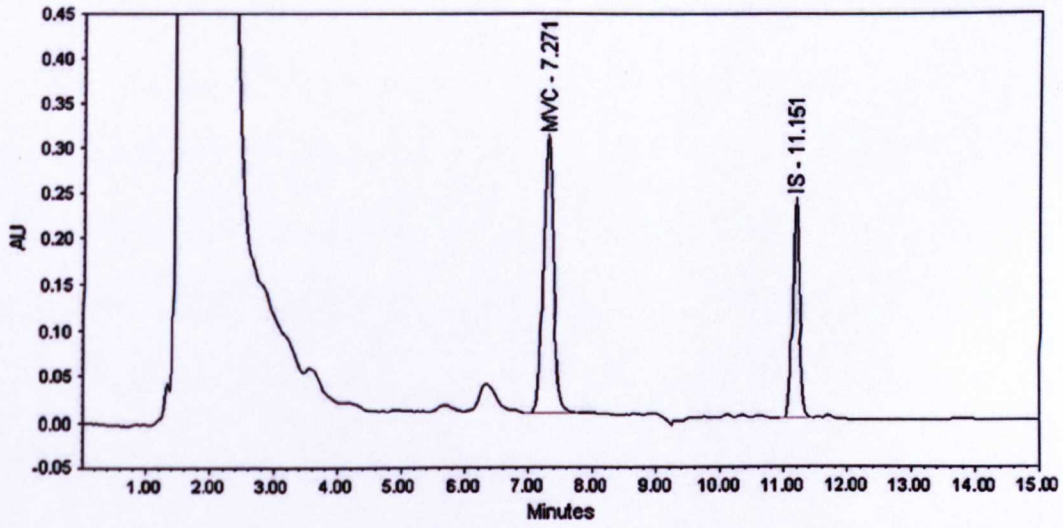

Figure 6.2. Chromatogram representing retention time for MVC and IS from extracted plasma samples at STD8 (overlapped with blank plasma extract).

The assays did not show any relevant interference with antiretrovirals or other concomitant drugs administered to the patients at therapeutic doses. A linear through zero regression was chosen and mean regression coefficient (r^2) of all calibration curves was at least 0.998. Results of the validation of the methods are listed in Table

6.2. All observed data (Intraday and Interday precision [RSD%]) were below 15.0 %, according to FDA guidelines(Food and Drug Administration 2001). This assay had a linear response, up to 2500 ng/ml. LOQ and LOD were 19.5 ng/mL and 5 ng/mL, respectively.

Table 6.2. Accuracy (%), Intraday and Interday Precision (RSD%) assayed for maraviroc (n=8).

	QC High			QC Medium			QC Low		
		Precision (RSD%)			Precision (RSD%)			Precision (RSD%)	
Drugs	Acc %	Intraday	Interday	Acc %	Intraday	Interday	Acc %	Intraday	Interday
MVC	4.16	2.16	3.59	5.54	2.87	4.72	-3.40	5.57	11.09

Multiple aliquots (n=8) at each of the three QCs concentration for MVC were assayed and mean recovery ranged from 91% to 101% (total mean = 96%). Mean recovery for IS was 95%. The stability study of MVC and IS in plasma extracts, kept for 24 h in the autosampler at room temperature, showed a variation below 9% for IS and MVC at each concentration, therefore the samples can be considered stable throughout the HPLC-UV analysis.

6.3.2 Genotyping analysis

For *ABCB1* 3435C>T, the fluorogenic probe complementary to the C allele had a FAM dye and the fluorogenic probe complementary to the T allele had a VIC dye. Amplification of both probes indicates the presence of both alleles and therefore heterozygosity. As shown in Figure 6.3, the three genetic groups were easily distinguishable: the Y axis represents the endpoint fluorescence for VIC dye and the

X axis represents endpoint fluorescence for FAM dye. Patients with CC genotype resulted in amplification of just the FAM-probe (open circle), patients with heterozygosity had amplification of both probes (open triangle) and patients with TT genotype had amplification of the VIC-probe (open square).

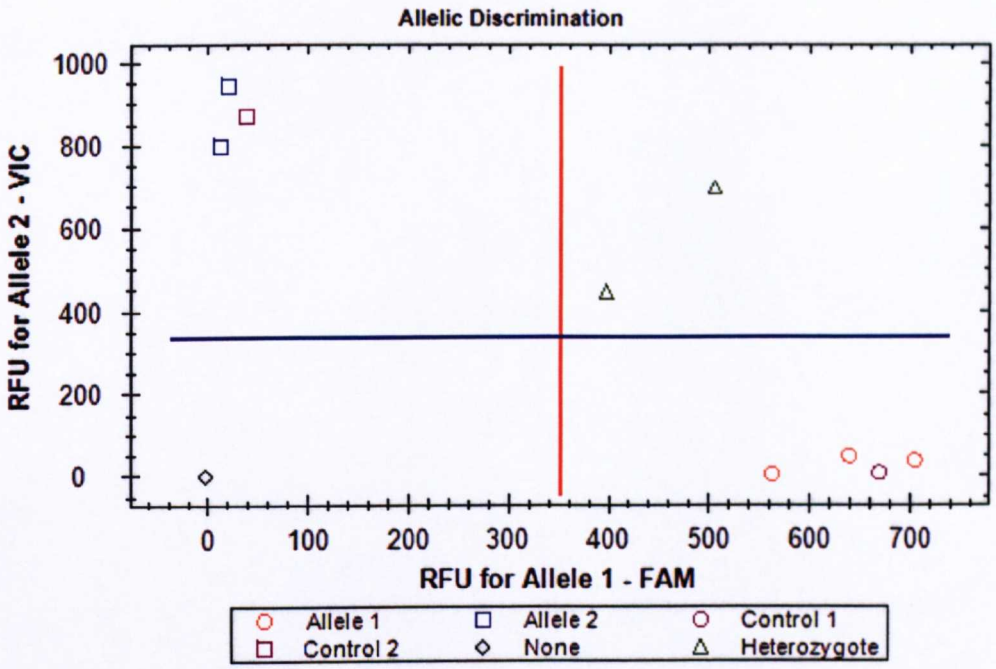

Figure 6.3. Representative allelic discrimination plot for *ABCB1* 3435C>T. Open square represents TT genotype, open triangle CT and open circle CC genotype. Orange line is the threshold for FAM-probe amplification and blue line for the amplification of VIC-probe.

For *SLCO1B1* 521T>C, the fluorogenic probe complementary to the T allele had a FAM dye and the fluorogenic probe complementary to the C allele had a VIC dye. Amplification of both probes indicates the presence of both alleles and therefore heterozygosis. A shown in Figure 6.4, patients with TT genotype resulted in amplification of just the FAM-probe (open circle), patients with heterozygosis had amplification of both probes (open triangle).

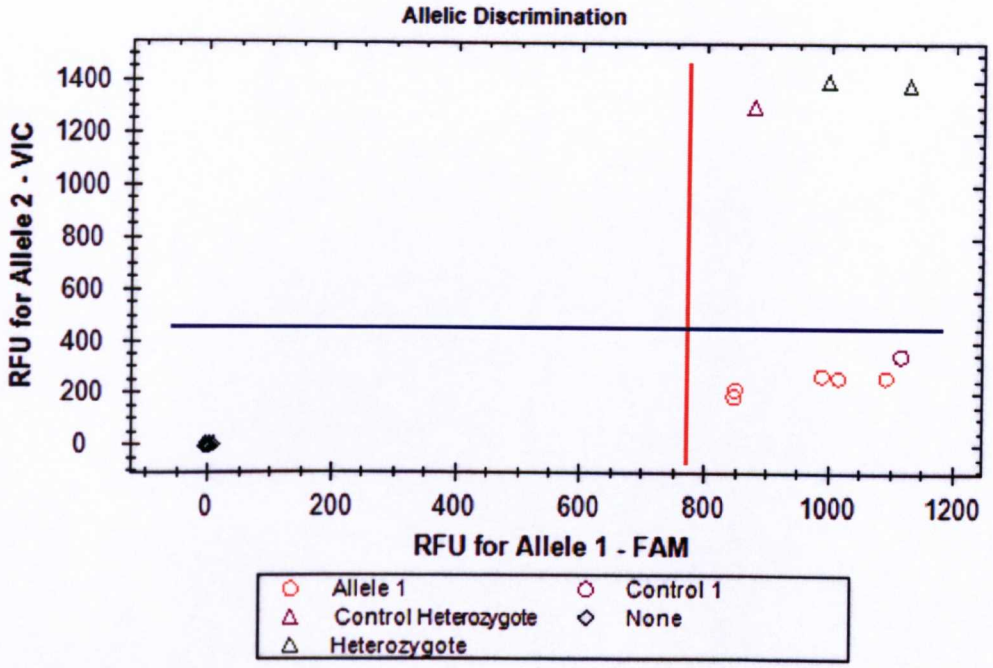

Figure 6.4. Representative allelic discrimination plot for *SLCO1B1* 521T>C. Open triangle represents TC genotype and open circle TT genotype. Orange line is the threshold for FAM-probe amplification and blue line for the amplification of VIC-probe.

For *PXR* 63396C>T, the fluorogenic probe complementary to the T allele had a FAM dye and the fluorogenic probe complementary to the C allele had a VIC dye. As shown in Figure 6.5, patients with TT genotype resulted in amplification of just the FAM-probe (open circle), patients with heterozygosis had amplification of both probes (open triangle) and patients with CC genotype resulted in amplification of just the VIC-probe.

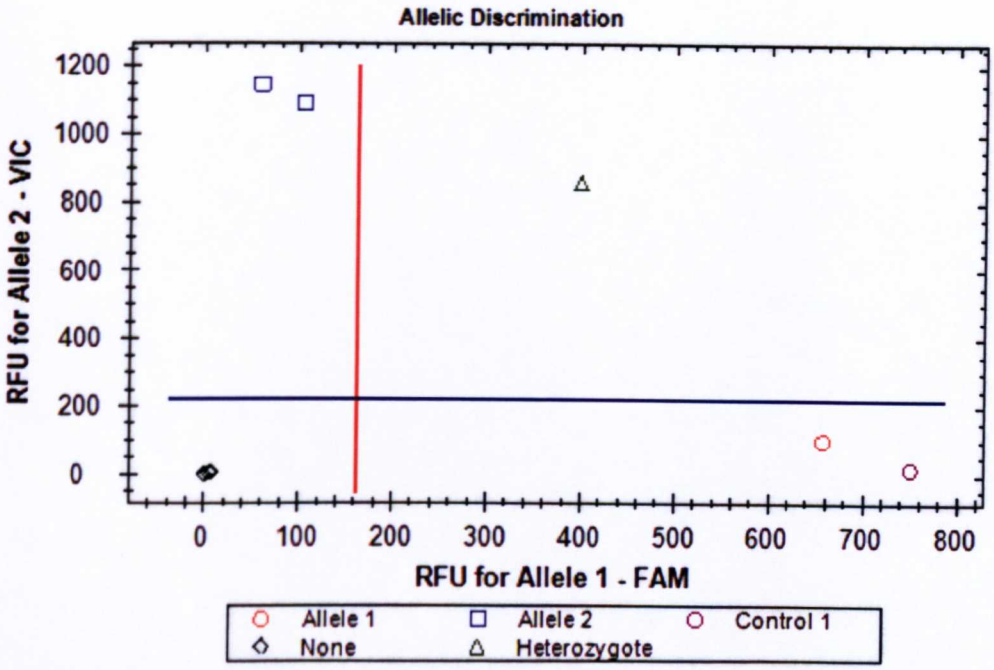

Figure 6.5. Representative allelic discrimination plot for *PXR 63396C*>T. Open square represents CC genotype open triangle CT and open circle TT genotype. Orange line is the threshold for FAM-probe amplification and blue line for the amplification of VIC-probe.

For *CYP3A4* *1B, the fluorogenic probe complementary to the *1 allele had a FAM dye and the fluorogenic probe complementary to the *1B allele had a VIC dye. As shown in Figure 6.6, patients with *1/*1 genotype resulted in amplification of just the FAM-probe (open circle), patients with heterozygosis had amplification of both probes (open triangle) and patients with *1B/*1B genotype resulted in amplification of just the VIC-probe.

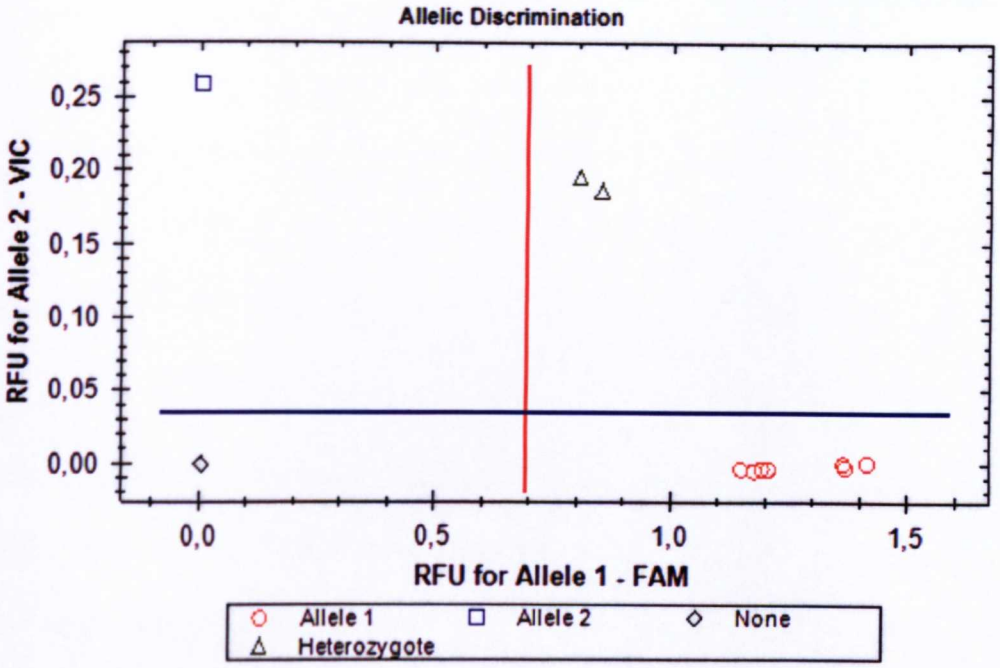

Figure 6.6. Representative allelic discrimination plot for *CYP3A4**1B . Open square represents *1/*1 genotype open triangle *1/*1B and open circle *1B/*1B genotype. Orange line is the threshold for FAM-probe amplification and blue line for the amplification of VIC-probe.

6.3.3 Clinical study

Patient demographics and clinical characteristics are summarized in Table 6.3. No association between patient demographics and MVC C_{trough} were observed. Gender did not influence median MVC C_{trough} values: men, 66 ng/ml (42.5–111) vs women, 50 ng/ml (15–78), $p = 0.28$). Similarly, MVC C_{trough} was not correlated with height ($\rho = -0.09$; $p = 0.56$), weight ($\rho = -0.25$; $p = 0.11$), or age ($\rho = -0.22$; $p = 0.17$).

Table 6.3. A summary of patient demographics and physical characteristics

Gender (Male, %)	37 (90)
Age	47 (44-54)
Weight (kg)	72 (66-80)
Height (cm)	175 (170-179)

The variant allele frequency for *ABCB1* 3435 was 0.47, for *CYP3A4**1B was 0.05, for *PXR* 63396 was 0.61 and for *SLCO1B1* 521 was 0.12. All SNPs were in Hardy Weinberg equilibrium. Effect of concomitant antiretrovirals on MVC C_{trough} is summarized in

Table 6.4 and Figure 6.7. MVC C_{trough} differed between patients treated with different concomitant antiretrovirals (p=0.033). Patients treated with 150mg bid of MVC plus a boosted protease inhibitor (n=7) had a median C_{trough} of 127 ng/mL (71-161); patients treated with 300 mg bid plus nevirapine (n=4) had a median C_{trough} of 51 ng/mL (30-128), and patients treated with 600mg bid plus etravirine (n=30) had a median C_{trough} of 59 ng/ml (36-82). MVC C_{trough} values were significantly higher in patients treated with 150 mg bid of MVC plus a boosted protease inhibitor, 127 ng/mL (71-161) than patients treated with 600 mg bid plus etravirine, 59 ng/ml (36-82), p=0.007.

Table 6.4. Effect of dose and concomitant antiretrovirals on MVC plasma concentrations.

MVC	N (%)	MVC C_{trough} (ng/ml)	p value
150mg + PI/r	7 (17)	127 (71-161)	0.033
300mg	4 (10)	51 (30-128)	
600 mg + ETV*	30 (73)	59 (36-82)	

*One patients received efavirenz (600 mg once daily)

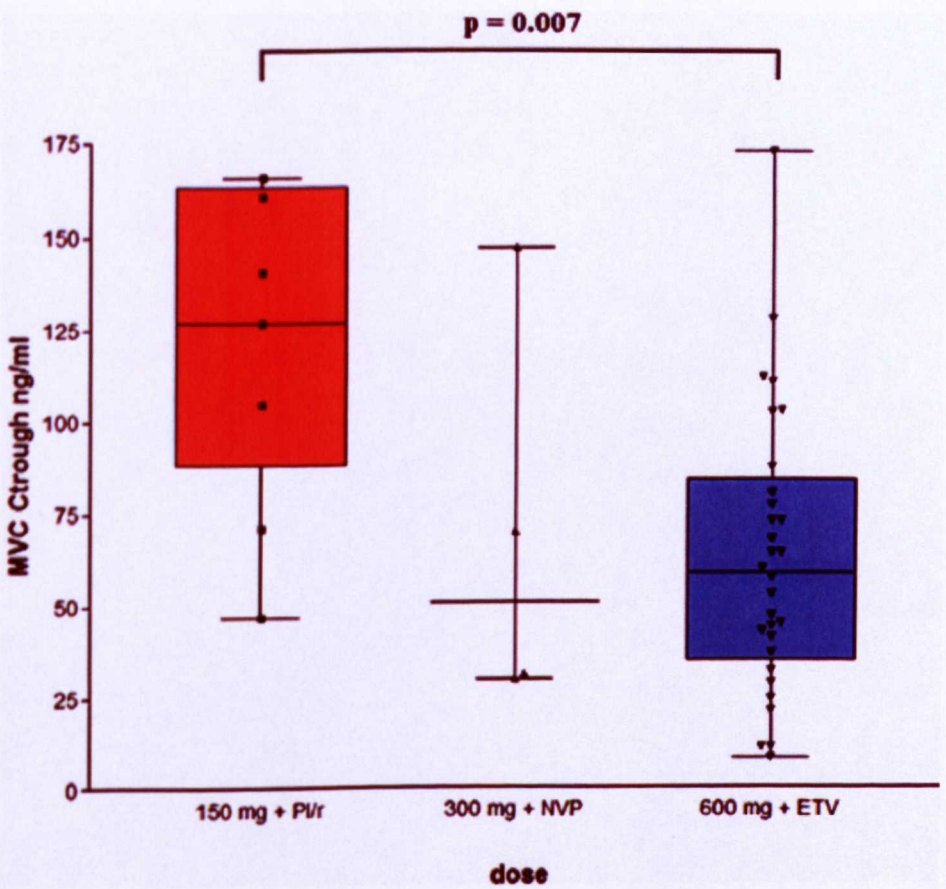

Figure 6.7. MVC C_{trough} and dose. Median values (horizontal thick line), IQR (bars), individual patient values (dots), highest and lowest value (whiskers) are given.

The majority of patients (30 out of 41) were receiving MVC 600 mg + ETV, which was selected for further pharmacogenetic analysis, avoiding the confounding effect of concomitant drugs. *PXR* 63396 C>T, *ABCB1* 3435 C>T and *CYP3A4**1B were not associated with MVC C_{trough}, as represented in Figure 6.8.

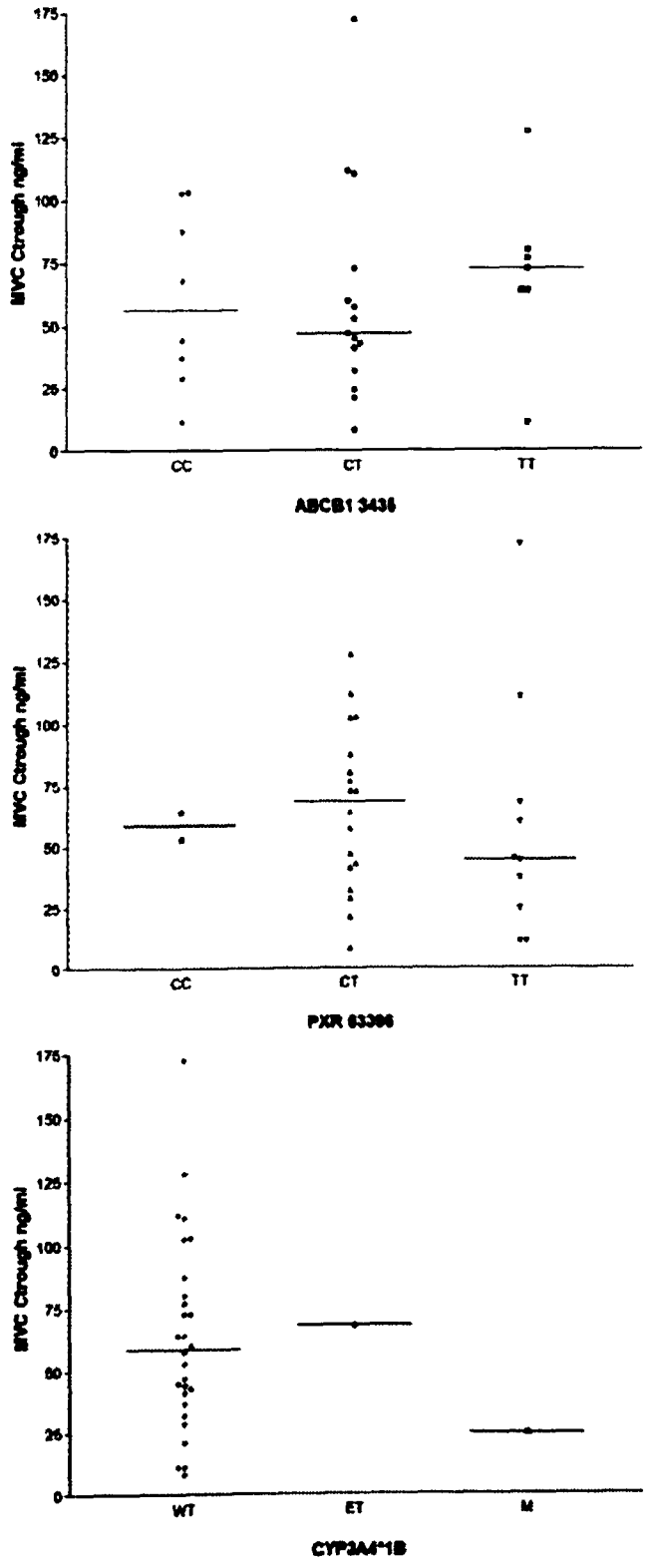

Figure 6.8. MVC C_{trough} and genotypes. Median values (horizontal thick line), IQR (bars), patient values (dots), highest and lowest value (whiskers) are given.

MVC C_{trough} in *SLCO1B1* 521 heterozygote patients (TC) (n=8) were higher than in wild type homozygotes (TT) (n=22) [103 ng/ml (69 - 124) vs 46 ng/ml (28 - 66), p=0.003], as shown in Figure 6.9.

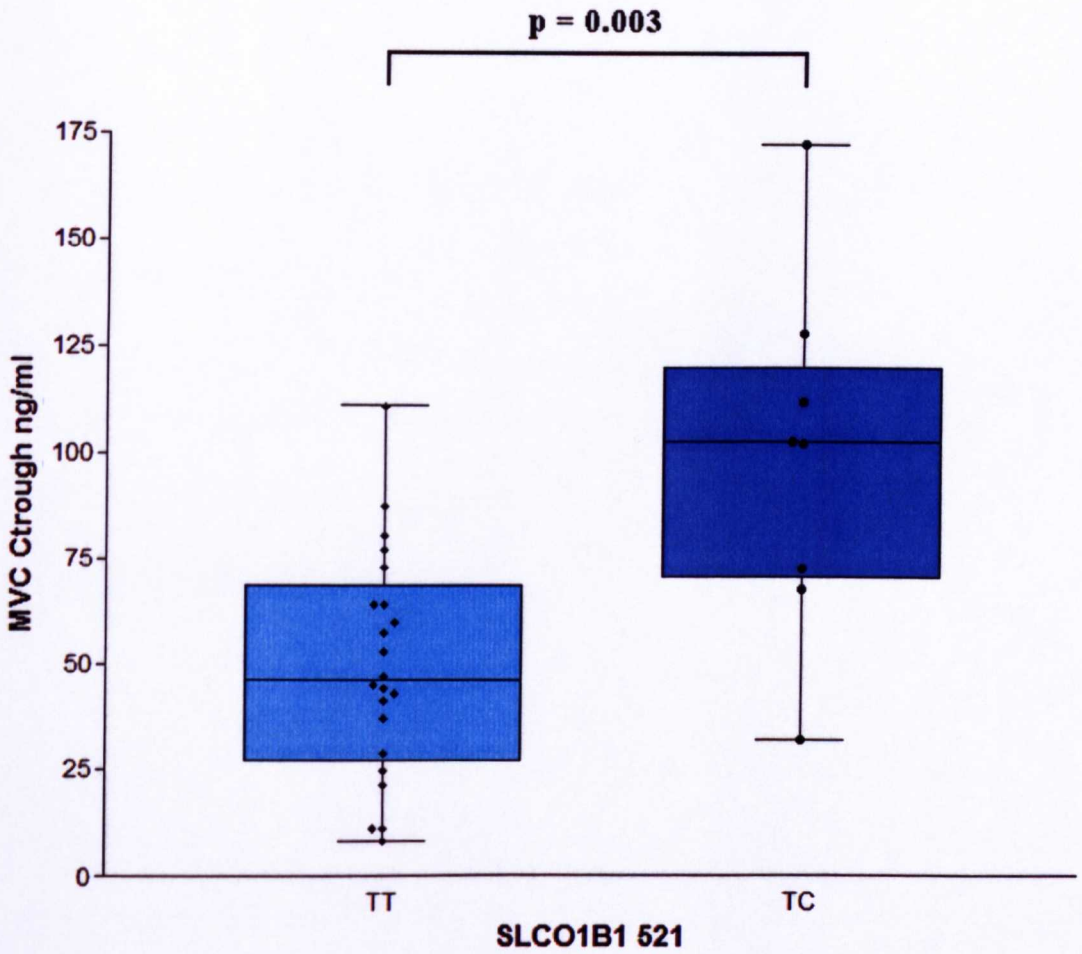

Figure 6.9. MVC C_{trough} and *SLCO1B1* 521 genotypes. Median values (horizontal thick line), IQR (bars), patient values (dots), highest and lowest value (whiskers) are given.

In multivariate logistic regression analyses, dose and SLCO1B1 521 TC genotype were the only factors independently associated with MVC C_{trough}. (Dose 600 mg; β = -47, 95% CI -74 to -19; P = 0.001; SLCO1B1 521 TC, (β = 31.5, 95% CI 3 to 60; P =

0.031). The final adjusted R squared value showed that 17.6% of interpatient variability was explained by the 600 mg dose, and 7.7% by SLCO1B1 TC genotype.

6.4 Discussion

Antiretroviral plasma exposure can be a crucial factor influencing the global efficacy of anti-HIV therapy. Viral suppression is promoted by therapeutic concentrations while excessive plasma levels can generate several forms of toxicity. A relationship between MVC exposure and viral response has been recently identified and a minimum effective concentration of 50 ng/ml has been proposed as a target in treatment guidelines (McFadyen et al. 2007; DHHS 2010). Therefore understanding factors which can alter MVC pharmacokinetics can be of crucial importance in improving therapy in the future.

Concomitant antiretrovirals are known to alter MVC pharmacokinetics but dose adjustments do not fully compensate for the alteration in MVC plasma concentrations {Sari-Chaaf, 2009 #57}. CYP3A4 and P-gp inhibition by RTV increases in MVC plasma concentrations, and a 50% dose reduction in MVC is therefore suggested in order to maintain maximal plasma concentrations below those associated with an increased incidence of postural hypotension (Abel et al. 2008). ETV and EFV both enhance the activity of CYP3A4 and 600 mg bid MVC is commonly prescribed with these drugs to correct MVC plasma exposure (Abel et al. 2008). Although these dose corrections can partially compensate the effect of the interacting drugs, in the present study a significant difference between patients treated with MVC 150mg bid plus a boosted protease inhibitor and patients treated

with 600 mg bid plus ETV or EFV was observed [127 (71-161) ng/ml] vs [59 (36-82) ng/ml], p =0.007.

The effect of the *SLCO1B1* 521C>T polymorphism on MVC concentrations could be detected in the 600 mg dose group. MVC C_{trough} in SLCO1B1 521 heterozygote patients (TC) (n=8) were higher than in wild type homozygotes (TT) (n=22) [103 ng/ml (69 - 124) vs 46 ng/ml (28 - 66), p=0.003], as shown in Figure 6.9. 7.7% of total interpatient variability could be accounted for by the SLCO1B1 TC genotype.

The magnitude of these polymorphism-related effects is comparable to that seen in several other reports where the 521TC or CC genotypes have been correlated with increased plasma concentrations of other SLCO1B1 substrates, such as atrasentan, fexofenadine, simvastatin acid, pitavastatin, atorvastatin, rosuvastatin, pravastatin and lopinavir (Niemi et al. 2004; Katz et al. 2006; Pasanen et al. 2006; Pasanen et al. 2007; Kohlrausch et al. 2010). A limitation of the present study is the low numbers of patients included in the genetic analysis. Inclusion of a higher number of patients treated with different doses of MVC could elucidate if the effect of the 521 C allele can be described for all doses or just for the 600 mg plus ETV group. Moreover more intense pharmacokinetic sampling including full AUC profiles could help in clarifying if the SLCO1B1 521 C allele exerts an effect on the first hours post dose or the subsequent portion of the dose interval. Population pharmacokinetic modelling could represent an alternative approach which will enable a more detailed characterisation of SLCO1B1 521 T>C relevance.

A dosing strategy including once daily administration of MVC has been recently proposed (Vourvahis 2010). Simplified regimens such as once daily administration are currently considered as an advantageous clinical option and can positively affect therapy efficacy, improving pill burden and consequently favouring adherence. Patients with *SLCO1B1* 521T variant allele benefit from higher plasma concentrations and could be optimal candidates for once daily administration.

In summary, our results confirm that MVC pharmacokinetics is influenced by concomitant antiretrovirals and for the first time, a genetic factor able to alter MVC plasma concentrations was identified. The correlation between the *SLCO1B1* 521T>C polymorphism and MVC pharmacokinetics and the results obtained using the X. *leavis* expression system in chapter 5 suggest that *SLCO1B1* can have an active role in the definition of MVC distribution and metabolism. A larger prospective cohort study is now required to define the true magnitude of the association between *SLCO1B1* 521T>C and MVC plasma concentrations and its clinical value in predicting MVC pharmacokinetics.

CHAPTER 7

General discussion

The overall efficacy of antiretroviral therapy is the result of an interplay of several factors involving the virus and the host. Each patient has a different combination of viral and host characteristics and therefore a unique scenario for treatment of HIV infection. The correct management of antiretroviral therapy can be challenging in some groups of patients with specific pharmacological or virological characteristics which can potentially jeopardise the antiretroviral efficacy. There is now a substantial knowledge base available to support the relevance of antiretroviral pharmacokinetics in the suppression of viral replication. Direct evidence of a correlation between NNRTI / CCR5 antagonist plasma exposure and probability of the achieving viral suppression has been described. For PIs, viral susceptibility and pharmacokinetics are merged into measures such as inhibitory quotient, for the quantification of antiviral pressure. Factors influencing antiretroviral pharmacokinetics have a major importance in the identification of patients with a higher risk of achieving insufficient exposure and therefore a higher chance of failing therapy.

A major aim of this thesis was to identify genetic factors influencing antiretroviral pharmacokinetics and explaining part of the variability observed in patients treated with various antiretroviral regimens. Secondarily, the role of other factors such as demographic and pharmacological variables was investigated. The convergence of different factors under study permitted partial definition of the complex interplay in which drug-drug interactions and physical characteristics interact with genetic variability to define the pharmacokinetic phenotype.

Delineation of how different combinations of factors impact on antiretroviral pharmacokinetics is challenging and several obstacles have to be overcome in order to give a reliable identification and estimation of pharmacokinetic predictors. Firstly, innovative and robust methods for the quantification of antiretroviral concentrations in plasma and other matrices have to be developed and validated. Complete reliability in the quantification methods is essential to guarantee a correct description of the pharmacokinetic phenotype and it is imperative that these methods are evaluated using international guidelines to ensure consistency within and between laboratories.

Development of new methods involves selection of appropriate technologies, consideration of biological matrices, range of concentrations, number of samples and physiochemical characteristic of the analytes. LC-MS/MS methods have high sensitivity and may be selected when very low concentrations are suspected. Furthermore, they need to be coupled with appropriate extraction procedures to avoid matrix effects. A valid alternative to LC-MS/MS is represented by HPLC-UV/PDA, a more classical approach which although lacking comparative sensitivity and requiring longer chromatographic runs, represents a reliable quantification method. Quantification methods have to be carefully validated considering numerous variables to reduce the risk of unreliable results. Accuracy and precision are key factors for correct measurement of analytes which have to be proven stable in different conditions and sufficiently extracted from the biological matrix under analysis. Interference from endogenous and exogenous molecules needs to be excluded by testing several blank matrices, and those containing all the potential environmental and pharmacological contaminants. In this thesis, four novel

chromatographic methods were developed and fully validated. An HPLC-PDA method for simultaneous quantification of 13 antiretrovirals was applied for unboosted ATV in plasma (Chapter 2). This methodology is now routinely used in the therapeutic drug monitoring (TDM) service in the Department of Infectious Diseases, University of Turin, Amedeo di Savoia Hospital, Turin, Italy and has also been applied in several clinical studies. Intracellular concentrations of 13 antiretrovirals can also be quantified using the method optimised and validated in Chapter 3. A HPLC-UV method for the quantification of MVC in plasma was developed in Chapter 6 and an original HPLC-MS method for the quantification of MVC in oocytes was validated in Chapter 5. This portfolio of analytical methods allow for the quantification of all currently used NNRTIs and PIs as well as raltegravir and maraviroc. Moreover, the methods may serve as a platform for addition of new antiretrovirals because of similarities in the physiochemical characteristics and the generic gradient used for resolving analytes.

Characterising antiretroviral pharmacokinetics in the clinical setting is a challenge and several factors should be considered when designing pharmacokinetic and pharmacogenetic studies. Pharmacogenetic studies require large sample sizes to clearly describe the effect of genetic variants on pharmacokinetics. Many variant alleles have low frequency that can vary substantially between ethnicities and multiple interactions between different genetic variants increase the complexity of patients' genetic profiles. Moreover, several variant alleles have an uncharacterised influence on protein activity and therefore their effect on ADME and pharmacokinetics is not always predictable. Consequently, a key priority for these studies is to maximise the sample size in order to have sufficient statistical power to

detect the effects of genetic variants in different ethnicities. Notwithstanding the necessity for large sample size, obtaining full pharmacokinetics profiles is not always feasible for a large number of patients. High numbers of samples will increase the cost of the studies and therefore decrease the opportunity for investigation. Thus, an accurate plan of sampling strategy needs to be executed to assess appropriate pharmacokinetic variables (e.g. C_{trough} or C_{max}) and to determine intra-patient variability.

In this thesis different strategies to investigate the role of genetic variants in the definition of pharmacokinetics were applied using a bottom up approach in all studies. Consequently, the candidate genes involved in the definition of the pharmacokinetic phenotype were already identified or were elucidated. Relevant SNPs in these genes were then selected and included in the investigations. A broad range of ADME processes were investigated, clarifying the role of genes influencing the regulation of metabolic enzymes and transporters (Chapter 2), the uptake of antiretrovirals into PBMC (Chapter 3) and hepatocytes (Chapter 5 and 6) and metabolic activity (Chapter 4).

As stated above, antiretroviral exposure results from several factors that can interplay to define the pharmacokinetic phenotype. As summarised in Figure 7.1, pharmacokinetics is influenced by factors such as concomitant drugs, adherence to therapy, age, co-morbidities and ADME processes mediated by transporters and metabolic enzymes which can be regulated by nuclear receptors. Genetic variability in genes encoding for these proteins influences their activity and consequently, each patient represents a unique combination of all these factors.

Figure 7.1. Factors influencing antiretroviral pharmacokinetics.

Recently, several prospective and retrospective clinical studies have been conducted in order to indentify physiological, pharmacological or genetic factors that alter antiretroviral pharmacokinetics. Co-morbidities can affect drug distribution and metabolism and one of the most common co-infections is hepatitis C virus (HCV) infection in 10% of HIV positive patients (Turner et al. 2010). In some cases HCV can cause an alteration in the antiretroviral plasma concentrations. Indeed, HCV positive patients have higher plasma concentration for unboosted atazanavir and efavirenz (Dominguez et al. 2010; Regazzi et al. 2011) but not some other HIV therapies (Vogel et al. 2009; Calza et al. 2011).

The effect has also been described for different classes of antiretrovirals due to the fat content altering absorption or ingredients that can inhibit CYP3A4 activity. (Kupferschmidt et al. 1998; Yeh et al. 1998; Damle et al. 2002; Brainard et al. 2011).

Additionally, several interactions with concomitant drugs can take place. Drug-drug interaction have become very common as HIV positive patients survive longer and consequently having higher frequency of treatment for diseases associated with aging. As recently demonstrated, the most frequent interactions with NNRTIs and PIs occur with therapeutic agents used for the treatment of cardiovascular diseases (Marzolini et al. 2010). The presence of numerous co-morbities and therapeutic agents give a complex clinical scenario that can result in unpredictable pharmacokinetic phenotypes. Moreover, expression of key metabolic enzymes and transporters can vary in geriatric and paediatric patients (Kerr et al. 1994; George et al. 1995; Rakhmanina and van den Anker 2006).

Genetic factors also clearly influence pharmacokinetic variability and many genes mediating different ADME processes have to be considered. Several studies demonstrating how antiretroviral pharmacokinetics are influenced by variability in different gene sequences have been published. Plasma exposure is influenced by genes encoding transporters that influence passage of antiretrovirals through membranes (e.g. *SLCO1B1* in hepatocytes). Recently the key role for *SLCO1B1* has been demonstrated for PIs such as LPV and in this thesis for MVC (Niemi et al. 2004; Hartkoorn et al. 2010). Other genes that have a role in the definition of antiretroviral pharmacokinetics are *CYPs* that are responsible for NNRTI and PI metabolism (Koudriakova et al. 1998; Erickson et al. 1999; Hyland et al. 2004; Walker et al. 2005; Faucette et al. 2007; di Iulio et al. 2009; Ogburn et al. 2010), and nuclear receptors (NRs) that are upstream regulators of both CYPs and transporters (Waxman 1999; Geick et al. 2001; Hagenbuch et al. 2001; Synold et al. 2001; Kast et al. 2002). In this thesis novel information regarding these genes have been described

and analysed, clarifying the role of NRs (*PXR* in chapter 2). transporters (*SLCO3A1* in chapter 3 and *SLCO1B1* in chapter 5 and 6), CYPs (*CYP2B6* in chapter 4).

Patients exposed to markedly lower concentrations of antiretrovirals have a higher chance to fail therapy and acquire drug resistance mutations within the virus. A correlation between plasma concentrations and therapeutic efficacy has been described for different classes of antiretrovirals (Csajka et al. 2003; Gonzalez de Requena et al. 2005; Leth et al. 2006; McFadyen et al. 2007). However, a clear description of the role of PK in the predisposition to side effects has not yet been finalised for the great majority of antiretrovirals. Predictors of antiretroviral pharmacokinetics will help identify patients likely to have extreme plasma concentrations and therefore adverse clinical phenotypes. To date, the only genetic marker that has found clinical application is the *HLA-B*5701* for dose-independent toxicity (Martin et al. 2004). It is important to recognise that pharmacokinetic phenotypes are likely to be influenced by multiple genetic variants and are as such not monogenic. Moreover, the great majority of single associations do not explain a sufficient degree of the variability in order to justify validation studies and thus be clinically implementable. Strategies to investigate the effect caused by combinations of different genetic factors need to be validated and simulation models such the ones developed in Chapter 2 and 4 may facilitate this process and help in design of prospective clinical trials.

The identification of factors influencing antiretroviral pharmacokinetics could help future optimisation of the therapy. Moreover, many patients may benefit from dose modification contrasting to the current standard practice to administer an equal dose

to all patients without regard to heterogeneity in biological and genetic factors. Patients that have already achieved complete suppression of viral replication (<50 copies/ml) may represent good candidates for dose reduction and simplification. The antiretroviral potency needed to inhibit viral replication for this group of patients is markedly lower compared with subjects having higher viral load and consequently dose simplification may be implemented more safely. This strategy has already been applied in clinical studies where patients treated with boosted ATV or EFV that were fully suppressed were switched to lower dose or alternative frequency dosing and successfully maintained viral suppression (Cohen et al. 2007; Ghosn et al. 2010). Reduction of dose and simplified posology reduces pill burden and has been shown to favour high adherence (Juday et al. 2011) which is in turn a predictor of sustained virological suppression (Paterson et al. 2000; Nachega et al. 2007). Another group of patients that might benefit from dose reduction are those characterised by high plasma concentrations at standard dosage. Thus, genetic markers of elevated antiretroviral exposure could find application in the selection of candidate patients to undergo dose reduction.

The selection of alternative regimens is another way in which pharmacogenetics may be deployed. This is challenging and may require prospective clinical trials for validation. To date, several strategies have been hypothesised. Firstly, the number of active antiretrovirals might be reduced to monotherapy, an effective choice for boosted protease inhibitors such as darunavir (Pulido et al. 2010; Clumeck et al. 2011). Secondly, the frequency of administration may be altered to once daily or brief interruption strategies that incorporate breaks from ART administration of a few days. Thirdly, a reduction of the dose without adjustment of the dosage

frequency might be introduced. All these options have to be carefully evaluated and analysed before planning validation studies. Retrospective analysis of available data is rarely possible because of the low number of patients that previously received the alternative regimens. Consequently, accurate models that can predict the pharmacokinetics and pharmacodynamics of alternative regimens are essential for a first evaluation of viable therapeutic options. In this thesis two examples of models that can find application in the prediction of pharmacokinetic effect of dose simplifications have been developed. In chapter 2, a pharmacogenetic based population pharmacokinetic model for unboosted ATV was assessed and in chapter 4 an *in vitro in vivo* extrapolation model for EFV was developed. Both models can be used to describe the role of genetic factors in pharmacokinetics for standard regimens or alternative dosages.

The primary benefit that patients might receive from dose personalisation is, as suggested above, the reduction of pill burden which can reflect an improvement of adherence. The decrease of plasma concentrations reduces the risk of dose-dependent toxicities and improves long term quality of a daily lifelong drug therapy. Additionally, personalisation of the therapy brings benefits not just for the single patient but can have a positive impact to the whole health system. The cost of antiretroviral therapy could be markedly decreased if dose reduction or personalisation is introduced for patients with stable suppression of viral replication and carriers of genetic markers of elevated antiretroviral exposure. This might be particularly relevant in middle-low income countries where the universal access to therapy is not achieved mainly due to insufficient financial resources.

In summary, a number of different strategies to investigate the role of genetic variability in antiretroviral exposure were developed in this thesis. Genetic variants of *SLCO1B1, PXR, SLCO3A1* and *CYP2B6* were significantly correlated with antiretroviral pharmacokinetics. These findings will help identify patients with a higher risk of achieving sub-therapeutic or potentially toxic plasma concentrations and will serve as a knowledge-base from which to grow and validate strategies for optimisation of therapy.

References

Aarons, L., M. O. Karlsson, et al. (2001). "Role of modelling and simulation in Phase I drug development." Eur J Pharm Sci 13(2): 115-122.

Abe, T., M. Kakyo, et al. (1999). "Identification of a novel gene family encoding human liver-specific organic anion transporter LST-1." J Biol Chem 274(24): 17159-17163.

Abel, S., T. M. Jenkins, et al. (2008). "Effects of CYP3A4 inducers with and without CYP3A4 inhibitors on the pharmacokinetics of maraviroc in healthy volunteers." Br J Clin Pharmacol 65 Suppl 1: 38-46.

Abel, S., D. Russell, et al. (2008). "Effects of CYP3A4 inhibitors on the pharmacokinetics of maraviroc in healthy volunteers." Br J Clin Pharmacol 65 Suppl 1: 27-37.

Adachi, H., T. Suzuki, et al. (2003). "Molecular characterization of human and rat organic anion transporter OATP-D." Am J Physiol Renal Physiol 285(6): F1188-1197.

Agarwala, S., T. Eley, et al. (2005). Pharmacokinetic interaction between tenofovir and atazanavir in healthy subjects. abstract WePe3.3C07. . 3rd IAS Conference on HIV Pathogenesis and Treatment. Rio de Janiero, Brazil.

Albermann, N., F. H. Schmitz-Winnenthal, et al. (2005). "Expression of the drug transporters MDR1/ABCB1, MRP1/ABCC1, MRP2/ABCC2, BCRP/ABCG2, and PXR in peripheral blood mononuclear cells and their relationship with the expression in intestine and liver." Biochem Pharmacol 70(6): 949-958.

Alnouti, Y. and C. D. Klaassen (2008). "Regulation of sulfotransferase enzymes by prototypical microsomal enzyme inducers in mice." J Pharmacol Exp Ther 324(2): 612-621.

Amacher, D. E. (2010). "The effects of cytochrome P450 induction by xenobiotics on endobiotic metabolism in pre-clinical safety studies." Toxicol Mech Methods 20(4): 159-166.

Amundsen, R., H. Christensen, et al. (2010). "Cyclosporine A, but not tacrolimus, shows relevant inhibition of organic anion-transporting protein 1B1-mediated transport of atorvastatin." Drug Metab Dispos 38(9): 1499-1504.

Arab-Alameddine, M., J. Di Iulio, et al. (2009). "Pharmacogenetics-based population pharmacokinetic analysis of efavirenz in HIV-1-infected individuals." Clin Pharmacol Ther 85(5): 485-494.

Avihingsanon, A., J. van der Lugt, et al. (2009). "A low dose of ritonavir-boosted atazanavir provides adequate pharmacokinetic parameters in HIV-1-infected Thai adults." Clin Pharmacol Ther 85(4): 402-408.

Aymard, G., M. Legrand, et al. (2000). "Determination of twelve antiretroviral agents in human plasma sample using reversed-phase high-performance liquid chromatography." J Chromatogr B Biomed Sci Appl 744(2): 227-240.

Babiker, H. M., C. M. Schlebusch, et al. (2011). "Genetic variation and population structure of Sudanese populations as indicated by 15 Identifiler sequence-tagged repeat (STR) loci." Investig Genet 2(1): 12.

Balani, S. K., L. R. Kauffman, et al. (1999). "Nonlinear pharmacokinetics of efavirenz (DMP-266), a potent HIV-1 reverse transcriptase inhibitor, in rats and monkeys." Drug Metab Dispos 27(1): 41-45.

Bazzoli, C., V. Jullien, et al. (2010). "Intracellular Pharmacokinetics of Antiretroviral Drugs in HIV-Infected Patients, and their Correlation with Drug Action." Clin Pharmacokinet 49(1): 17-45.

Belanger, A. S., P. Caron, et al. (2009). "Glucuronidation of the antiretroviral drug efavirenz by UGT2B7 and an in vitro investigation of drug-drug interaction with zidovudine." Drug Metab Dispos 37(9): 1793-1796.

Bertz, R. J. and G. R. Granneman (1997). "Use of in vitro and in vivo data to estimate the likelihood of metabolic pharmacokinetic interactions." Clin Pharmacokinet 32(3): 210-258.

Binet, I., A. Wallnofer, et al. (2000). "Renal hemodynamics and pharmacokinetics of bosentan with and without cyclosporine A." Kidney Int 57(1): 224-231.

Brainard, D. M., E. J. Friedman, et al. (2011). "Effect of low-, moderate-, and high-fat meals on raltegravir pharmacokinetics." J Clin Pharmacol 51(3): 422-427.

Breilh, D., I. Pellegrin, et al. (2004). "Virological, intracellular and plasma pharmacological parameters predicting response to lopinavir/ritonavir (KALEPHAR study)." AIDS 18(9): 1305-1310.

Bristol-Myers Squibb (2009). Approval documentation for Sustiva ™ (Efavirenz) NDA no 020972.

Cabrera Figueroa, S., A. Iglesias Gomez, et al. (2010). "Long-term efficacy and safety of efavirenz dose reduction to 200 mg once daily in a Caucasian patient with HIV." Clin Drug Investig 30(6): 405-411.

Cabrera, S. E., D. Santos, et al. (2009). "Influence of the cytochrome P450 2B6 genotype on population pharmacokinetics of efavirenz in human immunodeficiency virus patients." Antimicrob Agents Chemother 53(7): 2791-2798.

Caldwell, G. W., J. A. Masucci, et al. (2004). "Allometric scaling of pharmacokinetic parameters in drug discovery: can human CL, Vss and t1/2 be predicted from in-vivo rat data?" Eur J Drug Metab Pharmacokinet 29(2): 133-143.

Caldwell, M. D., R. L. Berg, et al. (2007). "Evaluation of genetic factors for warfarin dose prediction." Clin Med Res 5(1): 8-16.

Calza, L., L. Mosca, et al. (2011). "Assessing the impact of hepatitis C virus coinfection on lopinavir/ritonavir trough concentrations in HIV-infected patients." Eur J Clin Pharmacol 67(2): 143-149.

Cass, C. E., J. D. Young, et al. (1999). "Nucleoside transporters of mammalian cells." Pharm Biotechnol 12: 313-352.

Chan, L. M., S. Lowes, et al. (2004). "The ABCs of drug transport in intestine and liver: efflux proteins limiting drug absorption and bioavailability." Eur J Pharm Sci 21(1): 25-51.

Chandra, A., T. Gerber, et al. (1986). "Biochemical heterogeneity of reverse transcriptase purified from the AIDS virus, HTLV-III." FEBS Lett 197(1-2): 84-88.

Chen, J. and K. Raymond (2006). "Roles of rifampicin in drug-drug interactions: underlying molecular mechanisms involving the nuclear pregnane X receptor." Ann Clin Microbiol Antimicrob 5: 3.

Chetchotisakd, P. and S. Anunnatsiri (2008). "Low-dose, once-daily atazanavir/ritonavir (200/100): an effective treatment for HIV-infected patients in Thailand." J Acquir Immune Defic Syndr 49(2): 230-231.

Choi, S. O., N. L. Rezk, et al. (2007). "High-performance liquid chromatography assay for the determination of the HIV-protease inhibitor tipranavir in human

plasma in combination with nine other antiretroviral medications." J Pharm Biomed Anal 43(4): 1562-1567.

Choo, E. F., B. Leake, et al. (2000). "Pharmacological inhibition of P-glycoprotein transport enhances the distribution of HIV-1 protease inhibitors into brain and testes." Drug Metab Dispos 28(6): 655-660.

Clumeck, N., A. Rieger, et al. (2011). "96 week results from the MONET trial: a randomized comparison of darunavir/ritonavir with versus without nucleoside analogues, for patients with HIV RNA <50 copies/mL at baseline." J Antimicrob Chemother.

Cohen, C. J., A. E. Colson, et al. (2007). "Pilot study of a novel short-cycle antiretroviral treatment interruption strategy: 48-week results of the five-days-on, two-days-off (FOTO) study." HIV Clin Trials 8(1): 19-23.

Colombo, G., S. Serra, et al. (2006). "Baclofen-induced suppression of alcohol deprivation effect in Sardinian alcohol-preferring (sP) rats exposed to different alcohol concentrations." Eur J Pharmacol 550(1-3): 123-126.

Colombo, S., A. Beguin, et al. (2005). "Intracellular measurements of anti-HIV drugs indinavir, amprenavir, saquinavir, ritonavir, nelfinavir, lopinavir, atazanavir, efavirenz and nevirapine in peripheral blood mononuclear cells by liquid chromatography coupled to tandem mass spectrometry." J Chromatogr B Analyt Technol Biomed Life Sci 819(2): 259-276.

Colombo, S., T. Buclin, et al. (2006). "Population pharmacokinetics of atazanavir in patients with human immunodeficiency virus infection." Antimicrob Agents Chemother 50(11): 3801-3808.

Colombo, S., A. Telenti, et al. (2006). "Are plasma levels valid surrogates for cellular concentrations of antiretroviral drugs in HIV-infected patients?" Ther Drug Monit 28(3): 332-338.

Cooper, D. A., J. Gold, et al. (1985). "Acute AIDS retrovirus infection. Definition of a clinical illness associated with seroconversion." Lancet 1(8428): 537-540.

Cote, H. C., Z. L. Brumme, et al. (2002). "Changes in mitochondrial DNA as a marker of nucleoside toxicity in HIV-infected patients." N Engl J Med 346(11): 811-820.

Crommentuyn, K. M., J. W. Mulder, et al. (2004). "The plasma and intracellular steady-state pharmacokinetics of lopinavir/ritonavir in HIV-1-infected patients." Antivir Ther 9(5): 779-785.

Crommentuyn, K. M., H. Rosing, et al. (2004). "Simultaneous quantification of the new HIV protease inhibitors atazanavir and tipranavir in human plasma by high-performance liquid chromatography coupled with electrospray ionization tandem mass spectrometry." J Chromatogr B Analyt Technol Biomed Life Sci 804(2): 359-367.

Crommentuyn, K. M., H. Rosing, et al. (2003). "Rapid quantification of HIV protease inhibitors in human plasma by high-performance liquid chromatography coupled with electrospray ionization tandem mass spectrometry." J Mass Spectrom 38(2): 157-166.

Csajka, C., C. Marzolini, et al. (2003). "Population pharmacokinetics and effects of efavirenz in patients with human immunodeficiency virus infection." Clin Pharmacol Ther 73(1): 20-30.

D'Avolio, A., M. Siccardi, et al. (2007). "HPLC-MS method for the simultaneous quantification of the new HIV protease inhibitor darunavir, and 11 other

antiretroviral agents in plasma of HIV-infected patients." J Chromatogr B Analyt Technol Biomed Life Sci 859(2): 234-240.

Daar, E. S., T. Moudgil, et al. (1991). "Transient high levels of viremia in patients with primary human immunodeficiency virus type 1 infection." N Engl J Med 324(14): 961-964.

Dailly, E., F. Raffi, et al. (2004). "Determination of atazanavir and other antiretroviral drugs (indinavir, amprenavir, nelfinavir and its active metabolite M8, saquinavir, ritonavir, lopinavir, nevirapine and efavirenz) plasma levels by high performance liquid chromatography with UV detection." J Chromatogr B Analyt Technol Biomed Life Sci 813(1-2): 353-358.

Damle, B. D., J. H. Yan, et al. (2002). "Effect of food on the oral bioavailability of didanosine from encapsulated enteric-coated beads." J Clin Pharmacol 42(4): 419-427.

Delfraissy, J. F., S. Moreno, et al. (2008). Efficacy and safety of 48-week maintenance with QD ATV vs ATV/r (both + 2NRTIs) in patients with VL <50 c/mL after induction with ATV/r + 2NRTIs: study AI424136. Ninth International Congress on Drug Therapy in HIV Infection. Glasgow, UK.

Deng, J. W., I. S. Song, et al. (2008). "The effect of SLCO1B1*15 on the disposition of pravastatin and pitavastatin is substrate dependent: the contribution of transporting activity changes by SLCO1B1*15." Pharmacogenet Genomics 18(5): 424-433.

Dheda, K., J. F. Huggett, et al. (2004). "Validation of housekeeping genes for normalizing RNA expression in real-time PCR." Biotechniques 37(1): 112-114, 116, 118-119.

DHHS (2010). Panel on Antiretroviral Guidelines for Adult and Adolescents. Guidelines for the use of antiretroviral agents in HIV-infected adults and adolescents. Department of Health and Human Services 1-166.

di Iulio, J., A. Fayet, et al. (2009). "In vivo analysis of efavirenz metabolism in individuals with impaired CYP2A6 function." Pharmacogenet Genomics 19(4): 300-309.

Dickinson, L., M. Boffito, et al. (2009). "Population pharmacokinetics of ritonavir-boosted atazanavir in HIV-infected patients and healthy volunteers." J Antimicrob Chemother 63(6): 1233-1243.

Djabarouti, S., D. Breilh, et al. (2006). "Intracellular and plasma efavirenz concentrations in HIV-infected patients switching from successful protease inhibitor-based highly active antiretroviral therapy (HAART) to efavirenz-based HAART (SUSTIPHAR Study)." J Antimicrob Chemother 58(5): 1090-1093.

Dominguez, S., J. Ghosn, et al. (2010). "Impact of hepatitis C and liver fibrosis on antiretroviral plasma drug concentrations in HIV-HCV co-infected patients: the HEPADOSE study." J Antimicrob Chemother 65(11): 2445-2449.

Dumont, J. N. (1972). "Oogenesis in Xenopus laevis (Daudin). I. Stages of oocyte development in laboratory maintained animals." J Morphol 136(2): 153-179.

Eagling, V. A., D. J. Back, et al. (1997). "Differential inhibition of cytochrome P450 isoforms by the protease inhibitors, ritonavir, saquinavir and indinavir." Br J Clin Pharmacol 44(2): 190-194.

Elens, L., S. Veriter, et al. (2009). "Validation and clinical application of a high performance liquid chromatography tandem mass spectrometry (LC-MS/MS) method for the quantitative determination of 10 anti-retrovirals in human

peripheral blood mononuclear cells." J Chromatogr B Analyt Technol Biomed Life Sci 877(20-21): 1805-1814.

Erickson, D. A., G. Mather, et al. (1999). "Characterization of the in vitro biotransformation of the HIV-1 reverse transcriptase inhibitor nevirapine by human hepatic cytochromes P-450." Drug Metab Dispos 27(12): 1488-1495.

Ernest, C. S., 2nd, S. D. Hall, et al. (2005). "Mechanism-based inactivation of CYP3A by HIV protease inhibitors." J Pharmacol Exp Ther 312(2): 583-591.

Eron, J., J. Rockstroh, et al. (2011). QDMRK, a phase III study of the safety and efficacy of once daily vs twice daily RAL in combination therapy for treatment-naïve HIV-infected patients. CROI. Boston, MA, USA.

European Medicines Agency "Celsentri (maraviroc): summary of product characteristics. Updated 2010 Jan 11 [online]. Available from URL: http://www.emea.europa.eu/humandocs/PDFs/EPAR/celsentri/emea-combinedh811en.pdf Accessed 2010 May 23."

Evans, W. E. and M. V. Relling (1999). "Pharmacogenomics: translating functional genomics into rational therapeutics." Science 286(5439): 487-491.

Evers, R., M. Kool, et al. (1998). "Drug export activity of the human canalicular multispecific organic anion transporter in polarized kidney MDCK cells expressing cMOAT (MRP2) cDNA." J Clin Invest 101(7): 1310-1319.

Faucette, S. R., T. C. Zhang, et al. (2007). "Relative activation of human pregnane X receptor versus constitutive androstane receptor defines distinct classes of CYP2B6 and CYP3A4 inducers." J Pharmacol Exp Ther 320(1): 72-80.

Fauci, A. S. and H. C. Lane (2006). Human Immunodeficiency Virus Disease: AIDS and Related Disorders. Harrison's Principles of Internal Medicine. M.-H. P. Group: 1106-1169.

Fayet, A., A. Beguin, et al. (2009). "A LC-tandem MS assay for the simultaneous measurement of new antiretroviral agents: Raltegravir, maraviroc, darunavir, and etravirine." J Chromatogr B Analyt Technol Biomed Life Sci 877(11-12): 1057-1069.

Fayet Mello, A., T. Buclin, et al. (2011). "Successful efavirenz dose reduction guided by therapeutic drug monitoring." Antivir Ther 16(2): 189-197.

Feinberg, M. B., R. F. Jarrett, et al. (1986). "HTLV-III expression and production involve complex regulation at the levels of splicing and translation of viral RNA." Cell 46(6): 807-817.

Food and Drug Administration (2001). Guidance for Industry Bioanalytical Method Validation.

Ford, J., M. Boffito, et al. (2006). "Influence of atazanavir 200 mg on the intracellular and plasma pharmacokinetics of saquinavir and ritonavir 1600/100 mg administered once daily in HIV-infected patients." J Antimicrob Chemother 58(5): 1009-1016.

Ford, J., M. Boffito, et al. (2004). "Intracellular and plasma pharmacokinetics of saquinavir-ritonavir, administered at 1,600/100 milligrams once daily in human immunodeficiency virus-infected patients." Antimicrob Agents Chemother 48(7): 2388-2393.

Ford, J., D. Cornforth, et al. (2004). "Intracellular and plasma pharmacokinetics of nelfinavir and M8 in HIV-infected patients: relationship with P-glycoprotein expression." Antivir Ther 9(1): 77-84.

Ford, J., S. H. Khoo, et al. (2004). "The intracellular pharmacology of antiretroviral protease inhibitors." J Antimicrob Chemother 54(6): 982-990.

Fox, R. I., S. L. Morgan, et al. (2003). "Combined oral cyclosporin and methotrexate therapy in patients with rheumatoid arthritis elevates methotrexate levels and reduces 7-hydroxymethotrexate levels when compared with methotrexate alone." Rheumatology (Oxford) 42(8): 989-994.

Fujino, H., T. Saito, et al. (2005). "Transporter-mediated influx and efflux mechanisms of pitavastatin, a new inhibitor of HMG-CoA reductase." J Pharm Pharmacol 57(10): 1305-1311.

Fumaz, C. R., J. A. Munoz-Moreno, et al. (2005). "Long-term neuropsychiatric disorders on efavirenz-based approaches: quality of life, psychologic issues, and adherence." J Acquir Immune Defic Syndr 38(5): 560-565.

Gallego, L., P. Barreiro, et al. (2004). "Analyzing sleep abnormalities in HIV-infected patients treated with Efavirenz." Clin Infect Dis 38(3): 430-432.

Gallo, S. A., A. Puri, et al. (2001). "HIV-1 gp41 six-helix bundle formation occurs rapidly after the engagement of gp120 by CXCR4 in the HIV-1 Env-mediated fusion process." Biochemistry 40(41): 12231-12236.

Gao, W. Y., A. Cara, et al. (1993). "Low levels of deoxynucleotides in peripheral blood lymphocytes: a strategy to inhibit human immunodeficiency virus type 1 replication." Proc Natl Acad Sci U S A 90(19): 8925-8928.

Gatanaga, H., T. Hayashida, et al. (2007). "Successful efavirenz dose reduction in HIV type 1-infected individuals with cytochrome P450 2B6 *6 and *26." Clin Infect Dis 45(9): 1230-1237.

Geick, A., M. Eichelbaum, et al. (2001). "Nuclear receptor response elements mediate induction of intestinal MDR1 by rifampin." J Biol Chem 276(18): 14581-14587.

Gelmann, E. P., M. Popovic, et al. (1983). "Proviral DNA of a retrovirus, human T-cell leukemia virus, in two patients with AIDS." Science 220(4599): 862-865.

George, J., K. Byth, et al. (1995). "Age but not gender selectively affects expression of individual cytochrome P450 proteins in human liver." Biochem Pharmacol 50(5): 727-730.

Ghosn, J., G. Carosi, et al. (2010). "Unboosted atazanavir-based therapy maintains control of HIV type-1 replication as effectively as a ritonavir-boosted regimen." Antivir Ther 15(7): 993-1002.

Glaeser, H., D. G. Bailey, et al. (2007). "Intestinal drug transporter expression and the impact of grapefruit juice in humans." Clin Pharmacol Ther 81(3): 362-370.

Goldwirt, L., S. Chhun, et al. (2007). "Quantification of darunavir (TMC114) in human plasma by high-performance liquid chromatography with ultra-violet detection." J Chromatogr B Analyt Technol Biomed Life Sci 857(2): 327-331.

Gonzalez de Requena, D., S. Bonora, et al. (2005). "Nevirapine plasma exposure affects both durability of viral suppression and selection of nevirapine primary resistance mutations in a clinical setting." Antimicrob Agents Chemother 49(9): 3966-3969.

Gonzalez de Requena, D., S. Bonora, et al. (2011). "Comparative evaluation of seven resistance interpretation algorithms and their derived genotypic inhibitory quotients for the prediction of 48 week virological response to darunavir-based salvage regimens." J Antimicrob Chemother 66(1): 192-200.

Grinsztejn, B., B. Y. Nguyen, et al. (2007). "Safety and efficacy of the HIV-1 integrase inhibitor raltegravir (MK-0518) in treatment-experienced patients

with multidrug-resistant virus: a phase II randomised controlled trial." Lancet 369(9569): 1261-1269.

Gulick, R. M., J. Lalezari, et al. (2008). "Maraviroc for previously treated patients with R5 HIV-1 infection." N Engl J Med 359(14): 1429-1441.

Gutierrez, F., A. Navarro, et al. (2005). "Prediction of neuropsychiatric adverse events associated with long-term efavirenz therapy, using plasma drug level monitoring." Clin Infect Dis 41(11): 1648-1653.

Haas, D. W., H. J. Ribaudo, et al. (2004). "Pharmacogenetics of efavirenz and central nervous system side effects: an Adult AIDS Clinical Trials Group study." AIDS 18(18): 2391-2400.

Hagenbuch, N., C. Reichel, et al. (2001). "Effect of phenobarbital on the expression of bile salt and organic anion transporters of rat liver." J Hepatol 34(6): 881-887.

Hanson, D. L., C. R. Horsburgh, Jr., et al. (1993). "Survival prognosis of HIV-infected patients." J Acquir Immune Defic Syndr 6(6): 624-629.

Hartkoorn, R. C., W. S. Kwan, et al. (2010). "HIV protease inhibitors are substrates for OATP1A2, OATP1B1 and OATP1B3 and lopinavir plasma concentrations are influenced by SLCO1B1 polymorphisms." Pharmacogenet Genomics 20(2): 112-120.

Hedman, M., P. J. Neuvonen, et al. (2004). "Pharmacokinetics and pharmacodynamics of pravastatin in pediatric and adolescent cardiac transplant recipients on a regimen of triple immunosuppression." Clin Pharmacol Ther 75(1): 101-109.

Hennessy, M., S. Clarke, et al. (2004). "Intracellular accumulation of nelfinavir and its relationship to P-glycoprotein expression and function in HIV-infected patients." Antivir Ther 9(1): 115-122.

Hennessy, M., S. Clarke, et al. (2003). "Intracellular indinavir pharmacokinetics in HIV-infected patients: comparison with plasma pharmacokinetics." Antivir Ther 8(3): 191-198.

Hoefnagel, J. G., M. J. van der Lee, et al. (2006). "The genotypic inhibitory quotient and the (cumulative) number of mutations predict the response to lopinavir therapy." AIDS 20(7): 1069-1071.

Hsiang, B., Y. Zhu, et al. (1999). "A novel human hepatic organic anion transporting polypeptide (OATP2). Identification of a liver-specific human organic anion transporting polypeptide and identification of rat and human hydroxymethylglutaryl-CoA reductase inhibitor transporters." J Biol Chem 274(52): 37161-37168.

Hu, S., R. M. Franke, et al. (2008). "Interaction of imatinib with human organic ion carriers." Clin Cancer Res 14(10): 3141-3148.

Hughes, C. A., L. Robinson, et al. (2009). "New antiretroviral drugs: a review of the efficacy, safety, pharmacokinetics, and resistance profile of tipranavir, darunavir, etravirine, rilpivirine, maraviroc, and raltegravir." Expert Opin Pharmacother 10(15): 2445-2466.

Hustert, E., M. Haberl, et al. (2001). "The genetic determinants of the CYP3A5 polymorphism." Pharmacogenetics 11(9): 773-779.

Hyland, R., M. Dickins, et al. (2008). "Maraviroc: in vitro assessment of drug-drug interaction potential." Br J Clin Pharmacol 66(4): 498-507.

Hyland, R., B. Jones, et al. (2004). In vitro assessment of the CYP-based drug–drug interaction potential of UK-427,857. 5th International Workshop on Clinical Pharmacology of HIV Therapy, Rome, Italy.

Ingelman-Sundberg, M., S. C. Sim, et al. (2007). "Influence of cytochrome P450 polymorphisms on drug therapies: pharmacogenetic, pharmacoepigenetic and clinical aspects." Pharmacol Ther 116(3): 496-526.

Iwamoto, M., L. A. Wenning, et al. (2008). "Safety, tolerability, and pharmacokinetics of raltegravir after single and multiple doses in healthy subjects." Clin Pharmacol Ther 83(2): 293-299.

Iwazaki, N., K. Kobayashi, et al. (2008). "Involvement of hepatocyte nuclear factor 4 alpha in transcriptional regulation of the human pregnane X receptor gene in the human liver." Drug Metab Pharmacokinet 23(1): 59-66.

Jamei, M., G. L. Dickinson, et al. (2009). "A framework for assessing inter-individual variability in pharmacokinetics using virtual human populations and integrating general knowledge of physical chemistry, biology, anatomy, physiology and genetics: A tale of 'bottom-up' vs 'top-down' recognition of covariates." Drug Metab Pharmacokinet 24(1): 53-75.

Janneh, O., P. G. Bray, et al. (2010). "Concentration-dependent effects and intracellular accumulation of HIV protease inhibitors in cultured CD4 T cells and primary human lymphocytes." J Antimicrob Chemother 65(5): 906-916.

Janneh, O., B. Chandler, et al. (2009). "Intracellular accumulation of efavirenz and nevirapine is independent of P-glycoprotein activity in cultured CD4 T cells and primary human lymphocytes." J Antimicrob Chemother 64(5): 1002-1007.

Janneh, O., R. C. Hartkoorn, et al. (2008). "Cultured CD4T cells and primary human lymphocytes express hOATPs: intracellular accumulation of saquinavir and lopinavir." Br J Pharmacol 155(6): 875-883.

Jigorel, E., M. Le Vee, et al. (2006). "Differential regulation of sinusoidal and canalicular hepatic drug transporter expression by xenobiotics activating drug-sensing receptors in primary human hepatocytes." Drug Metab Dispos 34(10): 1756-1763.

Josephson, F., M. C. Andersson, et al. (2010). "The relation between treatment outcome and efavirenz, atazanavir or lopinavir exposure in the NORTHIV trial of treatment-naive HIV-1 infected patients." Eur J Clin Pharmacol 66(4): 349-357.

Juday, T., S. Gupta, et al. (2011). "Factors associated with complete adherence to HIV combination antiretroviral therapy." HIV Clin Trials 12(2): 71-78.

Justesen, U. S. (2008). "Protease inhibitor plasma concentrations in HIV antiretroviral therapy." Dan Med Bull 55(4): 165-185.

Kajosaari, L. I., M. Niemi, et al. (2006). "Telithromycin, but not montelukast, increases the plasma concentrations and effects of the cytochrome P450 3A4 and 2C8 substrate repaglinide." Clin Pharmacol Ther 79(3): 231-242.

Kajosaari, L. I., M. Niemi, et al. (2005). "Cyclosporine markedly raises the plasma concentrations of repaglinide." Clin Pharmacol Ther 78(4): 388-399.

Kalliokoski, A., J. T. Backman, et al. (2008). "Effects of gemfibrozil and atorvastatin on the pharmacokinetics of repaglinide in relation to SLCO1B1 polymorphism." Clin Pharmacol Ther 84(4): 488-496.

Kalow, W., L. Endrenyi, et al. (1999). "Repeat administration of drugs as a means to assess the genetic component in pharmacological variability." Pharmacology 58(6): 281-284.

Kameyama, Y., K. Yamashita, et al. (2005). "Functional characterization of SLCO1B1 (OATP-C) variants, SLCO1B1*5, SLCO1B1*15 and SLCO1B1*15+C1007G, by using transient expression systems of HeLa and HEK293 cells." Pharmacogenet Genomics 15(7): 513-522.

Kanamitsu, S. I., K. Ito, et al. (2000). "Prediction of in vivo drug-drug interactions based on mechanism-based inhibition from in vitro data: inhibition of 5-fluorouracil metabolism by (E)-5-(2-Bromovinyl)uracil." Drug Metab Dispos 28(4): 467-474.

Kappelhoff, B. S., K. M. Crommentuyn, et al. (2004). "Practical guidelines to interpret plasma concentrations of antiretroviral drugs." Clin Pharmacokinet 43(13): 845-853.

Kaslow, R. A., J. P. Phair, et al. (1987). "Infection with the human immunodeficiency virus: clinical manifestations and their relationship to immune deficiency. A report from the Multicenter AIDS Cohort Study." Ann Intern Med 107(4): 474-480.

Kassahun, K., I. McIntosh, et al. (2007). "Metabolism and disposition in humans of raltegravir (MK-0518), an anti-AIDS drug targeting the human immunodeficiency virus 1 integrase enzyme." Drug Metab Dispos 35(9): 1657-1663.

Kast, H. R., B. Goodwin, et al. (2002). "Regulation of multidrug resistance-associated protein 2 (ABCC2) by the nuclear receptors pregnane X receptor,

farnesoid X-activated receptor, and constitutive androstane receptor." J Biol Chem 277(4): 2908-2915.

Katsumoto, T., M. Asanaka, et al. (1990). "Budding process and maturation of human immunodeficiency virus examined by means of pre- and post-embedding immunocolloidal gold electron microscopy." J Electron Microsc (Tokyo) 39(1): 33-38.

Katz, D. A., R. Carr, et al. (2006). "Organic anion transporting polypeptide 1B1 activity classified by SLCO1B1 genotype influences atrasentan pharmacokinetics." Clin Pharmacol Ther 79(3): 186-196.

Kerr, B. M., K. E. Thummel, et al. (1994). "Human liver carbamazepine metabolism. Role of CYP3A4 and CYP2C8 in 10,11-epoxide formation." Biochem Pharmacol 47(11): 1969-1979.

Kim, R. B., M. F. Fromm, et al. (1998). "The drug transporter P-glycoprotein limits oral absorption and brain entry of HIV-1 protease inhibitors." J Clin Invest 101(2): 289-294.

Kitamura, A., S. Imai, et al. (2007). "The new acyl-CoA cholesterol acyltransferase inhibitor SMP-797 does not interact with statins via OATP1B1 in human cryopreserved hepatocytes and oocytes expressing systems." Biopharm Drug Dispos 28(9): 517-525.

Klein, K., T. Lang, et al. (2005). "Genetic variability of CYP2B6 in populations of African and Asian origin: allele frequencies, novel functional variants, and possible implications for anti-HIV therapy with efavirenz." Pharmacogenet Genomics 15(12): 861-873.

Knight, T. R., S. Choudhuri, et al. (2008). "Induction of hepatic glutathione S-transferases in male mice by prototypes of various classes of microsomal enzyme inducers." Toxicol Sci 106(2): 329-338.

Kobayashi, D., T. Nozawa, et al. (2003). "Involvement of human organic anion transporting polypeptide OATP-B (SLC21A9) in pH-dependent transport across intestinal apical membrane." J Pharmacol Exp Ther 306(2): 703-708.

Kobayashi, Y., R. Sakai, et al. (2005). "Possible involvement of organic anion transporter 2 on the interaction of theophylline with erythromycin in the human liver." Drug Metab Dispos 33(5): 619-622.

Kohlrausch, F. B., R. de Cassia Estrela, et al. (2010). "The impact of SLCO1B1 polymorphisms on the plasma concentration of lopinavir and ritonavir in HIV-infected men." Br J Clin Pharmacol 69(1): 95-98.

Kontorinis, N. and D. T. Dieterich (2003). "Toxicity of non-nucleoside analogue reverse transcriptase inhibitors." Semin Liver Dis 23(2): 173-182.

Koudriakova, T., E. Iatsimirskaia, et al. (1998). "Metabolism of the human immunodeficiency virus protease inhibitors indinavir and ritonavir by human intestinal microsomes and expressed cytochrome P4503A4/3A5: mechanism-based inactivation of cytochrome P4503A by ritonavir." Drug Metab Dispos 26(6): 552-561.

Kupferschmidt, H. H., K. E. Fattinger, et al. (1998). "Grapefruit juice enhances the bioavailability of the HIV protease inhibitor saquinavir in man." Br J Clin Pharmacol 45(4): 355-359.

Kwara, A., M. Lartey, et al. (2009). "CYP2B6, CYP2A6 and UGT2B7 genetic polymorphisms are predictors of efavirenz mid-dose concentration in HIV-infected patients." AIDS 23(16): 2101-2106.

la Porte, C. (2008). "Inhibitory quotient in HIV pharmacology." Curr Opin HIV AIDS 3(3): 283-287.

Lagas, J. S., M. L. Vlaming, et al. (2009). "Pharmacokinetic assessment of multiple ATP-binding cassette transporters: the power of combination knockout mice." Mol Interv 9(3): 136-145.

Lamba, J., V. Lamba, et al. (2008). "Novel single nucleotide polymorphisms in the promoter and intron 1 of human pregnane X receptor/NR1I2 and their association with CYP3A4 expression." Drug Metab Dispos 36(1): 169-181.

Lamba, J. K., Y. S. Lin, et al. (2002). "Genetic contribution to variable human CYP3A-mediated metabolism." Adv Drug Deliv Rev 54(10): 1271-1294.

Lang, T., K. Klein, et al. (2001). "Extensive genetic polymorphism in the human CYP2B6 gene with impact on expression and function in human liver." Pharmacogenetics 11(5): 399-415.

Lemmer, B. (2005). "Chronopharmacology and controlled drug release." Expert Opin Drug Deliv 2(4): 667-681.

Letendre, S., J. Marquie-Beck, et al. (2008). "Validation of the CNS Penetration-Effectiveness rank for quantifying antiretroviral penetration into the central nervous system." Arch Neurol 65(1): 65-70.

Leth, F. V., B. S. Kappelhoff, et al. (2006). "Pharmacokinetic parameters of nevirapine and efavirenz in relation to antiretroviral efficacy." AIDS Res Hum Retroviruses 22(3): 232-239.

Lewis, P., M. Hensel, et al. (1992). "Human immunodeficiency virus infection of cells arrested in the cell cycle." EMBO J 11(8): 3053-3058.

Lightfoote, M. M., J. E. Coligan, et al. (1986). "Structural characterization of reverse transcriptase and endonuclease polypeptides of the acquired immunodeficiency syndrome retrovirus." J Virol 60(2): 771-775.

Lim, Y. P. and J. D. Huang (2008). "Interplay of pregnane X receptor with other nuclear receptors on gene regulation." Drug Metab Pharmacokinet 23(1): 14-21.

Liptrott, N. J., S. H. Khoo, et al. (2008). "Detection of ABCC2, CYP2B6 and CYP3A4 in human peripheral blood mononuclear cells using flow cytometry." J Immunol Methods 339(2): 270-274.

Liptrott, N. J., M. Penny, et al. (2009). "The impact of cytokines on the expression of drug transporters, cytochrome P450 enzymes and chemokine receptors in human PBMC." Br J Pharmacol 156(3): 497-508.

Little, S. J., S. Holte, et al. (2002). "Antiretroviral-drug resistance among patients recently infected with HIV." N Engl J Med 347(6): 385-394.

Lubomirov, R., J. di Iulio, et al. (2010). "ADME pharmacogenetics: investigation of the pharmacokinetics of the antiretroviral agent lopinavir coformulated with ritonavir." Pharmacogenet Genomics 20(4): 217-230.

Lundin, K., A. Nygren, et al. (1987). "A specific assay measuring binding of 125I-Gp 120 from HIV to T4+/CD4+ cells." J Immunol Methods 97(1): 93-100.

Maartens, G., E. Decloedt, et al. (2009). "Effectiveness and safety of antiretrovirals with rifampicin: crucial issues for high-burden countries." Antivir Ther 14(8): 1039-1043.

MacArthur, R. D. and R. M. Novak (2008). "Reviews of anti-infective agents: maraviroc: the first of a new class of antiretroviral agents." Clin Infect Dis 47(2): 236-241.

Mackenzie, P. I., D. G. Hu, et al. (2010). "The regulation of UDP-glucuronosyltransferase genes by tissue-specific and ligand-activated transcription factors." Drug Metab Rev 42(1): 99-109.

Mahungu, T., C. Smith, et al. (2009). "Cytochrome P450 2B6 516G-->T is associated with plasma concentrations of nevirapine at both 200 mg twice daily and 400 mg once daily in an ethnically diverse population." HIV Med 10(5): 310-317.

Markowitz, M., J. O. Morales-Ramirez, et al. (2006). "Antiretroviral activity, pharmacokinetics, and tolerability of MK-0518, a novel inhibitor of HIV-1 integrase, dosed as monotherapy for 10 days in treatment-naive HIV-1-infected individuals." J Acquir Immune Defic Syndr 43(5): 509-515.

Markowitz, M., B. Y. Nguyen, et al. (2007). "Rapid and durable antiretroviral effect of the HIV-1 Integrase inhibitor raltegravir as part of combination therapy in treatment-naive patients with HIV-1 infection: results of a 48-week controlled study." J Acquir Immune Defic Syndr 46(2): 125-133.

Martin, A. M., D. Nolan, et al. (2004). "Predisposition to abacavir hypersensitivity conferred by HLA-B*5701 and a haplotypic Hsp70-Hom variant." Proc Natl Acad Sci U S A 101(12): 4180-4185.

Marzolini, C., A. Beguin, et al. (2002). "Determination of lopinavir and nevirapine by high-performance liquid chromatography after solid-phase extraction: application for the assessment of their transplacental passage at delivery." J Chromatogr B Analyt Technol Biomed Life Sci 774(2): 127-140.

Marzolini, C., L. Elzi, et al. (2010). "Prevalence of comedications and effect of potential drug-drug interactions in the Swiss HIV Cohort Study." Antivir Ther 15(3): 413-423.

Marzolini, C., A. Telenti, et al. (2000). "Simultaneous determination of the HIV protease inhibitors indinavir, amprenavir, saquinavir, ritonavir, nelfinavir and the non-nucleoside reverse transcriptase inhibitor efavirenz by high-performance liquid chromatography after solid-phase extraction." J Chromatogr B Biomed Sci Appl 740(1): 43-58.

Marzolini, C., A. Telenti, et al. (2001). "Efavirenz plasma levels can predict treatment failure and central nervous system side effects in HIV-1-infected patients." AIDS 15(1): 71-75.

Marzolini, C., N. Troillet, et al. (2000). "Efavirenz decreases methadone blood concentrations." AIDS 14(9): 1291-1292.

Masur, H., F. P. Ognibene, et al. (1989). "CD4 counts as predictors of opportunistic pneumonias in human immunodeficiency virus (HIV) infection." Ann Intern Med 111(3): 223-231.

Mathias, A. A., P. German, et al. (2010). "Pharmacokinetics and pharmacodynamics of GS-9350: a novel pharmacokinetic enhancer without anti-HIV activity." Clin Pharmacol Ther 87(3): 322-329.

McFadyen, L., P. Jacqmin, et al. (2007). Maraviroc (MVC) Exposure–Efficacy Relationship in Treatment-experienced HIV-1-infected Patients. AIDS Conference / EACS Madrid, Spain, .

McFadyen, L., J. R. Wade, et al. (2007). Maraviroc (MVC) Exposure–Effcacy Relationship in Treatment-experienced HIV-1-infected Patients. 11th European AIDS Conference / EACS Madrid, Spain.

Mellors, J. W., A. Munoz, et al. (1997). "Plasma viral load and CD4+ lymphocytes as prognostic markers of HIV-1 infection." Ann Intern Med 126(12): 946-954.

Mellors, J. W., C. R. Rinaldo, Jr., et al. (1996). "Prognosis in HIV-1 infection predicted by the quantity of virus in plasma." Science 272(5265): 1167-1170.

Merschman, S. A., P. T. Vallano, et al. (2007). "Determination of the HIV integrase inhibitor, MK-0518 (raltegravir), in human plasma using 96-well liquid-liquid extraction and HPLC-MS/MS." J Chromatogr B Analyt Technol Biomed Life Sci 857(1): 15-24.

Michael, N. L., M. Vahey, et al. (1992). "Viral DNA and mRNA expression correlate with the stage of human immunodeficiency virus (HIV) type 1 infection in humans: evidence for viral replication in all stages of HIV disease." J Virol 66(1): 310-316.

Mildvan, D., U. Mathur, et al. (1982). "Opportunistic infections and immune deficiency in homosexual men." Ann Intern Med 96(6 Pt 1): 700-704.

Moore, J. T. and S. A. Kliewer (2000). "Use of the nuclear receptor PXR to predict drug interactions." Toxicology 153(1-3): 1-10.

Moss, A. R., P. Bacchetti, et al. (1988). "Seropositivity for HIV and the development of AIDS or AIDS related condition: three year follow up of the San Francisco General Hospital cohort." Br Med J (Clin Res Ed) 296(6624): 745-750.

Moss, D. M., W. S. Kwan, et al. (2011). "Raltegravir is a substrate for SLC22A6: a putative mechanism for the interaction between raltegravir and tenofovir." Antimicrob Agents Chemother 55(2): 879-887.

Mouly, S., K. S. Lown, et al. (2002). "Hepatic but not intestinal CYP3A4 displays dose-dependent induction by efavirenz in humans." Clin Pharmacol Ther 72(1): 1-9.

Muck, W., I. Mai, et al. (1999). "Increase in cerivastatin systemic exposure after single and multiple dosing in cyclosporine-treated kidney transplant recipients." Clin Pharmacol Ther 65(3): 251-261.

Nachega, J. B., M. Hislop, et al. (2007). "Adherence to nonnucleoside reverse transcriptase inhibitor-based HIV therapy and virologic outcomes." Ann Intern Med 146(8): 564-573.

Nakagomi-Hagihara, R., D. Nakai, et al. (2006). "OATP1B1, OATP1B3, and mrp2 are involved in hepatobiliary transport of olmesartan, a novel angiotensin II blocker." Drug Metab Dispos 34(5): 862-869.

Nelson, D. R., L. Koymans, et al. (1996). "P450 superfamily: update on new sequences, gene mapping, accession numbers and nomenclature." Pharmacogenetics 6(1): 1-42.

Nicholson, J. K., T. J. Spira, et al. (1989). "Serial determinations of HIV-1 titers in HIV-infected homosexual men: association of rising titers with CD4 T cell depletion and progression to AIDS." AIDS Res Hum Retroviruses 5(2): 205-215.

Niemi, M., P. J. Neuvonen, et al. (2001). "The cytochrome P4503A4 inhibitor clarithromycin increases the plasma concentrations and effects of repaglinide." Clin Pharmacol Ther 70(1): 58-65.

Niemi, M., E. Schaeffeler, et al. (2004). "High plasma pravastatin concentrations are associated with single nucleotide polymorphisms and haplotypes of organic anion transporting polypeptide-C (OATP-C, SLCO1B1)." Pharmacogenetics 14(7): 429-440.

Notari, S., A. Bocedi, et al. (2006). "Simultaneous determination of 16 anti-HIV drugs in human plasma by high-performance liquid chromatography." J Chromatogr B Analyt Technol Biomed Life Sci 831(1-2): 258-266.

Notari, S., C. Tommasi, et al. (2009). "Simultaneous determination of maraviroc and raltegravir in human plasma by HPLC-UV." IUBMB Life 61(4): 470-475.

Nunez, M., D. Gonzalez de Requena, et al. (2001). "Higher efavirenz plasma levels correlate with development of insomnia." J Acquir Immune Defic Syndr 28(4): 399-400.

Nyakutira, C., D. Roshammar, et al. (2008). "High prevalence of the CYP2B6 516G->T(*6) variant and effect on the population pharmacokinetics of efavirenz in HIV/AIDS outpatients in Zimbabwe." Eur J Clin Pharmacol 64(4): 357-365.

Ogburn, E. T., D. R. Jones, et al. (2010). "Efavirenz primary and secondary metabolism in vitro and in vivo: identification of novel metabolic pathways and cytochrome P450 2A6 as the principal catalyst of efavirenz 7-hydroxylation." Drug Metab Dispos 38(7): 1218-1229.

Oroszlan, S., T. D. Copeland, et al. (1984). "Structural and antigenic characterization of the proteins of human T-cell leukemia viruses and their relationships to the gene products of other retroviruses." Princess Takamatsu Symp 15: 147-157.

Owen, A. (2006). "The impact of host pharmacogenetics on antiretroviral drug disposition." Curr Infect Dis Rep 8(5): 401-408.

Owen, A., B. Chandler, et al. (2004). "Expression of pregnane-X-receptor transcript in peripheral blood mononuclear cells and correlation with MDR1 mRNA." Antivir Ther 9(5): 819-821.

Palella, F. J., Jr., R. K. Baker, et al. (2006). "Mortality in the highly active antiretroviral therapy era: changing causes of death and disease in the HIV outpatient study." J Acquir Immune Defic Syndr 43(1): 27-34.

Pasanen, M. K., H. Fredrikson, et al. (2007). "Different effects of SLCO1B1 polymorphism on the pharmacokinetics of atorvastatin and rosuvastatin." Clin Pharmacol Ther 82(6): 726-733.

Pasanen, M. K., M. Neuvonen, et al. (2006). "SLCO1B1 polymorphism markedly affects the pharmacokinetics of simvastatin acid." Pharmacogenet Genomics 16(12): 873-879.

Pasanen, M. K., P. J. Neuvonen, et al. (2008). "Global analysis of genetic variation in SLCO1B1." Pharmacogenomics 9(1): 19-33.

Paterson, D. L., S. Swindells, et al. (2000). "Adherence to protease inhibitor therapy and outcomes in patients with HIV infection." Ann Intern Med 133(1): 21-30.

Pazin, M. J., P. L. Sheridan, et al. (1996). "NF-kappa B-mediated chromatin reconfiguration and transcriptional activation of the HIV-1 enhancer in vitro." Genes Dev 10(1): 37-49.

Pelerin, H., S. Compain, et al. (2005). "Development of an assay method for the detection and quantification of protease and non-nucleoside reverse transcriptase inhibitors in plasma and in peripherical blood mononuclear cells by liquid chromatography coupled with ultraviolet or tandem mass spectrometry detection." J Chromatogr B Analyt Technol Biomed Life Sci 819(1): 47-57.

Pellegrin, I., D. Breilh, et al. (2007). "Interpretation of genotype and pharmacokinetics for resistance to fosamprenavir-ritonavir-based regimens in

antiretroviral-experienced patients." Antimicrob Agents Chemother 51(4): 1473-1480.

Pellegrin, I., D. Breilh, et al. (2006). "Virological responses to atazanavir-ritonavir-based regimens: resistance-substitutions score and pharmacokinetic parameters (Reyaphar study)." Antivir Ther 11(4): 421-429.

Pfizer Inc (2010). "Selzentry (maraviroc) US prescribing information. Revised 11/2009 [online]. Available fromURL: http://us.gsk.com/products/assets/us_selzentry.pdf [Accessed 2010 May 23]."

Phillips, A. N. (1996). "Reduction of HIV concentration during acute infection: independence from a specific immune response." Science 271(5248): 497-499.

Prada, N. and M. Markowitz (2010). "Novel integrase inhibitors for HIV." Expert Opin Investig Drugs 19(9): 1087-1098.

Proctor, N. J., G. T. Tucker, et al. (2004). "Predicting drug clearance from recombinantly expressed CYPs: intersystem extrapolation factors." Xenobiotica 34(2): 151-178.

Pulido, F., M. Matarranz, et al. (2010). "Boosted protease inhibitor monotherapy. What have we learnt after seven years of research?" AIDS Rev 12(3): 127-134.

Quirino, T., E. Ricci, et al. (2008). Long-term efficacy of boosted and unboosted atazanavir-containing regimens: results from the SCOLTA Project. Ninth International Congress on Drug Therapy in HIV Infection. Glasgow, UK.

Rakhmanina, N. Y. and J. N. van den Anker (2006). "Pharmacological research in pediatrics: From neonates to adolescents." Adv Drug Deliv Rev 58(1): 4-14.

Rasar, M. a. and S. R. Hammes (2006). The physiology of the Xenopus laevis ovary. Methods in molecular biology (Clifton, N.J.). 322: 17-30.

Regazzi, M., P. Villani, et al. (2011). "Therapeutic Monitoring and Variability of Atazanavir in HIV-Infected Patients, With and Without HCV Coinfection, Receiving Boosted or Unboosted Regimens." Ther Drug Monit 33(3): 303-308.

Rivero, A., J. A. Mira, et al. (2007). "Liver toxicity induced by non-nucleoside reverse transcriptase inhibitors." J Antimicrob Chemother 59(3): 342-346.

Rosario, M. C., B. Poland, et al. (2006). "A pharmacokinetic-pharmacodynamic model to optimize the phase IIa development program of maraviroc." J Acquir Immune Defic Syndr 42(2): 183-191.

Rostami-Hodjegan, A. and G. T. Tucker (2007). "Simulation and prediction of in vivo drug metabolism in human populations from in vitro data." Nat Rev Drug Discov 6(2): 140-148.

Rotger, M., S. Colombo, et al. (2005). "Influence of CYP2B6 polymorphism on plasma and intracellular concentrations and toxicity of efavirenz and nevirapine in HIV-infected patients." Pharmacogenet Genomics 15(1): 1-5.

Rowe, S. M., S. R. Rabel, et al. (1999). Physical Chemical Properties of Efavirenz. Annual Meeting and Exposition, AAPS PharmSci Supplement.

Rowland Yeo, K., A. Rostami-Hodjegan, et al. (2003). Abundance of cytochromes P450 in human liver: a meta-analysis. 225P GKT, University of London Winter Meeting December 2003. London, UK.

Ruffault, A., C. Michelet, et al. (1995). "The prognostic value of plasma viremia in HIV-infected patients under AZT treatment: a two-year follow-up study." J Acquir Immune Defic Syndr Hum Retrovirol 9(3): 243-248.

Saitoh, A., E. Sarles, et al. (2007). "CYP2B6 genetic variants are associated with nevirapine pharmacokinetics and clinical response in HIV-1-infected children." AIDS 21(16): 2191-2199.

Sangviroon, A., D. Panomvana, et al. (2010). "Pharmacokinetic and pharmacodynamic variation associated with VKORC1 and CYP2C9 polymorphisms in Thai patients taking warfarin." Drug Metab Pharmacokinet 25(6): 531-538.

Sarasa-Nacenta, M., Y. Lopez-Pua, et al. (2001). "Simultaneous determination of the HIV-protease inhibitors indinavir, amprenavir, ritonavir, saquinavir and nelfinavir in human plasma by reversed-phase high-performance liquid chromatography." J Chromatogr B Biomed Sci Appl 757(2): 325-332.

Schuitemaker, H., M. Koot, et al. (1992). "Biological phenotype of human immunodeficiency virus type 1 clones at different stages of infection: progression of disease is associated with a shift from monocytotropic to T-cell-tropic virus population." J Virol 66(3): 1354-1360.

Shitara, Y., M. Hirano, et al. (2004). "Gemfibrozil and its glucuronide inhibit the organic anion transporting polypeptide 2 (OATP2/OATP1B1:SLC21A6)-mediated hepatic uptake and CYP2C8-mediated metabolism of cerivastatin: analysis of the mechanism of the clinically relevant drug-drug interaction between cerivastatin and gemfibrozil." J Pharmacol Exp Ther 311(1): 228-236.

Shitara, Y., T. Itoh, et al. (2003). "Inhibition of transporter-mediated hepatic uptake as a mechanism for drug-drug interaction between cerivastatin and cyclosporin A." J Pharmacol Exp Ther 304(2): 610-616.

Siccardi, M., A. D'Avolio, et al. (2008). "Association of a single-nucleotide polymorphism in the pregnane X receptor (PXR 63396C-->T) with reduced concentrations of unboosted atazanavir." Clin Infect Dis 47(9): 1222-1225.

Simon, V. A., M. D. Thiam, et al. (2001). "Determination of serum levels of thirteen human immunodeficiency virus-suppressing drugs by high-performance liquid chromatography." J Chromatogr A 913(1-2): 447-453.

Solas, C., M. C. Gagnieu, et al. (2008). "Population pharmacokinetics of atazanavir in human immunodeficiency virus-infected patients." Ther Drug Monit 30(6): 670-673.

Stahle, L., L. Moberg, et al. (2004). "Efavirenz plasma concentrations in HIV-infected patients: inter- and intraindividual variability and clinical effects." Ther Drug Monit 26(3): 267-270.

Starnes, M. C. and Y. C. Cheng (1989). "Human immunodeficiency virus reverse transcriptase-associated RNase H activity." J Biol Chem 264(12): 7073-7077.

Steigbigel, R. T., D. A. Cooper, et al. (2008). "Raltegravir with optimized background therapy for resistant HIV-1 infection." N Engl J Med 359(4): 339-354.

Stern, J. O., P. A. Robinson, et al. (2003). "A comprehensive hepatic safety analysis of nevirapine in different populations of HIV infected patients." J Acquir Immune Defic Syndr 34 Suppl 1: S21-33.

Stevens, S. W. and J. D. Griffith (1994). "Human immunodeficiency virus type 1 may preferentially integrate into chromatin occupied by L1Hs repetitive elements." Proc Natl Acad Sci U S A 91(12): 5557-5561.

Storch, C. H., D. Theile, et al. (2007). "Comparison of the inhibitory activity of anti-HIV drugs on P-glycoprotein." Biochem Pharmacol 73(10): 1573-1581.

Svard, J., J. P. Spiers, et al. (2008). Antivirals and nuclear receptor activation of CYP3A4 and 2B6. Ninth International Congress on Drug Therapy in HIV Infection. Glasgow, UK.

Synold, T. W., I. Dussault, et al. (2001). "The orphan nuclear receptor SXR coordinately regulates drug metabolism and efflux." Nat Med 7(5): 584-590.

Takahashi, M., Y. Kudaka, et al. (2007). "The validation of plasma darunavir concentrations determined by the HPLC method for protease inhibitors." Biol Pharm Bull 30(10): 1947-1949.

Takano, R., K. Sugano, et al. (2006). "Oral absorption of poorly water-soluble drugs: computer simulation of fraction absorbed in humans from a miniscale dissolution test." Pharm Res 23(6): 1144-1156.

Tamai, I., R. Ohashi, et al. (2000). "Molecular and functional characterization of organic cation/carnitine transporter family in mice." J Biol Chem 275(51): 40064-40072.

Taylor, P. J. (2005). "Matrix effects: the Achilles heel of quantitative high-performance liquid chromatography-electrospray-tandem mass spectrometry." Clin Biochem 38(4): 328-334.

ter Heine, R., M. Davids, et al. (2009). "Quantification of HIV protease inhibitors and non-nucleoside reverse transcriptase inhibitors in peripheral blood mononuclear cell lysate using liquid chromatography coupled with tandem mass spectrometry." J Chromatogr B Analyt Technol Biomed Life Sci 877(5-6): 575-580.

Ter Heine, R., M. J. Hillebrand, et al. (2009). "Quantification of the HIV-integrase inhibitor raltegravir and detection of its main metabolite in human plasma, dried blood spots and peripheral blood mononuclear cell lysate by means of

high-performance liquid chromatography tandem mass spectrometry." J Pharm Biomed Anal 49(2): 451-458.

Ter Heine, R., H. Rosing, et al. (2009). "Quantification of etravirine (TMC125) in plasma, dried blood spots and peripheral blood mononuclear cell lysate by liquid chromatography tandem mass spectrometry." J Pharm Biomed Anal 49(2): 393-400.

Tersmette, M., R. E. de Goede, et al. (1988). "Differential syncytium-inducing capacity of human immunodeficiency virus isolates: frequent detection of syncytium-inducing isolates in patients with acquired immunodeficiency syndrome (AIDS) and AIDS-related complex." J Virol 62(6): 2026-2032.

Tersmette, M., J. M. Lange, et al. (1989). "Association between biological properties of human immunodeficiency virus variants and risk for AIDS and AIDS mortality." Lancet 1(8645): 983-985.

Thelen, K. and J. B. Dressman (2009). "Cytochrome P450-mediated metabolism in the human gut wall." J Pharm Pharmacol 61(5): 541-558.

Tibotec (2006). "TMC125 Investigator Brochure. Edition 11."

Tirona, R. G., B. F. Leake, et al. (2001). "Polymorphisms in OATP-C: identification of multiple allelic variants associated with altered transport activity among European- and African-Americans." J Biol Chem 276(38): 35669-35675.

Turner, J., L. Bansi, et al. (2010). "The prevalence of hepatitis C virus (HCV) infection in HIV-positive individuals in the UK - trends in HCV testing and the impact of HCV on HIV treatment outcomes." J Viral Hepat 17(8): 569-577.

Turner, M. L., K. Reed-Walker, et al. (2003). "Simultaneous determination of nine antiretroviral compounds in human plasma using liquid chromatography." J Chromatogr B Analyt Technol Biomed Life Sci 784(2): 331-341.

UNAIDS/WHO (2010). Towards universal access: scaling up priority HIV/AIDS interventions in the health sector: progress report 2010.

Uwai, Y., H. Saito, et al. (2000). "Interaction between methotrexate and nonsteroidal anti-inflammatory drugs in organic anion transporter." Eur J Pharmacol 409(1): 31-36.

van Luin, M., L. Gras, et al. (2009). "Efavirenz dose reduction is safe in patients with high plasma concentrations and may prevent efavirenz discontinuations." J Acquir Immune Defic Syndr 52(2): 240-245.

Varatharajan, L. and S. A. Thomas (2009). "The transport of anti-HIV drugs across blood-CNS interfaces: summary of current knowledge and recommendations for further research." Antiviral Res 82(2): A99-109.

Vavricka, S. R., J. Van Montfoort, et al. (2002). "Interactions of rifamycin SV and rifampicin with organic anion uptake systems of human liver." Hepatology 36(1): 164-172.

Verbesselt, R., E. Van Wijngaerden, et al. (2007). "Simultaneous determination of 8 HIV protease inhibitors in human plasma by isocratic high-performance liquid chromatography with combined use of UV and fluorescence detection: amprenavir, indinavir, atazanavir, ritonavir, lopinavir, saquinavir, nelfinavir and M8-nelfinavir metabolite." J Chromatogr B Analyt Technol Biomed Life Sci 845(1): 51-60.

Vlahov, D., N. Graham, et al. (1998). "Prognostic indicators for AIDS and infectious disease death in HIV-infected injection drug users: plasma viral load and CD4+ cell count." JAMA 279(1): 35-40.

Vogel, M., N. Bertram, et al. (2009). "Nevirapine pharmacokinetics in HIV-infected and HIV/HCV-coinfected individuals." J Antimicrob Chemother 63(5): 988-991.

Volpi, S., C. Heaton, et al. (2009). "Whole genome association study identifies polymorphisms associated with QT prolongation during iloperidone treatment of schizophrenia." Mol Psychiatry 14(11): 1024-1031.

Vourvahis, M. (2010). Pharmacokinetics of QD maraviroc co-administered as part of a novel NRTI-sparing regimen with atazanavir/ritonavir in HIV treatment-naïve patients. 11th International Workshop on Clinical Pharmacology and HIV Therapy. . Sorrento, Italy.

Vrouenraets, S. M., F. W. Wit, et al. (2007). "Efavirenz: a review." Expert Opin Pharmacother 8(6): 851-871.

Walgren, R. A., K. J. Karnaky, Jr., et al. (2000). "Efflux of dietary flavonoid quercetin 4'-beta-glucoside across human intestinal Caco-2 cell monolayers by apical multidrug resistance-associated protein-2." J Pharmacol Exp Ther 294(3): 830-836.

Walker, D. K., S. Abel, et al. (2005). "Species differences in the disposition of the CCR5 antagonist, UK-427,857, a new potential treatment for HIV." Drug Metab Dispos 33(4): 587-595.

Ward, B. A., J. C. Gorski, et al. (2003). "The cytochrome P450 2B6 (CYP2B6) is the main catalyst of efavirenz primary and secondary metabolism: implication for

HIV/AIDS therapy and utility of efavirenz as a substrate marker of CYP2B6 catalytic activity." J Pharmacol Exp Ther 306(1): 287-300.

Washington, C. B., C. Flexner, et al. (2003). "Effect of simultaneous versus staggered dosing on pharmacokinetic interactions of protease inhibitors." Clin Pharmacol Ther 73(5): 406-416.

Waxman, D. J. (1999). "P450 gene induction by structurally diverse xenochemicals: central role of nuclear receptors CAR, PXR, and PPAR." Arch Biochem Biophys 369(1): 11-23.

Weiss, J., M. Herzog, et al. (2009). "Induction of multiple drug transporters by efavirenz." J Pharmacol Sci 109(2): 242-250.

Wenning, L., B.-Y. Nguyen, et al. (2008). Pharmacokinetic/Pharmacodynamic (PK/PD) analyses for Raltegravir (RAL) in phase II and III studies in treatment experienced HIV-infected patients 9th International Workshop on Clinical Pharmacology of HIV Therapy. New Orleans, USA.

Woods, C. G., J. P. Heuvel, et al. (2007). "Genomic profiling in nuclear receptor-mediated toxicity." Toxicol Pathol 35(4): 474-494.

Yeh, K. C., P. J. Deutsch, et al. (1998). "Single-dose pharmacokinetics of indinavir and the effect of food." Antimicrob Agents Chemother 42(2): 332-338.

Zhang, J., P. Kuehl, et al. (2001). "The human pregnane X receptor: genomic structure and identification and functional characterization of natural allelic variants." Pharmacogenetics 11(7): 555-572.

Zhu, T., D. Muthui, et al. (2002). "Evidence for human immunodeficiency virus type 1 replication in vivo in CD14(+) monocytes and its potential role as a source of virus in patients on highly active antiretroviral therapy." J Virol 76(2): 707-716.